

Distribution Agreement

In presenting this thesis or dissertation as a partial fulfillment of the requirements for an advanced degree from Emory University, I hereby grant to Emory University and its agents the non-exclusive license to archive, make accessible, and display my thesis or dissertation in whole or in part in all forms of media, now or hereafter known, including display on the world wide web. I understand that I may select some access restrictions as part of the online submission of this thesis or dissertation. I retain all ownership rights to the copyright of the thesis or dissertation. I also retain the right to use in future works (such as articles or books) all or part of this thesis or dissertation.

Signature:

Evan P. Lebois

Date

Discovery and Development of Selective M₁ Agonists that Protect Against Alzheimer's
Pathology and Bias Hippocampal Circuitry Dynamics in Rodents

By

Evan P. Lebois
Doctor of Philosophy

Graduate Division of Biological and Biomedical Science
Neuroscience

Allan I. Levey, MD, Ph.D.
Advisor

Joseph R. Manns, Ph.D.
Advisor

Elizabeth A. Buffalo, Ph.D.
Committee Member

Robert M. Cohen, Ph.D, MD.
Committee Member

P. Jeffrey Conn, Ph.D.
Committee Member

Accepted:

Lisa A. Tedesco, Ph.D.
Dean of the James T. Laney School of Graduate Studies

Date

Discovery and Development of Selective M₁ Agonists that Protect Against Alzheimer's
Pathology and Bias Hippocampal Circuitry Dynamics in Rodents

by

Evan P. Lebois
B.S., University of Delaware, 2007

Advisors: Allan I. Levey, MD, Ph.D.
Joseph R. Manns, Ph.D.

An abstract of
A dissertation submitted to the Faculty of the James T. Laney School of Graduate Studies
of Emory University in partial fulfillment of the requirements for the degree of
Doctor of Philosophy
in Graduate Division of Biological and Biomedical Science
Neuroscience
2014

Abstract

Discovery and Development of Selective M₁ Agonists that Protect Against Alzheimer's Pathology and Bias Hippocampal Circuitry Dynamics in Rodents

By Evan P. Lebois

M₁ muscarinic receptors are heavily expressed in brain areas important for memory (e.g. the hippocampus) and are known to both modulate hippocampal memory circuits and regulate amyloid pathology in AD mice. M₁^{-/-} mice develop memory impairments and high A β levels in their brain, highlighting a potentially disease-modifying role of M₁ receptors in AD. Although acute improvements in memory and pathology have been shown in AD mice with M₁ activators, it remains unclear whether chronically activating M₁ can lead to persistent disease-modifying effects that prevent memory impairments and neuropathology from forming. Thus, the present work used chronic dosing of the selective M₁ agonist, VU0364572, to 5X FAD mice from an age prior to appreciable amyloid pathology (2 months) to an age where these mice display memory impairments (6 months). M₁ activation was found to both prevent mice from becoming memory impaired as well as significantly reduce levels of soluble and insoluble A β _{40,42} in the cortex and hippocampus of these animals.

Although M₁ modulates hippocampal circuitry, how M₁ biases circuits *in vivo* to improve memory remains unclear. Pharmacological work indicates M₁ activation improves spatial memory, and *in vitro* studies with M₁^{-/-} mice have indicated M₁ activation suppresses CA3-CA1 transmission. However, the effects of M₁ activation on spatial representations and CA3-CA1 functional connectivity remains unclear. *In vivo* tetrode recording from dCA3 and dCA1 was used to obtain spiking and local field potential data in adult rats during open field exploration in a morph box. The M₁ agonist, VU0364572, was used to examine the impact of M₁ activation on hippocampal place fields and CA3-CA1 synchrony. Consistent with prior findings, the present results indicated that M₁ activation decreased CA3-CA1 functional connectivity yet benefitted spatial representations. Specifically, M₁ activation decreased CA3-CA1 spike-field synchrony in the theta range and the temporal organization of CA3 spikes to CA1. However, M₁ activation also increased responsiveness of hippocampal place fields to changes in the shape of the recording enclosure. One possible interpretation is that less coherent CA3-CA1 synaptic transmission might act to prioritize current information coming from entorhinal cortex.

Discovery and Development of Selective M₁ Agonists that Protect Against Alzheimer's
Pathology and Bias Hippocampal Circuitry Dynamics in Rodents

by

Evan P. Lebois
B.S., University of Delaware, 2007

Advisors: Allan I. Levey, MD, Ph.D.
Joseph R. Manns, Ph.D.

A dissertation submitted to the Faculty of the
James T. Laney School of Graduate Studies of Emory University
in partial fulfillment of the requirements for the degree of
Doctor of Philosophy
in Graduate Division of Biological and Biomedical Science
Neuroscience
2014

ACKNOWLEDGEMENTS

There are countless individuals who have helped me become the person whom I have developed into and enabled me to undertake this long, arduous journey towards a PhD. To every one of them I say “thank you!”

Among these countless individuals, however, are a certain select group which stand out. Firstly I would like to thank my graduate school advisors here at Emory, Drs. Allan Levey and Joseph Manns. You two have been absolutely incredible mentors for me during my time here at Emory and set a very high bar for your students to aspire to. You both have shown my colleagues and I how to work harder and think deeper in pursuit of the best effort that one can possibly put forth. For all of your encouragement and support through these past several years I cannot possibly thank you enough. I hope to someday be as good of a mentor as the example that you guys have set for me. Also, without you both agreeing to take me on I would have likely never been here at Emory in the first place. Again, the words cannot do justice to all that you have done for me.

Secondly, I would like to thank my prior grad school advisors, Drs. P. Jeffrey Conn and Craig W. Lindsley. I cannot say enough about the group that you all have established at the Vanderbilt Center for Neuroscience Drug Discovery—it is exceptional in every way and every single individual there, yourselves included, are outstanding mentors and human beings to work with. Your generosity and support for me over the years has been unwavering, in good times and in bad—and we have certainly been to both extremes! This support means everything to me and I look forward to continued collaboration and friendship with you both over the years ahead. Without your generous contribution of the drugs used in my dissertation work these studies never would have

been able to happen. It has been a long, hard road but I am thankful beyond words that you have been there to see me through to the end.

Thank you also to my committee members, Robert Cohen, Beth Buffalo and Jeff Conn. Conversations with you all have helped in guiding this work to make it the most polished product possible and I owe a great deal of that to you. Your input has been invaluable along the way and I look forward to continuing the scientific dialogue with each of you in the future.

One cannot complete such a journey through a PhD program without the day-to-day support of one's colleagues. From Vanderbilt to Emory I have had immense support and the best group of colleagues imaginable to work with. I would like to thank the entirety of the Vanderbilt Center for Neuroscience Drug Discovery (you guys have just gotten too numerous to list individually!), as well as Kwangho Kim, YY-Cheung and Rich Williams. As I was struggling to find my scientific niche coming out of my undergraduate years, all of you helped to ignite a passion for drug development in me that I can never thank you enough for. The years I spent working with you were some of the best of my life and I hope to keep in close touch over the years ahead.

At Emory, the Center for Neurodegenerative Disease is a very special place to work. It has proved an incredibly stimulating, enriching, and thought-provoking environment that has driven me to be creative and excel. For all of the many students and faculty who are part of the CNS who have helped me over my years at Emory I would like to say "thank you." The Lah-Levey Lab has been an amazing laboratory to be a part of for these past several years. A special thank you to my undergraduate mentee Jay Li for your invaluable technical assistance over my years at Emory. You were a pleasure to

work with and I am sure you will absolutely excel in medical school. All of you have been some of the best colleagues I could have hoped for in coming here to Emory. Thank you for everything you have done to support me over these years.

The CND is not the only truly special place at Emory, however. The Manns Lab I feel is one group that can truly match the CND for its support and nurturing of young investigators—it is a truly amazing place to work and I was absolutely blessed to spend my years at Emory working with this talented group of individuals. A special thank you to John Trimper, Claire Galloway, David Bass and Arick Wang for performing countless injections that enabled my *in vivo* electrophysiology studies to come to fruition. Also, a special thank you to Chun Hu, my undergraduate mentee who has excelled in helping me to build recording drives and train rats for behavioral studies—I could not have finished this project this quickly without you. In addition to technical assistance though, all of you have helped me through the day-to-day grunt of PhD studies in ways that mean so much more than just helping the science along. You all are great friends and I look forward to keeping in touch with you in the future.

I would be absolutely remiss to not thank those in Atlanta who have helped keep me sane outside of lab during these tough years of graduate study here at Emory. In particular, a huge thank you to Clan na nGael GAA Hurling and Gaelic Football Club. You all have been an amazing group of friends over the years who have truly helped me develop as a better person—in addition to helping Lauren and I with an emergency move! I cannot thank you enough for the times we have shared on and off the field and I will treasure these memories always.

Finally, I would like to thank my McDonough and Lebois families. Your support has been the strongest and most steadfast I could possibly imagine during both the best and the hardest of times during my graduate studies. Your cards and emails and messages and care packages and conversations and visits have helped carry me through these tough years. I am blessed to have you as the parents and siblings I do and cannot imagine a better family to have at my side through these past years and the years ahead—I really lucked out with each and every one of you guys! Lauren, my lovely wife, I could not have done this without you! Your love and support has truly meant—and will always mean—the world to me. Thank you so much for being at my side through not only the good times, but the bad, offering words of encouragement to pick me up and help me through. I am forever thankful that my time at Emory allowed us to meet and am excited for our next adventure together in Boston!

This dissertation is dedicated to my parents, Gus and Nora Lebois. My journey to complete a PhD is nothing compared to the countless hours and stress that you guys endured as parents to provide the best possible upbringing for Ryan and I. Your love and belief in me has made all of this possible.

TABLE OF CONTENTS

Chapter I: INTRODUCTION	1
Alzheimer's Disease: Overview and Significance.....	1
The Pathophysiology of Alzheimer's Disease.....	4
APP Processing and the Amyloid Cascade Hypothesis.....	9
A β -Induction of Synaptic Dysfunction.....	11
Cholinergic Neurotransmission and its Role in Alzheimer's Disease.....	12
Neuroanatomy of the Cholinergic System.....	12
Muscarinic Acetylcholine Receptor Expression and Function.....	14
Alzheimer's Disease Treatment.....	21
Currently Approved Therapeutics and Limitations.....	21
Therapeutic Strategies Under Investigation.....	23
Pro-muscarinic strategies under therapeutic development for AD.....	31
M ₁ Allosteric Agonist Development for Alzheimer's Disease.....	35
Animal Models of Alzheimer's Disease.....	44
The Hippocampal Memory System.....	49
Functional Neuroanatomy and Overview.....	49
Hippocampal Place Cells: Properties and Relevance to Memory.....	56
Place Field Properties.....	56
Place Cell Remapping.....	59

Local Field Potential Oscillations and Relevance to Memory.....	63
Proposed Research.....	76
Chapter II: MATERIALS AND METHODS.....	79
Subjects for Transgenic AD Mouse Studies.....	79
Animal Perfusion.....	79
Biochemical Tissue Fractionation.....	80
Behavioral Testing.....	82
Morris Water Maze.....	82
Cued and Contextual Fear Conditioning.....	83
Immunohistochemistry.....	84
Immunohistochemical Quantification.....	85
A β ₄₀ and A β ₄₂ ELISA.....	85
Drugs for Transgenic AD Mouse Studies.....	86
Determination of CNS VU572 Concentrations for Chronic Dosing.....	86
Primary Neuron Culture.....	87
Statistical Analyses.....	88
Drugs for <i>In Vivo</i> Electrophysiology Studies.....	89
Subjects for <i>In Vivo</i> Electrophysiology Studies.....	90
Morph Box Open Field Exploration Task.....	90
Surgeries and Positioning of Recording Electrodes.....	91
<i>In Vivo</i> Electrophysiology Data Acquisition.....	95
<i>In Vivo</i> Electrophysiology Data Analyses.....	95
Place Field Analyses and Spatial Discrimination Scores.....	95

Spatial Information Analyses.....	96
Relation of Local Field Potentials to Behavior.....	97
Analyses of Hippocampal Synchrony.....	97
Statistical Analyses.....	99
Electrolytic Lesioning.....	99
Chapter III: <i>IN VITRO</i> AND <i>IN VIVO</i> EFFECTS OF SELECTIVE M₁ AGONISTS ON NEUROPATHOLOGY AND BEHAVIORAL DEFICITS IN A CHRONIC, PREVENTATIVE TREATMENT TRIAL OF TRANSGENIC AD MICE.....	101
Introduction.....	101
Results.....	103
M ₁ Activation by VU572 Lowers A β ₄₀ and A β ₄₂ Levels <i>In Vitro</i> in Mouse Primary Cortical and Hippocampal Neurons.....	103
M ₁ Activation by VU572 Preserves Hippocampal Memory When Dosed Chronically in 5X FAD Transgenic Alzheimer's Mice.....	105
VU572 Decreases Soluble and Insoluble A β ₄₀ and A β ₄₂ Levels in Cortex and Hippocampus of 5X FAD Mice.....	113
M ₁ Activation by VU572 Treatment Abolishes Soluble A β ₄₂ Correlation with Memory Impairment.....	114
M ₁ Activation by VU572 Reduces A β ₄₀ Neuropathology in the Hippocampus and cortex of 5X FAD Mice.....	119
Effect of M ₁ Activation by VU572 on Contextual and Cued Fear Conditioning.....	122
Discussion.....	135

Chapter IV: EFFECTS OF SELECTIVE M₁ ACTIVATION ON HIPPOCAMPAL CIRCUITRY DYNAMICS	141
Introduction.....	141
Results.....	143
Place Cells Code Contextual Change in the Proposed Morph Box Test Paradigm.....	143
M ₁ Activation by VU572 Increases Spatial Discrimination of Hippocampal Place Cells.....	147
M ₁ Activation by VU572 Does Not Impair Spatial Information of CA3 or CA1 Place Cells, but Activation by the M ₁ PAM BQCA Does.....	153
M ₁ Activation by VU572 Suppresses CA3-CA1 Field-Field Coherence.....	156
M ₁ Activation by VU572 Suppresses CA3 Spike-CA1 Field Coherence.....	156
M ₁ Activation by VU572 Renders CA3 Spikes to CA1 Less Coherent.....	162
Discussion.....	165
Chapter V: SUMMARY AND FUTURE DIRECTIONS	173
DECLARATION OF CONFLICTS OF INTEREST	182
REFERENCES	183

LIST OF FIGURES

1.1 Alzheimer's Disease Pathology.....	3
1.2 Pathological Cascade of Alzheimer's Disease.....	5
1.3 Amyloid Cascade Hypothesis of AD: Amyloid Buildup is Responsible for AD.....	7
1.4 Cholinergic Hypothesis of AD: Decreased Acetylcholine is Responsible for AD....	14
1.5 Muscarinic Receptor Function and Expression in the CNS.....	16
1.6 Current Therapy for AD Patients.....	22
1.7 Novel Therapeutic Strategies for AD Patients.....	25
1.8 M ₁ Muscarinic Receptors Bias APP Toward Non-Amyloidogenic Processing.....	29
1.9 M ₁ Agonist Discovery and Characterization.....	38
1.10 M ₁ Agonist Optimization for <i>In Vivo</i> Studies.....	39
1.11 M ₁ Activation by VU572 Robustly Impacts Hippocampal Synaptic Plasticity.....	42
1.12 M ₁ Allosteric Agonists Do Not Robustly Desensitize M ₁ Receptor Signaling.....	43
1.13 Animal Models of AD: The 5X FAD Mouse is a Robust Animal Model of AD....	47
1.14 The Hippocampus Combines Spatial and Nonspatial Inputs in Order to Form Episodic Memories.....	51
1.15 Hippocampal Place Cells Form Place-Specific Firing Fields.....	57
1.16 Place Cells Form Context-Specific Representations.....	61
1.17 Oscillations Lay the Foundation for Spike-Timing Dependent Plasticity: They Serve to Turn Many Small Signals Into a Big Signal that Can Elicit Target Neuron Discharge	65
1.18 The Mammalian CNS Has Many Different Neural Oscillators Whose Frequencies Subserve Different Memory Processes.....	66

1.19 Intra- Versus Extra-Hippocampal Microcircuits Contribute to Different Aspects of Information Encoding, where Intrahippocampal Connectivity is Modulated by Muscarinic Receptors.....	69
1.20 CA3 and CA1 Hippocampal Subfields Show Theta-Modulated Gamma Activity That Serves to Organize Pyramidal Cell Spiking During Behavior	70
1.21 Coherence is a Measure of Functional Connectivity	72
1.22 Coherence Reflects How Much Two LFPs Co-Vary in Time	73
1.23 Coherograms are a Way of Simultaneously Depicting Coherence Across Many Frequency Bands of Interest	74
2.1 Terminal Pathology Processing.....	81
2.2 32-Tetrode Microdrive Permits High-Density Neuronal Recording From the Rodent Hippocampus.....	92
2.3 Tetrode Recordings Allow for Optimum Single Unit Isolation.....	93
3.1 M ₁ Activation by VU572 Lowers A β _{40/42} Levels in Mouse Primary Cortical and Hippocampal Neurons.....	104
3.2 M ₁ Agonist VU572 Preventative Treatment Trial in 5X FAD Mice.....	107
3.3 M ₁ Activation by VU572 Preserves Hippocampal Memory When Dosed Chronically in 5X FAD Transgenic Alzheimer’s Mice.....	111
3.4 M ₁ Activation by VU572 Does Not Influence Morris Water Maze Performance During Training.....	112
3.5 M ₁ Activation by VU572 Decreases Soluble A β ₄₀ and A β ₄₂ Levels in Cortex and Hippocampus of 5X FAD Mice	115

3.6 M ₁ Activation by VU572 Decreases Insoluble A β ₄₀ and A β ₄₂ Levels in Cortex and Hippocampus of 5X FAD Mice.....	116
3.7 M ₁ Activation by VU572 Treatment Abolishes Soluble A β ₄₂ Correlation with Memory Impairment.....	118
3.8 Insoluble A β ₄₂ Levels Are Not Correlated with Memory.....	120
3.9 M ₁ Activation by VU572 Does Not Impact Soluble or Insoluble A β _{40/42} Ratios in the Cortex or Hippocampus of 5X FAD Mice.....	121
3.10 M ₁ Activation by VU572 Reduces A β ₄₀ Neuropathology in the Hippocampus of 5X FAD Mice.....	123
3.11 M ₁ Activation by VU572 Reduces A β ₄₀ Neuropathology in the Cortex of 5X FAD Mice.....	125
3.12 M ₁ Activation by VU572 Reduces A β ₄₀ Neuropathology in the Brains of 5X FAD Mice.....	126
3.13 M ₁ Activation by VU572 Reduces A β ₄₂ Neuropathology in the Brains of 5X FAD Mice.....	128
3.14 M ₁ Activation by VU572 Reduces A β ₄₀ Neuropathology in the Brains of 5X FAD Mice.....	130
3.15 M ₁ Activation by VU572 Reduces A β ₄₀ Neuropathology in the Brains of 5X FAD Mice.....	131
3.16 M ₁ Activation by VU572 Does not Rescue Deficits in Contextual Fear Conditioning in 5X FAD Mice.....	133
3.17 Cued Fear Conditioning is Not Impacted by 5X FAD Genotype or M ₁ Activation by VU572 Treatment in 5X FAD Mice.....	134

4.1 Morph Box Test Paradigm to Manipulate Hippocampal Place Field Activity.....	144
4.2 Place Cells Code Contextual Change in the Proposed Morph Box Test Paradigm..	145
4.3 Representative Place Cell Examples From Experimental Drug Sessions.....	149
4.4 M ₁ Activation by VU572 Increases Spatial Discrimination of Hippocampal Place Cells.....	151
4.5 M ₁ Activation by VU572 Does Not Impair Spatial Information of CA3 or CA1 Place Cells, but Activation by the M ₁ PAM BQCA Does.....	154
4.6 M ₁ Activation by VU572 Suppresses CA3-CA1 Field-Field Coherence.....	157
4.7 M ₁ Activation by VU572 Suppresses CA3 Spike-CA1 Field Coherence.....	160
4.8 M ₁ Activation by VU572 Renders CA3 Spikes to CA1 Less Coherent.....	163
4.9 Under Normal Circumstances CA1 Listens Equally to Either CA3 or EC.....	168
4.10 The Suppression of CA3-CA1 Circuitry by M ₁ Agonists May Bias CA1 Towards Synchronizing More with Other Partners Such as EC to Drive Novel Information Encoding.....	169
5.1 Cholinergic Dysfunction is Central to Age-Associated Alterations in Hippocampal Function and May Be a Key Contributor to Age-Related Memory Impairment	176
5.2 Aging Detrimentally Impacts the Ability of Place Cells to Represent Space and Biases the Hippocampus Towards Pattern Completion.....	177
5.3 Mouse Models of AD Show Disrupted Place Fields and Decreased Spatial Information Content of Place Cells.....	179
5.4 M ₁ Agonists For the Treatment of Memory Dysfunction.....	181

Chapter 1. INTRODUCTION

Alzheimer's Disease: Overview and Significance

Alzheimer's disease (AD) is a progressive, neurodegenerative disease which is the most common cause of dementia worldwide and accounts for 60-70% of all cases of dementia (Barker, et al. 2002; Holtzman, et al. 2011). The economic impact of AD on the healthcare system and lives of caregivers is hard to overstate. The current cost of care for AD and dementia in the US alone is around \$172 billion and with the aging Baby Boomers the number of people with AD is expected to quadruple by the year 2050. Currently approximately 1 in 8 individuals over the age of 65 have AD and this number increases sharply to approximately 50% over the age of 85 (www.alz.org). Despite the emotional and financial impact of AD worldwide there currently exists no treatment to slow or halt the disease process. Thus, AD represents one of the most significant challenges facing society to-date.

AD was first characterized by the psychiatrist Alois Alzheimer back in 1906 (Alzheimer 1906). Alzheimer was the first to observe the neurofibrillary tangles, amyloid beta (A β) plaques, and overt neuronal loss in the brain of a patient he studied, Auguste Deter. Over the years in which Alzheimer observed Deter, she presented with memory loss, disorientation, hallucinations and vocal outbursts. Upon post-mortem examination of her brain, Alzheimer stained the tissue using then recently developed techniques by Franz Nissl, which allowed him to see the tangles and plaques that he subsequently used in his pathological characterization of the disorder. To this day,

Nissl's methods are still in use and the plaques, tangles, and neuronal loss described by Alzheimer remain the standard pathological hallmarks of AD (Figure 1.1).

Broadly-speaking, there are two different types of AD: early-onset AD (EOAD) and late-onset AD (LOAD). EOAD is much rarer, but some cases can be genetically-defined. That is, a small percentage of patients with EOAD have defined autosomal dominant genetic mutations that give rise to their disease phenotype, however the bulk of EOAD and LOAD cases without identified genetic causes clearly indicates that other, as of yet unidentified, genetic mechanisms are at play and need to be better understood (Kauwe, et al. 2008; Wingo, et al. 2012). As the name implies, these EOAD patients onset early with the disease (typically in their 40's-50's) and progress rapidly. Less than 5% of all AD cases are attributable to these genetic mutations, however it is important to note that virtually all animal models of AD are based upon some number of these human genetic mutations introduced into animals. The mutations that give rise to EOAD reside in one of three genes: *APP*, *PSEN1*, and *PSEN2*. *APP* codes for the amyloid precursor protein, while *PSEN1* and *PSEN2* code for members of the gamma secretase complex responsible for the proteolytic processing of APP that gives rise to the A β peptides associated with AD (Goate, Chartier-Harlin et al. 1991; Murrell, Farlow et al. 1991; Hendriks, van Duijn et al. 1992; Mullan, Crawford et al. 1992; Levy-Lahad, Wasco et al. 1995; Rogaev, Sherrington et al. 1995; Sherrington, Rogaev et al. 1995).

The remaining 95% of AD cases are termed LOAD cases or "sporadic" AD cases, as they are idiopathic in nature with as of yet no defined genetic cause. Several risk factors exist for LOAD, the biggest being age and *APOE* ϵ 4 status. Heterozygosity for the *APOE* ϵ 4 allele confers approximately a 3-fold risk and homozygosity confers

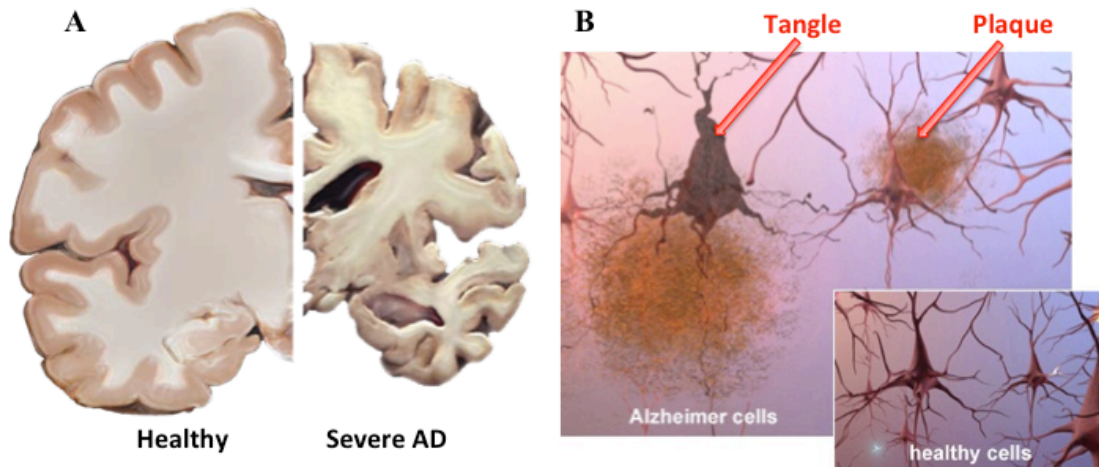


Figure 1.1. Alzheimer's Disease Pathology.

A) Example hemispheres depicting a healthy brain (left) and advanced AD brain showing severe disease pathology (right). Note the cortical atrophy that has taken place due to extensive neuronal death, resulting in enlargement of ventricles and marked loss of hippocampal volume. B) The two major hallmarks of AD depicted: amyloid beta plaques composed of aggregated amyloid beta ($A\beta$) peptides and neurofibrillary tangles composed of hyperphosphorylated tau protein. The plaques reside extracellularly, while the neurofibrillary tangles resides intracellularly.

Image From: http://www.alz.org/alzheimers_disease_facts_figures.asp

approximately a 12-fold risk (www.alzgene.org). Functionally, apoE is a lipoprotein that serves as a cargo adaptor for the vesicular transport of cholesterol and also has been shown to bind and transport A β (Corder, et al. 1993). Due to its involvement in trafficking, apoE plays a role in a wide range of processes in the CNS other than cholesterol transport including neuronal plasticity and inflammation (Kim, et al. 2009). Despite these findings, the exact role in healthy and disease brain states is yet unknown.

The Pathophysiology of Alzheimer's Disease

Neurodegeneration in AD progresses sequentially through certain brain structures and select subpopulations of vulnerable neurons. AD almost invariably begins with an insidious, gradual decline in memory, specifically, with problems encoding new memories. Consistently impacted early are those neurons in layer II of the entorhinal cortex, which acts as a gatekeeper of information flowing to and from the hippocampus. A β and tau pathologies accumulate in a circuit-dependent manner, deafferenting the entorhinal cortical projections to the hippocampus, and disrupting the molecular mechanisms necessary to form new episodic memories (Figure 1.2) (Buckner, et al. 2005; de Toledo-Morrell, et al. 2007; Palop, and Mucke 2010; Small, et al. 2011). A β pathology is believed to be upstream of tau pathology, as A β has been shown to directly induce tau hyperphosphorylation and neuritic degeneration (Jin, et al. 2011). The early accumulation of A β in AD has resulted in the “amyloid cascade hypothesis of AD,” which posits that all significant damage observed in the brains of advanced AD patients is a downstream consequence resulting from A β accumulation (Hardy and Selkoe 2002). This progressive accumulation of A β pathology results in patients becoming more

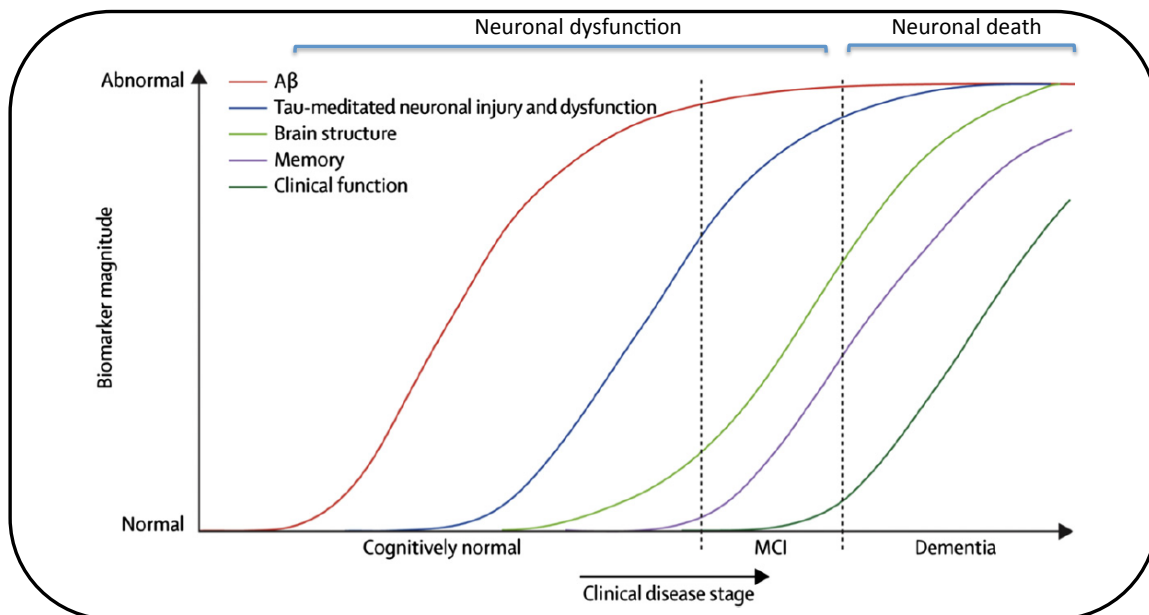


Figure 1.2. Pathological Cascade of Alzheimer's Disease.

The sigmoidal curves depict the temporal trajectory of various known AD-related biomarkers as they relate to the development of clinical symptoms (rightmost dark green curve). In recent years it has become clear that there is likely a very long protracted prodromal period of disease prior to clinical symptom onset, where A β levels begin to become elevated (red curve), tau pathology is then exacerbated to contribute to neuronal dysfunction (blue), and then these two pathologies combine to begin morphologically-altering brain structure (light green curve) and impairing memory (purple curve). Due to this long prodromal period prior to clinical symptom onset it would be useful for clinical trial design and to raise societal disease awareness to begin thinking of AD not as a disease of just the elderly, but a disease of younger people too, as shown by the red arrows on the plot above. Early therapeutic intervention needs to be a crucial goal for treatments moving forward.

Figure adapted from: Jack, C.R., et al. 2010

forgetful and repeating conversations, losing their belongings and often getting lost driving or otherwise spatially navigating (Buckner, et al. 2004). These initial disease symptoms reflect the increasing dysfunction of the medial temporal lobe memory system. Neuropsychological tests may be used to confirm memory loss and quantify problems of new learning, recall, and recognition memory for verbal and visual material. Additionally, functional MRI studies have demonstrated altered patterns of memory-related activation in the medial temporal lobe of individuals with prodromal AD (Bookheimer, et al. 2006). While the coding of nascent episodic memories is compromised in early AD, older semantic memories that have previously been consolidated in neocortex are relatively preserved.

As A β and tau pathologies become increasingly widespread with disease progression and lead to synaptic failure and neurodegeneration, early episodic memory impairment gives way to progressive deficits in other higher brain functions that result in patients coming into the clinic with memory impairments (Figure 1.3) (Scheff, et al. 2006). The number of affected neuronal circuits increases dramatically to impact frontal, cingulate and parietal cortices such that executive function, language, perception, praxis, and visuospatial abilities become impaired. With advanced disease, damage to higher cortices can also disrupt skilled motor actions (praxis) and compromise long-term semantic memory. Beyond widespread cortical pathology, cholinergic basal forebrain (CBF) neurons along with neurons of the locus coeruleus (LC) and raphe nuclei are vulnerable (Mossner, et al. 2000; Mufson, et al. 2008; Weinshenker 2008). CBF degeneration—particularly in the nucleus basalis of Meynert and the medial septum—contributes to AD symptoms including attention deficits, increased spatial memory

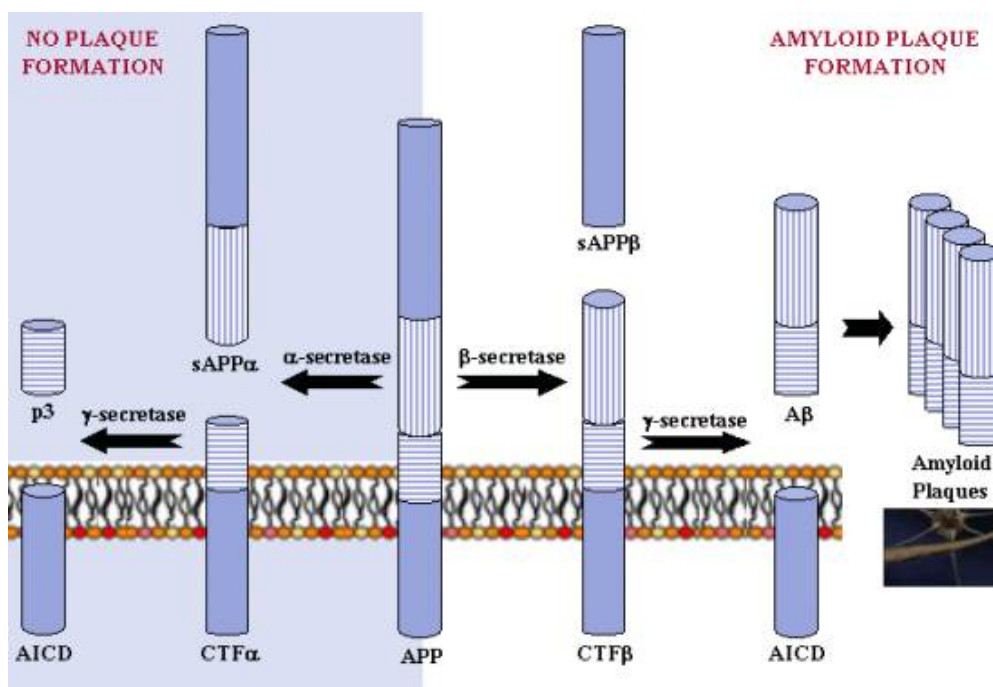


Figure 1.3. Amyloid Cascade Hypothesis of AD: Amyloid Buildup is Responsible for AD.

The processing of Amyloid Precursor Protein (APP) by the enzymatic secretase machinery is depicted here. APP can be processed in one of two ways: the non-amyloidogenic (i.e. non-plaque-forming) direction which is shown in the light blue half of the figure on the left and the amyloidogenic (i.e. plaque-forming) in the white half of the figure on the right. Sequential cleavages by α -secretase and γ -secretase liberate the extracellular sAPP α cleavage product, which is a soluble. However, sequential cleavages by β -secretase and γ -secretase liberate A β peptides (e.g. A β_{40} and A β_{42}), which are prone to self-aggregate into soluble oligomers and insoluble plaques that are thought to contribute to the memory impairments and neuronal cell death characteristic of AD.

Image from: http://www.ebi.ac.uk/interpro/potm/2006_7/Page2.htm

decline and further impairment in the coding of new episodic memories. Loss of serotonergic raphe projections likely contributes to behavioral symptoms such as irritability, apathy, depression, mood lability and aggression. Degeneration of LC neurons translates to noradrenergic transmission loss, which disrupts arousal, vigilance, sleep-wakefulness, working memory and properly interpreting and responding to autonomic stressors. Additionally, LC degeneration can also perturb microglial function yielding neurotoxic inflammation.

From a cellular perspective, A β and tau pathologies are the dominant hallmarks of disease. A β peptides can self-aggregate extracellularly to form larger A β plaques, which become sites of neuroinflammation in more advanced AD. This neuroinflammation likely contributes in large part to the massive neuronal death seen in advanced AD as axons and dendrites die off (McGeer, et al. 1995, 1999, 2003; Rogers, et al. 1996). Tau is a microtubule binding protein whose normal function is to bind to and stabilize microtubules to maintain intracellular transport. In AD tau becomes hyperphosphorylated and dissociates from microtubules to aggregate in the cytoplasm of neurons, forming neurofibrillary tangles. The presence of these tangles is known to contribute to neuronal dysfunction and correlates to the clinical progression of AD. Furthermore, these intracellular tangles profoundly compromise intracellular transport and, ultimately together with A β aggregates, cell viability (Small, et al. 2008). Recent experiments in triple transgenic AD mice (3xTg) that develop both plaque and tangle pathology indicate that A β pathology precedes tau pathology and thus may be the primary driver of disease pathogenesis (Oddo, et al. 2003; Oddo, et al. 2004; Oddo, et al.

2007). In the same studies neither severity nor the onset of amyloid pathology was obtained by genetically altering tau levels.

While particular cell populations and areas are impacted by cell death and A β and tau deposition, it is important to realize that these particular areas act as part of networks. That is to say, the majority of cognitive dysfunction that accompanies AD is likely not due to the loss of one neurotransmitter or neuromodulatory system, but rather, to how the loss of these various components impacts network connectivity between limbic and neocortical systems as a whole. For example, A β deposition appears disproportionate in members of the default mode network, which is involved in maintaining a default brain state of “wakeful rest” when the brain is not engaged in goal-directed behavior (Greicius, et al. 2004, 2009; Sperling, et al. 2010). The significance of this for AD is that this network has the highest baseline activity at rest and A β levels are regulated by neuronal activity (Kamenetz, et al. 2003; Cirrito, et al 2005; Dolev, et al. 2013). Since the human brains spends a lot of time at rest not engaged in goal-directed behavior, this could help explain the relatively specific accumulation of A β pathology in regions that comprise the default mode network.

APP Processing and the Amyloid Cascade Hypothesis

APP is an integral membrane protein of 695-700 amino acids expressed throughout the brain and periphery (Kang, et al. 1987; Tanzi, et al. 1987). There are three major isoforms of APP that exist: APP⁶⁹⁵, APP⁷⁵¹, and APP⁷⁷⁰, however APP⁶⁹⁵ is the predominant isoform expressed in the human brain. The normal function of APP has been the subject of considerable debate and is still not completely known. Roles for APP

have been implicated in trophic support, neural stem cell proliferation and differentiation, as well as effects on neurite outgrowth, synaptogenesis and synaptic plasticity (Dawkins and Small 2014). APP knockout mice are viable and can reproduce, however, it is worth mentioning that functional redundancy also exists with other APP family members APLP1 and APLP2. In this vein, APP/APLP2 knockout mice die shortly after birth (Zheng, et al. 1995; von Koch, et al. 1997).

What is abundantly clear, however, is that APP is proteolytically processed by the secretase enzymes (Figure 1.2) to yield the A β peptides that end up triggering synaptic dysfunction and aggregating into plaques in AD, particularly A β ₄₂ (Gandy, et al. 1993; Selkoe 1994; Selkoe and Yamazaki, 1996; Selkoe 2001; Suzuki and Nakaya 2008; Thinakaran and Koo 2008). APP is processed in essentially one of two directions. These directions are commonly referred to as “amyloidogenic” or “non-amyloidogenic.” That is to say, one way of processing produces plaques, while the other does not.

Amyloidogenic processing of APP arises from the sequential cleavage of APP by beta and gamma secretase enzymes in order to liberating the soluble APPs β ectodomain of APP and A β peptides. Since the cleavage of APP by gamma secretase is relatively non-specific, A β peptides of varying lengths are formed, but the two most predominant species are A β ₄₀ and A β ₄₂ (Steiner, et al. 2008).

On the other hand, non-amyloidogenic APP cleavage precludes the formation of A β peptides since APP is processed by different secretase machinery with different APP cleavage sites (Esch, et al. 1990; Sisodia, et al. 1990, 1992). Specifically, APP is cleaved sequentially by alpha secretase and gamma secretase in order to liberate the soluble APPs α domain. Importantly, alpha secretase cleavage occurs in the middle of the A β

peptide sequence, which is responsible for precluding the formation of the A β peptides observed in amyloidogenic APP processing. It is worth noting that gamma secretase is actually a complex of at least four different proteins (presenilin, APH-1, nicastric, and PEN-2) that works to catalyze the cleavage of many different type I transmembrane proteins including Notch, p75^{NTR}, and EGFR. The fact that gamma secretase cleaves these other critically important proteins has profound consequences for inhibitors targeting gamma secretase that will be discussed later. During the lifespan of the APP protein, it is trafficked to many subcellular compartments such as the Golgi, ER, and lipid rafts where it has the opportunity to interact with and undergo cleavage by secretase enzymes at any point (Thinakaran, et al. 1996; Wild-Bode, et al. 1997; Xu, et al. 1997; Skovronsky, et al. 2000). However, more recent work points to endosomal compartments and the trans-Golgi network as crucial sites of APP cleavage (Cataldo, et al. 1997; Lah and Levey 2000; Cataldo, et al. 2004).

A β -Induction of Synaptic Dysfunction

In recent years, an exciting literature to emerge has focused on the role soluble A β and the induction of synaptic dysfunction. While plaques were identified first and contribute to detrimental aspects of disease pathology such as neuroinflammation once they are present, it has become evident that there is cognitive dysfunction that precedes large buildup of A β plaque loads and this is increasingly attributed to the action of soluble A β peptides (Sperling, et al. 2009). In particular studies with transgenic AD mice bearing familial human AD mutations display significant deficits in synaptic transmission and hippocampal synaptic plasticity well in advance of detectable insoluble A β pathology

(Chapman, et al. 1999; Fitzjohn, et al. 2001). Specifically, intense focus has been placed on soluble A β oligomers as a causal source of synaptic dysfunction associated with AD (Walsh, et al. 2002; Bitan, et al. 2003; Takahashi, et al. 2004; Glabe 2005; Walsh, et al. 2005; Walsh, et al. 2005; Haas and Selkoe 2007). Microinjecting A β oligomers in the absence of any other amyloid pathology is sufficient to potently inhibit hippocampal LTP in rats (Li, et al. 2009). These animal studies dovetail nicely with a growing literature that memory deficits accompanying MCI and AD patients correlate much better with soluble A β levels than with plaque numbers (Kuo et al., 1996; Lue et al., 1999; McLean et al., 1999; Naslund et al., 2000). Furthermore, in human patients, synaptic loss is significantly correlated with soluble A β levels (Lue, et al. 1999).

Cholinergic Neurotransmission and its Role in Alzheimer's Disease

Neuroanatomy of the Cholinergic System

Acetylcholine (ACh) was the first neurotransmitter to be described and is intimately involved in many aspects of peripheral and central neurotransmission. The synthesis of ACh is carried out by choline acetyltransferase (ChAT) from the precursors acetyl-CoA and choline, whereas synaptic clearance of ACh is via synaptic degradation mediated by acetylcholinesterase (AChE) (Loewi and Navratil 1926; Nachmansohn and Machado 1943; Nachmansohn and John 1945). ACh is packaged into vesicles by the vesicular acetylcholine transporter (VACHT) for release from presynaptic nerve terminals and following degradation, choline is taken back up into the presynaptic nerve terminal by the high-affinity choline transporter (CHT).

The cholinergic system of the mammalian CNS is comprised of several major groups of nuclei that are the major source of ACh to the entire brain (Figure 1.4). These groups are the brainstem pontine nuclei, the cholinergic interneurons of the striatum, and the nuclei of the cholinergic basal forebrain (CBF), including the nucleus basalis of Meynert, as well as the medial septum, diagonal band of Broca and the lateral septum (Mufson and Kordower 2001). Specifically, the nucleus basalis is responsible for cholinergic innervation of the neocortex, whereas the medial septum/diagonal band of Broca is responsible for the cholinergic innervation to the hippocampus. Thus, it comes as no surprise that the nucleus basalis and medial septum play key roles in shaping memory processes mediated by the neocortex and hippocampus, respectively (Mizumori, et al. 1990). The neurons of the CBF are disproportionately impacted in advanced AD, with heavy (~80%) neuronal loss observed in these nuclei (Whitehouse, Price et al. 1982; Mufson, Bothwell et al. 1989; Mufson and Kordower 2001; Mufson, et al. 2002). Also, cholinergic enzyme activity is known to decline with aging, compromising the ability to maintain proper modulation of neocortical and hippocampal circuitry (Davies and Maloney 1976; Perry, et al. 1977; Perry, et al. 1978). The loss of ACh synthesis capacity in tandem with the dysfunction in cholinergic signaling nuclei that accompanies disease has led to the cholinergic hypothesis of AD, which posits that these cholinergic deficiencies are responsible for AD pathology.

Cholinergic neurons of the CBF can be identified by the molecular markers ChAT, CHT, p75^{NTR}, and TrkA. The p75^{NTR} and TrkA receptors are significant because these receptors bind nerve growth factor (NGF), which is a potent neurotrophin responsible for

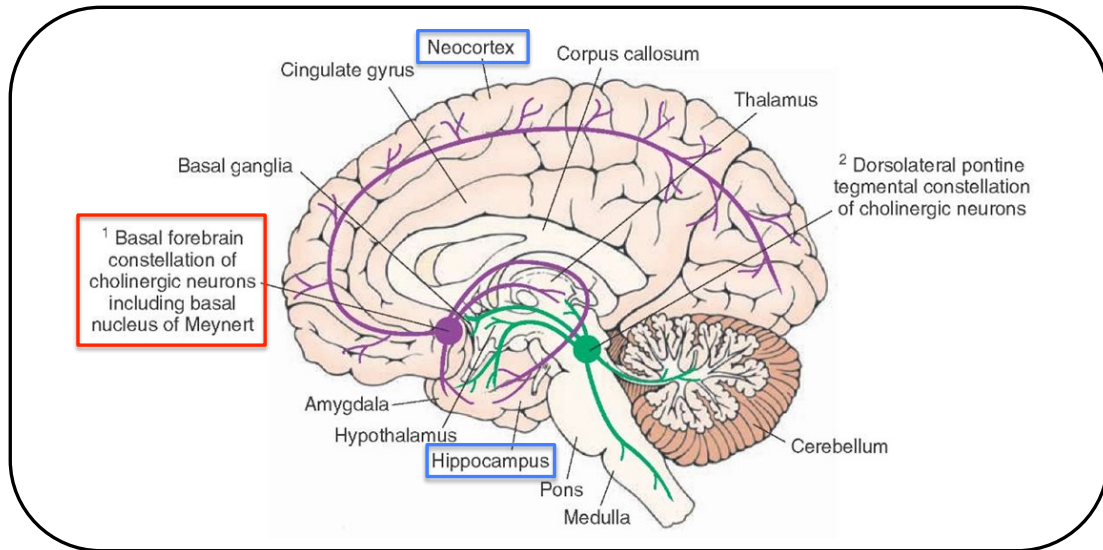


Figure 1.4. Cholinergic Hypothesis of AD: Decreased Acetylcholine is Responsible for AD.

The cholinergic neuromodulatory system is comprised of the brainstem pontine nuclei (green projections, above) as well as the nuclei of the cholinergic basal forebrain (CBF), including the nucleus basalis of Meynert, as well as the medial and lateral septum (purple projections, above). The nucleus basalis is responsible for cholinergic innervation of the neocortex, whereas the medial septum/diagonal band of Broca is responsible for the cholinergic innervation to the hippocampus. The nuclei of the CBF feature particularly prominently in AD since heavy (~80%) neuronal loss accompanies advanced disease in these nuclei. The decline in cholinergic enzyme activity with aging and the dysfunction in these cholinergic signaling centers with disease has led to the cholinergic hypothesis of AD, which posits that these cholinergic deficiencies are responsible for AD pathology.

Image adapted from: <http://what-when-how.com/neuroscience/neurotransmitters-the-neuron-part-2/>

the trophic support of cholinergic neurons. Therapeutic strategies aimed at boosting neurotrophin signaling will be discussed later.

Muscarinic Acetylcholine Receptor Expression and Function

The muscarinic acetylcholine receptors (mAChRs) are family A G-protein-coupled receptors (GPCRs), comprised of 5 different subtypes, M_1 - M_5 . $M_{1,3,5}$ couple through $G\alpha_q$ in order to increase intracellular calcium levels, thereby mediating excitatory neuromodulatory actions of ACh (Figure 1.5A). These receptors activate phospholipase C (PLC) in order to cause release of calcium from intracellular stores in the endoplasmic reticulum via protein kinase C (PKC) (Wess, et al. 1996, 2007). On the other hand, $M_{2,4}$ couple through $G\alpha_{i/o}$ to block adenylate cyclase (AC) activity, which causes a decrease in cAMP levels and thereby mediates the inhibitory neuromodulatory actions of ACh (Figure 1.5A). Within the CNS it is M_1 and M_4 receptors that are found most on principal cells postsynaptically and presynaptically, respectively.

Regarding mAChR function in the hippocampus specifically, early work by Auerbach and Segal who first characterized muscarinic LTP (LTP_m) in the hippocampus using carbachol, showed a concentration-dependent effect of muscarinic receptors in triggering LTP (Auerbach and Segal 1994, 1996; Segal and Auerbach 1997). The finding that muscarinic receptors can modulate LTP is significant since LTP is widely held to be a cellular correlate of learning and memory (Bliss and Collingridge, 1993). An abundance of work has arisen to demonstrate that mAChR activation is capable of enhancing LTP of excitatory synaptic responses in the hippocampus (Blitzer et al., 1990; Burgard and Sarvey 1990; Markram and Segal 1990; Abe, et al. 1994; Auerbach and

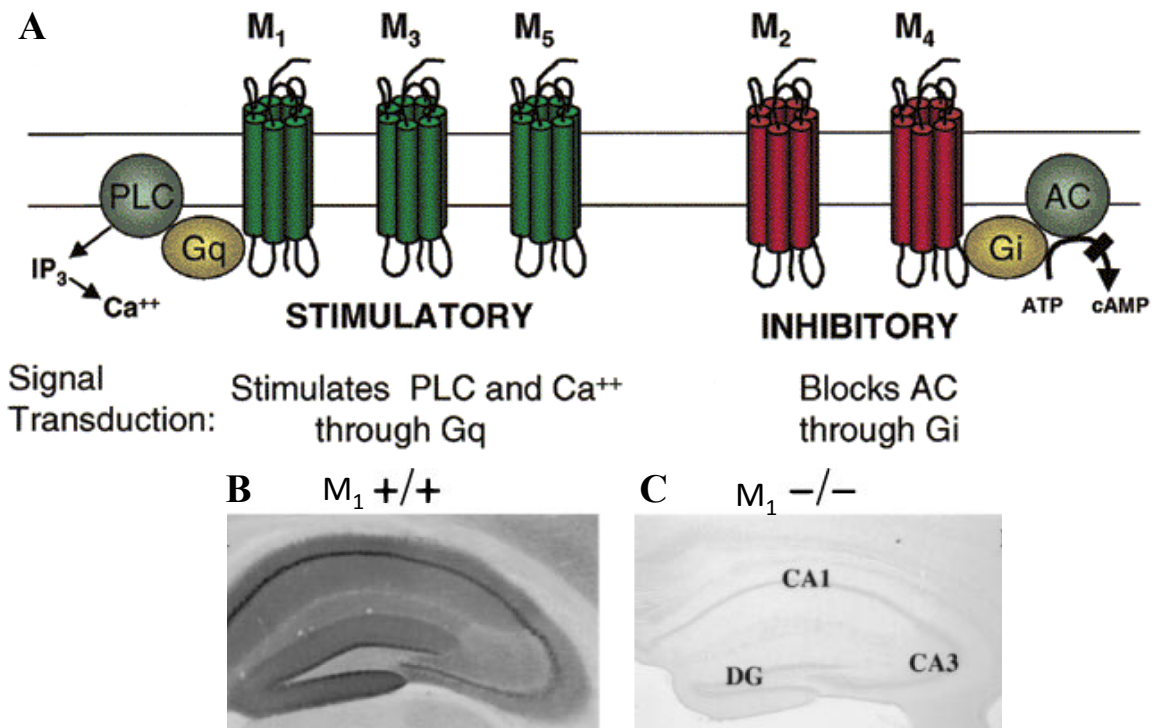


Figure 1.5. Muscarinic Receptor Function and Expression in the CNS.

A) The mAChRs are family A GPCRS, comprised of 5 subtypes, M₁-M₅. M_{1,3,5} couple through G_q in order to increase intracellular calcium levels, thereby mediating excitatory neuromodulatory actions of ACh. On the other hand, M_{2,4} couple through G_i to block adenylate cyclase activity and thereby mediate the inhibitory neuromodulatory actions of ACh. While M₂ receptors are the most abundant in the CNS, it is M₁ and M₄ receptors that are found most on principal cells postsynaptically and presynaptically, respectively.

B) M₁ receptors visualized by immunohistochemistry are particularly densely expressed in memory circuitry, such as in the hippocampus and an extensive literature demonstrates their importance in supporting memory, influencing hippocampal synaptic plasticity, and potential therapeutic role in diseases of memory (e.g. Alzheimer's Disease). C) Sections from an M₁ knockout mouse showing a stark contrast from the dense M₁ expression in B.

Image adapted from: Hamilton, S.E., et al. 1997.

Segal 1996; Shinoe, et al. 2005). More recent work has extended this observation to include LTD, as higher concentrations of carbachol have been found to trigger a sustained atropine-sensitive LTD at CA3-CA1 synapses that appeared to arise via a post-synaptic mechanism, termed muscarinic LTD (mLTD) (Scheiderer, et al. 2006, 2008).

The M₁ receptor is expressed in many regions but is found at the highest levels in the hippocampus, amygdala, neocortex, and striatum (Levey, et al. 1991, 1994, 1995; Levey 1996; Rouse and Levey 1996). In the hippocampus the M₁ receptor is expressed mainly postsynaptically throughout the stratum oriens and radiatum, as well as in the granule cells and molecular layer of the dentate gyrus (Figure 1.5B and 1.5C) (Levey, et al. 1995; Levey 1996; Rouse and Levey 1996). In the neocortex M₁ is heavily localized to layers II/III and VI (Levey, et al. 1991). Analysis of M₁ knockout mice has documented key roles for the M₁ mAChR in certain aspects of memory such as consolidation and working memory (Anagnostaras, et al. 2003; Wess, et al. 2007). The fact that M₁ signaling can potentiate NMDAR signaling in hippocampal pyramidal cells is well-established and plays a key role in the ability of M₁ to contribute so importantly to memory consolidation (Marino, et al. 1998; Quinn, et al. 2005; Lebois, et al. 2009). Additionally, further evidence shows that M₁ contributes to hippocampal synaptic plasticity, as M₁ knockout animals display deficient hippocampal LTP induction (Wess 1996; Agnostaras, et al. 2003; Wess, et al. 2007; Giessel and Sabatini 2010). The story is likely not as simple as deficient LTP though, as newer work has clarified a role for M₁ in mediating the induction of LTD at hippocampal CA3-CA1 synapses. Depending upon the degree of M₁ activation, M₁ can act either to potentiate LTP at lower levels of M₁ activation or induce LTD at higher levels of M₁ activation (Digby, et al. 2012). In

addition to effects on LTP and LTD, M₁ can also robustly activate ERK 1/2 in the brain, a key mediator of synaptic plasticity (Berkeley, et al. 2001; Hamilton and Nathanson 2001). Both the expression profile of M₁ in the hippocampus and functional consequences of M₁ activation have important implications for AD therapy, but this will be addressed in greater detail in the following sections of this thesis.

Apart from the extensive effects on hippocampal transmission, M₁ is known to play a critical role in regulating the excitability of layer II/III and V mPFC pyramidal cells. Taking this excitatory role into account with the previously described actions of M₁ on NMDAR receptor signaling, a potential therapeutic avenue of relief of cognitive symptoms in schizophrenia and psychosis via M₁ begins to emerge, as NMDARs are thought to play a central role in schizophrenia and psychosis (Coyle et al., 2002; Marino and Conn, 2002; Tsai and Coyle, 2002; Conn, et al. 2009; Bridges, et al. 2010; Jones, et al. 2011). In the striatum M₁ is found localized predominately in dopamine-2-(D₂) expressing medium spiny neurons (MSNs). Interestingly, M₁ has been shown to be involved in reward and reinforcement behaviors as well, as M₁ activation attenuates the ability of animals to discriminate cocaine from saline (Thomsen, et al. 2011). In the periphery M₁ is found at very low levels, but it is possible that activation of this receptor could contribute to syncope in clinical trials with muscarinic activators (Bodick, et al. 1997a; Bodick, et al. 1997b).

M₂ is the most abundant mAChR subtype found in the CNS. The expression of M₂ is mainly confined to interneurons and serves as a presynaptic autoreceptor in layers IV and V/VI in neocortex and other regions of the forebrains such as the hippocampus where it is found most in the CA3 subfield (Levey, et al. 1991; Levey, et al. 1995; Rouse

and Levey 1996). M_2 immunoreactivity is largely absent from pyramidal cells and granule cells of the hippocampus, but is robustly localized to interneurons (Levey, et al. 1995). M_2 functions as a presynaptic autoreceptor in the hippocampus and neocortex whose function is to regulate the synaptic release of ACh. M_2 is found at lower levels in the periphery, but is found at appreciable levels in the cardiac epithelium where it could give rise to bradycardia or other adverse peripheral side effects if activated (Grenlee, et al. 2001). Additionally, roles in locomotor activity as well as pain response have been documented for M_2 (Gomez, et al. 1999).

M_3 accounts for a smaller percentage of mAChRs (~5-10%) and is found mainly postsynaptically (Levey, et al. 1994). While only accounting for a small fraction of mAChRs, M_3 displays a wide-ranging expression profile including the hippocampus, amygdala, cortex, thalamus, striatum, and pons (Levey, et al. 1991, 1994, 1995; Rouse and Levey 1996). Despite this wide-ranging expression profile, relatively little is known about M_3 function in the CNS. In addition to the CNS, M_3 is the most abundant mAChR in the periphery and is thought to be the major mAChR that underlies off-target side effects of muscarinic activators (Grenlee, et al. 2001; Conn, et al. 2009). Work in M_3 knockout mice has shown roles for M_3 in salivation and vasodilation, as well as smooth muscle contraction in the urinary bladder, stomach and gut (Matsui, et al. 2000; Grenlee, et al. 2001; Yamada, et al. 2001; Duttaroy, et al. 2004; Khurana, et al. 2004).

M_4 is expressed throughout the CNS, but is found most heavily expressed in the hippocampus and striatum (Levey, et al. 1991, 1994, 1995; Rouse and Levey 1996). In both of these regions M_4 receptors are located primarily presynaptically where it acts as the major presynaptic mAChR autoreceptor to suppress ACh release. However, in the

hippocampus, striatum, and neocortex M₄ receptors can also act as postsynaptic modulatory receptors (Levey et al. 1991; Ziying and Creese 1997). In the striatum M₄ is expressed on medium spiny neurons and is known to play important roles in the modulation of dopaminergic signaling in the mesolimbic and nigrostriatal dopamine pathways. M₄ has also been shown to be involved in reward and reinforcement behaviors as well, as M₄ activation attenuates the ability of animals to discriminate cocaine from saline (Thomsen, et al. 2011). Due to its intimate involvement in modulating dopaminergic signaling in the basal ganglia, M₄ has long been a candidate for therapy in schizophrenia and psychosis, where dopamine hyperfunction in the basal ganglia is believed to strongly contribute to the cognitive deficits that schizophrenics display (Conn, et al. 2009).

M₅ is by far the weakest of the mAChRs in terms of expression in the CNS (Levey, et al. 1991, 1994, 1995). However, M₅ has been shown to be enriched in the cerebrovasculature where it plays a role in the dilation of blood vessels, modulates amyloid pathology, and is involved in reward and reinforcement behaviors in response to drugs of abuse (Yamada, et al. 2001b; Basile, et al. 2002; Thomsen, et al. 2011). Interestingly, M₅ knockout animals appear to exhibit a marked decrease in conditioned place preference to cocaine and reduced acute self-administration of cocaine (Fink-Jensen, et al. 2003; Thomsen, et al. 2011). In the vein of reward and reinforcement regulation, M₅ is also found to be expressed at low levels in the basal ganglia where it acts to regulate dopamine release. More recent work indicates that expression location in the basal ganglia can dictate the effect of M₅ activation, as activation of M₅ in the substantia

nigra increases neuronal firing, whereas activation of M₅ in the striatum decrease dopamine release (Foster, et al. 2014).

Alzheimer's Disease Treatment

Currently Approved Therapeutics and Limitations

At present, currently available FDA-approved therapies for AD are extremely limited. Our present understanding of the pathophysiology of AD has yielded mainly pro-cholinergic treatment strategies including acetylcholinesterase inhibitors (AChEIs) such as donepezil, physostigmine, and rivastigmine (Figure 1.6). The rationale for the development of AChEIs derives from the observation that enzymatic activity responsible for ACh synthesis declines with aging and cholinergic circuits in the brain become selectively vulnerable in advanced AD. AChEIs, by definition, are extremely non-selective in their action. They act by inhibiting acetylcholinesterase, the enzyme responsible for synaptic degradation of ACh, and thus activate all subtypes of both muscarinic and nicotinic receptors throughout the body. Therefore, AChEIs are known to trigger a variety of adverse side effects, including gastrointestinal side effects, extrapyramidal movement disorders, urination, defecation, salivation, lacrimation, cardiorespiratory effects, and sleep disturbances (Thompson, et al. 2004). Furthermore, since the muscarinic and nicotinic receptors are comprised of many different family members, some of whom mediate functionally-opposing actions, it comes as no surprise that the efficacy of AChEIs is quite limited. Despite the non-selective mechanism of action for AChEIs, they do confer a small symptomatic benefit in moderate-to-severe AD,

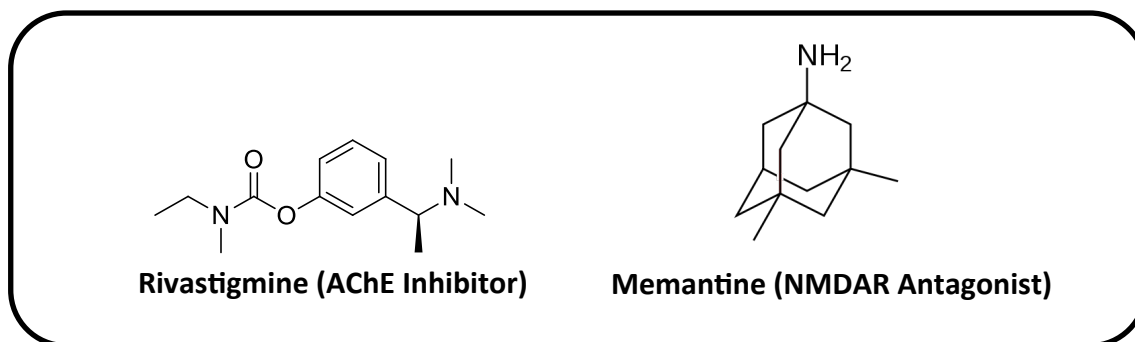


Figure 1.6. Current Therapy for AD Patients

Currently, FDA-approved therapeutics for AD are extremely limited to two classes of compounds: acetylcholinesterase inhibitors (AChEIs) such as rivastigmine and NMDAR antagonists, such as memantine. Both classes of compounds are very nonselective in their mechanisms of action and in the case of compounds such as memantine, the mechanism of action leading to clinical efficacy is not entirely apparent. The nonselectivity of the AChEIs, in particular, leads to the activation of all isoforms of muscarinic and nicotinic cholinergic receptors, some of which are excitatory and the others are inhibitory. Thus, the net effect of the compounds are very minimal since competing functional cascades are activated. The clinical utility of these compounds track with this nonselectivity, as the efficacy of both AChEIs and NMDAR is both very mild and short-lived. Aside from their mild and temporary efficacy, their nonselective pharmacological profile means that the potential for peripheral side effects due to off-target ACh or NMDAR activation is also much higher.

but do nothing to delay or alter the timecourse of the decline associated with AD (Mangialasche, et al. 2010). Other work indicates that AChEIs may be able to somewhat slow the progression from MCI to AD in *APOEε4* patients (Doody, et al. 2001). The modest symptomatic improvement obtained with AChEIs in the face of nonselectivity does highlight the importance of developing selective cholinergic activators, as there is much work described in the following section that indicates certain cholinergic subtypes are the therapeutically-beneficial ones (Conn, et al. 2009).

The second type of drug approved for use in AD is an uncompetitive NMDAR antagonist, memantine (Figure 1.6) (Reisberg, et al. 2003; Thomas, et al. 2009). How exactly NMDAR blockers such as memantine work *in vivo* to yield ultimate behavioral efficacy in AD patients is a matter of some debate, however, soluble A β oligomers have been shown to bind to NMDARs in order to mediate some of their detrimental effects on memory that occur with disease pathology. Thus, a beneficial role for NMDAR antagonists could be to at least temporarily counteract the impact of A β oligomers on memory circuits (Danysz and Parsons 2012). Secondly, NMDAR blockers could work to stem any excitotoxicity that accompanies disease in order to help prevent neuronal death (Danysz and Parsons 2012). Three randomized, double-blind, placebo-controlled trials have documented the safety and efficacy of memantine in moderate to severe AD, however the degree of efficacy obtained remains small and short-lived. As is the case for AChEIs, memantine offers acute symptomatic improvement without acting to halt the timecourse of AD. Thus, as disease pathology worsens, the beneficial effects of these drugs wear off.

The limited arsenal of currently approved therapeutics available to AD patients gives cause for alarm, as all are modestly acting and very short-lived. There is currently no treatment available to significantly delay or halt the development of AD pathology. Several promising new strategies will be discussed in the next section, but the need for a safe and effective therapy has never been more urgent.

Therapeutic Strategies Under Investigation

The pathophysiology of AD allows for several putative therapeutic avenues depending on disease stage (Figure 1.7) (Mangialasche, et al. 2010). Circuit abnormalities early in disease are only beginning to be understood, but it is clear that accumulation of soluble A β oligomers is capable of impairing hippocampal transmission in animals. Anatomically, the first neuronal connections that tend to become compromised are entorhinal afferents into the hippocampus which are crucial for maintaining the integrity whereby the hippocampus forms episodic memories. Furthermore, A β accumulation is associated with neuroinflammation in more advanced AD (McGeer and McGeer 1995, 1999, 2003). Once neuroinflammatory processes take hold, this is believed to contribute to neuronal death associated with AD. Apart from A β , cholinergic neurons of the CBF appear to be selectively vulnerable in late disease. Given the crucial role of cholinergic neurons in modulating memory circuitry, this is another ripe area for therapeutic intervention.

With regard to the development of therapeutics for AD, the focus has largely been on three main areas: pro-cholinergic strategies, anti-amyloid approaches, and other emerging approaches as our understanding regarding the pathophysiology of AD has

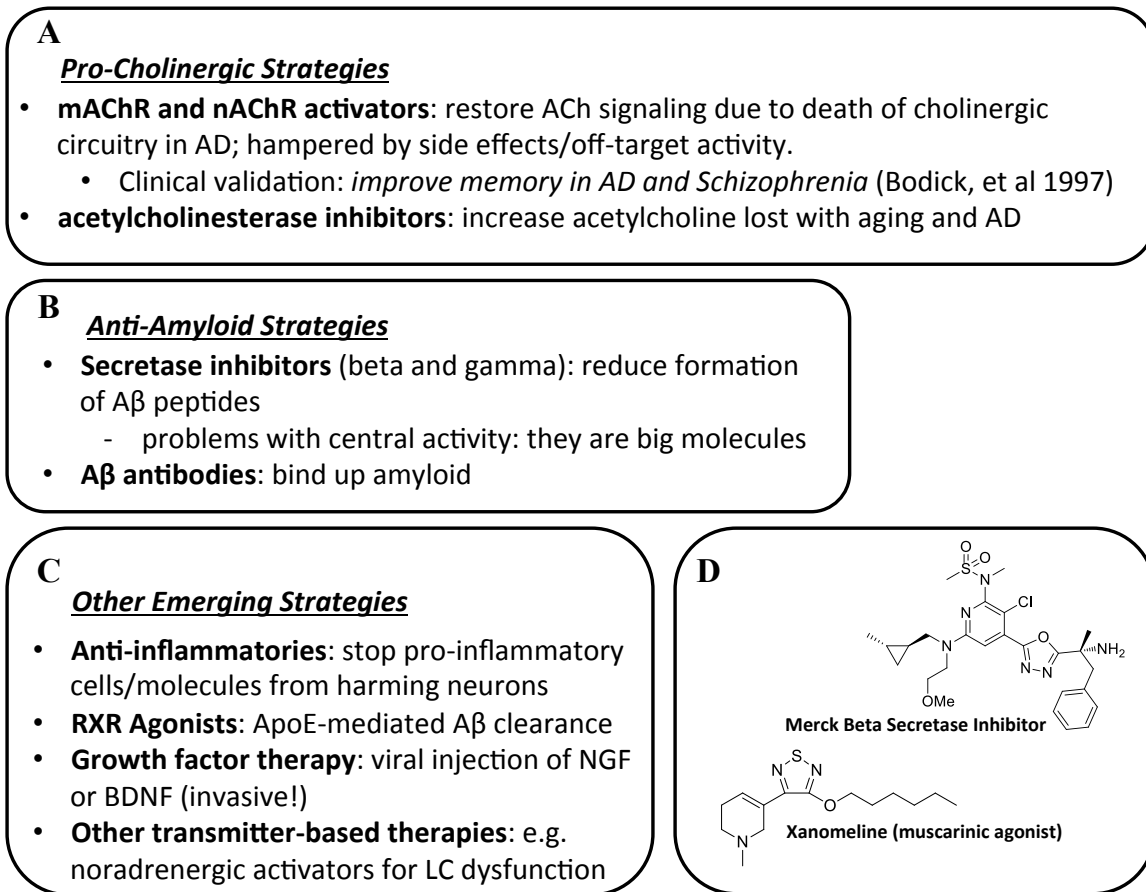


Figure 1.7. Therapeutic Strategies Under Investigation for AD Patients

Above is a non-exhaustive list that shows a mere snapshot of therapies being investigated for AD. A) Pro-cholinergic strategies include activating muscarinic receptors and AChEIs to boost deficient cholinergic signaling that accompanies aging and AD. B) Anti-amyloid strategies include inhibiting secretase machinery to prevent A β formation and antibodies to sequester A β . C) Other emerging strategies are developing novel anti-inflammatories to curb neuroinflammation that accompanies AD, RXR and nuclear receptor activators in attempt to trigger A β clearance mechanisms (e.g. via ApoE), viral delivery of neurotrophic factors to restore lost neuronal innervation to memory circuitry, and other transmitter-based approaches. D) Structures of prototypical beta secretase inhibitor and the M₁/M₄ muscarinic receptor agonist, Xanomeline.

increased. Anti-A β strategies have largely derived from our understanding of the deleterious roles that A β plays in AD and the amyloid cascade hypothesis (Karran, et al. 2011). Much of the work in anti-A β therapeutics has centered on small molecule inhibitors of beta and gamma secretase. As previously described, beta and gamma secretase are responsible for the proteolytic cleavage of APP to yield A β peptides. Beta secretase (BACE) inhibitors have traditionally had problems with size, poor central penetrance, and oral bioavailability, but these issues have been solved with newer compounds such as MK-8931, which is brain-penetrant (Yan and Vassar 2014). Furthermore, MK-8931 appears safe with no adverse events reported in a Phase I trial. Additionally, this compound can lower A $\beta_{40/42}$ levels in the CSF of patients, but efficacy remains to be seen in larger clinical trials. Other examples of newer generation BACE inhibitors include LY2886721 and E2609. While safety was demonstrated in phase I, trials for LY2886721 were halted in phase II due to drug-induced liver toxicity. E2609 represents one of the most promising small molecule BACE inhibitors to date, as it exerts very robust effects on decreasing CSF A β concentrations (up to 85%) in phase I. Efficacy remains to be seen in larger clinical patient populations, but is eagerly awaited. A problematic issue with developing BACE inhibitors is that BACE has been shown to be important for axon guidance and neurogenesis. Thus, BACE inhibitors may trigger axon mistargeting and deficits in neurogenesis.

Gamma secretase inhibition derives from the same rationale as that for BACE inhibitors of the desire to lower CNS A β levels. Like BACE inhibitors, gamma-secretase inhibitors have been shown to lower A β levels in laboratory animals. However, secretase inhibition has failed to translate in the clinic to an improvement in disease outcomes. At

least seven gamma secretase inhibitors have been evaluated in clinical trials, including semagacestat (LY-450139), MK-0752, E-2012, BMS-708163, PF-3084014, begacestat (GSI-953), and NIC5-15. In fact, in the most high-profile phase III trial to-date, Eli Lilly's semagacestat (LY450139) actually showed worse cognitive outcome than in the placebo group (Doody, et al. 2013)! Semagacestat also had no effect on CSF A β levels in AD patients. Like BACE, gamma secretase cleaves other proteins besides APP and one such target of gamma secretase is Notch, a very important developmental signaling pathway also involved in synaptic plasticity (De Strooper, et al. 1999). Other efforts in recent years have focused on gamma-secretase modulators (GSMs), which do not directly and completely inhibit gamma-secretase in an effort to prevent Notch cleavage (Dimitrov, et al. 2013). While these efforts have appeared promising in animals and several companies are developing GSMs, their efficacy in the clinic remains to be determined.

An exciting new class of anti-A β therapeutics has emerged designed to promote A β clearance in a novel way. Nuclear receptor activators, in particular RXR activators such as bexarotene, have been developed that stimulate the production of apoE in attempt to clear A β (Cramer, et al. 2012; Bomben, et al. 2014). Since apoE is a transport protein which binds A β , bexarotene is able to rapidly clear A β from the CNS of animals, reversing pathological deficits in mouse models of AD. More recent work has also shown that bexarotene treatment corresponds to a reduction in network excitability. RXR activation is still very much preclinical, but represents a promising new approach to get rid of A β that sidesteps the off-target and adverse proteolytic cleavages associated with secretase inactivators.

The last anti-A β strategy of note has been investigation of monoclonal antibodies in an effort to bind up A β in the CNS and thereby prevent it from triggering any pathological processes. Again, while this strategy showed promise in animals to lower A β , it failed in the clinic to slow cognitive or functional decline in AD patients. The findings from two high-profile phase III trials were recently announced, with Eli Lilly's solanezumab and Janssen/Pfizer's bapineuzumab failing to curb decline in AD patients (Salloway, et al. 2009, 2014; Doody, et al. 2014). In general, the anti-A β approach to treating AD needs to be called into question and undertaken with caution as to how A β is being lowered and to what degree, as recent studies by Puzzo and Arancio demonstrate that low concentrations of A β (in particular, A β_{42}) function normally in the CNS as vital signaling molecules that are actually vitally important for allowing synaptic plasticity and memory to occur (Puzzo and Arancio 2013). Finally, due to the realization that A β begins accumulating 10-20 years prior to symptom-onset in AD patients, one can make a strong argument that all anti-A β clinical trials have failed to-date because these trials have been more advanced clinical AD patients whose brains were already damaged beyond the point of repair. Indeed, these anti-A β therapeutic mechanisms will need to be revisited and vetted in preventative trials composed of prodromal AD patients before the anti-A β approach can be conclusively ruled out.

Apart from anti-A β strategies, other strategies under investigation for AD therapy include drugs that exert anti-inflammatory actions, drugs which stimulate A β clearance, and the employment of neurotrophic strategies. Neuroinflammation in AD is among the hottest current research areas of therapeutic interest in AD, as it has become clear that inflammation plays a large part in the damage dealt out to kill neurons over the course of

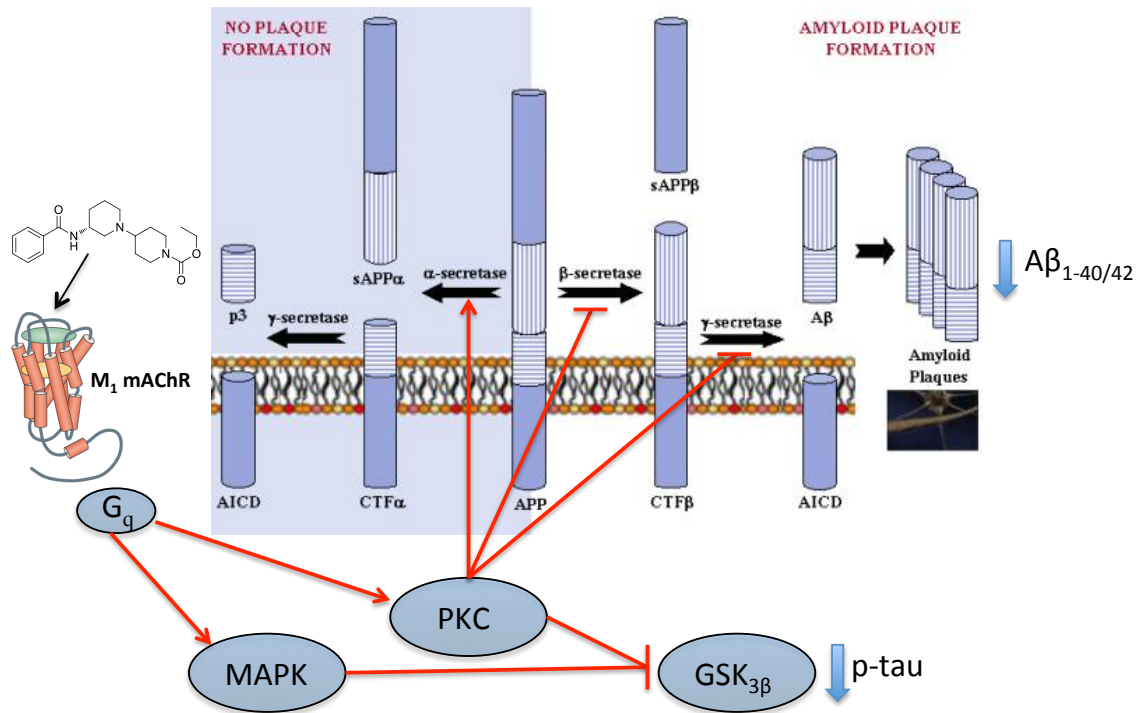


Figure 1.8. M₁ Muscarinic Receptors Bias APP Toward Non-Amyloidogenic Processing.

M₁ muscarinic receptors play a thoroughly documented and critical role in the processing of amyloid precursor protein (APP). M₁ activation (here, by the M₁ agonist VU572) leads to downstream effects on PKC to influence the cellular secretase machinery responsible for the proteolytic processing of APP. Namely, M₁ activation leads to a suppression in β-secretase and γ-secretase activity and concomitant promotion of α-secretase activity. This constellation of cellular effects results shifting of APP processing away from an amyloidogenic direction (e.g. decreased A β ₄₀ and A β ₄₂ formation) and towards a nonamyloidogenic direction (e.g. increased sAPP α formation).

Image adapted from: http://www.ebi.ac.uk/interpro/potm/2006_7/Page2.htm

the disease (McGeer and McGeer 1995, 1999, 2003; Morales, et al. 2014). The research in this area was largely sparked by the observation that long-term exposure to anti-inflammatories has been associated with a decreased risk in such individuals for developing AD (Akiyama, et al. 2000; Szekely, et al. 2004). Both natural products such as curcumin and small molecule strategies such as NSAIDs are under investigation for a beneficial role in suppressing the inflammation that is found to occur with AD progression. With all the recent activity in the area, understanding how neuroinflammation relates to AD pathology and how it might be leveraged therapeutically are still very much unclear.

Aside from anti-inflammatories, strategies designed to boost neurotrophic signaling arise in part from the observation that cholinergic neurons are selectively vulnerable in AD. Studies utilizing injection of viral vectors to drive NGF and BDNF in the entorhinal cortex of AD patients have demonstrated encouraging findings insofar as restoration of entorhinal cortical-hippocampal connections, but whether or not this translate to efficacy at the level of memory improvement in clinical patients remains to be seen (Nagahara, et al. 2009, 2013). The major caveat to the widespread utilization of this approach to AD treatment is the highly-invasive nature of the viral injections. Notably, work in animals looking at BDNF infusion has shown that BDNF can prevent lesion-induced death of entorhinal cortical neurons and act to reverse neuronal atrophy and memory impairments. In order to sidestep the highly-invasive viral injections, several efforts are currently underway to develop small molecule activators of TrkB receptors in order to mimic the therapeutic actions of BDNF, but all of these efforts remain preclinical (Castello, et al. 2014).

Arguably one of the largest areas for AD therapeutic development is in the area of pro-cholinergic therapeutics. Acetylcholine acts on two classes of receptors to mediate its actions: muscarinic receptors (mAChRs) and nicotinic receptors (nAChRs). Both types are found in the CNS and both types are found in key regions impacted by AD pathology, such as the hippocampus and neocortex. The nAChRs are ligand-gated ion channels responsible for the fast ionotropic actions of ACh, whereas the mAChRs are GPCRs responsible for mediating the slower, metabotropic actions of ACh (Haydar and Dunlop 2010). Among the nAChRs, the most abundant are the α_7 and $\alpha_4\beta_2$ and drugs targeting these receptors have been shown to have cognition-enhancing effects (Haydar and Dunlop 2010). The $\alpha_4\beta_2$ agonist Ispronicline (AZD-3480), for instance, has shown positive effects on cognition in healthy individuals, but failed to show improvement in the clinic for AD patients. A very similar story has been obtained with α_7 activators such as EVP-6124, where preclinical efficacy fails to translate to the clinic.

Pro-muscarinic strategies under therapeutic development for AD

Therapeutics targeting the mAChRs are uniquely poised to provide potentially disease-modifying benefit to AD patients. Work by Perry and colleagues has shown that chronic use of anticholinergic drugs (e.g. muscarinic receptor antagonists) for a variety of conditions (e.g. movement disorders, urinary incontinence, and dizziness) is associated with an increase in amyloid plaque and neurofibrillary tangle pathologies in post mortem brains of Parkinson's disease (PD) patients (Perry, et al. 2003). The elevated levels of post mortem amyloid following chronic anticholinergic use suggest that mAChRs play a particularly crucial role in regulating amyloid levels in humans. This ability of mAChRs

to regulate amyloid levels in humans has critically important implications for AD therapy, as it has recently become clear that A β levels are already maximally elevated in MCI patients prior to conversion to clinical AD, suggesting that A β plays an important upstream role in disease pathophysiology preceding the clinical progression to AD (Buchhave, et al. 2012).

Among the mAChRs, M₁ has received the most attention, as M₁ knockout mice display memory impairments and M₁ activation has been shown to be centrally important in the regulation of APP processing (Figure 1.8) (Anagnostaras, et al. 2002; Davis, et al. 2010). Recent studies have shown that M₁ activation leads to downstream effects on PKC which influence the cellular secretase machinery responsible for the proteolytic processing of APP (Caccamo, et al. 2006). Namely, M₁ activation leads to a suppression in β -secretase and γ -secretase activity and concomitant promotion of α -secretase activity in order to drive non-amyloidogenic APP processing. These effects by M₁ on APP processing combine to lower the levels of A β that are produced. This reduction in A β that has been observed with M₁ activators in animal models has translated nicely to the clinic in premortem studies in AD patients, where drugs targeting M₁ have been shown to lower A β levels in the CSF of AD patients (Hock, et al. 2000; Nitsch, et al. 2000; Fisher, et al. 2003). This has led to an immense interest in selective M₁ activators as potentially disease-modifying drugs for AD patients (Conn, et al. 2009a, 2009b). Furthermore, the dual M₁/M₄ agonist Xanomeline has shown significant effects on behavioral disturbances with a trend towards improved cognition in the clinic (Bodick, et al. 1997a; Bodick, et al. 1997b; Bymaster, et al. 1997). These lines of evidence implicating M₁ in beneficial effects on APP processing and positive outcomes on human

cognition in the clinic raised the exciting possibility that truly M_1 selective activators may be efficacious therapeutics for AD patients.

Why is it that M_1 activation, in particular, should be therapeutically-superior to conventional cholinergic strategies like AChEIs, which have been under investigation for decades? An important pharmacological point to consider is one of selectivity. Namely, that M_2 and M_4 receptors functionally oppose the actions of M_1 . As M_2 and M_4 do not have the same beneficial effects on APP processing and $A\beta$ -lowering that M_1 does, the focusing on development of selective M_1 activators has become very intense in recent years (Farber, et al. 1995; Davis, et al 2010). In this vein, the completely non-selective actions of AChEIs across all mAChR and nAChR subtypes drastically hampers the observed efficacy with these compounds, as functionally-opposing receptor subtypes are activated. Furthermore, the potential for central and peripheral adverse side effects becomes much greater (Conn, et al. 2009). For instance, M_3 mAChRs can become activated peripherally, which are believed to mediate the serious adverse gastrointestinal side effects observed with non-selective cholinergic activators. Several compounds such as AF206-B, 77-LH-28-1, AC-42, and AC260584 have been developed that have been touted as M_1 -selective, but all have off-target activity at other muscarinic family members, particularly M_2 and/or M_3 , that limits their clinical utility moving forward (Spalding, et al. 2006; Langmead, et al. 2008; Conn, et al. 2009a, 2009b; Jacobsen, et al. 2010). A breakthrough for the field came with the development of selective allosteric modulators such as BQCA and selective M_1 allosteric agonists such as VU0364572 (Ma, et al. 2009; Jones, et al. 2011; Lebois, et al. 2012). While central penetrance and solubility continues to be a problem that plagues the development of M_1 PAMs,

compounds such as VU0364572 have been shown to display M₁ specificity and cognition-enhancing properties in animal models, which is a large focus of this thesis and will be elaborated on in later portions of this document. While such compounds have shown great preclinical promise, the translation of selective M₁ PAMs and agonists to the clinic remains to be seen.

A final comment on the therapeutic progress observed for AD to-date is that, while tremendous effort has been poured into investigating multiple disease mechanisms, considerable challenges lay ahead. Namely, the need for a safe and effective intervention that translates to clinical efficacy in AD patients has never been greater. While much progress has been made in the mechanistic understanding of AD progression, progress in our circuit- and cellular-level understanding of functional deficits and therapeutic benefits *in vivo* has remained particularly challenging. Fully resolving this therapeutic impasse will likely require merging current histology and medicinal chemistry with increased systems-level understanding – through electrophysiology and imaging approaches – of how relevant neural circuits are being modulated pathologically and therapeutically *in vivo* so that our forward progress might be better informed. A large part of the reason why every intervention designed to slow or halt the disease timecourse has failed to-date is that these trials have been designed to target patients who already have AD (Holtzman, et al. 2011). By the time a patient presents with memory impairments in the clinic they already have marked pathological damage that has occurred to their brain and there is likely nothing that can be done to ameliorate this damage. The focus on patients with clinical AD has been entirely out of necessity, as certain inclusion criteria is needed to construct clinical trials. The reason prodromal AD patients have not been enrolled is that

our understanding of prodromal AD is only just unfolding and considerably lagging. This will be a focus of later discussion, but approaches such as functional imaging, eye-tracking technology, and *in vivo* electrophysiology designed to identify the earliest dysfunction in AD need to be employed in order to help inform the next generation of clinical trials and fully understand the dysfunction that occurs in prodromal AD.

M₁ Allosteric Agonist Development for Alzheimer's Disease

As previously described, M₁ mAChRs have long been an interest in laboratory research groups both academically and pharmaceutically for their demonstrated ability to reduce A β (Figure 1.8) pathology associated with AD as well as for their documented ability to improve several measures of memory (Conn, et al. 2009a, 2009b; Jones, et al. 2011). Although muscarinic activators such as Xanomeline have made it to the clinic and shown promising effects in AD patients and schizophrenics, the large reason selective M₁ activation has not borne fruit as an effective therapy is due to the fact that the muscarinic receptors are extremely difficult to target selectively (Bodick, et al. 1997a, 1997b; Conn, et al. 2009a, 2009b). In fact, GPCRs are notoriously hard to target selectively, in general, as most types of GPCRs comprise many different family members. An extreme example is the serotonin (5HT) receptor family that consists of at least 15 different isoforms! The muscarinic receptors consist of 5 different family members and M₂ and M₃ are believed to be the major subtypes expressed in the periphery that result in the dose-limiting side effects of drugs such as Xanomeline in the clinic (Conn, et al. 2009a, 2009b). Drugs that have been touted as M₁-selective, including AF206-B, 77-LH-28-1, AC-42, and AC260584 still have appreciable binding to M₂ and/or M₃ that dramatically hampers the

clinical utility of these compounds at a translational level and their use in probing the function of M_1 in the mammalian CNS at a more basic level (Conn, et al. 2009a, 2009b).

A breakthrough came in the development of the allosteric agonists VU0357017 and VU0364572, which represent the first ever M_1 specific agonists (Lebois, et al. 2009, 2011). This breakthrough came in large part due to the approach taken of designing allosterically-acting small molecule drugs (Conn, et al. 2009a, 2009b; Canals, et al. 2012). That is, drugs that act at a site on the M_1 receptor that is topologically-distinct from the orthosteric site where the endogenous ligand ACh acts (Avlani, et al. 2010; Lebois, et al. 2009, 2011). The rationale behind this approach is that all muscarinic receptors evolved to bind ACh so therefore the ACh binding site must be the most highly conserved part of these proteins. Thus, if one wants to selectively target a given family member one is substantially more likely to succeed by targeting the differences (e.g. the remainder of the protein structure outside of the orthosteric site) among muscarinic receptors rather than the similarities between them (Conn, et al. 2009). This novel approach employs functional screening assays that rely upon intracellular readouts of receptor activation, such as calcium release, rather than the classical competition binding assays with radioligands to used to detect orthosteric binding. By utilizing intracellular readouts of receptor activation, compounds acting anywhere on a receptor to activate it can be identified. The approach of functional screening by intracellular calcium release was the exact approach employed in order to identify the initial high-throughput screening (HTS) hits, VU0177548 and VU0207811 (Figure 1.9A). VU0177548 and VU0207811 display weak activity for activating M_1 , but incredibly, these compounds came off the screening deck selective for M_1 and displayed aqueous solubility.

Upon identification of VU0177548 and VU0207811 a lead optimization approach was rapidly developed in order to generate analogs of these compounds. In particular, western aryl, diamine linker, and eastern carbamate moieties were identified through retrosynthetic analysis as functional handles for optimization in attempt to increase the potency of the initial hits for M₁ while maintaining selectivity (Figure 1.9C and 1.9D). Using a diversity-oriented synthesis approach, each of these pieces identified from retrosynthesis was iteratively swapped out in favor of different analogs in order to fully sample the chemical space of these regions and round out structure-activity relation (SAR) studies to see how these chemical changes impacted the scaffold's ability to selectively activate the M₁ receptor.

These optimization efforts culminated in the development of VU0364572 (which, henceforth will be referred to as VU572), a potent and completely selective M₁ agonist (Lebois, et al. 2011) (Figure 1.10A). Notably, VU572 displayed enantiospecific activity with all activity attributable to the *R*-enantiomer. VU572 was found to be highly water soluble, orally bioavailable with a %*F* of 37. At a dose of 10 mg/kg VU572 achieves a Brain_{AUC}/Plasma_{AUC} of 1.35, providing high CNS exposure. These data provide extremely compelling evidence that VU572 represents the state-of-the-art tool with which to study M₁ receptor function *in vivo* in the mammalian CNS: it is completely selective for M₁, gets into the brain at therapeutically-relevant levels and is completely water soluble so that it can be dosed orally. In addition to its excellent pharmacological properties, VU572 has a clean ancillary pharmacological profile, as it was demonstrated to have no significant off-target activities at 68 different ion channels and GPCRs (Lebois, et al. 2011). VU572 was also functionally profiled at more than 100 other GPCRs with

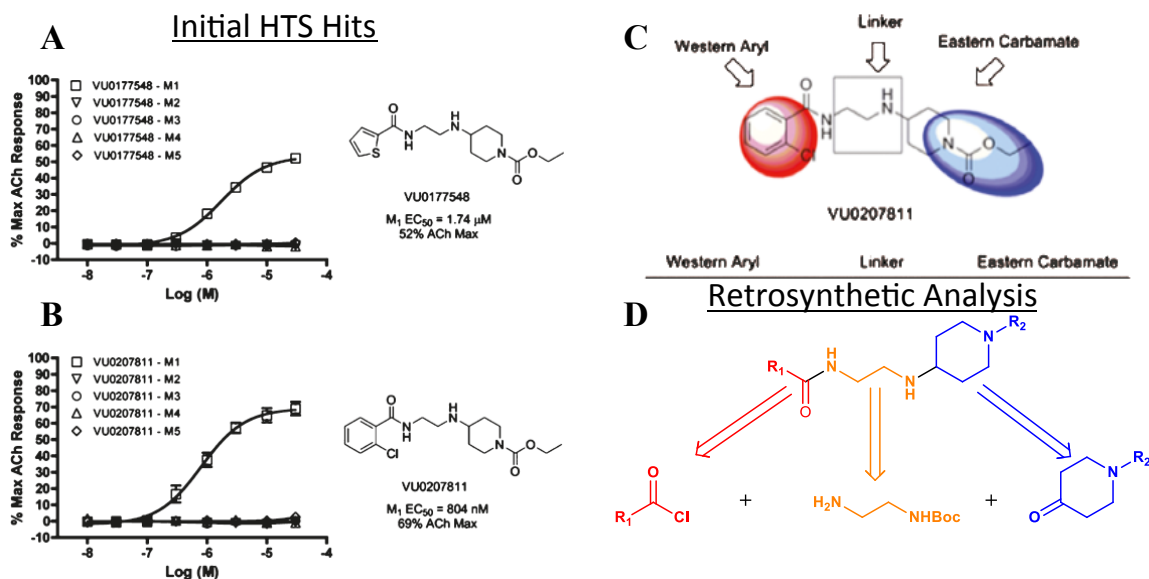


Figure 1.9. M₁ Agonist Discovery and Characterization.

A, B) Initial high-throughput screening (HTS) hits VU0177548 and VU0207811 which displayed weak potency and efficacy for activating intracellular calcium release.

Incredibly, these compounds came off the screening deck selective for M₁ and displayed aqueous solubility, so this provided a great starting point for lead-optimization. C) SAR breakdown showing areas of this diamine scaffold amenable for library synthesis.

Western aryl, diamine linker and eastern carbamate moieties all represent very easily tractable chemical regions to optimize. D) Retrosynthetic breakdown showing disconnections of diamine scaffold into cognate components for library synthesis.

Western aryl analogs were accessed through acylation of diamine scaffold using a library of acid chlorides and eastern carbamate analogs were accessed through reductive amination of the opposing end of the diamine linker. A rapid solid-phase synthesis approach with very high yields (~98%) and crude product purity (~95-98%) was developed for library generation.

Images from: Lebois, et al. 2010.

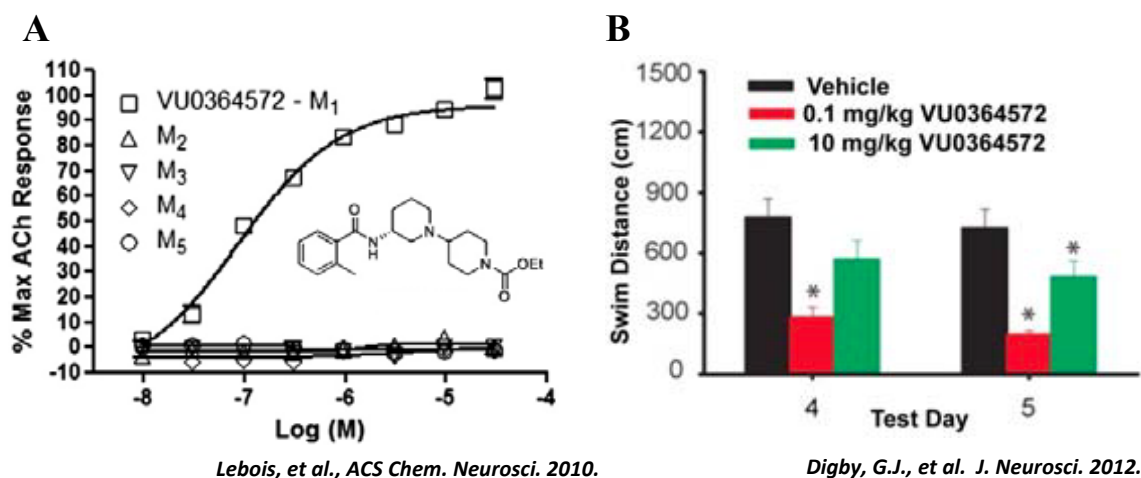


Figure 1.10. M₁ Agonist Optimization for *In Vivo* Studies.

A) Optimization of western aryl, diamine linker region and eastern carbamate moieties yielded VU0364572, a potent and completely selective M₁ agonist. Notably, VU0364572 displayed enantiospecific activity with all activity attributable to the *R*-enantiomer. VU0364572 is highly water soluble, orally bioavailable with a %*F* of 37. At a dose of 10 mg/kg VU0364572 achieves a Brain_{AUC}/Plasma_{AUC} of 1.35, providing high CNS exposure (Lebois, et al. 2011). B) *In vivo* development of VU0364572 demonstrated that this M₁ agonist is able to significantly improve memory on the Morris water maze task compared to saline. Animals administered doses of 0.1 mg/kg or 10 mg/kg VU0364572 learned much better than their saline counterparts. The inverse dose response is notable and tracks well with subsequent work of ours demonstrating the concentration-dependent effects observed with VU0364572 where lower concentrations promote hippocampal LTP, whereas higher concentrations promote LTD (Digby, et al., 2012).

no evidence of off-target liabilities. While, the development of selective M₁ PAMs preceded VU572, the poor solubility profile of these compounds and poor central penetrance has hampered their effective application in M₁ proof of concept studies *in vivo*. The development of VU572 has allowed M₁ receptor function in the mammalian CNS to be probed with small molecule activators *in vivo* for the first time.

In vivo studies with VU572 are now currently taking place to validate the role of M₁ in improving memory in order to apply M₁ activators in a host of different therapeutic conditions, including Alzheimer's disease and schizophrenia. The roles of M₁ receptor signaling for combatting disease pathology in AD and how M₁ acts at a basic level to contribute to the representation of information by the hippocampus constitute a major theme of this thesis and will be discussed shortly. In particular, it is not clear whether administering an M₁ agonist chronically before onset of neuropathology would guard against the subsequent development of pathology and cognitive deficits in animal models of AD. Also, while M₁ mAChRs have been shown to contribute critically to memory and synaptic plasticity process, how M₁ is acting at a circuit level *in vivo* in order to mediate these effects is unclear.

Subsequent characterization of VU572 *in vivo* showed that this compound is behaviorally-active at improving memory in the Morris water maze at doses of 0.1 and 10 mg/kg (Figure 1.10B). The inverse dose response noted for the efficacy obtained in the Morris water maze tracks well with the impact of VU572 on synaptic plasticity in the hippocampus, as VU572 was found to robustly potentiate theta-burst stimulation (TBS)-induced LTP (Figure 1.11A-C) at lower concentrations of 500 nM, yet induce LTD

(Figure 1.11D-F) at higher concentrations up to 30 μM at CA3-CA1 synapses in fEPSP recordings (Digby, et al. 2012).

A major concern moving forward with direct-acting agonists as therapeutics is that with chronic dosing one possibility is that tolerance is rapidly achieved to these drugs, which could abolish efficacy. This is due to the fact that receptor activation by exposure to agonists potently recruits intracellular arrestin machinery and is known to robustly desensitize receptor signaling (Thomas, et al. 2009; Davis, et al. 2010a). Any chronic dosing of a direct-acting agonist would therefore be expected to rapidly internalize receptors and keep them desensitized henceforth. Fortunately, this robust desensitization does not appear to be the rule for allosteric agonists of M_1 receptors (Thomas, et al. 2009; Avlani, et al. 2010). Exposure of M_1 -CHO cells to the general orthosteric mAChR agonist, carbachol, versus the more allosterically-acting agonists AC260584 and TBPB demonstrate that M_1 receptors are rapidly lost from the cell surface following activation by the orthosteric agonist carbachol, but are retained at the cell surface following allosteric activation (Davis, et al. 2010b). Subsequent work with VU572 demonstrated that, like AC260584 and TBPB, this compound is a weak beta-arrestin recruiter (Figure 1.12C). The fact that VU572 is such a weak arrestin recruiter suggests that it does not robustly desensitize M_1 receptor signaling as well. This is an extremely important observation, as a lack of desensitization following allosteric M_1 activation implies that allosteric M_1 activators can be delivered chronically to animals and patients in order to obtain lasting efficacy at improving disease pathology.

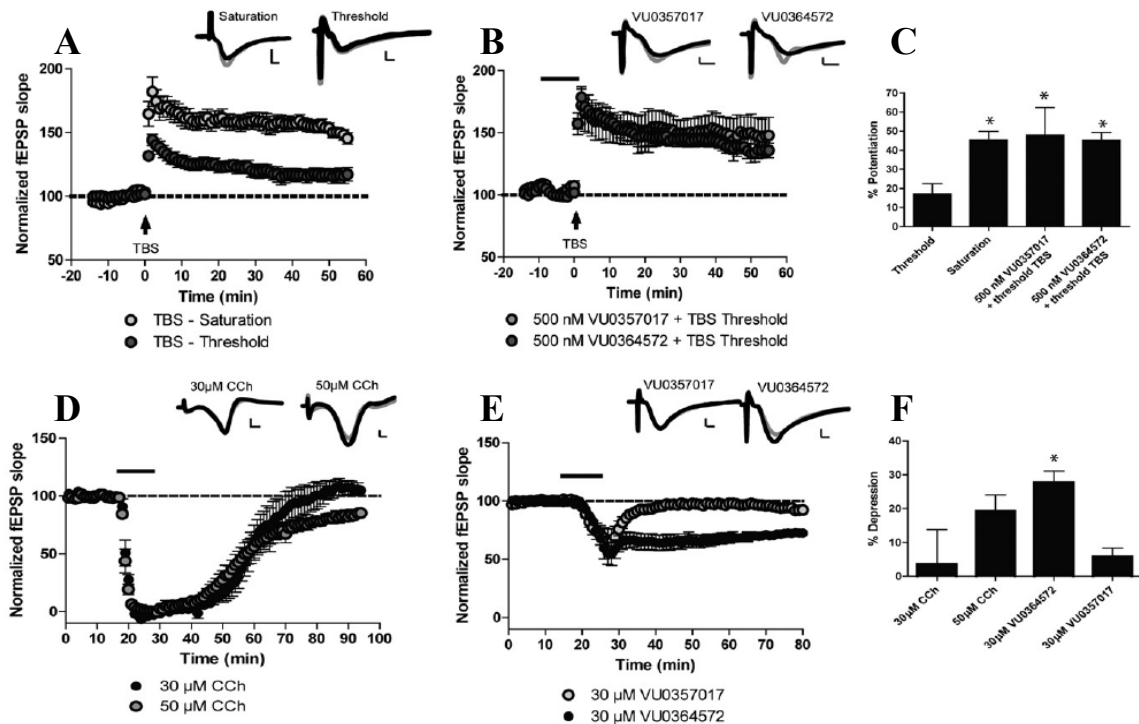
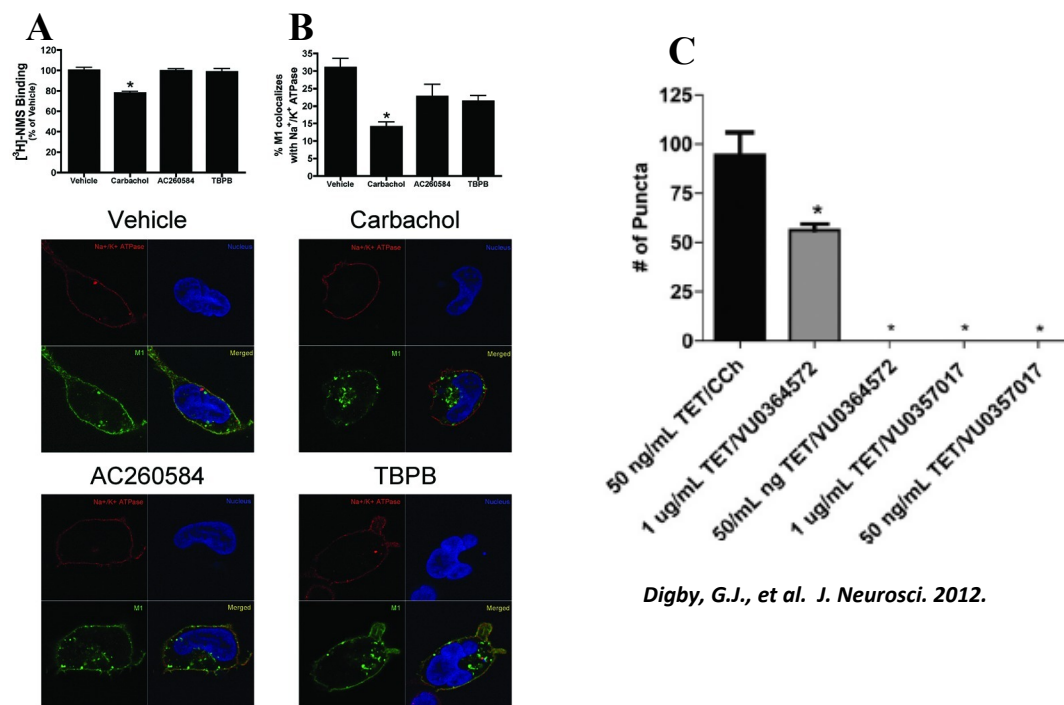


Figure 1.11. M_1 Activation by VU572 Has Robust Effects on Hippocampal Synaptic Plasticity.

A, B) Slice recordings from healthy adult rats demonstrating that doses of 500 nM of VU0364572 and an earlier structural analog, VU0357017, are capable of robustly potentiating (by ~40%, shown in panel C) a threshold level of LTP attained by delivering a theta burst stimulus train to the slice. D, E) Interestingly, higher concentrations of VU0364572 engages differential circuitry that leads to a chemical induction of LTD (termed mLTD; muscarinic LTD) with a robust and sustained ~30% depression as shown in panel F.

Figure from: Digby, et al., 2012.



Davis, et al., ACS Chem. Neurosci. 2010. 1(8): 542-551

Digby, G.J., et al. J. Neurosci. 2012.

Figure 1.12. M₁ Allosteric Agonists Do Not Robustly Desensitize M₁ Receptor Signaling.

A classic worry about developing direct acting agonists is that they traditionally rapidly desensitize receptor signaling and can do so for a long time such that treatment benefits wane or are completely abolished altogether. A, B) Demonstrates via radiolabeling M₁ receptors in M₁-CHO cells with [³H]-NMS that the allosteric agonists AC260584 and TBPB do not detectably internalize M₁ receptors following application. C) Importantly, work investigating the M₁ agonist utilized for the present studies, VU0364572, demonstrated that this compound is a weak (note the concentration here is 100 μM, more than an order of magnitude above therapeutic CNS levels) recruiter of β-arrestin, suggesting that chronic dosing of VU0364572 and other M₁ allosteric agonists may be possible with sustained efficacy.

Animal Models of Alzheimer's Disease

Many mouse models of AD have been developed to-date, but perhaps the two most influential are the original Tg2576 mouse and the so-called triple-transgenic mouse (3x-Tg) developed by Oddo, et al (Oddo, et al. 2003a). The Tg2576 mouse was the beginning of a first generation of mice that were engineered to express human amyloid mutations and harbor two APP Swedish mutations, K670N and M671L. These mice are characterized by progressive cortical and hippocampal deposition of amyloid as well as spatial learning and memory deficits that mirror those seen in AD patients. The disadvantages to this model are several-fold, though. Firstly, the amyloid pathology and memory deficits that these mice develop is very mild and does not reach appreciable levels until later in life. Thus, from a standpoint of preclinical drug development, these models may allow one to see an effect of a drug on pathology, but the mild nature of the pathology may mean that drug might not translate as well to the clinic when a more robust pathology is encountered. Secondly, the memory impairments that these mice develop take a long time to manifest, commonly 12-14 months. This makes conducting experiments with these animals extremely long-term and does not provide as realistic of a turnaround time in terms of effectively developing drugs.

One aspect of the Tg2576 models and other amyloid-based models that gave some investigators pause was that they only developed amyloid and displayed no evidence of the tau neurofibrillary tangle (NFT) pathology seen in human AD patients. In order to address this lack of NFTs, the 3x-Tg model was the first model developed as a full-spectrum AD mouse model (Oddo, et al. 2003a). These mice have been engineered to express APP (Swedish), PS1(M146V), and tau (P301L) mutations. This model

accumulates intraneuronal A β with plaques at around 3 months in the neocortex, at around 6 months in the hippocampus, with the first tangles appearing at around 12 months in the hippocampus and thereafter spreading to the cortex (Oddo, et al. 2003a; Oddo, et al. 2003b). Importantly, the appearance of amyloid pathology so long prior to tau pathology along with subsequent experiments demonstrating that amyloid pathology can exacerbate tau pathology but not vice-versa strongly support the amyloid cascade hypothesis of AD, which favors amyloid as the causative agent preceding tau.

Furthermore, LTP deficits that precede both plaque and tangle formation have been documented in these mice and are consistent with the idea that soluble amyloid may be playing a role in establishing a framework for disease prior to any plaque pathology.

These LTP deficits have been shown to correlate well with the accumulation of intraneuronal A β and soluble A β oligomers (Oddo, et al. 2003b; Billings, et al. 2005).

While both A β as well as tau pathology have been successfully modeled using 3x-Tg mice the work pointing to A β as a causative factor in AD upstream of tau suggests that cost in terms of experimental time in waiting for the 3x-Tg to develop pathology may not be worth it from the standpoint of drug development. One can argue that unless a drug is modeled in a system displaying both plaques and tangles that the drug is not being modeled in as physiologically-relevant system as possible. The goal for AD therapy should be to intervene at an early point before significant insoluble A β and tau pathology manifests and prevent the development of subsequent pathology in a preventative manner in order to stop patients from progressing into the decline characteristic of AD. Thus, the concern that tangles are present or not is largely irrelevant since soluble A β oligomers are likely acting before any tau deposition takes place.

Taking A β pathology as the proximal pathological event in AD in-hand with the desire to create an animal model that develops disease-relevant timecourse of A β expression and memory impairments on a reasonable timescale for drug development has led to the creation of the 5X FAD mouse model (Figure 1.13) by Vassar, et al. (Oakley, et al). The 5X FAD mouse model is so-called since it bears five familial AD (FAD) mutations known to give rise to AD: three of which are in APP (K670N/M671L, I716V, and V717I) and two of which are in PS1 (M146L and L286V). These mice begin accumulating intraneuronal A β and the first detectable A β deposits around 1.5-2 months of age in the subiculum and areas of the hippocampus. From 2-6 months of age these mice develop large amounts of insoluble amyloid deposits throughout the hippocampus and neocortex. 5X FAD mice accumulate both A β_{40} and A β_{42} , but in general develop much heavier A β_{42} deposition (Figure 1.13A and B). Notably, female mice develop approximately 30% more A β males do and at 6 months of age display significant memory impairments in the Morris water maze relative to WT littermate controls. This Morris water Maze data is a large focus of the present thesis and is not shown here, but will be discussed at length in later sections. Thus, the 5X FAD mouse model represents the most aggressive model of A β deposition to-date that subsequently develops the most rapid-onset of memory impairments. This rapid accumulation of pathology and onset of memory impairments makes the 5X FAD mouse model particularly attractive as a model for drug development since it potentially allows for *in vivo* drug testing with a rapid turnaround time compared to other transgenic models. While the concern with early transgenic models such as the Tg2576 mouse is that the pathology is so mild as to not be reliably predictive of clinical efficacy, the concern with the 5X FAD mouse is the

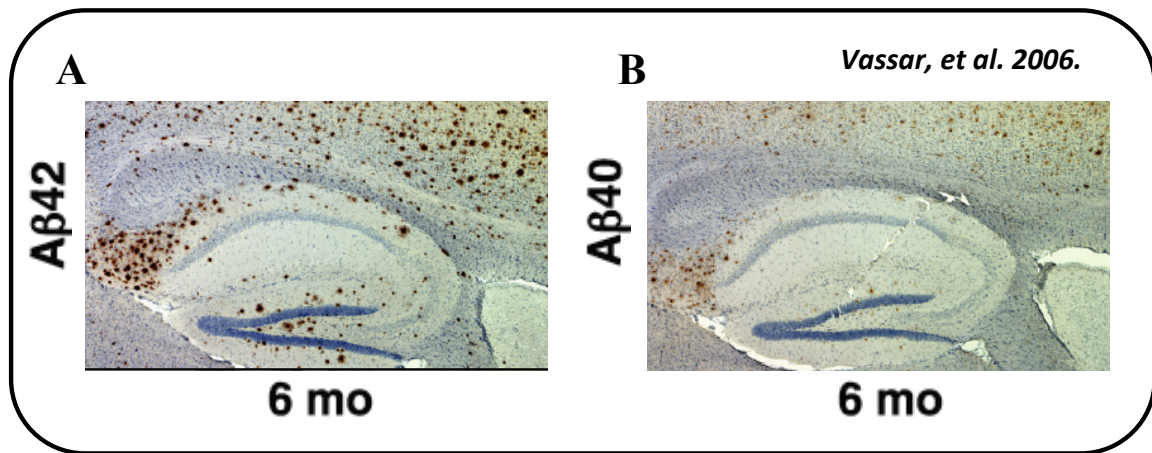


Figure 1.13. Animal Models of AD: The 5X FAD Mouse is a Robust Animal Model of AD.

A, B) Many mouse models of AD have been developed in the past, but perhaps the most aggressive is the 5X FAD mouse developed by Vassar and colleagues that bears 5 familial AD mutations. Three of these familial mutations are in APP (K670N/M671L, I716V, and V717I) and two are in PS1 (M146L and L286V). The confluence of 5 familial AD mutations gives rise to a mouse that develops detectable amyloid deposits beginning at 1.5-2 months of age. Detectable memory impairments are evident by 6 months of age, with very high Aβ₄₂ (panel A) and Aβ₄₀ (panel B) levels observed in the brains of these mice, particularly in the hippocampus and cortex.

Image from: Oakley, H., et al. 2006.

opposite. Namely, the 5X FAD mouse may be such an aggressive model of disease that it overwhelms the effect of activating any therapeutic mechanism. Even though this aggressive pathology sets the bar very high in terms of therapeutic modification of disease pathology, a drug intervention which blunts or prevents pathology in such an aggressive model may have the greatest potential of translating in the clinic to efficacy in terms of preventing or slowing the progression to AD.

The Hippocampal Memory System

Functional Neuroanatomy and Overview

The hippocampus is a brain structure responsible for the formation of episodic memories and functions as one component of the hippocampal memory system (Figure 1.14) (Squire 1992, 1993; Eichenbaum 2000; Burgess, et al. 2002). In addition to the hippocampus, the hippocampal memory system is composed of the adjacent hippocampal cortices including the perirhinal cortex, the parahippocampal cortex, and the medial and lateral entorhinal cortex (Witter 1993). In order to form episodic memories the hippocampus receives its main input via the perforant path from the medial and lateral entorhinal cortices to the dentate gyrus. A particularly important characteristic of this input to the hippocampus is that it is both highly-processed and segregated into spatial and non-spatial information. Spatial and non-spatial information originating in higher level associational cortices flows through the parahippocampal (postrhinal cortex in rats) and perirhinal cortex, respectively. After processing by the parahippocampal and perirhinal cortex, this spatial and non-spatial information then is passed on to the medial and lateral cortex for subsequent processing, respectively. From the medial and lateral entorhinal cortex the information is passed onward to the hippocampus, whose job it is to bind the nonspatial information to a particular set of spatial information (context) in a temporally-graded fashion.

The classical view of information processing by the hippocampus focuses on the tri-synaptic pathway composed of the dentate gyrus (DG), CA3, CA1, and subiculum (Witter 1993). Information first flows in from layer II of the EC through the perforant

path to the DG. Following processing by the DG, the information is then routed along mossy fiber afferents to the CA3 subfield of the hippocampus. After being processed by CA3 the information then passes to the CA1 subfield along the Schaffer collaterals to the subiculum. In the trisynaptic circuit view of hippocampal processing the subiculum serves as the main output of information from the hippocampus via the fornix back to the cortex.

In recent years after numerous anatomical and functional studies it has become apparent that the trisynaptic view of hippocampal processing is overly-simplified. The view of the hippocampus as an isolated trisynaptic circuit drastically underplays the interconnected and complex connections between the hippocampus, its adjacent cortical partners, and other extrahippocampal brain regions that serve as important sources of input and modulation of hippocampal processing (Eichenbaum 2000). The concerted action between all of these components is the important determining factor in how the hippocampus does its job at all to bind information and how well it is able to do it. A crucial connection in this vein arises from layer II/III of the entorhinal cortex and provides direct input to the CA fields of the hippocampus. Layer II EC afferents comprising the perforant path project to both the molecular layer of the DG as well as the stratum lacunosum-moleculare of CA3 (Nafstad, 1967; Steward and Scoville, 1976; Witter, 1993). Hence, incoming information to the hippocampus flows both to the DG, as well as directly to the CA fields. One might expect this to cause a traffic jam of sorts at the level of the hippocampus, however, each module of the hippocampus is specialized in the information processing that it carries out. The information flow through the perforant path from EC to DG and CA3 arises from EC layer II and is thought to be

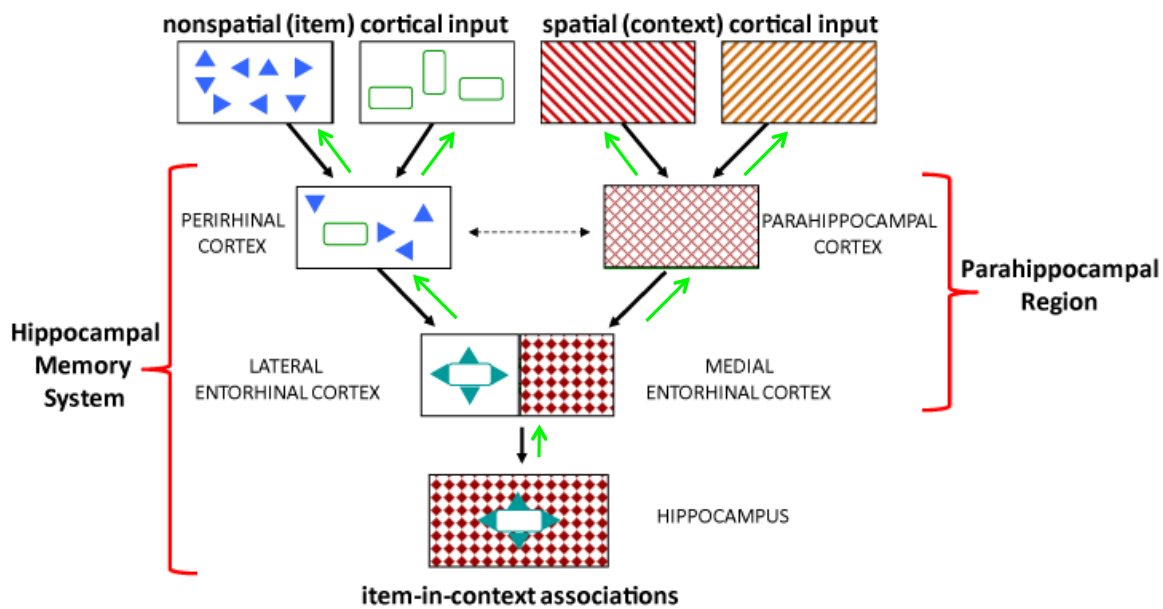


Figure 1.14. The Hippocampus Combines Spatial and Nonspatial Inputs in Order to Form Episodic Memories.

The hippocampal memory system is comprised of the CA fields of the hippocampus as well as adjacent hippocampal cortices, namely the lateral and medial entorhinal cortex, the perirhinal cortex, and the parahippocampal cortex. The primary job of the hippocampus in the brain is to contribute to forming episodic memories. In order to form episodic memories, the hippocampus is constantly binding spatial and nonspatial information together simultaneously into episodes representing “what” happened “where.” The perirhinal and parahippocampal cortices synthesize information they receive from higher level association cortex and then send this processed information on to the lateral and medial entorhinal cortices, respectively. An interesting feature of episodic memory formation is that spatial and nonspatial information stay very anatomically segregated in the brain until the level of the hippocampus where the two types are combined. The perirhinal-lateral entorhinal circuits are responsible for handling nonspatial information, whereas the parahippocampal-medial entorhinal circuits handle spatial information.

important for triggering pattern completion events in CA3 to aid in the recall of past representations. In deciding whether incoming information is novel and needs to be coded as a new memory, the hippocampus must have something to compare this incoming information to in order to make this decision. The CA3 subfield of the hippocampus has an extensive autoassociation network with a highly connected system of recurrent collaterals. Previous studies suggest that up to 80-90% of synapses onto CA3 cells are recurrent connections from other CA3 cells. This extensive recurrent network allows activity to reverberate in it and is therefore extremely efficient at taking a partial sensory input (e.g. a sight or a smell) and rapidly reconstructing an entire episodic experience with minimal energy expenditure (e.g. a smell of cookies at a friend's house triggers the memory of Grandmother's kitchen in New York on Christmas Eve of 1992). In this way, the CA3 subfield is intrinsically wired to emphasize the similarities of current online inputs to previously-encoded inputs. CA1, on the other hand does not have such a recurrent collateral system and differs in its handling of information. The two major inputs to CA1 are from CA3 and also a direct projection from EC layer III to the stratum lacunosum-moleculare of CA1 (Steward and Scoville, 1976; Kajiwara, et al. 2008). The responsibility of CA1 is then to compare the previous information retrieved by CA3 with the current online information being received from the EC. In the event that the previous information called up by CA3 differs from the online information being received from EC, CA1 needs to code the current information as a new memory. In the event the previous information called up by CA3 matches the current information from EC, CA1 needs to recognize that the information is the same so that it does not code a new memory. In any event, CA1 projects not only to the subiculum, but also to the deep

layers of the EC, perirhinal cortex, as well as to a number of other cortical and subcortical regions. In this vein, the subiculum also projects to a number of cortical and subcortical regions, as well as deep layers of the EC and perirhinal cortex in the parahippocampal region.

Since the EC acts as such a privileged gatekeeper of information flowing to and from the hippocampus, the functional consequence of EC projections to the hippocampus warrant further examination. Perforant path connectivity from EC to the hippocampal formation is comprised of input from medial entorhinal and lateral entorhinal areas (LEA and MEA, respectively) responsible for carrying spatial and nonspatial information, respectively (Hargreaves, et al. 2005). The perforant path projections of EC layer II to DG and CA3 are known to terminate in the outer one-third of the DG molecular layer and CA3 stratum lacunosum-moleculare. However, these EC layer II perforant path projections do not discriminate along the transverse axis of DG or CA3 (Van Strien, et al. 2009). Thus, DG and CA3 are likely to receive an equal blending of both spatial and nonspatial input from MEA and LEA (McNaughton and Barnes 1977). In stark contrast, inputs from EC layer III to CA1 are more discriminatory and non-overlapping. Specifically, LEA projects mainly to the medial and distal third of CA1, whereas MEA projects most robustly to the proximal and medial portions of CA1 (Van Strien, et al. 2009). This connectivity has great functional implications for both CA3 and CA1, as the positioning along the transverse axis of CA1 matters a great deal for the relative influence of spatial versus nonspatial information. By virtue of this topographically-distinct connectivity the hippocampus is able to simultaneously handle two parallel streams of information in order to form episodic memories. This blending of spatial and nonspatial

information at the level of CA3 and separation in CA1 makes good sense with regard to the functions ascribed to these regions in information processing (Guzowski, et al. 2004). If what CA3 truly cares about is whether incoming information is part of a previously coded memory, a blend of spatial and nonspatial information will increase the likelihood that this prior memory is called up. In contrast, if CA1 cares more about whether incoming information from EC is different from a previous memory called up by CA3, keeping spatial versus nonspatial information segregated makes good sense in order to compare aspects of this incoming information in a more piecemeal way to the previous memory. In this way, either 1) certain spatial and nonspatial aspects of this previous memory can be updated in a very accurate manner if need be while setting aside the familiar aspects if the current and previous episodes are similar or 2) an entirely new memory can be formed if the current and previous episodes dramatically differ.

In addition to the differences in EC projections along the transverse axis of CA3 and CA1, EC also projects in a topographically distinct manner along the septal-temporal (dorsal-ventral in the rat) axis of the hippocampus (Van Strien, et al. 2009). The major difference is that the more rostromedial portions of EC receive amygdalar and limbic input, whereas the more caudomedial portions of EC receive robust visuospatial, auditory, and sensory inputs. The implications for this differential input to EC have important consequences for what kind of information is emphasized along the septal-temporal axis of the hippocampus. Specifically, this organization of EC inputs implies that the temporal hippocampus (ventral hippocampus in rodents) is involved more in representing affective and visceral information, whereas the septal hippocampus is more involved in the in the representation of spatial information (Fanselow and Dong 2010). This pattern

of EC-hippocampal projection tracks well in experimental studies that have observed little to no effect of ventral hippocampal lesions on tests of spatial memory (e.g. the Morris water maze), whereas lesions restricted to the dorsal hippocampus are much more disruptive. Furthermore (and more relevant to the work in this thesis), place cells of the dorsal hippocampus care a great deal about spatial information and show very high spatial selectivity and spatial information content compared to ventral hippocampal cells which can be as large as the recording room an animal is placed in and consequently carry very little spatial information.

Aside from inputs to the hippocampus from adjacent cortices, the hippocampus also receives crucial inputs from a variety of other structures including the medial septum and diagonal band of Broca (DBB), amygdala, brainstem (including locus ceruleus and raphé nuclei), and hypothalamus. For the purposes of the work in this thesis, the most relevant of these regions are the medial septum and DBB. Septohippocampal afferents provide the major source of cholinergic innervation and modulation to the hippocampal formation and project diffusely to all hippocampal subfields (Wainer, et al. 1985). These septohippocampal afferents provide a powerful inhibitory innervation to the hippocampus that acts as a pacemaker to generate a large part of the theta rhythm in the hippocampus. This entrainment of the hippocampal formation to the theta rhythm provides an ordered framework in which information can be organized and bound at different frequencies. Importantly, mAChRs are responsible for the ability of the medial septum to pace the hippocampal theta rhythm, although the exact receptor subtypes responsible for this is unclear.

Hippocampal Place Cells: Properties and Relevance to Memory

Place Field Properties

O'Keefe and Dostrovsky made the seminal observation in 1971 that hippocampal pyramidal cells can form place specific firing fields (O'Keefe and Dostrovsky 1971). Specifically, while recording the activity of hippocampal pyramidal cells from rats as the animals engaged in open field exploration they noticed that certain neurons appeared to preferentially fire only in certain portions of the testing enclosure. This place-specific firing has led to the terms "place cell" to refer to hippocampal pyramidal cell and "place field" to refer to the preferred area in space in which hippocampal cells fire. Place cells are found in both CA3 and CA1, as well as along the entire dorsal-ventral axis of these regions, although as previously described the relative influence of spatial information varies dramatically along this axis (Moser, et al. 2008).

A stereotypical place field is very ordered and symmetric, displaying a high organization of firing rates (Figure 1.15) (Skaggs, et al. 1993; Skaggs and McNaughton 1998). Specifically, as an animal enters a place field for a particular neuron, the neuron starts firing at a very low rate (e.g. 1-2 Hz) at the edges of the place field and then, as the animal passes through the place field, the firing rate ramps up until the very center of the place field is represented by a focus of the highest firing rate (e.g. 5-20 Hz is common). This focus of high firing rate represents a discrete point in space represented by that particular neuron. If one could theoretically record from all neurons in the hippocampus simultaneously while an animal engaged in open field exploration, one would see active cells that represented every point in the test enclosure. Thus, place cells should not be

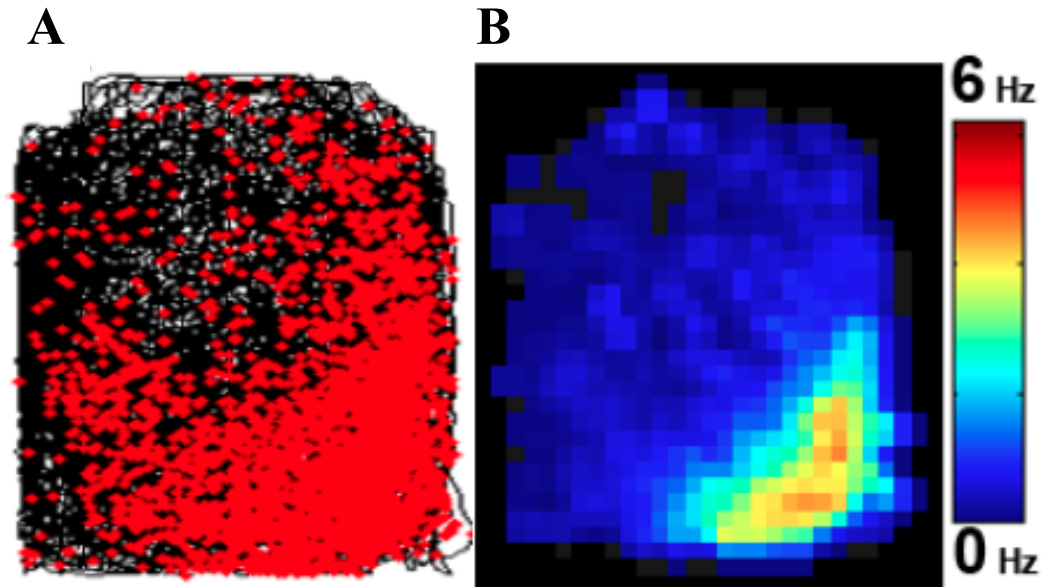


Figure 1.15. Hippocampal Place Cells Form Place-Specific Firing Fields.

Hippocampal “place cell” is another name for a hippocampal pyramidal cell which has a place-specific firing field. Such cells are found throughout the CA fields of the hippocampus and are thought to be a neural correlate of episodic memory since their firing fields are determined by the recognition (pattern completion) or differentiation (pattern separation) of a constellation of sensory cues available to an animal at one moment versus another. A) Movement trace depicting a rat freely exploring a square test enclosure for 15 minutes for randomly scattered chocolate food rewards. Shown in black is the rat’s movement over time and superimposed on this black movement trace are red dots, which depict every time this particular place cell fires an action potential. B) The red dots from A have been plotted over time as a rate-map or “place field” to depict cellular firing rate (in Hz) over time for the 15 minute test session. One can appreciate from A and B together that this place cell prefers the bottom right-hand corner of the testing enclosure.

thought of entirely in isolation, but rather as components of larger ensembles of many place cells, with each ensemble uniquely representing a collection of many cells that uniquely represent a given context. The size of place fields can vary considerably, but in general place fields in the dorsal hippocampus are a similar size and place fields in ventral hippocampus are a similar size. The only difference is that the size of place fields expands along the dorsal-ventral axis (Jung, et al. 1994; Komorowski, et al. 2013). Furthermore, place fields have been shown to be responsive to external cues (Beattie, et al. 1988). For instance if a stripe is painted on the wall of a testing enclosure and the animal is allowed to explore that enclosure the place cells will form place fields in certain locations. However if the animal is removed and the enclosure is rotated, the place fields will rotate with the external cues when an animal is placed back into the enclosure. Similarly, if the walls of an enclosure are “stretched” or “compressed” the place fields observed will be stretched or compressed to a corresponding degree compared to the original context (O’Keefe and Burgess 1996). It is generally accepted that place specific firing fields arise at the level of the hippocampus and entorhinal cortex due to a unique combination of spatial and sensory information at every point an animal passes through in space (Brun 2002, 2008; Knierim, et al. 2006; Moser, et al. 2008). Visual information undoubtedly exerts a strong influence on the formation of place fields, as just described and in many previous studies (O’Keefe and Conway 1978; Muller and Kubie 1987; Jeffrey and O’Keefe 1999). Interestingly, visual cues are neither necessary nor sufficient in order for place fields to form. Animals placed in darkness, animals blind from birth, or animals rendered blind in adulthood experimentally are all capable of forming place fields (O’Keefe and Dostrovsky 1971; O’Keefe 1976; Quirk, et al. 1990; Save, et al.

1998). Even animals that are blind and deaf show an ability to form place fields (Hill and Best 1981). These intriguing studies suggest that visuospatial information, while it exerts a strong influence over the ability to modulate place field formation, is not the only type of information important for forming place fields. Namely, nonspatial information and information about the animal's internal state are important in determining place field firing.

Place Cell Remapping

An important property of place cells that is especially relevant to this thesis is their ability to form distinct, characteristic representations in distinct contexts (Figure 1.16) (Leutgeb, et al. 2005). For instance, if an animal is allowed to explore a square box for 15 minutes such that place fields have a chance to form and then the walls of the enclosure are morphed to an octagon, as in Figure 1.16, the animal will presumably recognize it has changed contexts and place fields will code this change accordingly (Leutgeb, et al. 2005). This change in response properties of place fields in response to contextual change is referred to as “remapping” and reflects an updating of the animal's internal map for a given context (Leutgeb, et al. 2004, 2005a, 2005b, 2005c, 2007). Furthermore, if the animal is reintroduced to the original square shape following exploration of the octagon, the original firing properties and location observed in the initial square encounter will be recovered, indicating that the animal recognizes it is exploring a familiar square context. In this manner, the hippocampus is able to form and recall distinct spatial maps (neural ensembles) for distinct contexts.

Depending on the degree of contextual change an animal encounters there are three main types of remapping that have been observed to occur (Leutgeb, et al. 2005). These types of remapping have been termed partial remapping, rate remapping and global remapping. Partial remapping and rate remapping are typically observed in response to small or subtle degrees of contextual information (e.g. a circular box changing to an octagonal box). Partial remapping manifests at the level of place fields as a place field changing its firing rate at an initial location, while simultaneously beginning to fire at a new location. Thus, the place field looks like it is split between two distinct locations. Rate-remapping can be said to be a type of partial remapping, but is a slightly different representation of spatial information at the level of place fields. Specifically, place fields alter their overall firing rate in response to contextual change, as opposed to changing the physical position in which they fire. Finally, global remapping is where a place field changes its response entirely in response to contextual manipulation and is reserved for large contextual changes (e.g. encountering a square box versus a hexagonally-shaped box). One of two outcomes is possible with global remapping: either a place field is observed at an entirely new position or a place cell stops responding to the differing contexts altogether.

It is pertinent to this thesis and worth mentioning that this open field exploration can be made “harder” for place cells by manipulating the appearance of the testing enclosure to make the visual cues available to the animal more subtle. For instance, note in Figure 1.16 that the animal goes from exploring a square box to exploring an octagonal box. At first glance this seems like a large contextual change and one might expect to see more global remapping of place fields occur. However, the result depicted in Figure 1.16

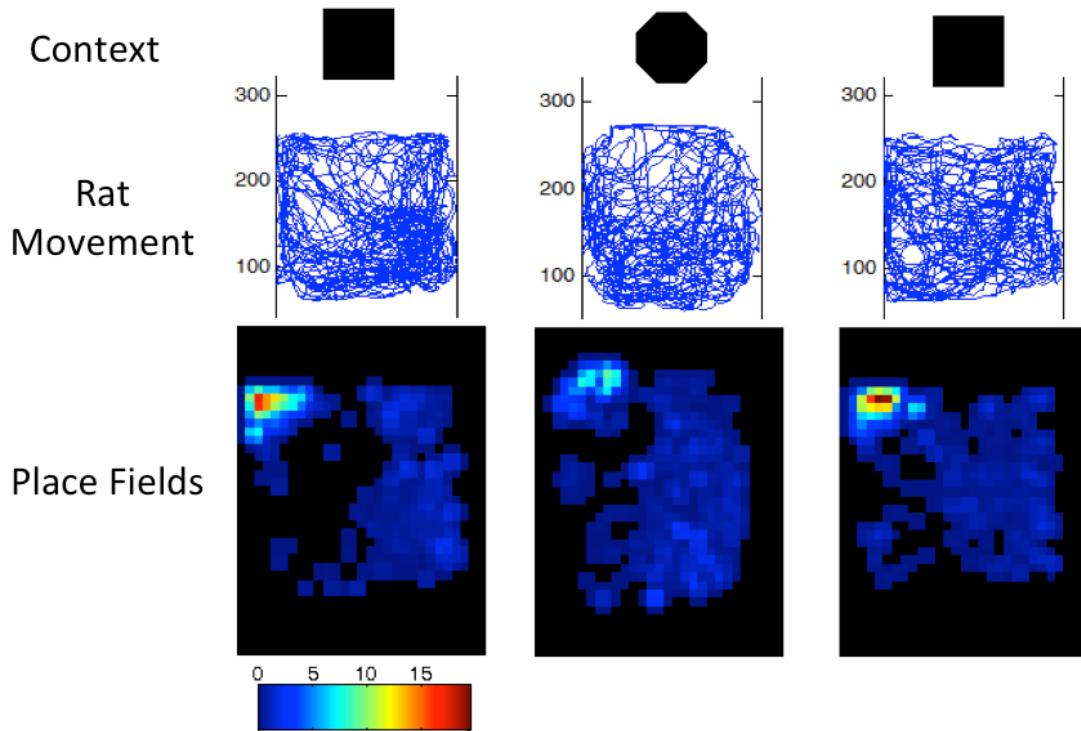


Figure 1.16. Place Cells Form Context-Specific Representations.

An example of a rat exploring 3 differently-shaped testing enclosures for 15 minutes each. Shown at the top of the figure are the 3 shapes the rat explored: square, octagon, and square. In the middle panels of the figures the rat's movement over the entire 15 minutes is plotted as a blue wire trace so one can see that the rat explores the entire surface area of the test enclosure. Finally, the bottom panels depict the place field of this particular place cell, with the cellular firing rate depicted in Hz as a heat map along the bottom edge of the figure. A prototypical place field forms in the upper left-hand corner of the initial square box, which subsequently reduces its firing rate in response to the novel octagon enclosure (rate-remapping), and the original firing rate is recovered when the animal is reintroduced to the square enclosure. This alteration in response to contextual manipulation and recognition of contextual identity are why place cells are considered a

neural correlate of episodic memory, as they can be thought of as coding for “what” happens “where.”

shows rate-remapping in response to this contextual change. In fact, rate-remapping is seen reliably and consistently in response to virtually all contextual manipulations described in this thesis. This consistency in obtaining rate-remapping of place fields is likely attributable to the fact that all of the walls of our recording enclosure are colored black and there are no extra visuospatial cues added to the walls. Thus, the manipulation of the shape of the enclosure is harder for the animal to pick up on when the test session is conducted in low-level lighting. This reliability in inducing rate-remapping is a great strength of our approach, as the intent of this thesis is to characterize the effects of cognition-enhancing drugs on spatial representations in CA3 and CA1 place cells, with the expectation that these drugs will increase the ability of place cells to change in response to contextual manipulation. If what we saw under baseline conditions was predominately global remapping, this would pose a problem for us, as we would effectively be at the ceiling in terms of any drug effect we might see in the task. That is, it would be very difficult (in fact, impossible) to make cells change to a greater degree than is observed with global remapping.

Local Field Potential Oscillations and Relevance to Memory

The local field potential represents the summed electrical perturbations (e.g. EPSPs and IPSPs) in membrane potentials surrounding a recording electrode over time (Draguhn, et al. 1998; Buzsaki, and Watson 2012). Neurons can oscillate between one of two electrical states: polarized (negative) or depolarized (positive). It is important to realize that the membrane potential of individual neurons is constantly changing between positive and negative over time. During the transfer of information, a principle of

neuronal function in the CNS is that membrane potentials of large groups of neurons termed “ensembles” synchronize with each other (Buzsaki 2004; Buzsaki and Watson 2012). As neurons synchronize their membrane potentials they oscillate between polarized and depolarized states together as an ensemble. The important consequence of this synchronization is that large collections of neurons are polarized and depolarized together. That is, they are most likely to fire and not fire together at any given point in time. Thus, oscillations provide the fundamental neural framework for Hebbian plasticity and spike-timing dependent plasticity, as they provide a means for ensuring that an ensemble of neurons sends its action potentials to downstream anatomically-connected target cells at the same time (Figure 1.17). Since the principles of spike-timing dependent plasticity dictate that only signals arriving on target cells within a very small time window act constructively to depolarize and elicit target cell discharge, oscillations ensure that many spikes can arrive on a target cell at the same time in order to elicit firing and information transfer (Dan and Poo 2004; Buzsaki 2012). Thus, it is hard to overstate the importance of oscillations in providing a framework for neural communication, as without this means of synchronization, spikes would fall seemingly at random on target cells and these target neurons would never fire.

The oscillation of neural ensembles can take place at many different frequencies, which reflect different types of information processing in different regions (Figure 1.18) (Buzsaki and Draguhn 2004). In the hippocampus, theta (6-12 Hz), beta (12-30 Hz), gamma (30-140 Hz) and ripple (> 140 Hz) frequencies have all been observed. Although these various different oscillators have been observed, theta, gamma and ripple

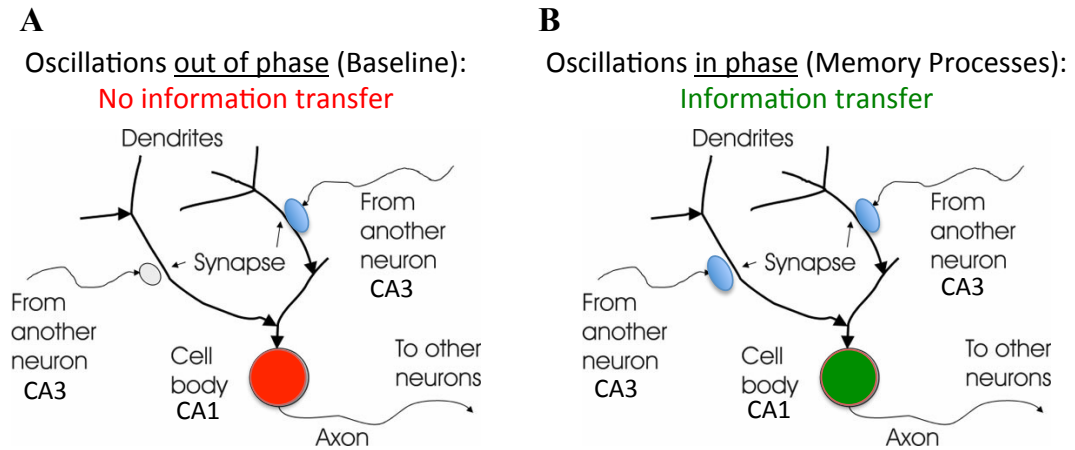


Figure 1.17. Oscillations Lay the Foundation for Spike-Timing Dependent Plasticity: They Serve to Turn Many Small Signals Into a Big Signal that Can Elicit Target Neuron Discharge.

The main point of oscillations is that provide a mechanism whereby a large ensemble of neurons can fire together in concert with one another. This is a vital property of neural communication, as it is well known that target neurons fire in response to the summation of all inputs at any given time along their somato-dendritic axis within a short time window. Thus, the more inputs a given neuron receives telling it to fire, the greater the likelihood that it actually fires (the converse is also true). A) Under baseline conditions with little neuronal synchrony, inputs to the examples CA1 cell come at random and it remains silent. B) Under memory processes when a high degree of neuronal synchrony is apparent, inputs can arrive onto the CA1 target cell at the same time and this summation of inputs gives rise to spike-timing dependent plasticity that enables target cell discharge and information transfer to take place.

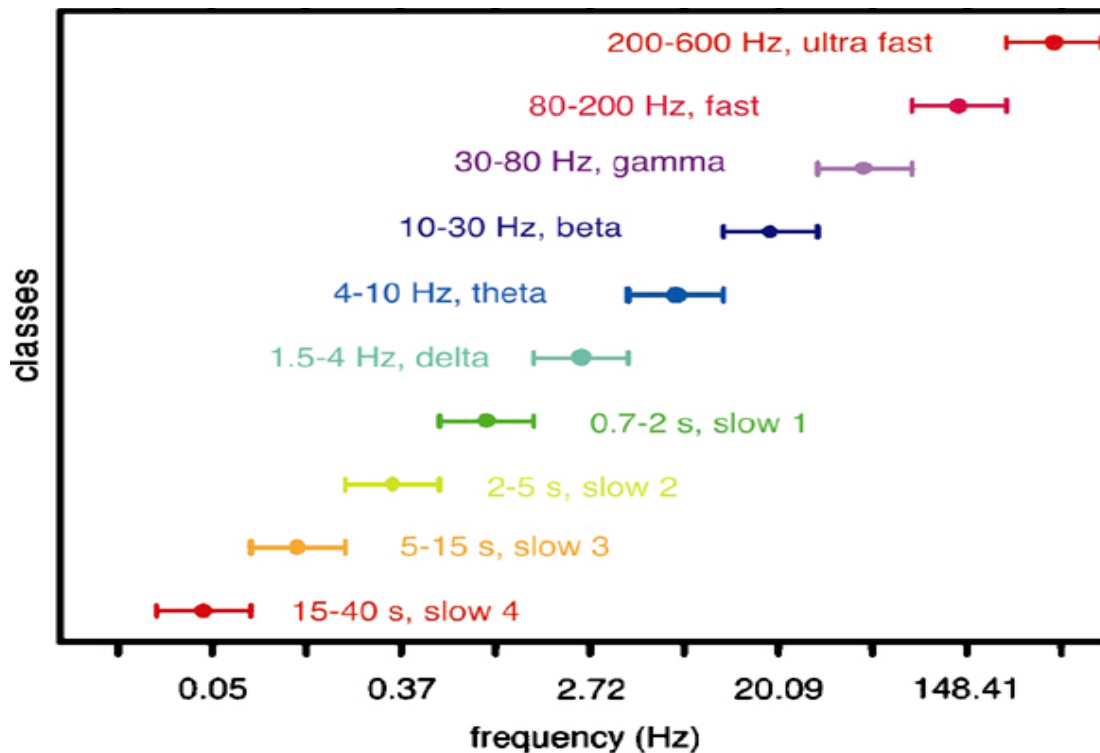


Figure 1.18. The Mammalian CNS Has Many Different Neural Oscillators Whose Frequencies Subserve Different Memory Processes.

Membrane oscillations act as timing mechanisms to organize neuronal communication in the brain. Large ensembles of neurons can synchronize themselves to a particular frequency, which creates an electrical signal large enough to measure called the Local Field Potential (LFP). Oscillations in the theta (4-10 Hz) and gamma ranges (30-200 Hz) are particularly important for memory processes mediated by the hippocampus. The longer wavelength oscillations are generally considered as a longer range (i.e. inter-regional) way of organizing neural ensembles, whereas the higher-frequency oscillations are generally reflective of very transient short-range local communication.

Image from: Buzsaki and Draguhn, 2004.

frequencies appear most prominently in the hippocampus (Mizuseki, et al. 2009; Sullivan, et al. 2011).

Theta, as previously described, is vital for entraining the hippocampus into a common baseline state for information processing to take place (Mizuseki, et al. 2009). Theta arises mainly from pacing and entrainment of the hippocampal subfields by the modulatory action of the medial septum cholinergic neurons, which express mAChRs. Thus, muscarinic antagonists such as atropine and scopolamine are capable of abolishing most theta observed at the level of the hippocampus. There is an atropine-resistant component of theta that is believed to be internally-generated by the hippocampus, however, it is clear from work with muscarinic antagonists that in the presence of compromised septal input with muscarinic antagonists spatial memory and representations are profoundly disrupted. Theta oscillations are observed during periods of movement or attention, termed t-theta and a-theta, respectively. The two types of theta are known to display distinct pharmacology relevant to this thesis, as t-theta is known to be the atropine-resistant component of theta, while a-theta is known to be the atropine-sensitive component.

Gamma oscillations occur at higher frequencies (30-140) and can be subdivided into a low gamma range (30-50 Hz) and high gamma range (90-140 Hz) (Colgin, et al. 2009; Buzsaki and Moser 2013). In particular, CA3 is known to communicate with CA1 at low gamma frequencies and this is thought to reflect processes of information retrieval by the hippocampus. Importantly, CA3 transmission has been shown to be modulated by cholinergic circuitry and mAChR signaling (Vogt and Regehr 2001). In contrast, EC has been shown to communicate with CA1 at high gamma frequencies, which is thought to

reflect ongoing memory encoding processes by the hippocampus (Giocomo and Hasselmo 2007; Hasselmo 2007). Importantly, CA3-CA1 connectivity has been shown to be under the control of muscarinic receptors, which act to suppress CA3-CA1 connectivity during states of memory encoding when EC-CA1 inputs are emphasized (Figure 1.19) (Giocomo and Hasselmo 2007; Hasselmo 1995, 1999, 2007). Additionally, M1 receptors have been shown to influence Hp gamma oscillations *in vitro* (Fisahn, et al. 2002). The precise subtype(s) of mAChR responsible for this suppression of CA3-CA1 activity are unknown and a central theme of this thesis. Since theta acts as a common organizational framework to entrain the entire hippocampus, it is an important observation that gamma oscillations occur nested inside theta cycles (Figure 1.20). Gamma has been proposed to act as a mechanism whereby memories are encoded and formed in the hippocampus. Specifically, during memory encoding both in rats (Figure 1.20) and primates (Jutras, et al. 2009; Jutras and Buffalo 2010), gamma band synchronization of hippocampal neurons is evident in response to behavioral task performance such as when rats are sniffing novel objects or primates are viewing novel scenes. The fundamental action of gamma oscillations, therefore, is to organize hippocampal pyramidal cell spiking inside individual phases of the theta wave in order to organize this information in a precise temporal fashion (Buzsaki and Moser 2013).

Oscillations and the degree of synchronization between brain regions can be used to measure the degree of functional connectivity between two regions (Brown, et al. 2004). That is, how strongly or weakly those two regions are functionally connected with one another. Such analysis relies upon measures of coherence, which is defined as how much the phase and amplitude of two oscillators co-varies in time (Figures 1.21 and 1.22).

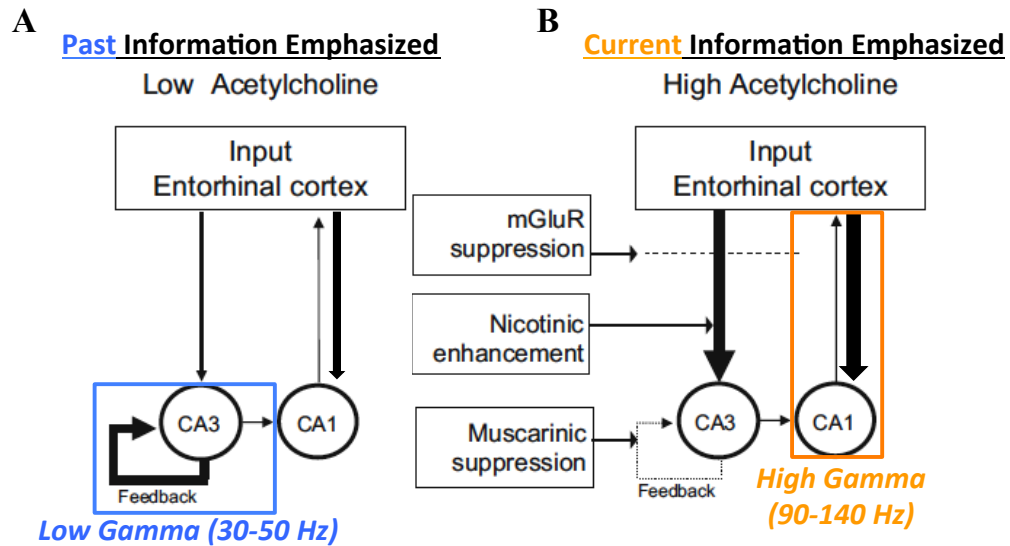


Figure 1.19. Intra- Versus Extra-Hippocampal Microcircuits Contribute to Different Aspects of Information Encoding, where Intrahippocampal Connectivity is Modulated by Muscarinic Receptors.

The hippocampus constantly toggles back and forth between encoding current information and retrieving past information and various neuromodulatory systems are critical for mediating this switch. With regard to the hippocampus, acetylcholine is undoubtedly one of the most important neuromodulators. Muscarinic receptors are known to play a role in suppressing intrahippocampal activity, although which subtypes underlie this are unclear. A) Under low acetylcholine levels, the hippocampus is primed for information retrieval where the auto-association network of the CA3 recurrent collateral system fires very robustly to CA1 in the low gamma range (30-50 Hz). B) Under high acetylcholine levels when the hippocampus is tasked with encoding new information the CA3 system is suppressed and deemphasized by muscarinic receptor signaling, while the entorhinal afferents into the hippocampus are potentiated with communication taking place in the gamma range (90-140 Hz).

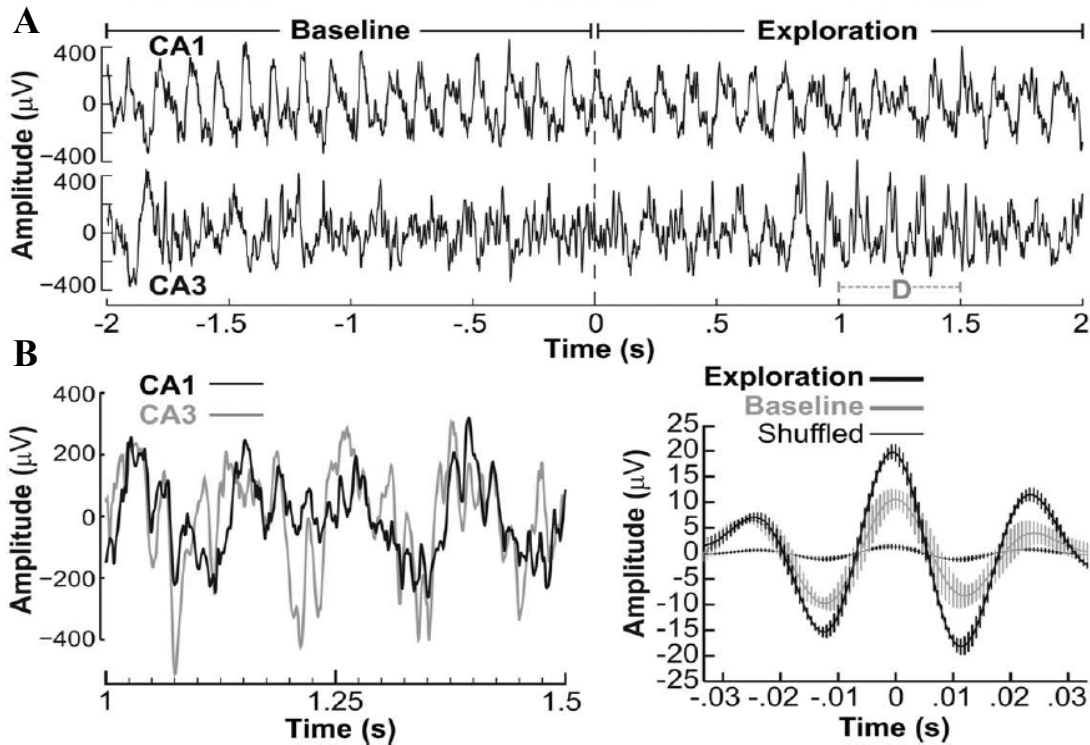


Figure 1.20. CA3 and CA1 Hippocampal Subfields Show Theta-Modulated Gamma Activity That Serves to Organize Pyramidal Cell Spiking During Behavior.

A,B) LFP traces showing prototypical CA3 and CA1 LFP oscillations under baseline conditions and a period in which an animal is engaged in a memory task (object exploration). Theta is a particularly prominent frequency observed as animals locomote, but also serves as a slower, longer wavelength frequency which can serve to organize higher-frequency, shorter wavelength oscillations (e.g. gamma) by nesting them inside of these larger theta cycles during memory processes. Panel B shows a zoomed in view of the 1-1.5s time period from panel A. In B the presence of the nested higher frequency gamma oscillations inside the theta waves becomes very apparent. Furthermore, the troughs of CA3 gamma oscillations tend to line up with the peaks of CA1 gamma oscillations, particularly during object exploration (B, right panel).

Image from: Trimper, et al. 2013.

The higher the phase and amplitude co-variance the higher the coherence is said to be between the two regions. Coherence analysis comes in one of two varieties: field-field coherence or spike-field coherence. Field-field coherence is the comparison of two LFP oscillations taken from two similar or different brain areas (e.g. CA3 and CA1) and asking how their phase and amplitude co-vary in time. Spike-field coherence on the other hand is the comparison of how regular the spikes of one region fall onto the phases of the LFP oscillation in another region (e.g. CA3 spikes onto a CA1 field oscillation). The higher the spike-field coherence the greater the regularity of the phases in which spikes fall onto phases of the target field oscillation.

Coherence measures can be calculated by subjecting the raw LFP recorded to a Fourier transform to dissect this LFP into its constituent frequency components that comprise it (Figure 1.22). The difference between field-field and spike field coherence is that a Fourier transform is applied twice (once to each LFP oscillation) in the case of field-field coherence and once in the case of spike-field coherence. For field-field analysis, one can then ask how much the phase and amplitude of each frequency band in the resulting spectrum from the Fourier transform co-varies in phase and amplitude over time. In so doing, a coherence value can be calculated for each frequency band and plotted in a broadband spectrum called a coherogram to display coherence across all frequency bands during a test session (Figure 1.23). For the work in the present thesis, this plot can be extended in order to control for the behavioral state of the animal, such as the animal's running speed since this behavioral state may impact the baseline coherence among these various oscillators or rather act to dictate drug responsiveness. In this vein, all of the LFP data from an entire test session can be broken down into short segments

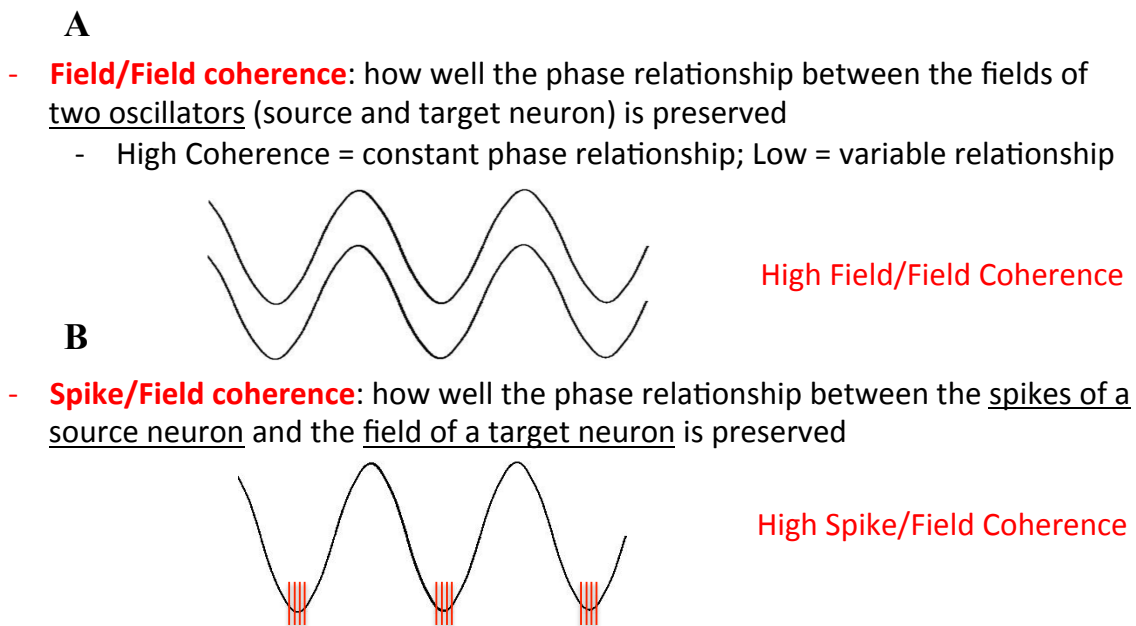


Figure 1.21. Coherence is a Measure of Functional Connectivity.

Coherence is a measure of the degree of functional connectivity between two different oscillators that reflects how well the phase and amplitude of the two oscillators co-vary with time. In the present case, these will be CA3 and CA1 hippocampal oscillators. A) Field-field coherence is when two LFP oscillations are compared (e.g. CA3 and CA1). If their phases and amplitudes closely match up over time, as the example oscillations in A do, the oscillators are said to be highly coherent. B) A second type of coherence one can calculate is spike-field coherence. This type of coherence compares how consistently spikes from a particular region (e.g. CA3) fall onto the field oscillation of another region (e.g. CA1). Unlike field-field coherence, spike field coherence can give much more information about the actual nature of the functional relationship being affected, as it deals with the actual action potentials (information) being transferred from one region to another.

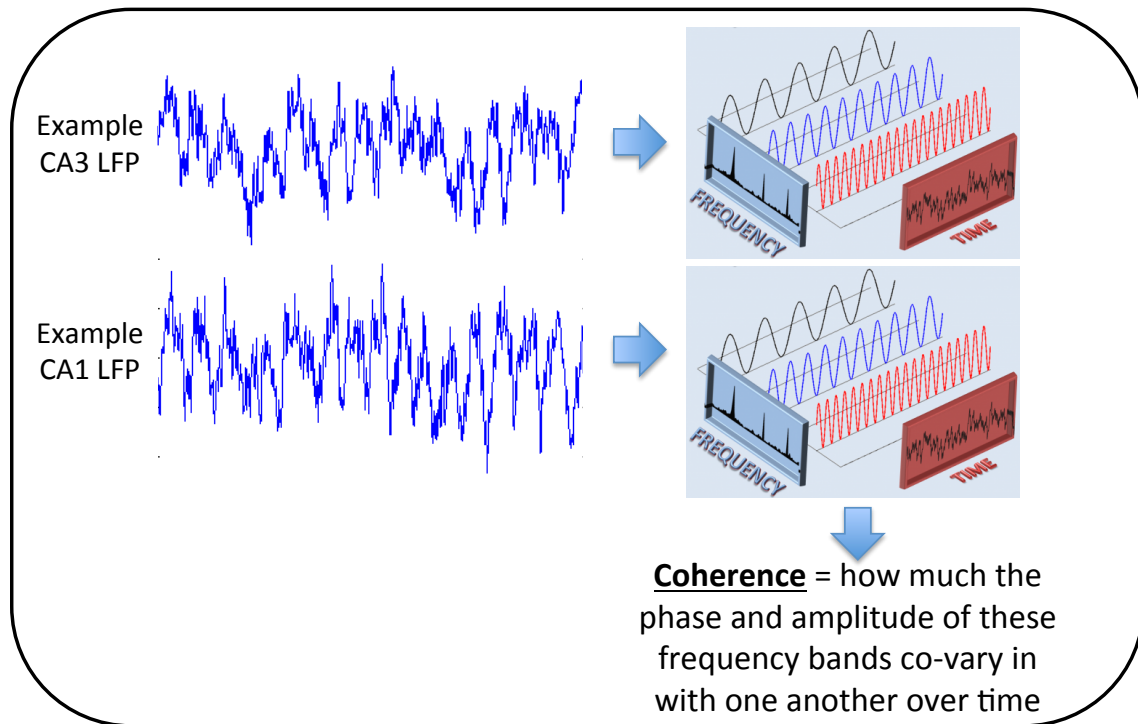
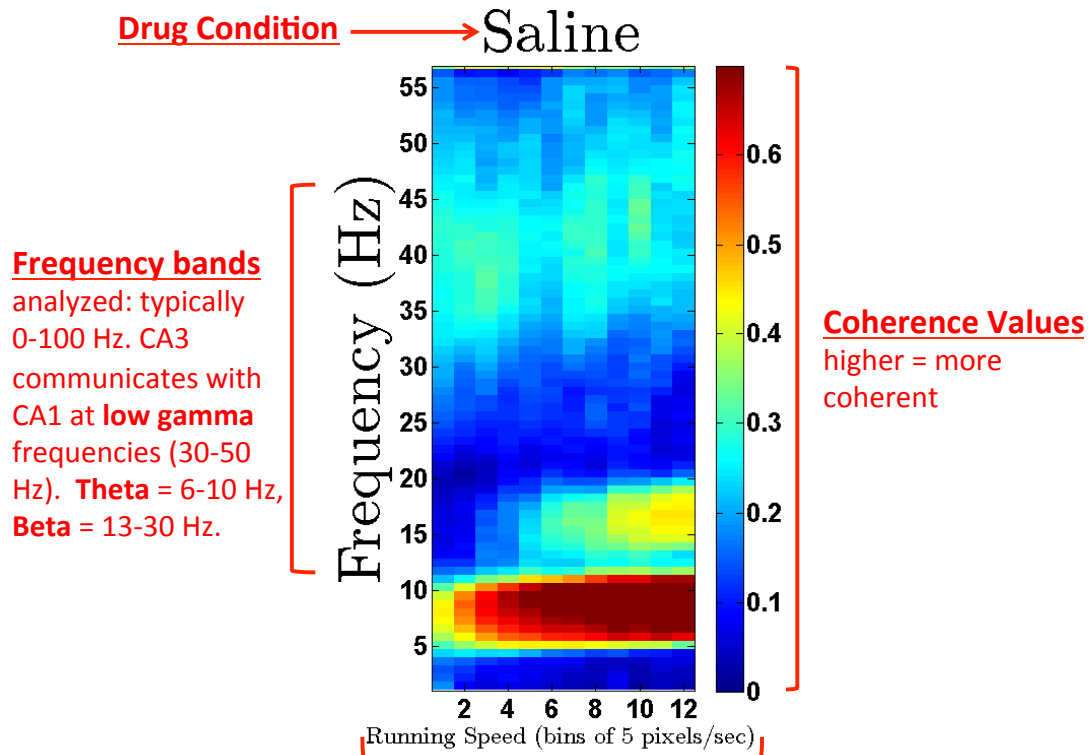


Figure 1.22. Coherence Reflects How Much Two LFPs Co-Vary in Time.

Field-Field coherence reflects how much the amplitude and phase of two LFP oscillations (e.g. CA3 and CA1) co-vary in time. The more they co-vary, the more highly coherent the two LFP oscillations are said to be. For coherence calculation, each LFP trace of interest is decomposed via a Fourier transform into its individual frequency components. The phase and amplitude co-variance can then be calculated across each of these frequency bands and compared between the oscillators over time to yield a coherence value.

Image from: <http://groups.csail.mit.edu/netmit/wordpress/projects/sparse-fourier-transform/>



Running speed (in bins of 5 pixels/sec): behavioral state may impact coherence, also drugs may have an effect (or not) depending upon behavioral state.

Figure 1.23. Coherograms are a Way of Simultaneously Depicting Coherence Across Many Frequency Bands of Interest.

Coherograms are a convenient way to display coherence values across a broad frequency spectrum. The above coherogram depicts frequency bands from 0-55 Hz and represents the coherence between a CA3 LFP oscillation and a CA1 LFP oscillation as a rat freely forages around various differently-shaped contexts for chocolate food rewards for approximately 1.5 hr. Coherence is depicted by a heat map along the right y-axis, with hotter colors representing higher coherence values. The dark red band from 6-12 Hz is indicative of coherence in the theta frequency, which an extremely prominent frequency since the animal is constantly locomoting for 1.5 hr. The middle yellow 13-20 Hz band is indicative of the beta frequency and the higher 30-50 Hz band is indicative of the low

gamma frequency. The low gamma frequency is of particular interest for the present work, as it is in this frequency range that CA3 is known to communicate with CA1. Finally, the LFP data is binned along the x-axis by running speed into bins of 5 pixels/second. This is crucial to control as much as possible for the behavioral state of the animal when deciphering how drugs might impact coherence values and in comparing data across animals (that is, one wants to compare equal behavioral states across animals).

(e.g. 1 second chunks) and assigned a running speed for how fast the animal was moving during that 1 second period. This data can then be binned according to running speed (e.g. bin size of 5 pixels/second) and then used to plot the coherogram. Importantly, by binning the data this way, data can be compared across animals for equivalent behavioral states (that is, equivalent running speed bins).

Proposed Research

The proposed studies will address memory impairments in aging and Alzheimer's Disease (AD) by focusing on cutting-edge mAChR activators: a highly-selective, best-in-class, M₁ mAChR agonist (VU0364572), and an M₁-selective positive allosteric modulator (PAM), BQCA. The goal of the research will be to test the hypothesis that selective M₁ activation can delay the onset of memory impairments and neuropathology in a mouse model of AD (Specific Aim 1) and to test the hypothesis that M₁-selective activation will improve the ability of hippocampal place cells to represent spatial information (Specific Aim 2). Previous studies indicate memory impairments in both aging and early AD arise from a decrease in cholinergic modulation of the hippocampus. In particular, M₁ knockout mice have documented hippocampal memory impairments and M₁ agonists have been found to robustly improve hippocampal memory. Although it is known that M₁ activators can improve memory, how exactly they act *in vivo* to mediate these effects is not known. Additionally, selective M₁ activators can reduce AD pathology both *in vitro* and *in vivo*. Therefore, selective M₁ activation has the potential to not only treat memory symptoms in aging and AD, but also prevent or delay AD onset. Here we assess the efficacy of two novel M₁ activators, VU0364572 and BQCA, in a

mouse model of AD and dissect the effect of M₁ activation on hippocampal circuits in freely-behaving rats. Specific Aim 1 will take place in mice since mice currently provide the greatest array of genetic models of AD to-date, specifically, the most aggressive rodent models of AD to-date. On the other hand, Specific Aim 2 will take place in rats since the physical size of rats means that one can record much larger collections of neurons simultaneously *in vivo*. Additionally, rats exhibit more robust behavior than do mice. Specific Aim 1 will take advantage of primary neuronal culture to assess the efficacy of VU0364572 and BQCA in lowering A β _{40/42} levels in hippocampal and cortical neurons transduced with human APP^{695WT}. These experiments in primary neurons will be used to guide selection of an optimal M₁ activator to use for chronic dosing in 5X FAD transgenic mice to ask if M₁ activation can slow or prevent the onset of AD pathology and spatial memory impairments when dosed through the developmental time window where neuropathology arises in these mice. Specific Aim 2 will use *in vivo* electrophysiology to record from hippocampal neurons in freely-moving healthy adult rats to test whether selective M₁ activation can improve the ability of hippocampal place cells to represent spatial information and whether this corresponds to a decrease in CA3-CA1 connectivity. This experiment will take advantage of the well-studied finding that many rat hippocampal pyramidal cells ("place cells") show spatially-specific receptive fields ("place fields").

Aim 1: To test the hypothesis that M₁ selective activators promote non-amyloidogenic APP processing in primary neuronal culture and that chronic

administration of a selective M₁ activator will improve spatial memory and reduce A β _{40/42} pathology in a 5XFAD mouse model of AD.

We predict that acutely dosing M₁ selective activators VU0364572 and BQCA will dose-dependently decrease A β _{40/42} levels in primary wild-type hippocampal and cortical neurons transduced with human APP695. We hypothesize that chronically activating M₁ in transgenic mice with VU0364572 will dose-dependently slow or prevent neuropathology and spatial memory deficits from arising in these mice. M₁ activator treatment is predicted to increase APP α levels in the brains of these mice with a concomitant reduction in A β _{40/42} levels.

Aim 2: To test the hypothesis that acute administration of the selective M₁ agonist, VU0364572, will increase the ability of hippocampal place cells to represent novel spatial information.

We predict that acute administration of VU0364572 will act to increase the ability of hippocampal place cells to code for space, thereby improving spatial memory and that this will correspond to a suppression in connectivity between CA3 and CA1.

The long-term goal of this work is to provide new small molecule drugs that will be effective in treating the memory impairments that accompany aging and AD and also delay the onset of AD. The outcomes of the proposed experiments will contribute critically to developing new therapeutic approaches to help treat memory dysfunction in aging and AD and also slow or prevent AD progression. Also, a better understanding of the role of individual mAChR subtypes—and how they can be leveraged therapeutically—at the network level will be gained from this work.

Chapter II. MATERIALS AND METHODS

Subjects for Transgenic AD Mouse Studies

5XFAD transgenic AD mice from Jackson Labs were utilized for this study (Oakley, H., et al. 2006). The 5XFAD strain is a double transgenic APP/PS1 strain that expresses five AD mutations. These mice bear Florida, London, and Swedish familial AD mutations in the gene coding for APP. Additionally, these mice bear M146L and L286V familial AD mutations in the PS1 gene. These mutations result in higher overall levels of A β , as well as increased production of A β 42, the major plaque forming species in AD. The 5XFAD mice show intraneuronal A β 42 at 1.5 months of age, amyloid deposition at 2 months, and memory deficits at 6 months (Eimer and Vassar). All procedures involving mice were approved by the Emory University Institutional Animal Care and Use Committee.

These mice were chronically dosed with VU0364572 (10 mg/kg, 30 mg/kg orally through drinking water) for 4.5 months (from age 1.5 months to 6 months). At 6 months, drug was washed out of the system for 24 hours, then the mice were behaviorally tested. Thus, no drug was on-board for any behavioral testing performed. Immediately after testing, the mice were perfused and brains were then collected, as described below.

Animal Perfusion

Mice were deeply anesthetized by delivering an overdose of sodium pentobarbital i.p. and monitored until no longer responsive to a toe pinch. Animals were then transcardially perfused with ice-cold normal saline for 4 minutes at a flow rate of 10

mL/min. Following perfusion, the brain was cut sagittally along the midline (Figure 2.1). One hemisphere was immediately snap-frozen on dry ice for biochemical analysis and placed at -80°C until analysis. The other hemisphere was immersion-fixed in 4% paraformaldehyde for 4 hr followed by cryoprotection in 30% sucrose until tissue sectioning.

Biochemical Tissue Fractionation

Fresh-frozen sagittal hemibrains were removed from -80°C storage after which neocortex and total hippocampus were microdissected from each hemisphere (Figure 2.1). Wet tissue weight for each cortex and hippocampus sample was recorded and tissue homogenized using a Konte's Dounce tissue grinder in phosphate-buffered saline with 1X protease inhibitor cocktail (Roche, Indianapolis, IN). Cortical samples were homogenized to a concentration of 150 mg/mL, whereas hippocampal samples were homogenized to a concentration of 100 mg/mL. Total homogenate was then sonicated for ~ 30 s using a microtip sonicator at 20% total amplitude. 2 % SDS was then added to the homogenate in order to enable soluble amyloid extraction. Homogenates were spun for 1 hour at $53,000 \times g$ at -4°C (Optima TLX Ultracentrifuge, Beckman-Coulter, Fullerton, CA) to separate soluble from insoluble amyloid species. The supernatant containing soluble amyloid was then collected and the pellet containing insoluble amyloid resuspended in 70% formic acid. Once resuspended, the insoluble fraction was re-sonicated as previously for ~ 30 s at 20% total amplitude. Individual tissue fractions were analyzed fresh and never subjected to more than one freeze-thaw

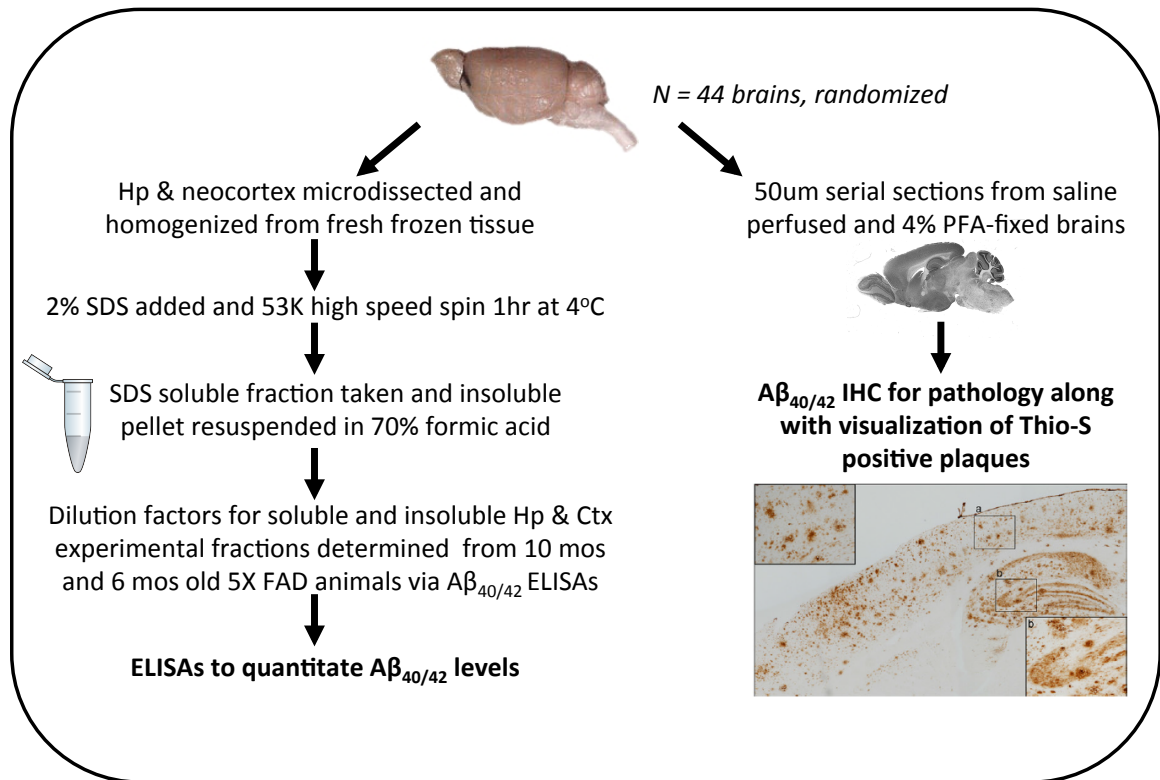


Figure 2.1. Terminal Pathology Processing.

Following behavioral testing, hemibrains from chronically-treated 5X FAD mice and WT littermate controls were harvested. One hemibrain was snap frozen and saved for biochemical analysis, while the other was immersion-fixed in 4% para-formaldehyde for sectioning. All hemibrains ($N = 44$) were randomized prior to analysis. For biochemical analysis, hippocampus and cortex were microdissected from brains, homogenized and then subjected to biochemical fractionation where soluble and insoluble amyloid fractions were collected. ELISA analysis on all fractions was then performed. Immersion-fixed hemibrains were serially-sectioned at 50 μm and then subjected to $A\beta$ immunohistochemical analysis.

cycle. All brains were randomized prior to microdissection so that experimenters were blinded during downstream biochemical analyses (e.g. A β ₄₀ and A β ₄₂ ELISAs).

Behavioral Testing

Morris Water Maze

Morris water maze training took place in a round, water-filled tub (52 inch diameter) in an environment rich with ambient cues in the testing room visible to animals navigating the maze. These ambient cues help facilitate the ability of animals to navigate the maze. Mice were placed in the water maze with their paws touching the wall from 4 different starting position (N, S, E, W) in water that started at 25° C and typically declined to 22° C by the time a whole group of mice was tested. An invisible escape platform was located in the same spatial location 1 cm below the water surface independent of a subject's start position on a particular trial. In this manner subjects are able to utilize ambient testing room cues to determine the submerged platform's location. Each subject was given 4 trials/day for 5 days with a 15-min intertrial interval. The maximum trial length was 60 s and if subjects did not reach the platform in the allotted time, they were manually guided to it. At the end of each day of testing, water was drained and the tank was cleaned with quatracide.

Upon reaching the invisible escape platform, subjects were left on it for an additional 5 s to allow for survey of the spatial cues in the environment to guide future navigation to the platform. After each trial subjects were dried and kept in a dry plastic holding cage filled with paper towels, which allowed the subjects to dry off. Following the 5 days of task acquisition, a probe trial was presented during which time the platform

was removed and the amount of time and distance swam in the quadrant which previously contained the escape platform during task acquisition was measured over 60 s. All trials will be videotaped and performance analyzed by means of MazeScan (Clever Sys, Inc.).

Cued and Contextual Fear Conditioning

Cued and contextual conditioning are fear conditioning tasks which measures the ability of a rodent to form and retain an association between an aversive experience and environmental cues. This task requires a slightly different set of sensory and motor abilities than the water maze and can be performed in a much more time efficient manner. While contextual fear conditioning tests solely hippocampal circuitry, cued fear conditioning tests both hippocampal and amygdala circuitry.

Fear conditioning took place over a period of three days. Animals were placed in the fear conditioning apparatus (Colbourn) and allowed to explore the enclosure for 3 min. Following this habituation period 3 conditioned stimulus (CS)-unconditioned stimulus (US) pairings were presented with a 1 min intertrial interval. The CS consisted of a 20 second 85 db tone and US consisted of 2 seconds of a 0.5 mA foot shock which co-terminated with each CS presentation. One minute following the last CS-US presentation animals were returned to their home cage. On day 2 the animals were presented with a context test during which subjects were placed in the same chamber used during conditioning on Day 1, and the amount of freezing was recorded via a camera and the software provided by Colbourn. On day 3, a tone test was presented during which time subjects were exposed to the CS in a novel compartment. Initially

animals were allowed to explore the novel context for 2 min. Following this habituation period the 85 db tone was presented for 6-min and the amount of freezing behavior recorded.

Immunohistochemistry

Sagittal hemibrains (Figure 2.1) were removed from storage in 30% sucrose and serially-sectioned at a thickness of 50 μm on a freezing stage sliding microtome. Sections were immediately submerged in cryoprotectant and placed at -20°C until analysis. For immunohistochemical staining 6 consecutive tissue sections were taken from equivalent depths across all mice enrolled in the 5X FAD chronic dosing trial.

For immunohistochemical analysis, free-floating brain sections were then rinsed in 0.1 M phosphate buffer pH 7.2 (PB) 5 times x 5 min. Next, PB was used to dilute 30% H_2O_2 (Sigma) to 3%. Tissue was washed with 3% H_2O_2 for 15 min in order to remove any endogenous peroxidase activity, after which the sections were again rinsed with PB 5 x 5min. Sections were then blocked with a solution of 10 $\mu\text{g}/\text{mL}$ avidin (1:1), 8% normal serum, and 0.1% Triton-X in TBS. Sections were blocked for 1 hour at 4°C , then rinsed with TBS 3 x 5min. Primary antibody incubation then took place in a solution of 50 $\mu\text{g}/\text{mL}$ biotin, 2% normal serum, and $\alpha\text{-hA}\beta_{1-40}$ (rabbit polyclonal, BioSource Invitrogen, Carlsbad, CA, 1:5000) or $\alpha\text{-hA}\beta_{1-42}$ (rabbit polyclonal, BioSource Invitrogen, Carlsbad, CA, 1:1000) in TBS. Incubation in the primary antibody solution took place for 48 hr at 4°C with shaking.

Following primary incubation, tissue was rinsed with TBS 4 x 5min. Sections were then incubated with a biotinylated secondary antibody (bG α Rb) for 3 hours at 4°C

with shaking and washed again with TBS 4 x 5 min. Secondary signal was then visualized using the avidin-biotin-peroxidase complex (ABC) method (ABC kit; Vector Labs, Burlingame, CA). ABC reagent was prepared according to the manufacturer's instructions in TBS and allowed to stand on ice for 30 min prior to use. Sections were then incubated in the ABC solution for 1 hr with shaking at 4°C. Sections were then rinsed 4 x 5 min with TBS and stained with diaminobenzidine (DAB). Following DAB staining, tissue was removed and rinsed with TBS 4 x 5 min. Brain sections were then mounted on precleaned Superfrost Plus slides (Fisher) in 0.1 M NaNO₃. Slides were then allowed to air dry after which they were then immersed in dH₂O 3min, 70% ethanol 3min, 95% ethanol 2 x 3 min, 100% ethanol 2 x 3 min, and Histoclear 3 x 3 min. Slides were then coverslipped with DPX and allowed to dry overnight.

Immunohistochemical Quantification

To quantify hA β ₄₀ and hA β ₄₂ immunoreactivity, cortex and hippocampus were photographed at low power (4X) from each of 6 consecutive sections stained for either hA β ₄₀ or hA β ₄₂. Total A β ₄₀ and A β ₄₂ immunoreactive surface area was then measured in a blinded manner using MetaMorph 5.0 software (Molecular Devices).

A β ₄₀ and A β ₄₂ ELISA

hA β ₄₀ and hA β ₄₂ levels in conditioned media from primary neuronal cultures and tissue homogenates from biochemically-fractionated mouse brains (Figure 2.1) were measured using human A β ₄₀ and A β ₄₂ ELISA kits according to the manufacturer's protocols (Biosource, Invitrogen). Insoluble amyloid fractions from mouse tissue

homogenates containing 70% formic acid were first neutralized by performing a 1:100 dilution in a solution of 1.0 M Tris (pH 11) prior to performing dilution series in ELISA diluent buffer supplied with ELISA kits. Soluble amyloid fractions were diluted as normal directly in ELISA diluent buffer. Plates were read at 450 nm using a Spectra Max Plus plate reader (Molecular Devices, Sunnyvale, CA).

Drugs for Transgenic AD Mouse Studies

VU0364572 was synthesized as a mono-HCl salt and provided as a jet-milled powder to aid in drug solubilization and systemic absorption. All drug was kindly provided by P. Jeffrey Conn and Craig Lindsley in the Vanderbilt Center for Neuroscience Drug Discovery (Vanderbilt University, Nashville, TN). Due to the documented oral bioavailability of VU0364572, drug was delivered to transgenic mice ad lib. in their drinking water from 2 months of age to 6 months of age. Mice had continuous access to drug-treated water at all times during this 4-month dosing window. Mouse cages were coded so that experimenters testing transgenic 5X FAD mice were blinded to treatment.

Determination of CNS VU572 Concentrations for Chronic Dosing

Doses of 10 mg/kg and 30 mg/kg VU572 were delivered ad lib. to wild type B6SJL mice (the genetic background that the 5X FAD mice are on) for 5 days. Doses were calculated based upon the average weight of mice (30 grams) and the average volume of drinking water a mouse was found to consume during a given 24 hour period (4 mL). Determination of doses in this manner was used to calculate doses of 10 and 30

mg/kg/day. Following this 5 day dosing to steady-state, mice were decapitated, brains removed and immediately washed with ice-cold phosphate-buffered saline, and brains then immediately frozen on dry ice until analysis. Trunk blood was immediately collected in EDTA Vacutainer tubes and plasma was separated by centrifugation and stored at -80°C until analysis. Treatment groups consisted of 6 mice per group.

Pharmacokinetic analysis of samples for plasma and tissue VU572 concentration was as described previously (Lebois, et al. 2010).

Primary Neuron Culture

Cortical and hippocampal neurons were isolated from mouse pups harvested from an E18 pregnant C57Bl/6 dam. Embryos were dissected and then cortical hemispheres and hippocampi were isolated in dissection buffer (Hanks Balanced Salt Solution (HBSS), 10 mM HEPES, 1 penicillin/streptomycin). The cortices and hippocampi were then pooled in separate tubes, whereupon they were digested with 0.25% trypsin (Gibco) and 0.01% deoxyribonuclease in dissection buffer for 15 min at 37°C. Following digestion, the tissue was rinsed gently twice with dissection buffer and twice with plating media (buffered MEM (Gibco), 0.6% glucose (Gibco), 2 mM L-glutamine (Cellgro), 10% heat-inactivated horse serum, and 1% penicillin/streptomycin). After rinsing, the tissue was then mechanically-dissociated with large bore and small bore fire-polished Pasteur pipettes. The tissue was triturated 10 times with a large bore pipette, followed by another 10 times with a small bore pipette.

Once dissociated, the neurons were seeded on 12-well poly-L-lysine plates in a volume of 1 mL high-glucose plating media at 80,000-100,000 cells/cm² for 2.5 hours

(Davis, et al. 2010). Following seeding, an additional 2.5 mL of neurobasal (Gibco) growth media was added gently to the wells containing B-27 growth supplement (Gibco), 2 mM L-glutamine, and 1% penicillin/streptomycin at 37°C, 5% CO₂. On day 2 in vitro, the neurons were then transduced with a human amyloid precursor protein (hAPP) cassette using lentiviral delivery for 72 hours. Following transduction, the cells were treated with a vehicle and a dose response of VU0364572 (10µM, and 30µM). These cells were incubated in neuronal growth media containing drug for 16 hours and then cell lysates and conditioned media containing extracellular Aβ were collected, as previously described (Davis, et al. 2010).

Lentiviruses expressing hAPP⁶⁹⁵ were packaged by calcium phosphate triple transfection of HEK293FT cells with the transgene/FUW cassette Δ8.9 HIV-1 packaging vector and pVSVG envelope glycoprotein. High titer (~1 x 10⁹ infectious virus particles/mL) virus was then used to transduce primary neurons.

Statistical Analyses

For all behavioral, primary culture data and ELISA data, graphs were generated using GraphPad Prism 4.0. For all of the above experiments, strong data exists in the literature which enabled us to strongly hypothesize with confidence that VU0364572 would mediate beneficial effects on tests of hippocampal memory and decrease amyloid levels. All p-values reported for these tests are two-tailed p-values. For analysis of Morris water maze probe data, ELISA data from primary culture conditioned media, and ELISAs run on 5X FAD tissue fractions, unpaired t-tests were used to compare vehicle treated groups with drug-treated groups. Due to the small number of subjects in the drug

treatment trial of 5X FAD mice, outlier detection/exclusion was performed using a test of Median Absolute Deviation (MAD), which is much less biased by any outliers themselves than tests which rely upon standard deviations from the mean (Leys, C., et al. 2013). Samples with a $MAD > 3$ were excluded as outliers.

Drugs for *In Vivo* Electrophysiology Studies

VU0364572 and BQCA were synthesized and obtained from the Vanderbilt Center for Neuroscience Drug Discovery, as previously described (Ma, et al. 2009; Shirey, et al. 2009; Lebois, et al. 2011). VU0364572 was formulated as a mono-HCl salt, whereas BQCA was formulated as a sodium salt. Since VU0364572 has previously been shown to be very water soluble and have excellent brain penetration following oral and systemic dosing, the present work utilized an oral dose-response of VU0364572, dissolved in water and delivered in strawberry Jell-O (pH 6.5) (Lebois, et al. 2011). Based upon the pharmacokinetics of VU0364572, drug delivery took place 30 minutes prior to testing. BQCA was delivered subcutaneously in all instances 30 minutes prior to testing in a solution of 20% 2-hydroxypropyl-beta-cyclodextrin in water (pH 6.5-8.5) (Ma, et al. 2009). Donepezil-HCl (Tocris) was dosed according to previous studies showing efficacy in Morris water maze testing (REFS). Donepezil formulation took place identically to VU0364572, with drug being dissolved in water and then being delivered in strawberry Jell-O (pH 6.5) 30 minutes prior to testing. Scopolamine (Sigma) was subcutaneously in a solution of saline (pH 6.5-8.5). All drugs were adjusted to target pH using solutions of 1 N NaOH and 1 M HCl.

Subjects for *In Vivo* Electrophysiology Studies

Three 8-13 month old Fisher 344 x Brown Norway hybrid rats were utilized for *in vivo* electrophysiology studies. Rats were trained to navigate a morph box for scattered chocolate food rewards. Training consisted of rats navigating a square-circle-square shape sequence and rats were considered to have reached criteria when they evenly covered the surface area of the testing enclosure multiple times for 20 minutes in each shape (1 hour of running total). During testing and training rats were always given approximately a 5 minute break from activity between morph shapes. For drug testing, rats were tasked with navigating a square-octagon-hexagon-circle-square sequence for the same scattered chocolate food rewards in order to contrast hippocampal representations of current information (octagon-hexagon-circle shapes) with familiar previous information (square shape). All procedures involving rats were approved by the Emory University Institutional Animal Care and Use Committee.

Morph Box Open Field Exploration Task

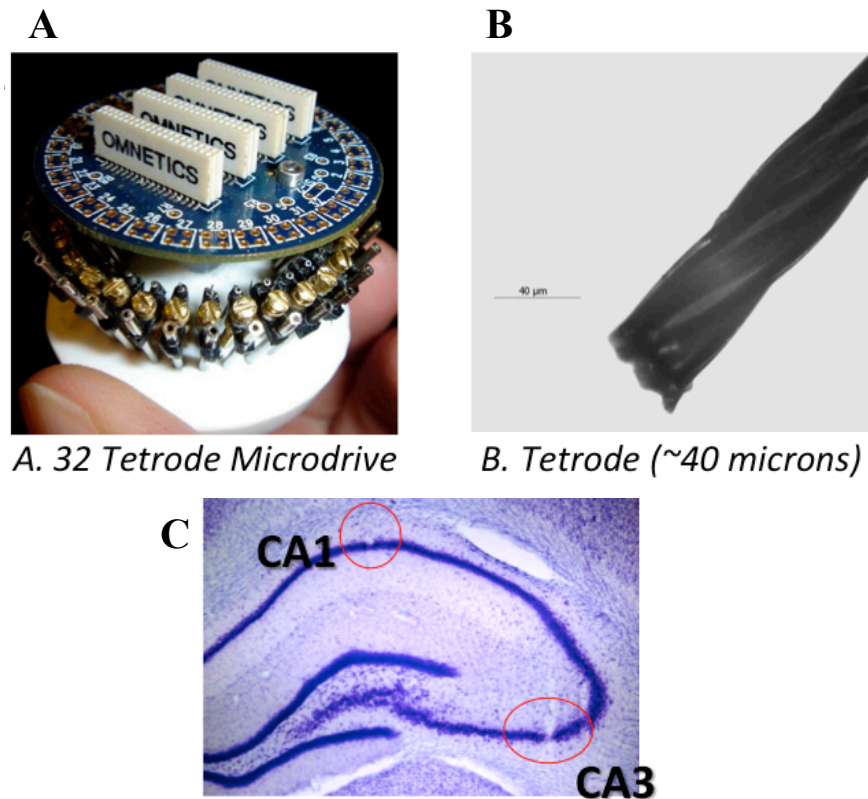
In order to examine drug effects on spatial representations in the hippocampus, place cell activity was manipulated using a morph box approach, as taken by previously laboratories (Leutgeb, et al. 2005; Leutgeb, et al. 2007). The morph box was constructed of segmented panels that were all hinged together so that the box could be changed into each respective test session shape: square, octagon, hexagon, and circle. The square measured 30 cm (*l*) x 30 cm (*w*) x 20 cm (*h*) and was composed of 6 panels per side. The height of the box measured 30 cm and was tall enough that the rats could see neither the testing room nor the experimenter as they were navigating each shape. The entire interior

of the box was painted black and no other extra cues besides the materials used in constructing the box were introduced. The seams were covered on the outside of the box with flexible black rubber strips so that the rats could not see out between the panels that made up the walls of the testing enclosure.

Rats were allowed to habituate on the stool for 15 minutes prior to testing. During testing, rats were free to explore each contextual shape for 15 minutes as the experimenter stood outside the testing enclosure tossing chocolate pellets (Bioserv) randomly about the testing enclosure. The goal in tossing the pellets was always to have the rats explore the entire surface area of the testing enclosure multiple times throughout each shape. At the end of 15 minutes, the experimenter removed the rat from the testing enclosure and transferred the animal to an adjacent stool for 5 minutes of rest while the shape was changed to the next shape in the test sequence. Data were analyzed for test sessions in which rats fully covered the entire surface area of all test enclosures so that any difference in place fields that may have occurred did not result simply from a rat not exploring a particular area of a test shape.

Surgeries and Positioning of Recording Electrodes

Rats were implanted with custom-built, high-density 32 tetrode recording arrays (Figure 2.2A and B) over the right dorsal hippocampus with 16 tetrodes targeting dorsal CA1 and 16 tetrodes targeting dorsal CA3. Each tetrode (Figure 2.2B) was comprised of four 12.5 μm nichrome wires whose tips were subsequently gold-plated to 200 k Ω at 1 kHz in order to bring the impedance of the wires into an appropriate range for recording and separating single neuronal signals (Figure 2.3A-C). Prior to stereotaxic surgery, rats



Example recording sites in CA1 and CA3

Figure 2.2. 32-Tetrode Microdrive Permits High-Density Neuronal Recording From the Rodent Hippocampus.

Custom-built tetrode recording implant for high-density recording of hippocampal pyramidal cells. A) Close-up of the exact design of the micro-drives that are utilized in the present study. Each drive contains 32 independently-adjustable tetrodes wired to an electrode interface board. B) Close-up of one individual tetrode showing the bundle of 4 individual wires that comprise a given tetrode. C) A cresyl-violet stained coronal section through the dorsal hippocampus, showing the target regions of interest: the dorsal CA3 and CA1 subfields. The red circles show representative electrolytic lesion marks that are made following recording from an animal in order to localize the final position of particular tetrodes in the hippocampus.

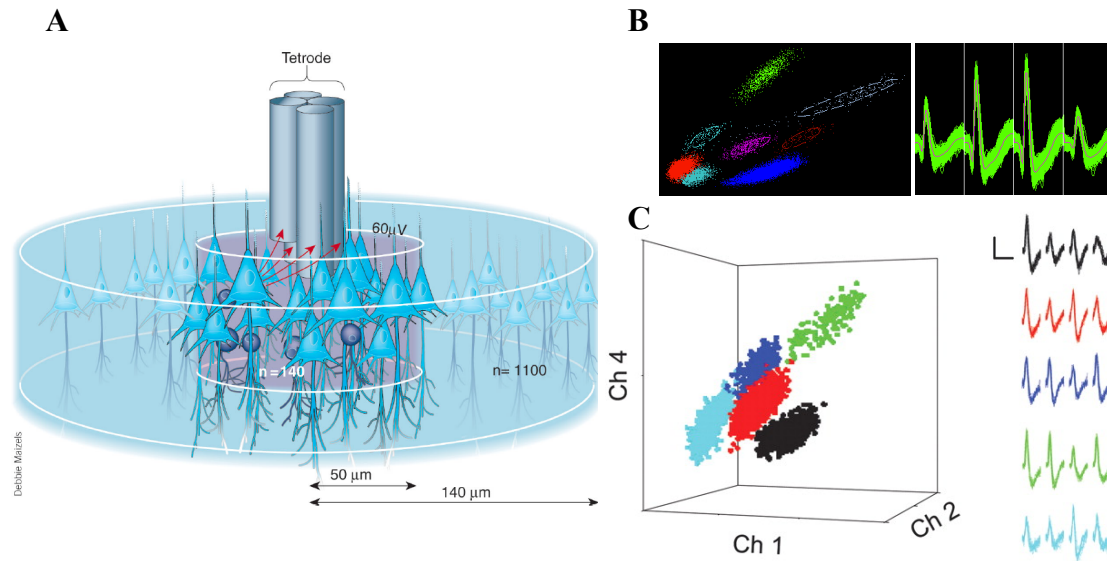


Figure 2.3. Tetrode Recordings Allow for Optimum Single Unit Isolation.

A) Schematic showing the advantage of using tetrodes to record from neurons. By using a bundle of 4 wires, the amplitude of signal from any given neuron will vary as a function of distance from each wire of the tetrode. Thus, a particular cell will give an activity “fingerprint” across all 4 wires over time that can distinguish it from other neurons in the same manner. B, C) The right panels show the neuronal waveforms with peak amplitudes across all 4 wires of a given tetrodes (wires 1, 2, and 4 in this case). The left panels show the peak amplitudes from 3 of the wires plotted in 3-dimensional space. This method of plotting peak amplitudes causes the spikes from single units to group into distinct “clusters” in 3-dimensional space, whereby they can then be separated from each other for analysis.

Image A and C from: Buzsaki, 2004.

were deeply anesthetized with isoflurane (1-3% in oxygen) and given a s.c. dose of buprenorphine (0.05 mg/kg) as a pre-operative analgesic. Craniotomies were performed 3.8 mm posterior to Bregma and arrays fixed over the craniotomy window using dental acrylic in order to anchor the recording implant to a ring of skull screws drilled into the skull. A stainless steel ground screw anchored in the skull above the cerebellum served as the electrical grounding for the tetrode array. Immediately following implantation, CA1 tetrodes were lowered 1 mm and CA3 tetrodes lowered 1.5 mm towards their targets. Rats were then administered a post-operative dose of buprenorphine (0.05 mg/kg) and 0.75 mL metacam to help alleviate post-operative pain and inflammation. Following a 1-week recovery period and over the course of the next several weeks thereafter, rats were re-trained to criteria on the morph box task and tetrodes advanced towards CA1 and CA3 subfields of the hippocampus. During testing, tetrodes were never turned on the day of testing so that the firing properties of neurons were stable during all test sessions. For recording of both CA3 and CA1 local field potentials (LFP), data was taken from tetrodes that were not moved during all days of testing so that any differences that resulted in the LFP could be attributed to the effect of drugs rather than tetrodes simply moving relative to pyramidal cells. For all LFP analyses, tetrode pairings were taken between tetrodes positioned in the medial third of the proximal-distal axis (relative to the dentate gyrus) of both CA3 and CA1. The medial third was chosen because the microcircuitry of the hippocampal subfields is such that medial CA3 shares the greatest connectivity with medial CA1. Additionally, this middle third receives input from both medial and lateral entorhinal cortex, reflecting a blending of spatial and nonspatial input (Witter and Amaral, 2004).

***In Vivo* Electrophysiology Data Acquisition**

Recordings were gathered using the NSpike data acquisition system (nspike.sourceforge.net) in order to simultaneously record local field potentials (sampling rate = 1500 Hz; bandpass filter 1-400 Hz) and spiking data. For animals whose recordings included a detectable 60 Hz electromagnetic noise artifact, a 60 Hz sine wave was fit to the local field potential data and then subtracted. Importantly this impacts a very targeted and narrow frequency range of ~59.9-60.1 Hz.

***In Vivo* Electrophysiology Data Analyses**

Place Field Analyses and Spatial Discrimination Scores

Test enclosure surface area was broken into a grid of boxes spanning 8 square pixels in order to downsample the space in which the animal could possibly be occupying at any given time. The movement trajectory of the rat was obtained by tracking the X-Y position over time of a red and green LED light affixed to the animal's head. Firing rate maps were calculated based upon the number of spikes that occurred in a given spatial bin divided by an animal's dwell time in that bin. In plotting place fields, this rate map was then subjected to Gaussian smoothing with a kernel size of 4 in order to visualize place fields.

In order to calculate spatial discrimination (SD) scores, the place field rate maps were plotted for each recorded cell across all 5 spatial contexts that comprised a given test session. Bin-by-bin correlations were then performed between the initial square enclosure (SC_1) and all subsequent contexts (SC_{1v1}) and (SC_{1v234}), with (SC_{1v1}) representing the spatial correlation between initial and final square contexts and

(SC_{1v234}) representing the mean spatial correlation of the initial square context with intervening octagon, hexagon and circular contexts. The mean spatial correlation between initial square and all intervening contexts was used since place cells appeared to recognize these middle contexts as “different” from the square, but not necessarily characteristically different in any consistent manner between cells. The degree to which place cells discriminated the intervening novel contexts was given by the following spatial discrimination score:

$$SD = \frac{(SC_{1v1} - SC_{1v234})}{SC_{1v1}}$$

where higher SD scores reflect a greater degree of discriminating the intervening octagon, hexagon, and circular contexts by place cells. A SD score of 0 indicates that the activity in the middle shapes did not change from the initial square shape and thus represents no discrimination of the contexts by place cells.

Spatial Information Analyses

Spatial information scores were computed according to the spatial information measure introduced by Skaggs, et al. (1993). The spatial information score I represents the extent to which one can use any given cell’s firing in order to predict the position of the rat (Skaggs, et al. 1993) and is reflected in units of bits per spike:

$$I(R|X) \approx \sum_i p(\vec{x}_i) f(\vec{x}_i) \log_2 \left(\frac{\vec{x}_i}{F} \right)$$

where $p(\vec{x}_i)$ is the probability that a rat occupies location \vec{x}_i at a given time, $f(\vec{x}_i)$ is the cell’s firing rate observed at location \vec{x}_i and F is the overall firing rate of the particular cell.

Relation of Local Field Potentials to Behavior

The analysis of local field potentials for this work focused on oscillatory activity recorded during animals engaging in bouts of open field exploration. Since any given animal's behavioral state is wildly fluctuating over time (e.g. an animal can be running very fast at one instant and then sitting still in the corner the next instant), all LFP data for an entire test session (1.5 hours) was segmented into 1 second chunks and binned according to the average running speed of the animal in pixels/second during that chunk. Plotting spectral data by running speed bins thus permits the comparison of equal running speed bins across animals to control for behavioral state.

Field-field and spike-field analysis of local field potential data was largely carried out assisted by the open source signal processing library, Chronux, for calculating coherence and other spectral estimates (Bokil, et al. 2010). Multitaper analyses were used (rather than a single taper fast Fourier transform) since they allow for a reduction in the variance and bias in calculating spectral estimates (Bokil, et al. 2010). For a sample of local field potential data spanning T seconds, $2TW-1$ orthogonal tapers (discrete prolate spheroidal sequences known as Slepian Sequences) were used that were concentrated in the frequency bandwidth $-W$ to $+W$ (Slepian 1978).

Analyses of Hippocampal Synchrony

Power analyses were performed in order to quantify the amount of a particular frequency of interest under drug treatment. Coherence analyses for CA3-CA3, CA1-CA1, and CA3-CA1 were also performed, whose estimates reflected functional connectivity within and between hippocampal subregions (e.g. Mitra and Pesaran, 1999). Coherence

reflects the degree to which the phase and amplitude of two oscillations (e.g. a CA3 oscillation with a CA1 oscillation) co-vary in time, with higher coherence values reflecting stronger functional connectivity. Coherence for the present study was based upon the phase consistency and amplitude in each 1 second bin of local field potential data taken from a particular test session. In order to allow comparison across treatment conditions, coherence values were Fisher transformed and bias-corrected (Bokil, et al. 2007), whereas power estimates were \log_{10} transformed. Notably, the transformed and bias corrected estimates differed very little from the original coherence estimates.

For spike-field analyses, pyramidal cells were included which had between 100-20000 spikes emitted in a test session. The lower limit of 100 spikes was designated to eliminate units with very low spike counts which may bias coherence estimates and the upper limit of 20000 spikes was set to restrict the analyses to pyramidal cells and filter out interneurons. Spike-field coherence estimates were obtained using Chronux, as well as Fisher transformed and bias corrected, as described above. Spike-field analyses were restricted to the theta range since theta oscillations are by far the most prominent frequency present during open field exploration test sessions.

Since spike-field coherence is a biased estimate, another statistic called the pairwise phase consistency was also used in order to determine how coherent information being sent from one region to a target region is (e.g. spikes from CA3 to field oscillations of CA1). The pairwise phase consistency is calculated as the average dot product of the angular distance between spike pairs for a given unit (Vinck, et al. 2010).

Statistical Analyses

Statistical analysis was carried out using GraphPad Prism 4.0 software. For spatial discrimination analysis of place cells and spatial information scores, data were combined for all animals and t-tests taken performed between saline and drug conditions in order to determine significance of drug treatment. For field-field coherence, a single mean coherence value from running speed bins 4-10 was taken for low gamma and theta ranges and plotted for each animal in order to test for significant differences using a two-tailed t-test. Pairwise phase consistency (PPC) values were combined for all units with > 100 spikes in each of running speed bins 4-10 and a two-tailed t-test used to compare the significance of saline PPC values to drug sessions.

Electrolytic Lesioning

Following the last test session for each rat, every tetrode from which data was recorded was used to electrolytically lesion the brain (Figure 2.2C). Rats were deeply anesthetized with isoflurane and currents of 20-40 μA were passed through each of these tetrodes for 20 s to lesion the pyramidal cell layer, which served to mark the final position of each tetrode in the brain. Adjacent tetrodes from which data was recorded were staggered with regard to the size of the current they received during lesioning (e.g. one tetrode would receive 40 μA , whereas its neighbor would receive 20 μA). This staggering of electrical current during lesioning enabled these tetrodes that were closer in space to be more easily distinguished during histology by virtue of their different small versus large lesion sizes.

After the last lesion was performed, rats were administered a lethal dose of euthanasia solution (Euthasol) and transcardially perfused for 4 min with normal saline in order to remove all traces of blood from the systemic circulation. Following saline, the animals were then perfused for 15 minutes with formalin in order to fix the brain inside the skull. Once fixation was complete, tetrodes were completely retracted to the surface of the skull and the brain was removed and placed in formalin for at least 48 hours. The brain was then subsequently placed in 30% sucrose for cryoprotection until it sunk to the bottom of the vial. Following cryoprotection of brains in 30% sucrose, the brains were then blocked in the coronal plane and serial sectioned at a thickness of 50 μm on a freezing stage sliding microtome. Sections were then mounted on slides and histochemically stained with cresyl violet in order to localize tetrode lesion marks.

Chapter III: *IN VITRO* AND *IN VIVO* EFFECTS OF SELECTIVE M₁ AGONISTS ON NEUROPATHOLOGY AND BEHAVIORAL DEFICITS IN A CHRONIC, PREVENTATIVE TREATMENT TRIAL OF TRANSGENIC AD MICE

Introduction

M₁ muscarinic receptor activation has been thoroughly demonstrated to play a critical role in the regulating APP processing in order to promote non-amyloidogenic APP cleavage and abrogate A β peptide formation. However, only recently has the first ever M₁-specific agonist, VU572, been identified and whether this compounds is able to influence APP processing in a similar manner to other M₁ activator chemotypes remains to be seen. Due to the fact there is no effective disease-modifying treatment available for AD, it is urgent that the potential for disease-modification of VU572 be critically evaluated in physiologically-relevant systems. By examining the effects of VU572 on APP processing in cultured mouse embryonic hippocampal and cortical neurons engineered to express hAPP^{695WT} we can establish the disease modification potential for VU572 and obtain the necessary proof-of-concept for advancing this compound *in vivo* to an aggressive mouse model of AD.

Furthermore, with the widespread failure of clinical trials aimed at disease-modification for AD to-date, the emphasis is rapidly shifting to “earlier” for clinical trial design. That is, investigators are looking to deliver therapies in the 20-year asymptomatic period of progressive neuropathology that precedes the onset of clinical AD symptoms, as opposed to an AD brain that has already been significantly and irreversibly damaged. Therefore, an outstanding and very timely question is whether or

not M_1 activation represents a viable mechanism for activation in prodromal AD in order to slow or halt the clinical disease timecourse. Does chronic delivery of a selective M_1 agonist in an aggressive mouse model of AD before detectable pathology onset result in significantly reduced pathology and prevention of memory deficits later in life when these animals are otherwise known to be impaired? For the first time, thanks to the development of VU572 we have the tools to answer this important question. The oral bioavailability, clean ancillary pharmacology, M_1 selectivity, and allosteric nature of VU572 make it the ideal tool to assess the proof-of-mechanism for chronic M_1 activation in AD treatment. Since VU572 does not robustly desensitize M_1 receptor signaling, long-term efficacy should be realized with chronic dosing.

A large part of why past studies showing efficacy in mice may have failed in the clinic may also be due to the fact that early models of AD such as the Tg2576 mouse develop a very mild pathology that set the pathological bar very low in terms of therapeutic effect required to show a benefit. Thus, these models likely yield much poorer predictive validity than newer, more aggressive mouse models of AD. We utilize the 5X FAD model, which has been shown to develop a very aggressive $A\beta$ pathology and rapid onset of memory impairments at 6 months of age in order to examine the drug effects of VU572. The rationale for selecting such a model is that, if therapeutic efficacy is obtained, the mechanism of chronic M_1 activation will be more likely to translate to human AD patients in the clinic. Furthermore, the impact of selective M_1 activation has never been appreciated at the resolution of soluble and insoluble $A\beta$ species for both neocortex and hippocampus previously. Understanding how M_1 impacts both soluble and insoluble $A\beta_{40}$ and $A\beta_{42}$ is very important given the documented roles for soluble forms

of A β in disrupting hippocampal synaptic plasticity and for insoluble A β in triggering neuroinflammatory responses. By delivering VU572 chronically to 5X FAD mice over a period of 1.5-6 months of age and then examining the neuropathology and memory impairments of drug-treated mice relative to vehicle-treated 5X FAD mice, we validate chronic M₁ activation as a mechanism with the potential to protect against AD-related neuropathology and memory impairments from forming.

Results

M₁ Activation by VU572 Lowers A β ₄₀ and A β ₄₂ Levels In Vitro in Mouse Primary Cortical and Hippocampal Neurons

In order to examine the potential of the M₁ agonist, VU572, for disease modification in AD, cortical and hippocampal neurons from E18 wildtype mice were cultured *in vitro* for analysis of VU572 effects on APP processing. Neurons were subsequently transduced with a lentiviral vector encoding hAPP^{695WT} in order to drive the expression of hAPP in these neurons and then incubated overnight in the presence of varying concentrations of VU572. Figure 3.1 shows that following ELISA analysis of the secreted A β content of the conditioned media these neurons were incubated in, that 10-30 μ M concentrations of VU572 is able to lower A β ₄₀ levels in cultures of primary hippocampal (* $p < 0.05$) and cortical (* $p < 0.05$; ** $p < 0.01$) neurons (Figure 3.1A and B). Furthermore, ELISAs also showed a decrease for A β ₄₂ levels in primary hippocampal (** $p < 0.01$) neurons incubated with 30 μ M VU572 and a trend towards a decrease in A β ₄₂ levels in cortical neurons (Figure 3.1C and D). Together these results indicate that M₁ activation by VU572 is able to drive non-amyloidogenic processing in

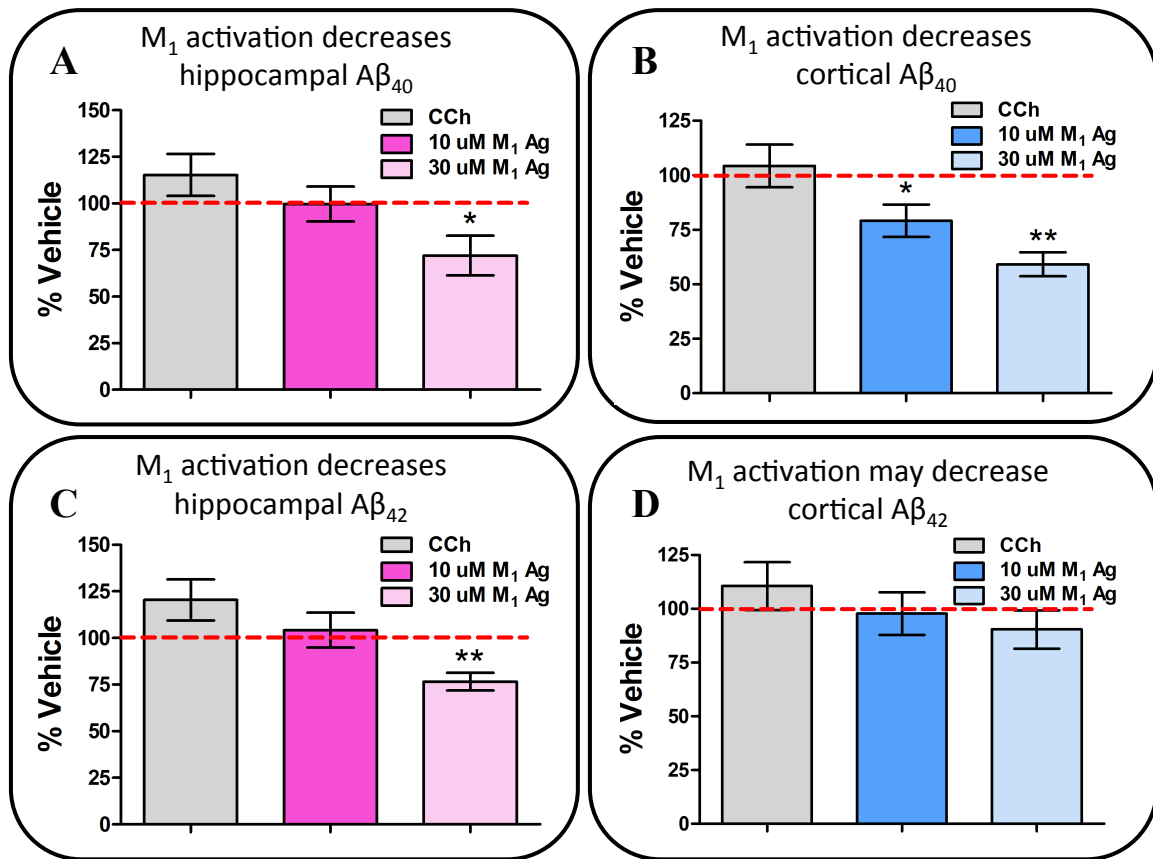


Figure 3.1. M₁ Activation by VU572 Lowers Aβ_{40/42} Levels in Mouse Primary Cortical and Hippocampal Neurons.

A) M₁ activation by VU572 at 30 μM was found to dose-dependently decrease Aβ₄₀ in conditioned media harvested from E18 primary mouse hippocampal neurons transduced with hAPP^{695WT} (* *p* < 0.05). B) 10 μM and 30 μM VU572 were found to dose-dependently decrease Aβ₄₀ in conditioned media harvested from E18 primary mouse cortical neurons transduced with hAPP^{695WT} (* *p* < 0.05; ** *p* < 0.01). C) 30 μM VU572 was found to dose-dependently decrease Aβ₄₂ in conditioned media harvested from E18 primary mouse cortical neurons transduced with hAPP^{695WT} (** *p* < 0.01), but not from hippocampal neurons (D). Error bars show ± SEM across triplicate samples for each drug condition.

the hippocampus and cortex and provide convincing proof-of-concept that VU572 has disease-modifying potential for *in vivo* studies using transgenic AD mice.

M₁ Activation by VU572 Preserves Hippocampal Memory When Dosed Chronically in 5X FAD Transgenic Alzheimer's Mice

Upon obtaining critical proof-of-concept that VU572 can lower A β ₄₀ and A β ₄₂ pathology in primary cultures of cortical and hippocampal neurons, the next key step in validating the potential of VU572 for disease modification in AD was then to assess whether chronic M₁ activation by VU572 could prevent neuropathology and memory impairments from forming in a mouse model of AD. Specifically, we sought to use a very aggressive mouse model of AD, taking the view that such a model would provide the most rigorous test of predictive validity in terms of preclinical therapeutic effects that might successfully translate to human clinical trials for AD. Further more, our selection of mouse model was guided by taking the view supported by the literature that A β accumulation is the proximal pathological event that occurs in AD and that impacts on tau pathology might derive largely due to effects arising from the presence of A β . Thus, we sought to focus in on preventing pathology in an aggressive A β model of the disease and ruled out possible effects due to the presence of tau in the current trial. Finally, in choosing an appropriate mouse model, we sought to utilize a model that developed an aggressive pathology and memory impairments quickly in order to provide a realistic turnaround time for follow-up testing of different drugs or different doses in order to aid in mechanistic validation of rigorously testing the mechanism of M₁ for disease modification *in vivo*.

Taking all of the above criteria into account, we elected to utilize the 5X FAD mouse model developed by Vassar (Oakley, et al. 2006) and structured a chronic, preventative trial to test whether chronic activation of M_1 by VU572 is sufficient to prevent neuropathology and memory impairments from forming in these mice according to the treatment schematic shown in Figure 3.2A. The 5X FAD mouse model develops a very aggressive $A\beta$ pathology starting at around 1.5-2 months of age, with female mice developing detectable memory impairments on the probe trial of the Morris water maze at 6 months of age (black arrows in Figure 3.2A). Female 5X FAD mice, in general, exhibit a much more robust deposition of $A\beta$ (~30% more than males) and earlier onset of memory impairments. Thus, we proposed to use all-female dose groups of wildtype (WT) littermate controls, 5X FAD animals which received vehicle (regular drinking water), and 5X FAD animals which received a chronic dose of M_1 agonist (calculated so that each mouse receives, on average, 10 mg/kg/day VU572 in drinking water spiked with VU572) from an age of 2 months to an age of 6 months in order to carry out this test of chronic M_1 efficacy (red arrow in Figure 3.2A). Dosing of vehicle or VU572 to animals was carried out by allowing the mice access to regular drinking water or drinking water spiked with VU572, respectively. Crucially, an independent pharmacokinetic assessment of plasma-brain-levels of VU572 achieved by various doses of VU572 helped guide the selection of 10 mg/kg VU572 in drinking water as the dose which provided acceptable average brain concentrations of 170 ng/mL (~450 nM) of drug for chronic activation of M_1 in light of efficacy obtained in previous studies performed with VU572 (data not shown; Lebois, et al. 2011).

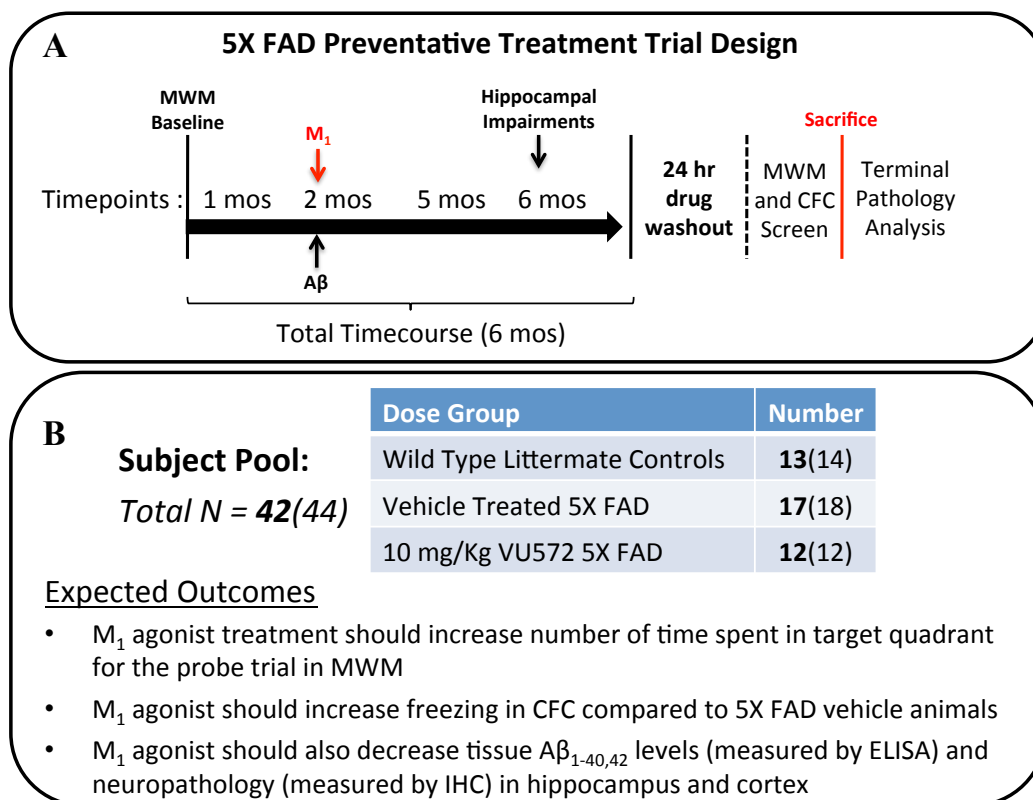


Figure 3.2. M₁ Agonist VU572 Preventative Treatment Trial in 5X FAD Mice.

A) Schematic depicting design of chronic treatment trial of 5X FAD mice with M₁ agonist, VU572. Mice were dosed from 2 months to 6 months of age, corresponding to the age before they develop detectable amyloid pathology and the age at which they develop memory impairments, respectively. Drug was delivered to the mice ad lib. in their drinking water to allow mice continuous access to drug over this 4 month period. Importantly, a pharmacokinetic study was done preceding this chronic dosing trial demonstrating that sufficient brain levels of VU572 can be attained to activate M₁ via the proposed dosing route. Crucially, following completion of the trial, drug was allowed to completely wash out for a period of at least 24 hours prior to behavioral testing and animal perfusion. The $t_{1/2}$ of VU572 is on the order of 46 min, so this washout period of 24 hours far exceeds the 4.5 half-life period required to completely clear a drug from the

body. This drug washout allows any observed effects of the drug on behavior or pathology to be attributed to the drug impacting underlying disease pathology rather than simply acute, symptomatic improvement. B) Breakdown of the experimental animal subject groups for the chronic treatment trial along with expected trial outcomes. Final numbers following exclusions for brain tissue that went into the present analyses were 13 WT littermate controls, 17 vehicle-treated 5X FAD transgenic mice, and 12 VU572-treated 5X FAD transgenic mice (N = 42 mice total). Numbers in parentheses reflect the original number of animals (N=44) prior to exclusion. Exclusions were pre-determined and occurred as a result of one mouse in the WT control group found to be a high amyloid expresser and one mouse in the 5X FAD vehicle-treated control group found to express no amyloid.

The chronic treatment trial was structured in such a way as to test for the ability of VU572 to modify underlying disease pathology in the 5X FAD animals. Drug was allowed to wash out of the system of these animals for at least 24 hours. Since the half-life of VU572 is on the order of ~46 min, the drug is thoroughly washed out of the mice following a 24-hour period (Lebois, et al. 2011). Following drug washout the mice were screened on the Morris water maze as well as in contextual and cued fear conditioning in order to assess drug effects on preventing memory impairments. Finally the brains of these mice were immediately harvested after behavioral testing and subjected to ELISA biochemical analysis for levels of soluble and insoluble A β ₄₀ and A β ₄₂ in the cortex and hippocampus as well as for serial sectioning to examine A β ₄₀ and A β ₄₂ pathology in tissue sections. Importantly, experimenters conducting behavioral and pathological analyses were blind to treatment type and treatment type/genotype, respectively.

Figure 3.2 shows a breakdown of the treatment group numbers that went into analysis. From previous work, the minimum size for dose groups we could utilize to see a statistically significant memory deficit was 10 animals, so we endeavored to utilize closer to 15 animals with the expectation of drop outs due to deaths, lack of pathology, treatment or testing mix-ups or other as-then unforeseen reasons. Thus, the numbers of mice that were tested behaviorally were 14 WT littermate controls, 18 vehicle-treated 5X FAD animals, and 12 VU572-treated 5X FAD animals. For the various reasons just mentioned, the final number of animals which are reflected in our data analyses is 13 WT littermate controls, 17 vehicle-treated 5X FAD animals, and 12 VU572-treated 5X FAD animals.

Following placebo treatment and behavioral testing at 6 months of age we observed a significant deficit of ~15-20% in 5X FAD mice for the probe trial of the Morris water maze that was in good agreement with previous results obtained for this mouse model (Figure 3.3). A significant effect of VU572 treatment on preventing behavioral deficits was seen following drug dosing, indicating that VU572 can act to prevent behavioral deficits from forming in an aggressive A β mouse model of AD and providing proof-of-mechanism that chronic M₁ activation is a valid mechanism to move forward for investigating the prevention of cognitive decline in AD ($*p < 0.05$, $t = 2.092$, $df = 27$) (Figure 3.3).

Importantly, non-memory metrics of Morris water maze performance, such as swim speed were found to be unimpacted relative to WT littermate controls by either genotype or treatment (Figure 3.4 B). Interestingly, distance traveled over training days was also found to be non-statistically different between any of the treatment groups, suggesting that performance differences do not emerge until the memory circuitry of mice is truly taxed during the probe trial. This indicates that the 5X FAD pathology is not introducing any non-drug-related confounds into the performance data we record for the Morris water maze. Similarly, the fact that these non-memory metrics are not impacted by drug means that the behavioral improvement we document in the Morris water maze is attributable to a drug effect on underlying pathology rather than a drug effect working to alter the behavioral baseline of animals relative to WT littermate controls.

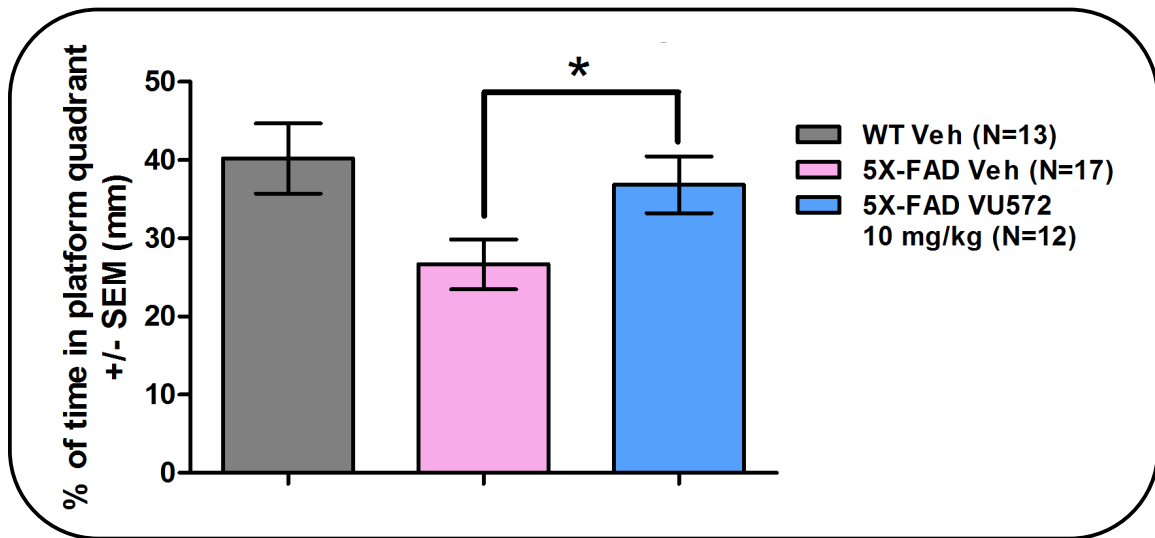


Figure 3.3. M_1 Activation by VU572 Preserves Hippocampal Memory When Dosed Chronically in 5X FAD Transgenic Alzheimer’s Mice.

Following dosing VU572 at 10 mg/kg to 5X FAD mice for 4 months, a significant improvement was observed in their performance on the probe trial of the Morris water maze relative to vehicle-treated 5X FAD mice ($*p < 0.05$, $t = 2.092$, $df = 27$). Drug was allowed to completely wash out for a period of at least 24 hours prior to behavioral testing so there was no drug on board the animals during testing. This preservation of hippocampal memory by M_1 activation is notable since the 5X FAD model is such an aggressive model of disease. Furthermore, the observed memory preservation provides the first ever compelling proof of mechanism that early prodromal intervention by M_1 activation could potentially lead to a delay in or prevention of the memory deficits observed in AD. Error bars show \pm SEM across all mice within a treatment group.

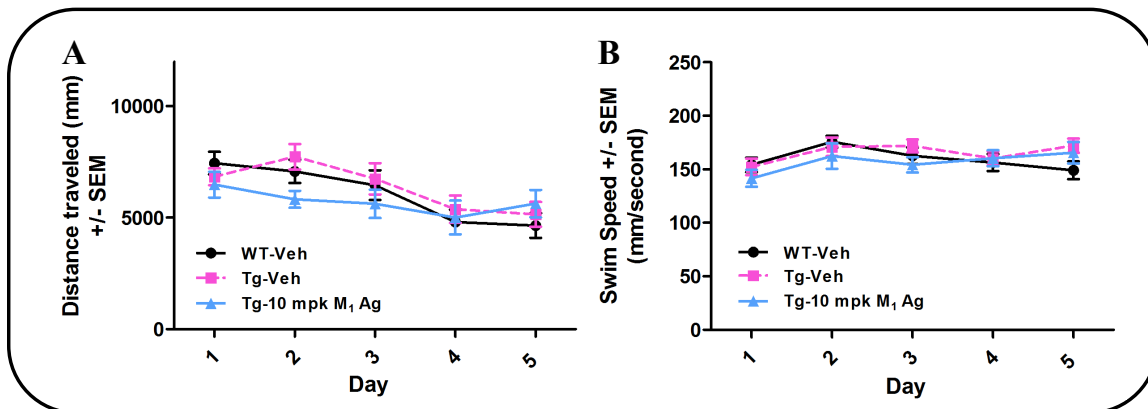


Figure 3.4. M₁ Activation by VU572 Does Not Influence Morris Water Maze Performance During Training.

Following dosing VU572 at 10 mg/kg to 5X FAD mice for 4 months no statistically significant difference was observed during training in either distance traveled during a test session (A) or swim speed (B) for either WT mice (N = 13), 5X FAD vehicle-treated mice (N = 17), or 5X FAD mice receiving 10 mg/kg VU572 (N = 12). Error bars show \pm SEM across all mice within a treatment group for individual training days.

VU572 Decreases Soluble and Insoluble A β ₄₀ and A β ₄₂ Levels in Cortex and Hippocampus of 5X FAD Mice

We next sought to pathologically-characterize the A β pathology in the brains of these animals in order to ascertain whether or not the improvement in memory performance we documented tracked with an improvement in underlying disease pathology. In order to do this, total hippocampus and neocortex was taken from a hemibrain of each mouse and subjected to biochemical fractionation to separate SDS-soluble and formic acid-insoluble A β fractions. The A β ₄₀ and A β ₄₂ levels for each sample were then analyzed by A β ₄₀ and A β ₄₂ ELISA, respectively.

Upon quantifying ELISA data, we documented a significant VU572-mediated decrease of 40.4% (* $p < 0.05$, $t = 1.96$, $df = 25$) in soluble hippocampal A β ₄₀ levels, with a decrease of 33.6% approaching significance for soluble cortical A β ₄₀ levels versus vehicle-treated 5X FAD mice (* $p < 0.05$, $t = 2.20$, $df = 25$) (Figure 3.5 A). Levels of soluble hippocampal A β ₄₂ were found to be significantly decreased by VU572 treatment (* $p < 0.05$, $t = 1.76$, $df = 26$), as were levels of soluble cortical A β ₄₂ (* $p < 0.05$, $t = 1.76$, $df = 26$) (Figure 3.5 B). Insoluble A β ₄₀ levels were found to be significantly decreased by 38.9% and 43.3% in cortex (* $p < 0.05$, $t = 2.20$, $df = 26$) and hippocampus (* $p < 0.05$, $t = 2.44$, $df = 26$), respectively (Figure 3.6 A). For insoluble A β ₄₂, we documented a significant decrease of 34.2% (* $p < 0.05$, $t = 1.87$, $df = 26$) in cortex and trend ($p < 0.1$, $t = 1.22$, $df = 26$) towards a decrease of 23.7% in hippocampus following VU572 treatment (Figure 3.6 B). Taken together, these results provide significant and compelling evidence to suggest that chronic M₁ activation by VU572 administration can act to modify underlying disease pathology in AD-relevant regions of the neocortex and hippocampus.

This is the first evidence to suggest that chronic M_1 activation initiated prior to detectable disease pathology can lead sustained and lasting improvements in disease pathophysiology that act to protect against the onset of overt neuropathology and memory impairments relevant to AD.

M₁ Activation by VU572 Treatment Abolishes Soluble A β ₄₂ Correlation with Memory Impairment

Following the observation that VU572 can fundamentally alter the underlying A β pathology in drug-treated 5X FAD mice relative to vehicle-treated controls, a question of interest became whether or not any aspects of A β ₄₀ or A β ₄₂ pathology correlated with behavioral performance in the Morris water maze. To this end, all pairwise-correlations were performed between soluble and insoluble A β ₄₀ and A β ₄₂ fractions for both the cortex and the hippocampus of all mice. Figure 3.7A depicts the only statistically-significant correlation obtained for A β levels with memory performance on the Morris water maze probe trial. A significant correlation ($R^2 = 0.4$; $**p < 0.01$) was obtained between soluble A β ₄₂ levels and hippocampal memory performance, with higher levels of A β ₄₂ corresponding to worse behavioral performance. Indeed, Zhang, et al. have also observed that soluble A β levels are highly correlated with spatial memory deficits in APP/PS1 mice, with no correlation observed between insoluble A β levels and memory impairments (Zhang, et al. 2011). The present correlation of soluble A β ₄₂ levels with memory impairment makes logical sense, as A β ₄₂ is the predominant self-aggregating species of A β that gives rise to the soluble A β oligomers that have been found to be so profoundly disruptive to hippocampal synaptic plasticity and therefore, to memory. To-

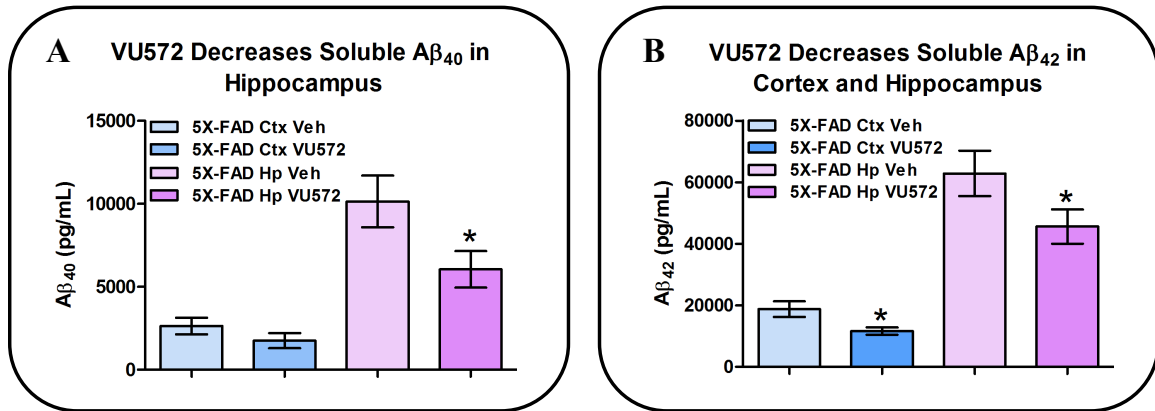


Figure 3.5. M₁ Activation by VU572 Decreases Soluble A β_{40} and A β_{42} Levels in Cortex and Hippocampus of 5X FAD Mice.

Neocortex and hippocampus were microdissected from 5X FAD animals and WT littermate controls and biochemically-fractionated in order to obtain soluble A β fractions. Fractions were then subjected to A β_{40} and A β_{42} ELISA analysis. A) VU572 significantly decreases soluble A β_{40} levels in the hippocampus of 5X FAD mice by 40.4% relative to vehicle-treated 5X FAD animals (* $p < 0.05$, $t = 1.96$, $df = 25$). A trend towards a decrease of 33.6% in soluble A β_{40} was observed in the cortex. B) VU572 significantly decreases soluble A β_{42} levels in both the neocortex (* $p < 0.05$, $t = 2.20$, $df = 25$) and hippocampus (* $p < 0.05$, $t = 1.76$, $df = 26$) of 5X FAD mice relative to vehicle-treated 5X FAD animals by 38.1% and 27.4%, respectively. Error bars show \pm SEM across all mice within a treatment group.

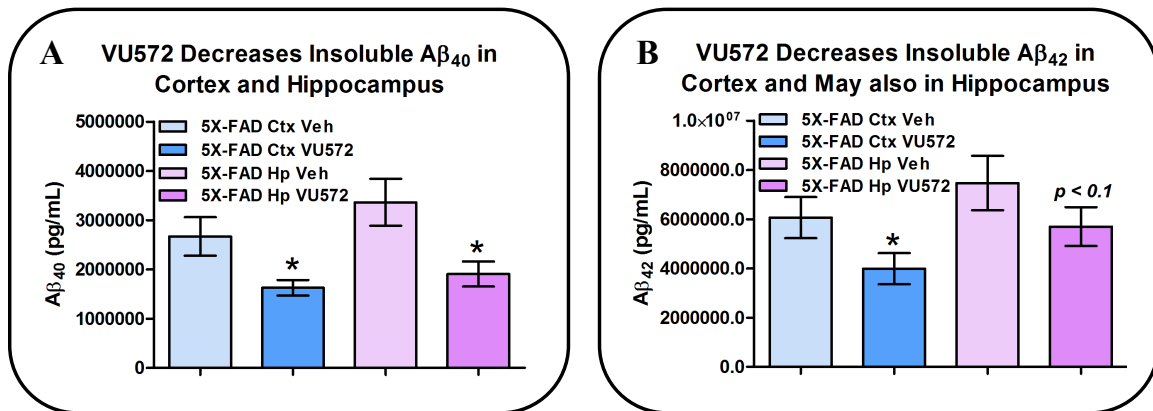


Figure 3.6. M₁ Activation by VU572 Decreases Insoluble A β_{40} and A β_{42} Levels in Cortex and Hippocampus of 5X FAD Mice.

Neocortex and hippocampus were microdissected from 5X FAD animals and WT littermate controls and biochemically-fractionated in order to obtain insoluble A β fractions. Fractions were then subjected to A β_{40} and A β_{42} ELISA analysis. A) VU572 significantly decreases insoluble A β_{40} levels in both the neocortex (* $p < 0.05$, $t = 2.20$, $df = 26$) and hippocampus (* $p < 0.05$, $t = 2.44$, $df = 26$) of 5X FAD mice relative to vehicle-treated 5X FAD animals by 38.9% and 43.3%, respectively. B) VU572 significantly decreases insoluble A β_{42} levels in the neocortex of 5X FAD mice relative to vehicle-treated 5X FAD animals by 34.2% (* $p < 0.05$, $t = 1.87$, $df = 26$), with a trend towards a decrease in hippocampus of 23.7% ($p < 0.1$, $t = 1.22$, $df = 26$). Since the insoluble levels of A β_{42} are so incredibly high in the brains of 5X FAD animals, the presence of any decrease at all is noteworthy. Error bars show \pm SEM across all mice within a treatment group.

date, it is these A β oligomers that appear the most significant and direct tie to the memory-impairing effects of A β in AD. Thus, one would expect higher levels of A β_{42} to equate to higher levels of soluble A β oligomers in a stoichiometric fashion. Importantly, the correlation between soluble A β_{42} levels and probe trial memory performance survives addition of the WT littermate controls, providing yet further evidence that this correlation is, indeed, real ($R^2 = 0.45$; $**p < 0.01$, data not shown). Furthermore, the correlation between soluble A β_{42} levels and probe trial memory performance is completely abolished in mice treated with VU572 ($R^2 = 0.02$), providing further evidence that VU572 is acting to fundamentally-alter underlying A β pathology and that this improvement corresponds to better memory outcomes. Additionally, the impact of VU572 to decrease soluble A β_{42} levels suggests the exciting likelihood that VU572 is functioning to decrease the formation of soluble A β_{42} oligomers in order to protect memory circuits of the hippocampus from disruption.

As previously mentioned, the correlation between soluble A β_{42} levels and probe trial memory performance was the only significant correlation to be observed. Figure 3.8 shows the corresponding correlation for insoluble A β_{42} levels and probe trial memory performance. One can readily see that there is no observable relationship between A β_{42} levels and probe trial memory performance ($R^2 = 0.06$). Since A β_{40} and A β_{42} might contribute differentially to disease pathology or VU572 might be acting preferentially to influence the levels of the individual A β peptides relative to one another, a final question is whether VU572 is acting to perturb the normal ratio of A β_{40} and A β_{42} observed in vehicle-treated 5X FAD animals. As expected, therapeutic effects remain evenly split

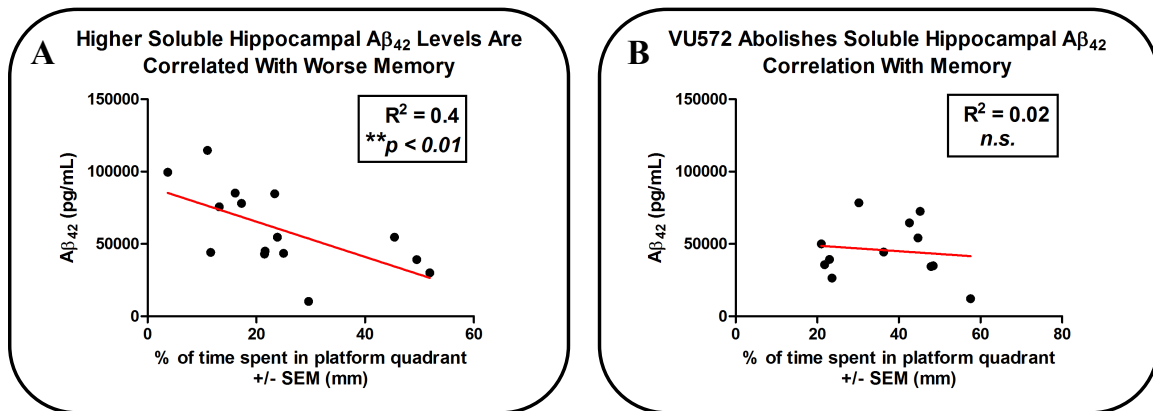


Figure 3.7. M₁ Activation by VU572 Treatment Abolishes Soluble A β_{42} Correlation with Memory Impairment.

The behavioral performance of 5X FAD mice on the probe trial of the Morris water maze was correlated with soluble and insoluble A β_{40} and A β_{42} levels from the cortex and hippocampus of these mice. The only significant correlation was observed between soluble A β_{42} levels and probe trial performance (A), where higher soluble A β_{42} levels correlated with worse probe trial performance ($R^2 = 0.4$; $**p < 0.01$). Notably the correlation in A survived even when the WT littermate controls were added to the data, indicating further that this is indeed a real effect of pathology on probe trial performance. Furthermore, the correlation in A was abolished by drug treatment with VU572, providing further evidence for the ability of M₁ activation to guard against the onset of disease pathology and memory impairments ($R^2 = 0.02$; n.s.).

across $A\beta_{40}$ and $A\beta_{42}$ species and thus, no significant perturbations in $A\beta_{40/42}$ ratios are noted in VU572-treated samples relative to controls (Figure 3.9).

M₁ Activation by VU572 Reduces $A\beta_{40}$ Neuropathology in the Hippocampus and Cortex of 5X FAD Mice

The effects of VU572 on insoluble $A\beta_{40}$ and $A\beta_{42}$ suggests a protective effect on $A\beta$ plaque burden. To determine if VU572 treatment altered the number of plaques, cortical and hippocampal sections were assayed by IHC analysis to permit the detection of $A\beta$ pathology at a brain-wide resolution that was not permitted by our $A\beta$ ELISAs. That is, since we took total neocortex and total hippocampus for ELISA experiments out of necessity, we have no idea how $A\beta$ deposition is being altered to impact $A\beta$ plaque number, size or regional deposition.

In order to determine whether VU572 is acting in either a brain-wide manner to globally decrease $A\beta$ or a more subregion-specific manner to decrease $A\beta$ pathology, sagittal section from VU572-treated 5X FAD mice, vehicle-treated 5X FAD mice, and WT littermate controls were stained with an antibody against human $A\beta_{40}$ (Figures 3.10-3.12) and $A\beta_{42}$ (Figure 3.13). Upon staining the brains of 5X FAD mice for $A\beta_{40}$, it became readily apparent that VU572 acted to cause global decreases in $A\beta_{40}$ levels in both the cortex and hippocampus of 5X FAD mice (3.10B and H-K; 3.11D and E; 3.12 G-L) relative to vehicle-treated 5X FAD mice (3.10C and D-G; 3.11B and C; 3.12 A-F). In the hippocampus, substantial decreases were noted across all hippocampal subfields: the subiculum (3.11H), dentate gyrus (3.11I), CA3 (3.11J), and CA1 (3.11K). As expected, very intense staining was observed in the hippocampus and cortex of vehicle-

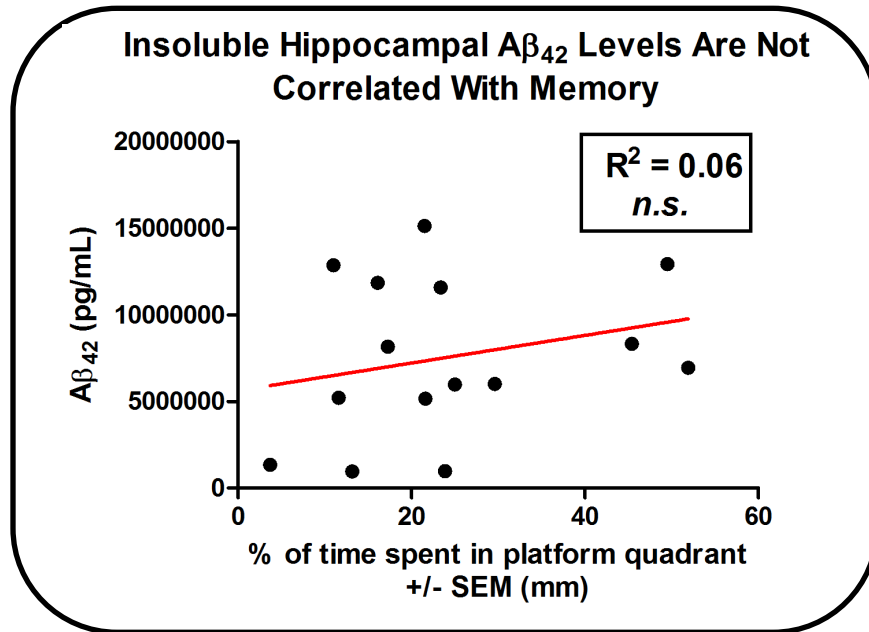


Figure 3.8. Insoluble A β_{42} Levels Are Not Correlated with Memory.

The behavioral performance of 5X FAD mice on the probe trial of the Morris water maze was correlated with soluble and insoluble A β_{40} and A β_{42} levels from the cortex and hippocampus of these mice. No significant correlation was observed between either insoluble A β_{42} (shown) or A β_{40} levels (not shown) and probe trial performance ($R^2 = 0.02$; n.s.).

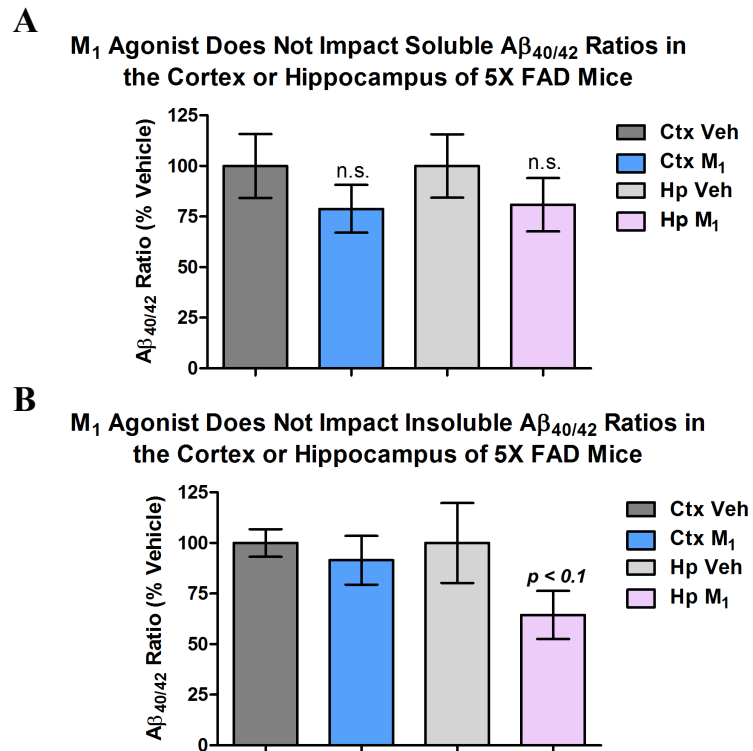


Figure 3.9. M₁ Activation by VU572 Does Not Impact Soluble or Insoluble A β _{40/42} Ratios in the Cortex or Hippocampus of 5X FAD Mice.

The ability of VU572 to impact soluble and insoluble A β _{40/42} ratios in the cortex and hippocampus was assessed. There was no significant effect of VU572 treatment on any of the soluble (A) or insoluble (B) A β _{40/42} ratios tested. Error bars show \pm SEM across all mice within a treatment group.

treated 5X FAD control mice (3.10C and D-G; 3.11B and C) relative to the brains of WT littermate controls, where no $A\beta_{40}$ immunoreactivity was observed (3.10A and 3.11A). In order to quantify VU572-induced changes on $A\beta_{40}$ pathology, total $A\beta_{40}$ immunoreactivity was measured in a blinded manner in equivalent regions of neocortex and hippocampus from 6 sections per experimental animal. 5X FAD vehicle-treated animals showed robust $A\beta_{40}$ pathology that is significantly mitigated by VU572 treatment in both the neocortex ($**p < 0.01$ $t = 3.66$, $df = 25$) and hippocampus ($**p < 0.01$ $t = 3.52$, $df = 25$) (Figure 3.14). Similarly, VU572 acted to cause global decreases in $A\beta_{42}$ levels in both the cortex and hippocampus of 5X FAD mice (3.13 G-L) relative to vehicle-treated 5X FAD mice (3.13 A-F). Quantification of $A\beta_{42}$ immunoreactivity in a similar fashion yielded a robust decrease in $A\beta_{42}$ pathology following VU572 treatment in both the neocortex ($***p < 0.01$ $t = 4.37$, $df = 25$) and hippocampus ($***p < 0.01$ $t = 4.73$, $df = 25$) (Figure 3.15).

Effect of M_1 Activation by VU572 on Contextual and Cued Fear Conditioning

Apart from the Morris water maze, we sought to characterize the memory of drug- and vehicle-treated 5X FAD animals and WT controls further using different a different test of hippocampal memory and a test of amygdala-mediated memory. In this vein, we tested all 5X FAD and WT control animals in the contextual and cued fear conditioning

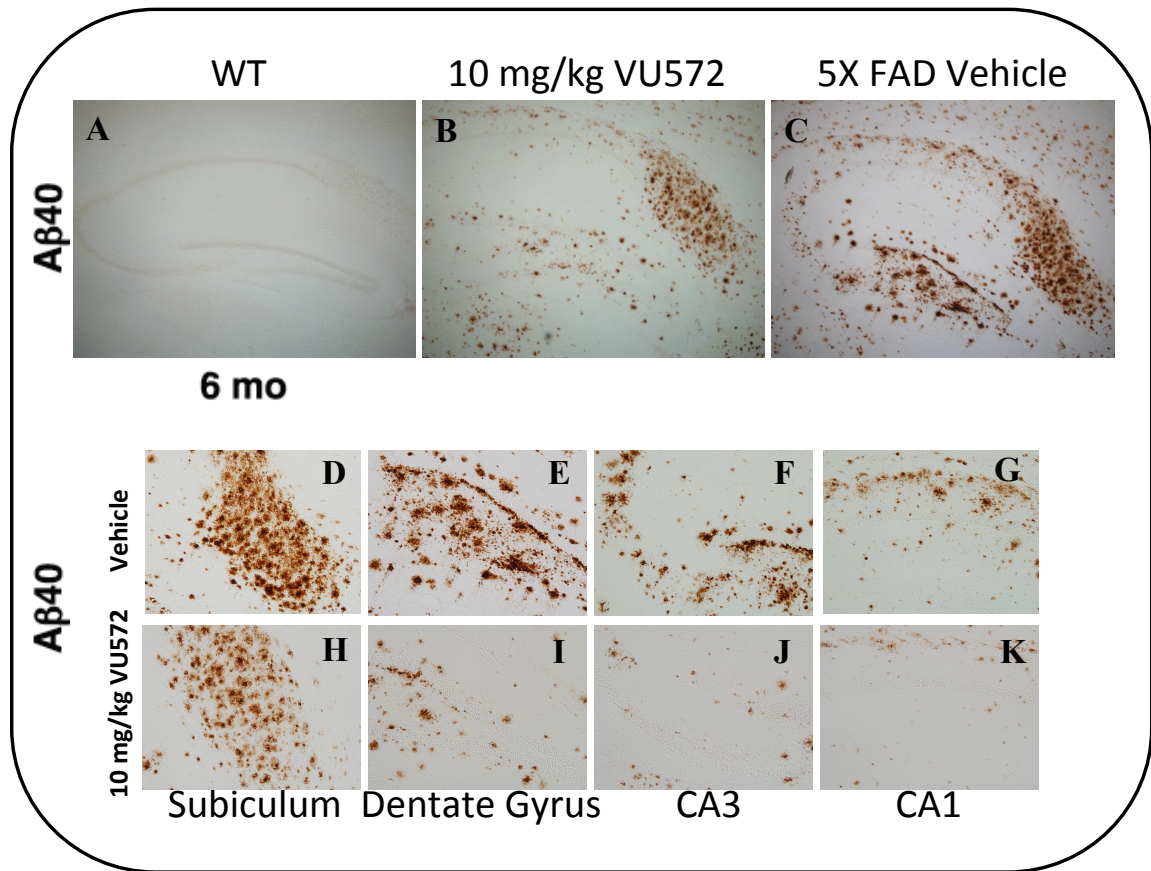


Figure 3.10. M_1 Activation by VU572 Reduces $A\beta_{40}$ Neuropathology in the Hippocampus of 5X FAD Mice.

Serial sections at 50 μ m were taken from 5X FAD mice and WT littermate controls and 6 sections per animal were then subjected to $A\beta_{40}$ immunohistochemical analysis with anti human $A\beta_{40}$ antibody (1:5000; Biosource) in order to examine $A\beta_{40}$ pathology in the hippocampus. As expected, WT littermate controls show no observable $A\beta_{40}$ pathology following staining (A). However, 5X FAD vehicle-treated animals show robust $A\beta_{40}$ pathology (C) that is substantially mitigated across all hippocampal subfields by VU572 treatment (B). High-magnification images show substantial $A\beta_{40}$ reduction in the subiculum (H), dentate gyrus (I), CA3 (J), and CA1 (K) subfields compared to the same subfields in vehicle-treated 5X FAD animals (D-G). Taken together, these results

strongly indicate that VU572 exerts sustained, disease-modifying effects on underlying $A\beta$ neuropathology in 5X FAD mice and that these beneficial effects occur in all areas of the hippocampus and cortex known to be impacted by AD.

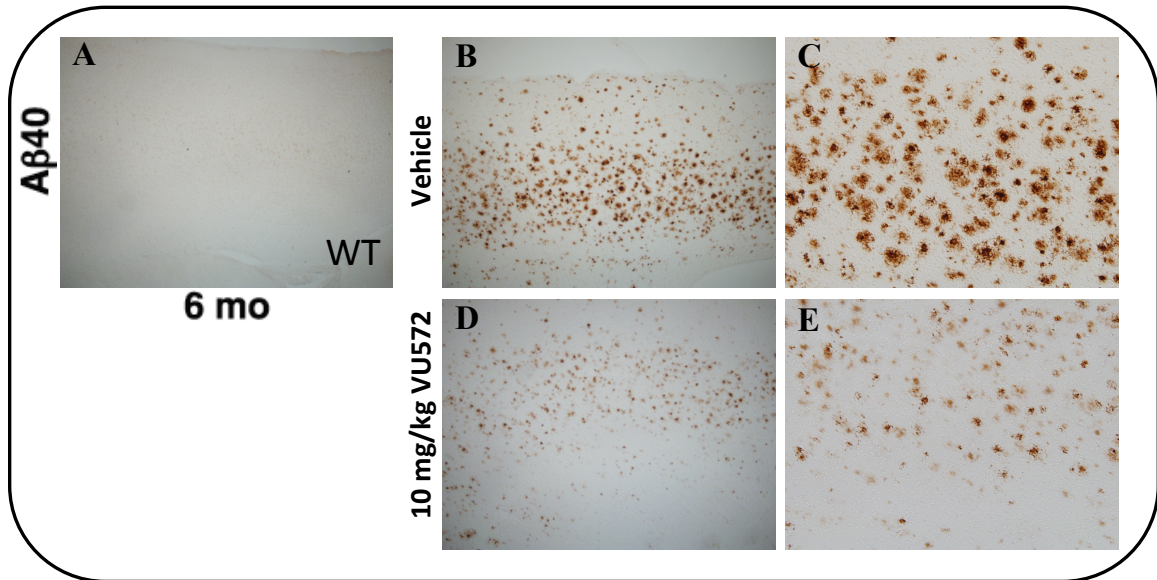


Figure 3.11. M₁ Activation by VU572 Reduces Aβ₄₀ Neuropathology in the Cortex of 5X FAD Mice.

Serial sections at 50 μm were taken from 5X FAD mice and WT littermate controls and 6 sections per animal were then subjected to Aβ₄₀ immunohistochemical analysis with anti human Aβ₄₀ antibody (1:5000; Biosource) in order to examine Aβ₄₀ pathology in the neocortex. As expected, WT littermate controls show no observable Aβ₄₀ pathology following staining (A). However, 5X FAD vehicle-treated animals show robust Aβ₄₀ pathology (B and C) that is substantially mitigated by VU572 treatment (D and E).

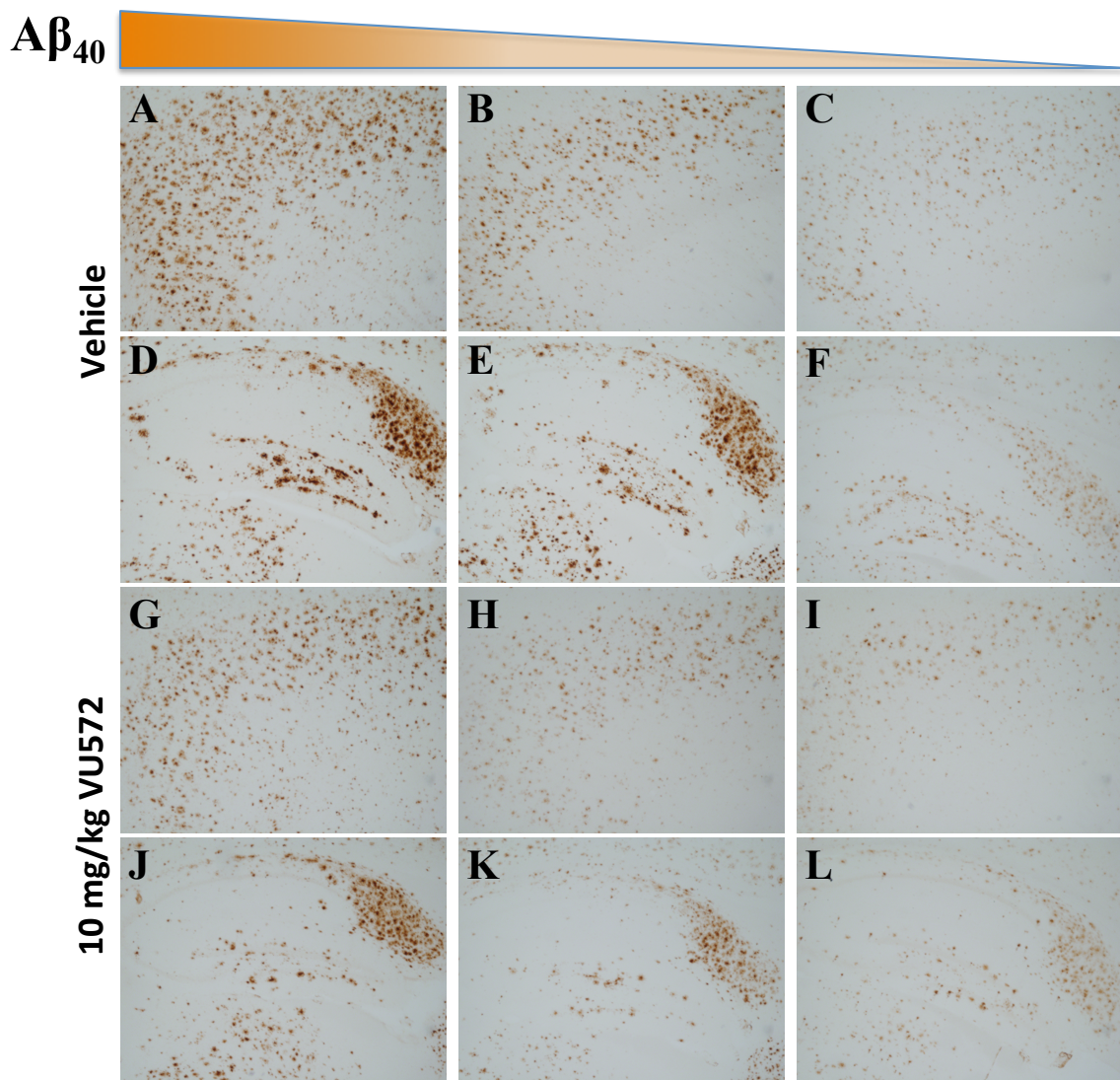


Figure 3.12. M₁ Activation by VU572 Reduces Aβ₄₀ Neuropathology in the Brains of 5X FAD Mice.

Serial sections at 50 μm were taken from 5X FAD mice and WT littermate controls and 6 sections per animal were then subjected to Aβ₄₀ immunohistochemical analysis with anti human Aβ₄₀ antibody (1:5000; Biosource) in order to examine Aβ₄₀ pathology.

Representative range of pathology showing high, medium and low Aβ₄₀-expressing animals for 5X FAD vehicle-treated animals (A-F) and 5X FAD drug-treated animals (G-

L). Cortex and hippocampus are shown for both 5X FAD vehicle-treated animals (A-C and D-F, respectively) and 5X FAD VU572-treated animals (G-I and J-L, respectively).

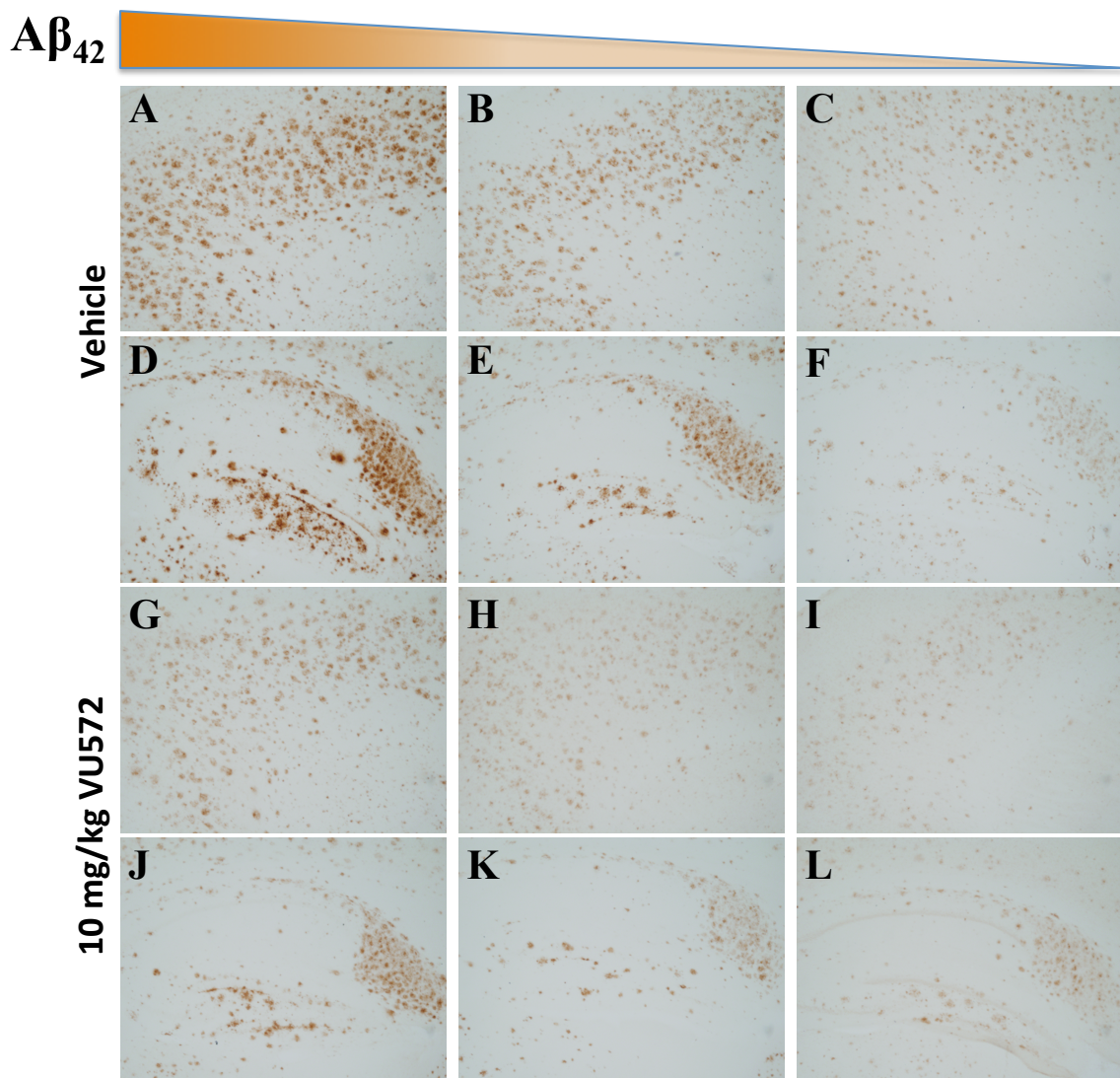


Figure 3.13. M₁ Activation by VU572 Reduces Aβ₄₂ Neuropathology in the Brains of 5X FAD Mice.

Serial sections at 50 μm were taken from 5X FAD mice and WT littermate controls and 6 sections per animal were then subjected to Aβ₄₂ immunohistochemical analysis with anti human Aβ₄₂ antibody (1:1000; Biosource) in order to examine Aβ₄₂ pathology.

Representative range of pathology showing high, medium and low Aβ₄₂-expressing animals for 5X FAD vehicle-treated animals (A-F) and 5X FAD drug-treated animals (G-

L). Cortex and hippocampus are shown for both 5X FAD vehicle-treated animals (A-C and D-F, respectively) and 5X FAD VU572-treated animals (G-I and J-L, respectively).

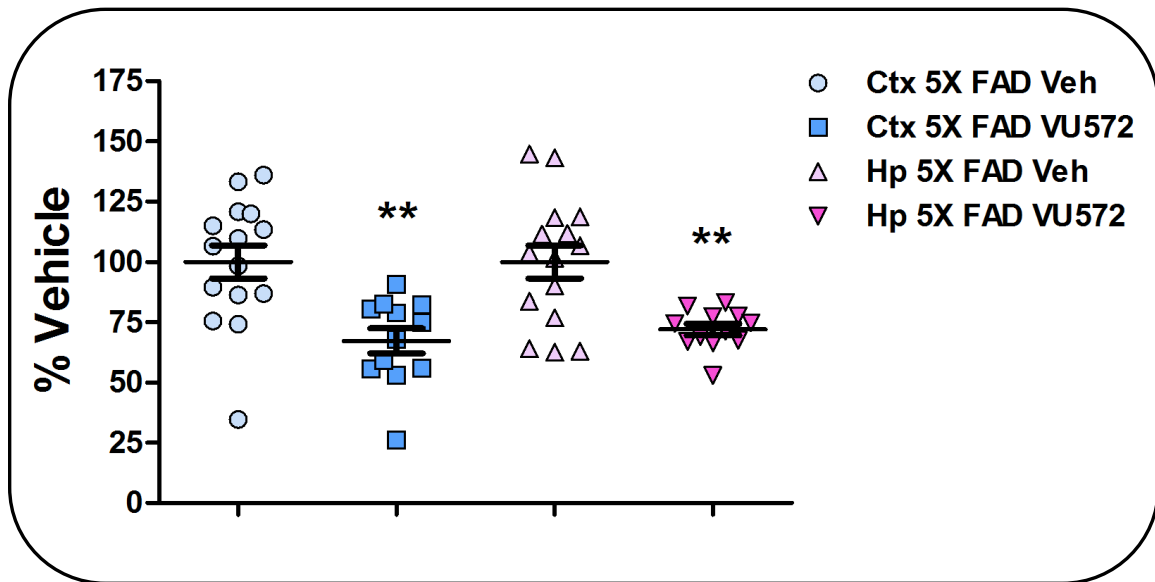


Figure 3.14. M₁ Activation by VU572 Reduces A β ₄₀ Neuropathology in the Brains of 5X FAD Mice.

Serial sections at 50 μ m were taken from 5X FAD mice and WT littermate controls and 6 sections per animal were then subjected to A β ₄₀ immunohistochemical analysis with anti human A β ₄₀ antibody (1:5000; Biosource) in order to examine A β ₄₀ pathology. Total A β ₄₀ immunoreactive surface area was measured for 6 slices of comparable depth per animal and the mean immunoreactive surface area plotted for individual animals. As expected, 5X FAD vehicle-treated animals show robust A β ₄₀ pathology that is significantly mitigated by VU572 treatment in both the neocortex (** $p < 0.01$ $t = 3.66$, $df = 25$) and hippocampus (** $p < 0.01$ $t = 3.52$, $df = 25$). Error bars show \pm SEM across all mice within a treatment group.

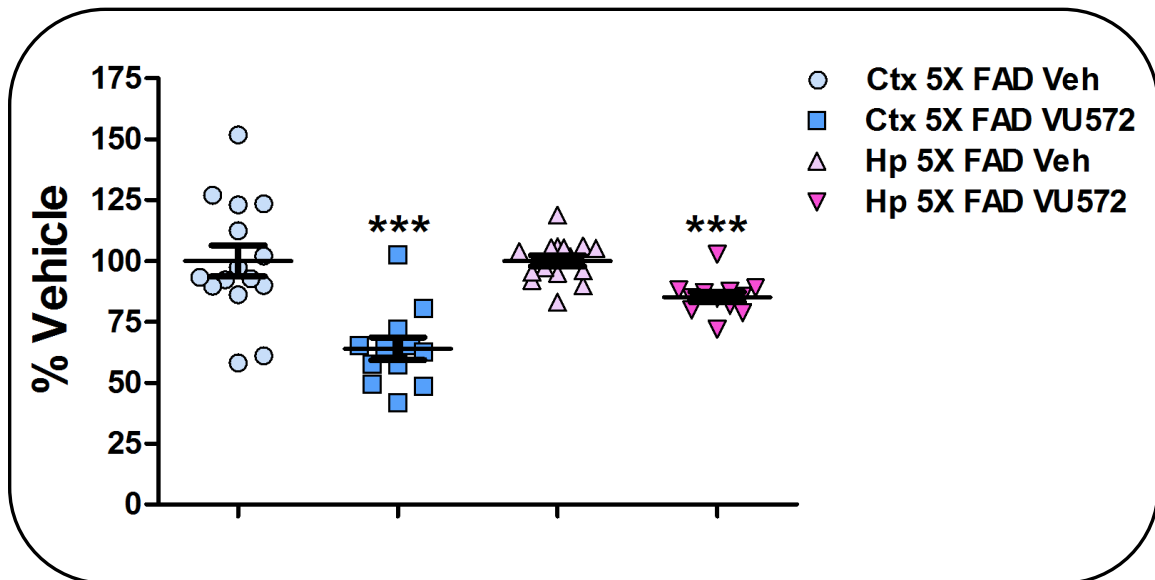


Figure 3.15. M₁ Activation by VU572 Reduces A β ₄₂ Neuropathology in the Brains of 5X FAD Mice.

Serial sections at 50 μ m were taken from 5X FAD mice and WT littermate controls and 6 sections per animal were then subjected to A β ₄₀ immunohistochemical analysis with anti human A β ₄₂ antibody (1:1000; Biosource) in order to examine A β ₄₂ pathology. Total A β ₄₂ immunoreactive surface area was measured for 6 slices of comparable depth per animal and the mean immunoreactive surface area plotted for individual animals. As expected, 5X FAD vehicle-treated animals show robust A β ₄₂ pathology that is significantly mitigated by VU572 treatment in both the neocortex (***p* < 0.01 *t* = 4.37, *df* = 25) and hippocampus (***p* < 0.01 *t* = 4.73, *df* = 25). Error bars show \pm SEM across all mice within a treatment group.

paradigms (Figures 3.12 and 3.13). We predicted a deficit in 5X FAD animals in contextual fear conditioning, as hippocampal memory has been previously described to be impaired in these mice at this age. Additionally, these mice develop robust hippocampal A β pathology at this age. What we observed, was the expected deficit in behavioral performance (% freezing in response to context) in vehicle-treated 5X FAD animals relative to WT littermate controls, however, there was no effect of VU572 treatment (Figure 3.12). This could likely be due how the mice were conditioned for this assay, which will be discussed shortly. In tests of cued fear conditioning we predicted we would see no deficit in vehicle-treated 5X FAD mice, as A β pathology is not quite as robust in the amygdala at 6 months of age. As expected, we observed no deficits in vehicle-treated 5X FAD control animals and no effect of treatment by VU572 on 5X FAD animals (Figure 3.13).

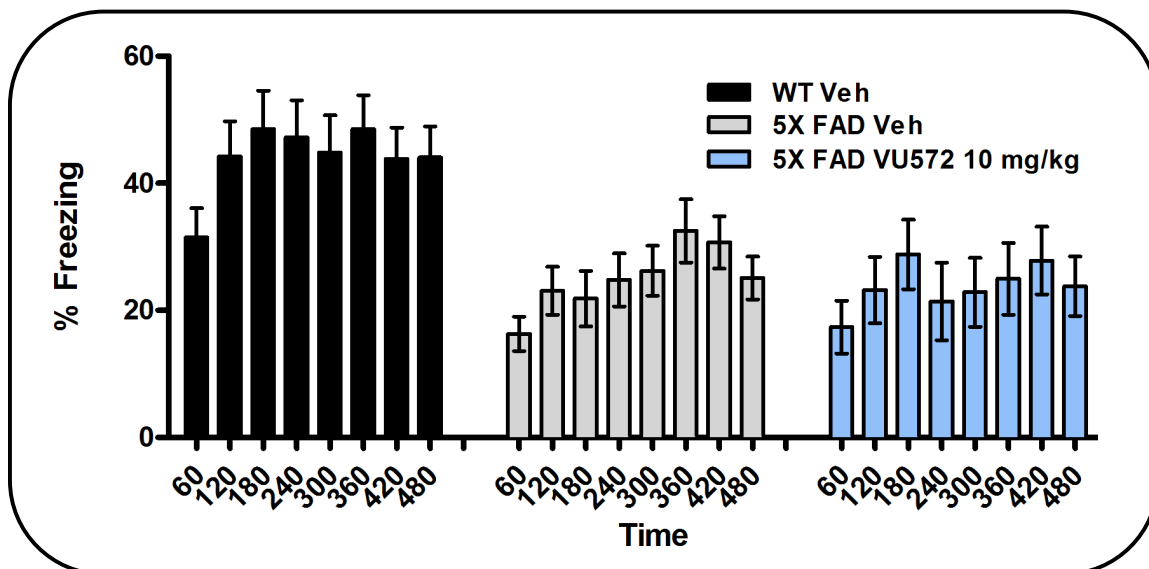


Figure 3.16. M_1 Activation by VU572 Does not Rescue Deficits in Contextual Fear Conditioning in 5X FAD Mice.

At 6 months of age a significant deficit was observed in vehicle-treated 5X FAD animals in contextual fear conditioning test of memory, however no significant improvement was observed following 4 months of dosing VU572 at 10 mg/kg. Drug was allowed to completely wash out for a period of at least 24 hours prior to behavioral testing so there was no drug on board the animals during testing. Error bars show \pm SEM across 60s time bins for all mice within a treatment group.

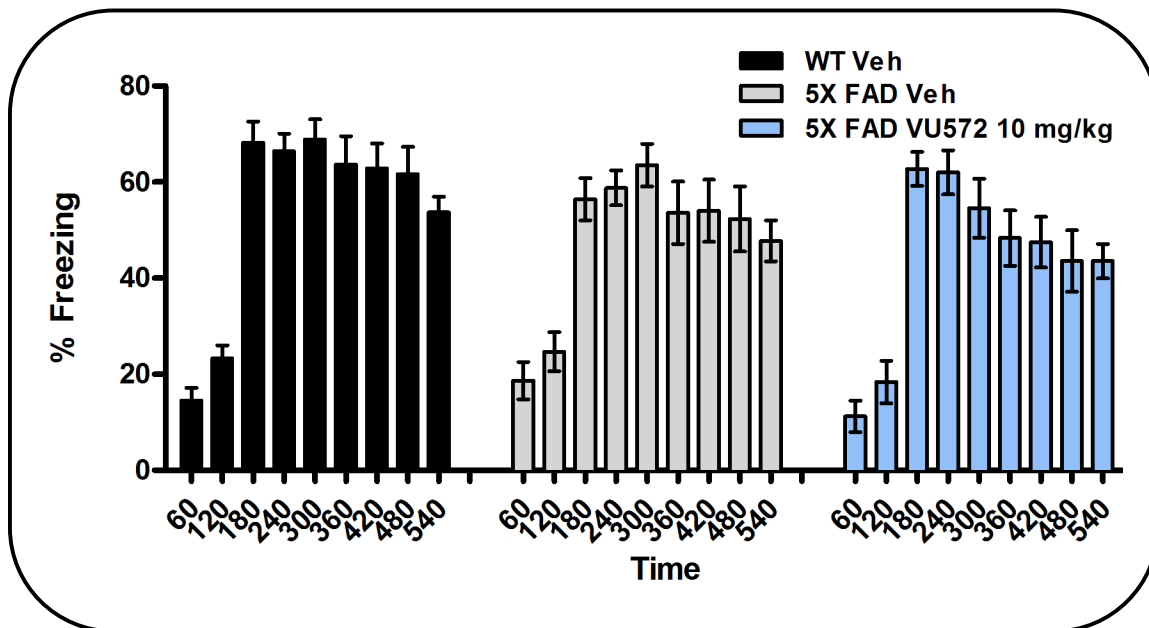


Figure 3.17. Cued Fear Conditioning is Not Impacted by 5X FAD Genotype or M_1 Activation by VU572 Treatment in 5X FAD Mice.

At 6 months of age, no significant deficit was observed in cued fear conditioning in 5X FAD vehicle-treated transgenic animals. There was similarly no significant effect of VU572 treatment on 5X FAD animals relative to WT littermate controls. Error bars show \pm SEM across 60s time bins for all mice within a treatment group.

Discussion

The M₁ receptor has long been regarded as a highly promising target for disease modification in AD by many academic and pharmaceutical groups. A number of studies have described the ability of M₁ to exert non-amyloidogenic effects on APP processing *in vitro*. Furthermore, other work in genetic studies with M₁ knockout mice has demonstrated the importance of the M₁ receptor for regulating amyloid levels *in vivo*. However, a paucity of truly selective M₁ agonist that display druggable characteristics acceptable for *in vivo* dosing has severely hampered the investigation of whether M₁ can exert preventative, disease-modifying effects to prevent the accumulation of A β pathology and manifestation of memory impairments in AD models. Several studies have obtained improvements in pathology in transgenic AD models, but these were with ligands not wholly selective for the M₁ receptor and were also studies performed in very mild models of disease (e.g. in Tg2576 mice), where a more aggressive model of disease with a higher translational potential (e.g. the 5X FAD mouse) would be superior. Thus, these improvements in pathology implicate M₁ activation in disease modification, but do not address in a preventative manner whether or not M₁ activation is a viable mechanism for protecting against the development of AD pathology or memory impairments. After all, many treatments have advanced to the clinic after showing improvements in animal models with mild disease phenotypes and to-date none have translated into an effective treatment that blunts or blocks AD pathophysiology. Thus, the elephant in the room is not whether M₁ is capable of lowering amyloid, but whether this action of M₁ is a therapeutically-viable mechanism for sustained treatment that can be initiated during prodromal AD and block clinical progression.

Here, we present for the first time compelling evidence using the M_1 specific allosteric agonist, VU572, that chronic activation of M_1 is a therapeutically-valid mechanism that acts to protect against neuropathology and prevent memory impairments from forming in the aggressive 5X FAD mouse model of AD. Specifically, chronic M_1 activation by VU572 from 2 months to 6 months of age was found to prevent the memory impairments observed in the vehicle-treated 5X FAD animals in the Morris water maze. The unexpected result obtained where VU572 failed to rescue impairments in contextual fear conditioning suggests that the brain circuitry necessary to mediate fear conditioning is still impacted by disease pathology despite therapeutic intervention with VU572. Thus, future analyses will need to investigate the ability of VU572 to counteract amyloid pathology in the amygdala of 5X FAD mice.

At a pathological level, VU572 was found to exert sustained and lasting benefits on lowering soluble and insoluble $A\beta_{40}$ and $A\beta_{42}$ pathology in the cortex and hippocampus of 5X FAD mice and this corresponds to a prevention of the memory impairments observed in vehicle-treated 5X FAD animals. Although the reduction in insoluble $A\beta_{42}$ pathology for the hippocampus did not reach significance by ELISA, there was a strong trend noted ($p < 0.1$). It is important to note that the failure to reach statistical significance for insoluble $A\beta_{42}$ levels was not wholly surprising and the observed reduction was still a substantial reduction in amyloid pathology—it is just that the levels of insoluble $A\beta_{42}$ in the 5X FAD mice are so high to lower them enough to reach significance may not be within the physiological realm of M_1 activation.

The observed correlation of higher soluble $A\beta_{42}$ levels with worse memory performance is especially interesting and highly consistent with recent research on the

role of soluble A β species in AD. A number of studies suggest that the pathological aspects of A β on impairing memory arise as a result of the actions of soluble A β oligomers on hippocampal synaptic plasticity, where these oligomers have been found to profoundly disrupt LTP. The significant decrease in hippocampal A β_{42} pathology observed in our studies and the fact that VU572 abolishes the correlation between soluble A β_{42} levels and memory performance is consistent with the view that M $_1$ activation by VU572 can act to lower the circulating levels of A β oligomers available to disrupt synaptic plasticity.

Apart from the observed behavioral and pathological results, the pharmacology of the observed efficacy of VU572 bears discussion. From the present studies it is clear that VU572 exerts a beneficial effect on protecting against neuropathology and preventing memory impairments from forming in 5X FAD mice. This is pharmacologically exciting for many reasons. First, this finding is consistent with a body of earlier work on M $_1$ allosteric agonists, including VU572, demonstrating that they do not robustly couple to intracellular signaling cascades to desensitize M $_1$ receptor signaling. The observation that we obtained sustained efficacy for the treatment duration of 4 months in the 5X FAD animals is highly consistent with the ability of VU572 to not desensitize M $_1$ receptor signaling. Also, the extensive molecular pharmacological characterization done with VU572 indicates that, while this compound is the most selective M $_1$ -agonist to-date, it is far from the most potent or efficacious. In fact, VU572 is, at best, a strong partial agonist whose potency approaches micromolar levels in low receptor reserve systems. Thus, the present findings indicate that it may not take a particularly high amount of efficacy for M $_1$ activation to exert therapeutically-beneficial effects as long as treatment is initiated

early enough in the disease timecourse. This finding is especially exciting with regard to the clinical translation of M_1 activators for treating AD, as the therapeutic dose one has to deliver to achieve sustained beneficial effects may be much lower than the dose one might have to deliver to an mild-to-advanced AD patients. An important implication of this is that it dramatically reduces the probability that off-target side effects or nonselective effects at other muscarinic family members will be observed, which otherwise might be provoked by a higher dose used to treat a mild-to-advanced AD patient. For a class of drugs (M_1 activators) plagued in the clinic by dose-limited side effects this is extremely welcome news!

Finally, an important note with regard to our chronic 5X FAD trial design is worth discussing. This trial was performed with all female mice because female 5X FAD mice (as do many other transgenic mouse models) express much higher levels (~30% more) of $A\beta$ and onset with memory impairments sooner than do males. Thus, for our purposes, females represented the more therapeutically challenging gender to tackle as far as translating observed effects to the clinic. Female animals in preclinical trials and female subjects in clinical trials represent often excluded and understudied groups. This is partly out of necessity, as research and clinical trials are expensive and as much control needs to be maintained over subject patient populations as possible. However, with regard to developing effective therapies, the exclusion of one gender is detrimental to the goal of improving patient health. Particularly with diseases that disproportionately impact women, this gender-bias is problematic. Interestingly, the pathological disparities between the genders in animal models of AD are mirrored in humans. That is, women are almost twice as likely (1:6 versus 1:11 for men) as men to develop AD by the age of

65. The choosing to structure our 5X FAD mouse trial with all females is therapeutically hugely-significant, as it indicates that chronic M₁ activation can prevent AD relevant neuropathology and memory impairments in females, where many other trials have used males. However, it does intentionally exclude males from the design. One would expect chronic M₁ activation with VU572 to have the same therapeutic effect in males as it does in females, however, our current study cannot speak to this. Future preclinical work is warranted to further investigate this and the inclusion of males along with females is certainly a factor that should be considered in translating chronic M₁ activation to the clinic.

While VU572 represents an important advance forward for selective M₁ receptor agonists that provides proof of mechanism for chronic M₁ activation in AD, there are a couple of reasons that may preclude VU572 from clinical development in humans. First, although VU572 represents a potent, selective M₁ agonist in rats, a right-shift of ~10-fold into the low-micromolar range was noted on human isoforms of the M₁ receptor (EC₅₀ = 1.3 μM). Additionally, the synthesis of more potent analogs of a chemical scaffold related to VU572 engendered detectable micromolar activity at M₂₋₅ (Melancon, et al. 2012). Thus, even though no hM₂₋₅ activity was noted at concentrations up to 30 μM, pushing the dose of VU572 or more potent analogs into micromolar ranges may increase the likelihood of observing adverse side effects with dosing in humans. Second, VU572 is a relatively short-lived compound with a *t*_{1/2} of only 46 min, which precludes formulation for optimal dosing in human studies. Ideally, compounds for human studies are developed for once, twice, or, at most, three times daily oral dosing in order to maximize patient compliance with taking all doses. Despite these shortcomings, VU572

displays excellent oral bioavailability and ancillary pharmacology. Therefore, in light of the beneficial effects on AD pathology and prevention of memory impairments reported in the present work, a more advanced analog of VU572 that displays increased potency for hM₁ (while maintaining M₁ selectivity) with a longer half-life is recommended for subsequent clinical development in humans.

Chapter IV: EFFECTS OF SELECTIVE M₁ ACTIVATION ON HIPPOCAMPAL CIRCUITRY DYNAMICS

Introduction

While the M₁ muscarinic receptor has been shown to play a key role in memory and the actions whereby ACh exerts a modulatory influence on hippocampal circuitry, how exactly M₁ acts at the level of brain circuits *in vivo* to mediate this effect is a significant unanswered question. The question of how M₁ exerts influence over the activity of hippocampal circuits *in vivo* has not yet been answered partly due to a couple of different reasons. Namely, developing specific small molecule M₁ activators that possess druggable properties for *in vivo* studies has proven incredibly difficult after over two decades of effort by the pharmaceutical industry. Only recently was the first small molecule M₁ specific activator suitable for *in vivo* studies described (Lebois, et al. 2011). Aside from the difficulty in developing sufficiently selective tools to study M₁ function, only recently has the technology in high-density neural recording *in vivo* progressed to a point where large collections of neurons can be recorded simultaneously across multiple brain areas. The confluence of these factors has allowed us for the first time to interrogate how previously documented therapeutically efficacious levels of M₁ receptor function act in the CNS to bias the activity of hippocampal circuits.

The discovery and characterization of hippocampal place cells by O'Keefe and colleagues and subsequent characterization of the spatial firing properties of hippocampal place fields has enabled us to utilize place cells as a window into hippocampal function in order to observe how well the hippocampus is doing its job to represent current

information. Subsequent work by Hasselmo and colleagues has implicated muscarinic receptors in the suppression of intrahippocampal circuits. Specifically, muscarinic receptors have been shown to suppress CA3 signaling to CA1. This signaling to CA1 by CA3 occurs in a distinct frequency band of the low gamma (30-50 Hz) range and is thought to represent the recall of previous information by the hippocampus. On the other hand, CA1 also communicates with EC in a separate distinct high gamma (90-140 Hz) band and this microcircuit is thought to convey current, online information to the hippocampus. Given the fact that CA1 also communicates directly with EC, this raises the intriguing possibility that muscarinic receptors can act as a switch to modulate the relative familiarity of information in the hippocampus. That is, by suppressing CA3-CA1 activity, muscarinic receptors may bias the hippocampus towards the ability to code current information.

We hypothesize that M_1 receptors play a role in this suppression of intrahippocampal CA3 and CA1 circuitry and examine the ability of the M_1 allosteric agonist VU572 to influence hippocampal place cell representations in response to graded contextual manipulation using a morph-box (Figures 4.1 and 4.2). In this study we record simultaneously from dorsal CA3 and CA1 as animals engage in open field exploration. We show compelling evidence to suggest that M_1 improves spatial representations by the hippocampus and that this corresponds to a suppression of CA3-CA1 connectivity. Specifically, we demonstrate that spikes from CA3 hippocampal pyramidal cells become dose-dependently desynchronized with increasing levels of M_1 activation by VU572.

Results

Place Cells Code Contextual Change in the Proposed Morph Box Test Paradigm

In order to examine whether M_1 activation by VU572 is capable of exerting a beneficial effect on the degree to which hippocampal place cells represent space, we first need an experimental paradigm that induces changes in hippocampal place field representations. In this manner, the influence of a drug on these place field representations can then be measured. Several different studies have now utilized a morph-box to manipulate place field representations and this is the approach we elected to utilize for the present studies (Figures 4.1 and 4.2). A morph box is exactly as the name implies: a box that changes shape. Specifically, we utilize a sequence of geometrically-graded contextual morphs (square-octagon-hexagon-circle-square) in order to manipulate the place cell representation of contextual information. We hypothesize that under baseline conditions, the animal will recognize the intermediate contexts as different from the initial square context and the final square context as the same shape in which he started. Therefore, place cell representations should track with this expectation, where place fields change in response to the octagon-hexagon-circle encounters and look the same in the square-square encounter (Figure 4.1). Furthermore, we expect that M_1 activation by VU572 will act to increase the degree to which place cells represent the octagon-hexagon-circle contexts relative to the square.

Plotting representative actual data from a single place cell from an actual test session under baseline conditions with no drug on board allows one to see several things (Figure 4.2). First and foremost is that place cells show an expected response to contextual manipulation in our morph box paradigm (Figure 4.2A). As rats navigate the

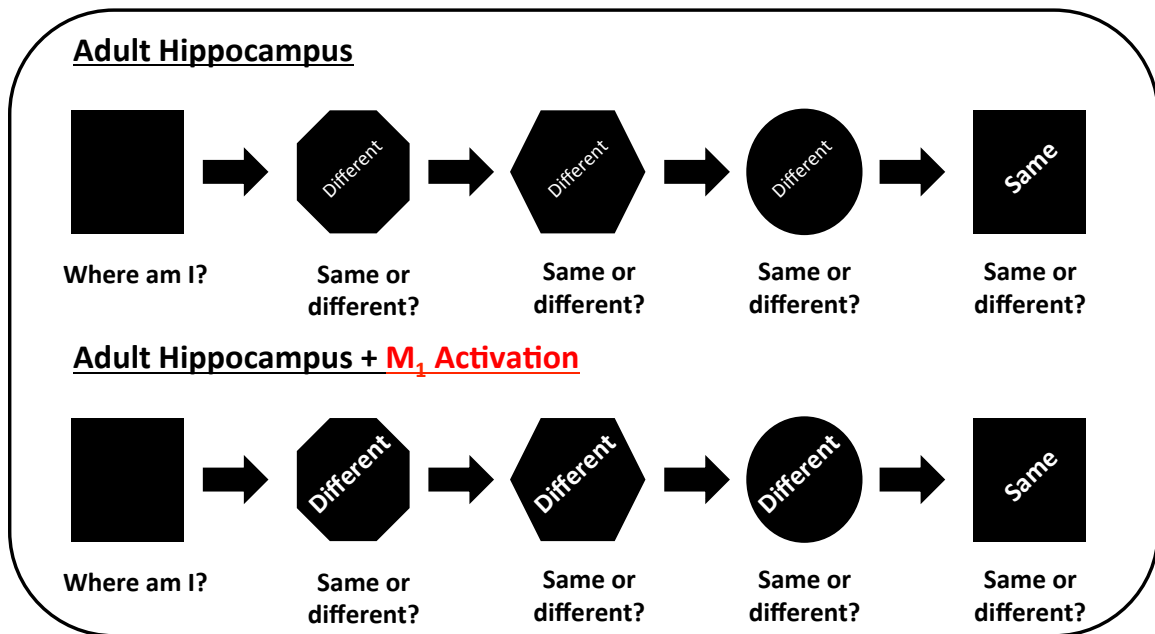


Figure 4.1. Morph Box Test Paradigm to Manipulate Hippocampal Place Field Activity.

Test sequence utilized in order to manipulate hippocampal place field activity (Top).

This study relies upon a morph box with segmented walls that allow the same testing enclosure to be “morphed” into a variety of different shapes for animals to explore.

Shown above is the actual test sequence of shapes: square-octagon-hexagon-circle-square.

Animals were trained to navigate square-circle-square to criteria (15 minutes each) prior

to surgery and then retrained to criteria on these shapes. During actual test sessions,

animals then encountered the full 5 shape sequence in the same order every time. The

bottom row shows the anticipated outcome of M_1 activation on hippocampal place cell activity, whereby place cells will change their firing properties to a greater degree in the intervening (octagon-hexagon-circle) contexts compared to a familiar context (square).

M_1 activation should not impact the ability to initially form a spatial representation in square 1 or subsequently recall it in square 2.

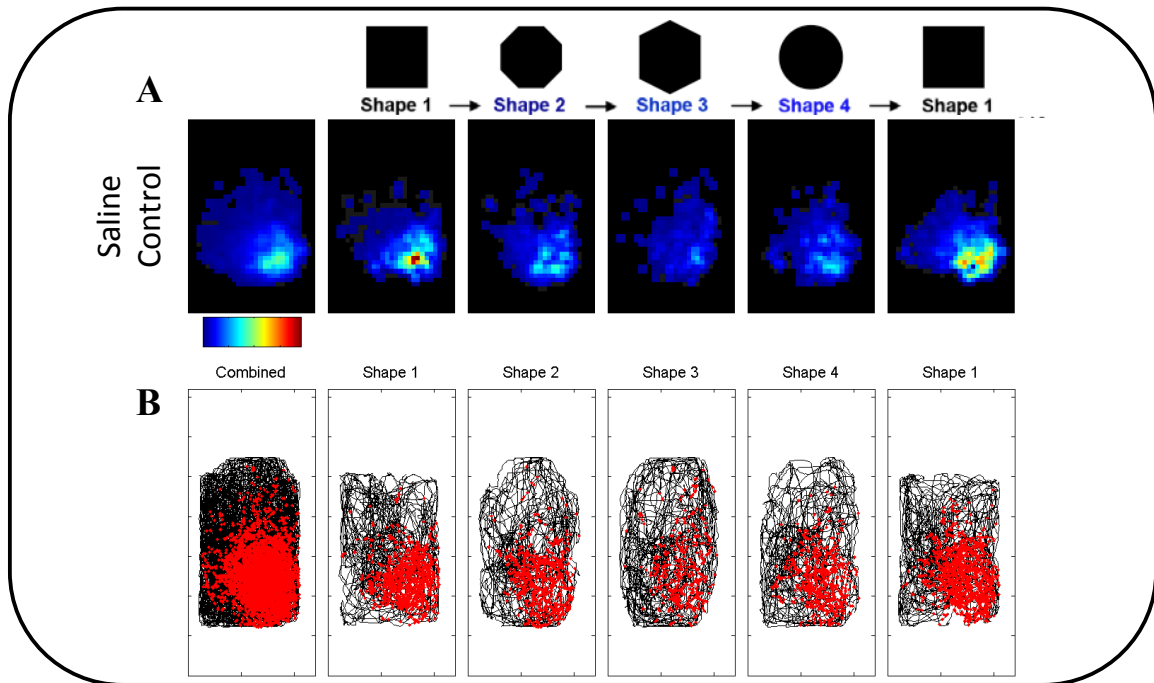


Figure 4.2. Place Cells Code Contextual Change in the Proposed Morph Box Test Paradigm.

A) Depiction of one representative hippocampal place cell from a test session in which a rat was administered a s.c. dose of saline. Rate maps show that this place cell has a place field in the bottom right hand area of all contexts encountered, where hotter colors equal higher firing rates. However, the firing rate of the place field markedly decreases in square, hexagon, and circular contexts, indicating that the rat is coding these contexts as different than the square. Furthermore, the original location and firing rate is recovered when the animals is reintroduced to the square enclosure indicating that he remembers the context as one he previously visited. B) The animal's movement trajectory is plotted as a black wire trace for each 15 minute exploration bout in individual shapes.

Superimposed upon this black wire trace are red dots, indicating every position at which this pyramidal cell emits an action potential. This figure allows one to see that even though the animal thoroughly explored all of the surface area available to him in the test

enclosure, the cell has a very particular place that it prefers to fire. In this vein, this also shows that any differences in place cell activity in a given context are not simply due to an animal not exploring a particular location.

full complement of differently-shaped testing enclosures, the place field representations in octagon-hexagon-circle differ from square, indicating that place fields are responding to the change in contextual information. Furthermore, the activity in square-square looks similar, which provides important information about how well the hippocampus is functioning to recall previous information. Also, the movement of the animal can be plotted over time (Figure 4B, black wire trace) with spikes superimposed upon this movement trace for every time during a test session at which a neuron being recorded emits an action potential. Taking the unit in figure 4B as an example, this unit spikes robustly in the bottom right-hand corner of the box where the neuron has its place field, but is relatively silent in much of the rest of the box even though it is clear the animal has explored all of the testing enclosure available to him. This illustrates nicely a fundamental property of place cell firing, that these cells respond to unique combinations of visuospatial and sensory cues to represent distinct points in space. While the movement traces are not shown for every cell in every test session for the present study, only data from test sessions in which the animal explored the entirety of the testing enclosure for every individual test context were included in the final analyses.

M₁ Activation by VU572 Increases Spatial Discrimination of Hippocampal Place Cells

A central question of interest in this work is whether M₁ activation by VU572 is able to increase the degree to which hippocampal place cells represent current information. In order to ascertain this, rats were run through the full complement of test-shapes, as described, under saline and randomized drug conditions. Prior to all test sessions rats were given strawberry Jell-O and an injection regardless of whether there

was drug in the Jell-O or syringe. On days where drug was in the Jell-O rats received a saline injection. The rats were administered 1 mg/kg, 10 mg/kg, and 30 mg/kg of the M₁ allosteric agonist, VU572, 30 mg/kg of the M₁ PAM, BQCA, and 3 mg/kg of the AChEI, donepezil and then tested at the time in which each of these drugs is known to be at its maximal concentration in the brain (~30 min post-injection). As expected, place fields were observed under all treatment conditions and these place fields changed in an anticipated manner with contextual change (Figure 4.3).

However, figure 4.3 illustrates a key point of why one needs to record from as many neurons in the CNS as possible when interrogating drug effects *in vivo*. Namely, that if one compares place fields from a single neuron under saline, 30 mg/kg VU572, and 3 mg/kg donepezil (rows 1, 3, and 5 in figure 4.3) the change in octagon-hexagon-circle for each of these conditions appears to be relatively equivalent when compared to square. Thus, it becomes critical to average over large populations of cells in order to appreciate drug effects on neural circuits. The observation that BQCA appears to be profoundly disruptive of place cell activity at the present dose of 30 mg/kg was completely unexpected and will be discussed at length shortly.

By averaging over all of the hippocampal units recorded (~100 units per drug condition represented) from 3 rats, we observe in Figure 4.4 that M₁ activation by VU572 at 1 mg/kg ($*p < 0.05$, $t = 2.00$, $df = 116$), 10 mg/kg ($*p < 0.05$, $t = 2.00$, $df = 180$) or 30 mg/kg ($*p < 0.05$, $t = 2.18$, $df = 164$) increases the ability of hippocampal place cells to represent the octagon-hexagon-circle shapes as more different than the square relative to saline. This exciting finding suggests that M₁ is biasing hippocampal circuitry towards the coding of current information. Furthermore, as expected, donepezil appears to have

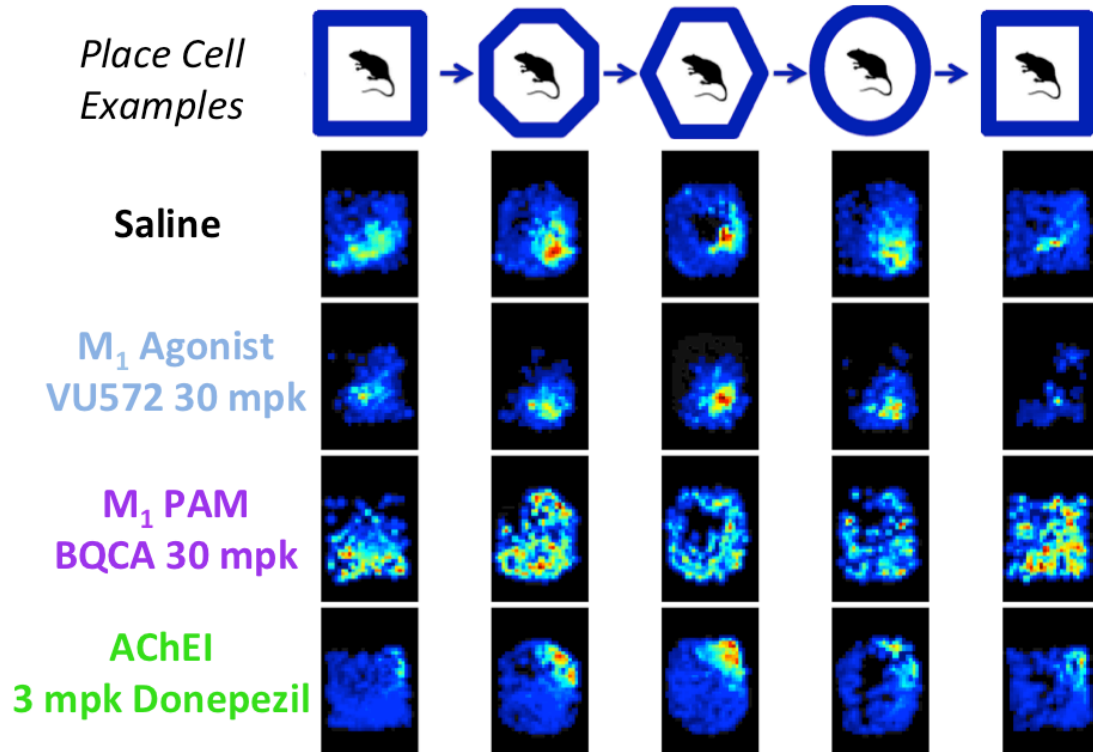


Figure 4.3. Representative Place Cell Examples From Experimental Drug Sessions.

Example place fields are shown for selected drug conditions to depict representative effects of the M₁ agonist, VU572, the M₁ PAM, BQCA, and the acetylcholinesterase inhibitor, donepezil, on place field activity following contextual manipulation. The top saline row shows expected changes in place field firing rate that accompany the octagon, hexagon, and circular morphs, as well as the recovery of initial firing rate upon the animal's return to a square enclosure. This same pattern of change was also observed in the 30 mg/kg M₁ agonist and 3 mg/kg donepezil test sessions. When comparing the degree of change to saline for just one cell as is shown here, though, the change looks no greater than that observed under saline conditions. This critically illustrates why, in order to appreciate drug effects on place cell activity, it is important to average over as large a cell population as possible in order to observe such effects. In the present studies we record from a total of ~100 hippocampal pyramidal cells that the following analyses will

focus on. Unexpectedly, BQCA at a dose of 30 mg/kg profoundly disrupted place cell activity, which could be due to a variety of reasons addressed in the manuscript.

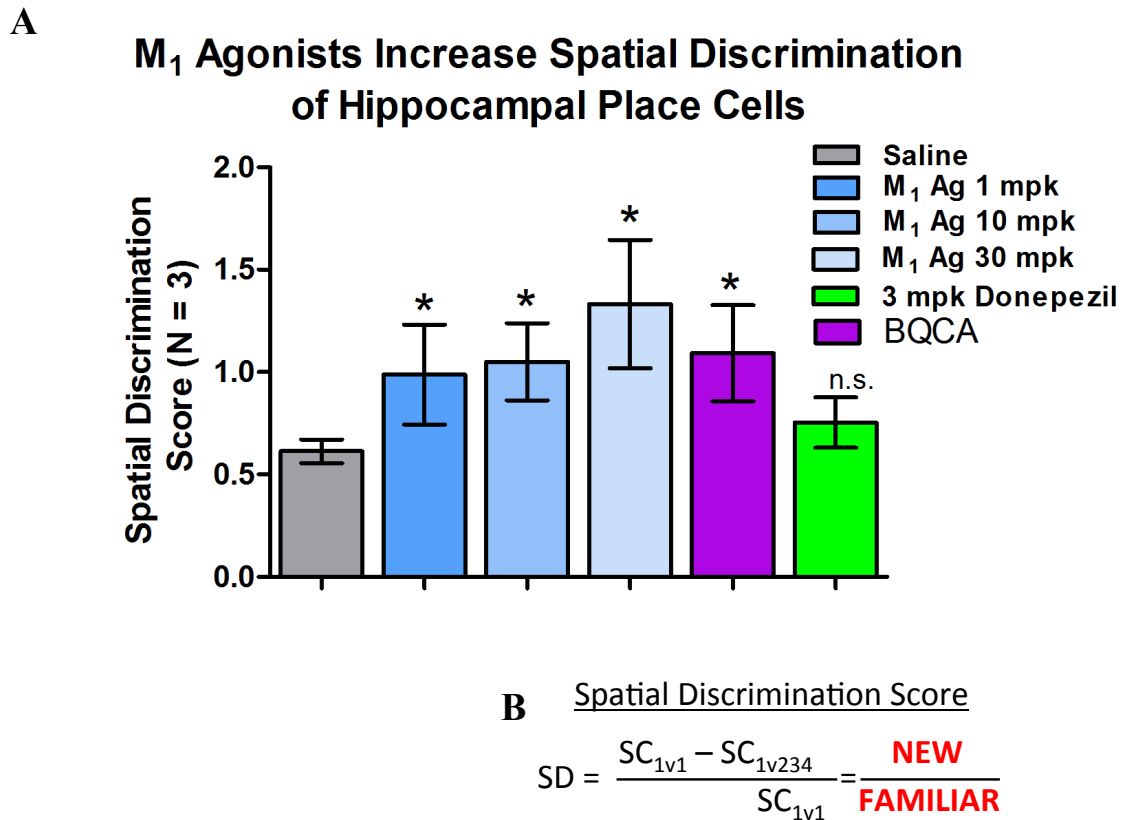


Figure 4.4. M₁ Activation by VU572 Increases Spatial Discrimination of Hippocampal Place Cells.

A) M₁ activation by VU572 at doses of 1 mg/kg ($*p < 0.05$, $t = 2.00$, $df = 116$), 10 mg/kg ($*p < 0.05$, $t = 2.00$, $df = 180$), and 30 mg/kg ($*p < 0.05$, $t = 2.18$, $df = 164$) significantly increases the degree to which place cells code novel spatial information in the octagon, hexagon, and circular contexts. BQCA was also found to significantly improve spatial discrimination scores ($*p < 0.05$, $t = 2.08$, $df = 176$). The apparent increase for BQCA is due to reasons that will be addressed in the subsequent analysis. No significant effect was observed on place cell representation of spatial information with donepezil. B) Spatial discrimination (SD) scores were calculated according to the formula shown. Pixel-by-pixel spatial correlations were taken pairwise between square 1 and square 2 (SC_{1v1}), from which the average spatial correlation of intervening contexts

(SC_{1v234}) and expressed in a ratio over SC_{1v1} . This calculation yields the SD score, where a higher SD score indicates that place fields are changing to a greater degree in the intervening octagon, hexagon, and circular shapes. Error bars show \pm SEM across single units for all rats.

no effect due to its nonselective action at activating functionally-opposing ACh receptor subtypes.

M₁ Activation by VU572 Does Not Impair Spatial Information of CA3 or CA1 Place Cells, but Activation by the M₁ PAM BQCA Does

Given the observation that BQCA appeared to significantly increase the ability of hippocampal place cells to code current information in a similar manner to VU572, this prompted us to quantify the effect of BQCA on the spatial information content of place cells to explain this unexpected result. It is important to realize that the spatial discrimination we use to calculate the degree of place cell change in octagon-hexagon-circle can increase for one of two reasons: either a) a place cell truly becomes better at tracking and representing contextual change, or b) a drug destabilizes a place field representation such that the fields look profoundly different in octagon-hexagon-circle. Based upon visual inspection of such place fields for BQCA from figure 4.3 and others in figure 4.5A, quantifying the impact of all drugs on the spatial information content of place cells was necessary to clarify the discrepancy with BQCA. This allowed us to verify that VU572 was not detrimentally impacting spatial information and distinguish why BQCA appeared to be increasing spatial discrimination scores. The resulting spatial information plots overwhelmingly showed a profound decrease for BQCA in the spatial information content of both CA3 and CA1 place cells ($*p < 0.05$, $t = 2.32$, $df = 72$; $**p < 0.01$, $t = 3.29$, $df = 109$; $***p < 0.001$, $t = 4.07$, $df = 175$) (Figure 4.5). On the other hand, no significant effect on spatial information content for CA3 or CA1 place cells was noted for all doses of VU572 or donepezil (Figure 4.5C-E).

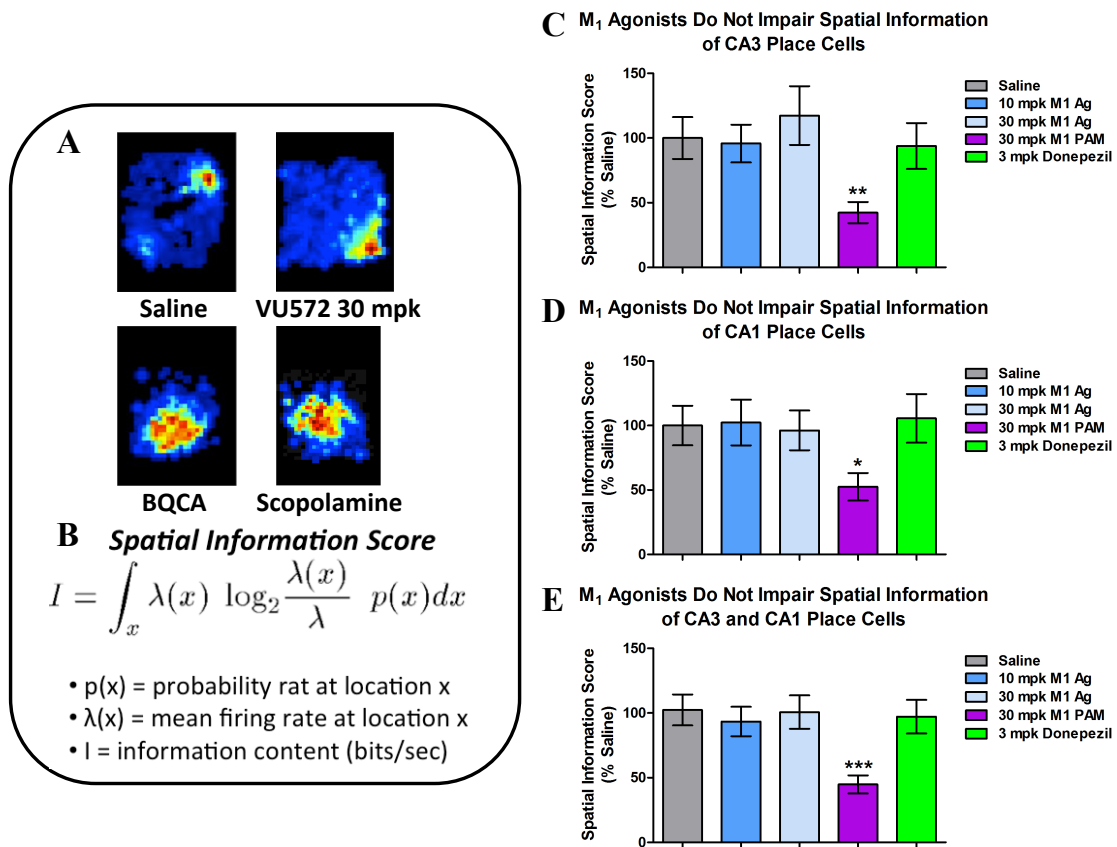


Figure 4.5. M₁ Activation by VU572 Does Not Impair Spatial Information of CA3 or CA1 Place Cells, but Activation by the M₁ PAM BQCA Does.

A) Representative examples of place fields obtained under various drug conditions. Note the prototypical acuity in organization of firing rate with place fields under saline and VU572 conditions. That is, the place fields start off cool at the edges and then smoothly ascend to a focal point of high firing rate at the very center of the place field, indicating a very accurate representation of a point in space. In contrast, place fields under BQCA and scopolamine treatment look enlarged and very disordered, indicating that the representation of spatial information is compromised. B) The quantity of spatial information contained in place fields can be quantified in bits/sec using the Skaggs spatial information score (Skaggs, et al. 1993). C-E) Plotting the Skaggs score for CA3

and CA1 place fields shows that M_1 activation by VU572 has no effect on the amount of spatial information contained in these place fields. However, BQCA appears to dramatically decrease the amount of spatial information in both CA3 and CA1 place fields ($*p < 0.05$, $t = 2.32$, $df = 72$; $**p < 0.01$, $t = 3.29$, $df = 109$; $***p < 0.001$, $t = 4.07$, $df = 175$). Possible reasons for this BQCA-mediated reduction in place field spatial information content are addressed in the manuscript. Error bars show \pm SEM across single place cells for all rats.

M₁ Activation by VU572 Suppresses CA3-CA1 Field-Field Coherence

Following the observation that M₁ activation by VU572 can act to increase the ability of hippocampal place cells to code current spatial information we next wondered what changes might be taking place at the level of CA3-CA1 circuitry in order to mediate this effect. Thus, we examined several measures of CA3-CA1 activity in response to M₁ activation by VU572. The first measure of CA3-CA1 connectivity analyzed was CA3-CA1 field-field coherence. Again, since CA3 is known to communicate with CA1 at low gamma frequencies (30-50 Hz) we hypothesize that we would see a decrease in this frequency band. In this vein, in figure 4.6 we observed a significant decrease of ~12% relative to saline in the low gamma band following increasing doses of VU572 (* $p < 0.05$; $t = 2.31$, $df = 16$). BQCA was also found to suppress CA3-CA1 low gamma activity (** $p < 0.01$; $t = 2.977$, $df = 16$), while donepezil had no significant effect. Importantly, VU572 had no effect on CA3-CA1 field-field coherence in the theta range, suggesting that the baseline information processing state the hippocampus uses to organize information remains unaffected by drug treatment.

M₁ Activation by VU572 Suppresses CA3 Spike-CA1 Field Coherence

In light of the exciting finding that M₁ activation can act to suppress CA3-CA1 field-field coherence we endeavored to further pursue the mechanism whereby M₁ appears to be biasing hippocampal circuitry. Since field-field coherence is a general measure of functional connectivity it gives very little information about the nature of the information being sent from CA3 to CA1. That is, a high field-field coherence value could indicate that two oscillations are perfectly phase locked peak-to-peak and trough-

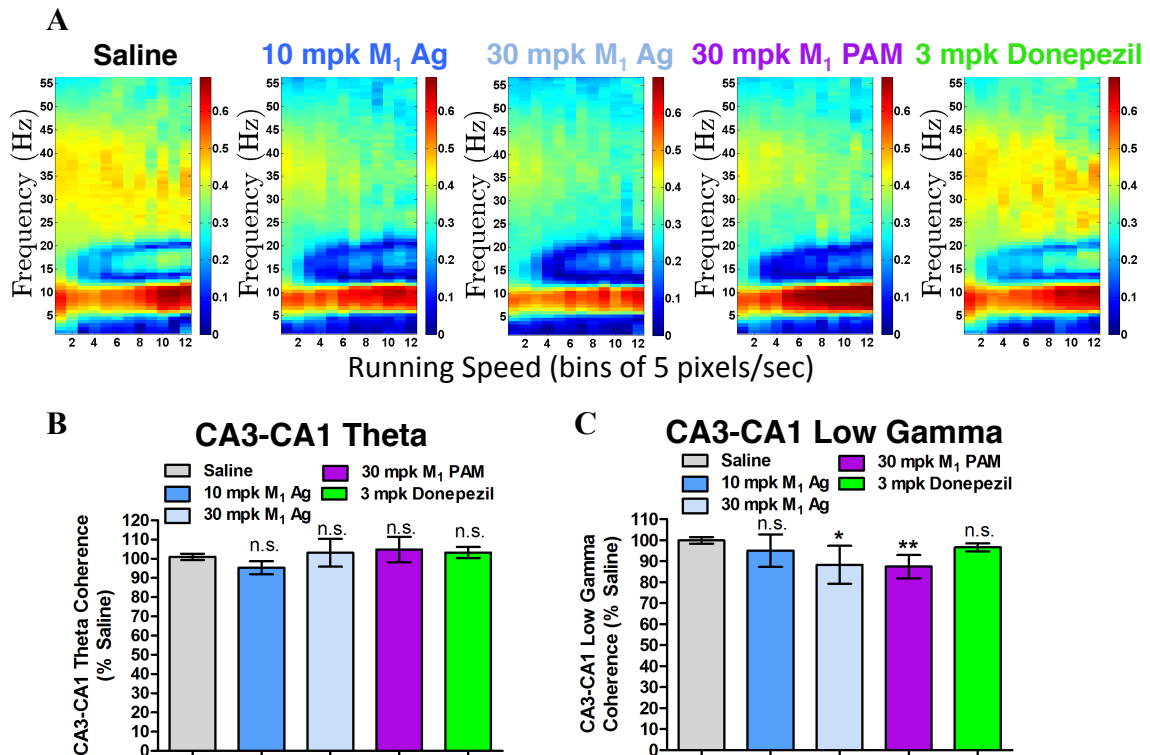


Figure 4.6. M₁ Activation by VU572 Suppresses CA3-CA1 Field-Field Coherence.

A) CA3-CA1 field-field coherence plots were constructed from a tetrode pair located in the middle third of the proximal-distal axis of both CA3 and CA1. Tetrodes in this region were chosen both because the microcircuitry of the hippocampus is such that the middle third of CA3 communicates most robustly with the middle third of CA1 and because the middle third of the subfields receives an equivalent blending of both lateral and medial entorhinal cortical inputs. As it is uncertain to what degree, if any, M₁ activation will impact nonspatial versus spatial information representation, the presence of this blending of nonspatial and spatial information in the present spectral analyses is ideal. Furthermore, the coherograms display data along the x-axis binned by running speed in order to control for the behavioral state of the animal. M₁ activation by VU572 shows a dose-dependent reduction in low gamma frequency (30-50 Hz), indicating that

VU572 can suppress CA3-CA1 functional connectivity since CA3 communicates with CA1 at low gamma frequencies. A decrease was also noted with BQCA and none was observed with donepezil. B) Quantification of the theta and low gamma spectral bands across equivalent running speed bins of LFP data (bins 4-10) for all three rats utilized in the present study show that M₁ activation by VU572 has no appreciable impact on theta field coherence, but significantly dose-dependently suppresses coherence in the low gamma range by 12% ($*p < 0.05$; $t = 2.31$, $df = 16$). BQCA also yielded a significant reduction in low gamma coherence of approximately 10% ($**p < 0.01$; $t = 2.977$, $df = 16$). For saline conditions, the mean coherence in each of running speed bin 6-10 is plotted \pm SEM across rats. For drug conditions a single average coherence value was obtained for the frequency band of interest and plotted \pm SEM across rats.

to-trough, or rather perfectly 180 degrees out of phase. The important determinant for a high coherence value is that the relationship between the oscillators is maintained over time. In the case of two perfectly in-phase oscillators or two perfectly 180 degrees out-of-phase oscillators, these scenarios would likely have exactly the opposite functional consequence.

Thus, it became crucial to determine what M_1 activation by VU572 is doing at the level of CA3 to impact spiking. By analyzing the organization of CA3 spikes being received by CA1, it can be determined whether or not VU572 is truly suppressing the integrity of actual information being sent to CA1. Spike-field coherence allows the determination of how coherent a particular spike train is relative to the phases of a field oscillation (Figure 4.7). Here, the coherence of CA3 spikes was measured relative CA1 theta oscillations since theta is by far the most prominent frequency that occurs as an animal locomoted around a testing enclosure engaging in open-field exploration. Under saline conditions when the spike field coherence between CA3 spikes and CA1 theta field oscillations was calculated an appreciable degree of baseline coherence was observed, as one would expect (Figure 4.7B). M_1 activation by increasing doses of VU572 was found to trigger a decrease in CA3-CA1 spike-field coherence relative to saline (Figure 4.7C). This decrease in CA3-CA1 spike-field coherence suggested that as the level of M_1 activation is increased, the information (spikes) flowing to CA1 became temporally desynchronized. CA1 theta was chosen as a frequency to compare CA3 spikes to, as it is by far the most prominent frequency observed during a test session in which animals are engaged free navigation. Future analyses will examine CA3 spike-CA1 low gamma coherence, as the low gamma frequency band should directly reflect CA3-CA1 activity.

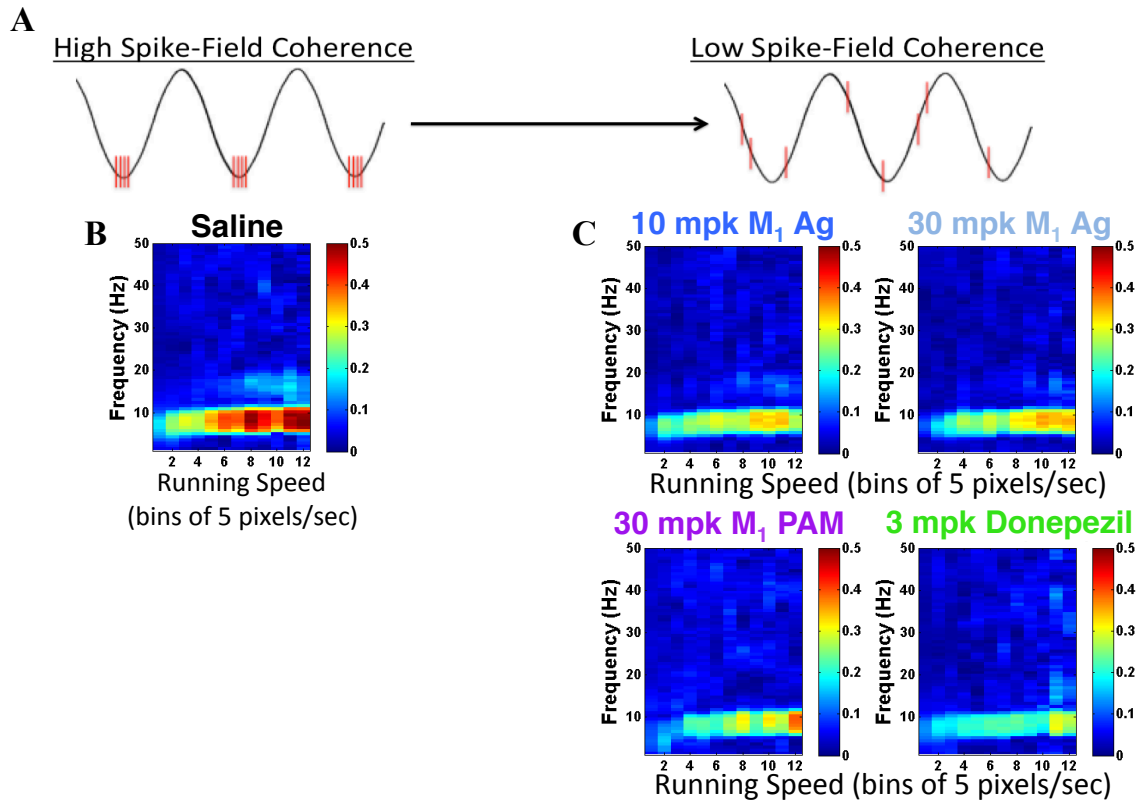


Figure 4.7. M_1 Activation by VU572 Suppresses CA3 Spike-CA1 Field Coherence.

A) Examples of high and low spike-field coherence. Under conditions of high spike-field coherence there is a very strong consistency in the relationship between the spikes from one region (e.g. CA3; spikes shown by red lines) and the field of another region (e.g. CA1; field shown by black oscillation). The exact converse is true for conditions of low-spike-field coherence where at the extreme spikes from one region fall in a seemingly random manner onto the field oscillation of another region (right portion of panel A). B) CA1 LFPs were filtered for theta frequency oscillations and phases were compared against incoming CA3 spikes in order to generate a spike-field coherence value. CA3 spikes from all units were combined and compared against the entire test session's worth of LFP data. Under saline conditions, there is an appreciable degree of CA3 spike-CA1 field coherence in the theta range, as one might expect since theta oscillations are so

prominent during locomotion and open-field exploration. C) M_1 activation by VU572 shows a suppression of CA3 spike-CA1 field coherence, indicating that M_1 muscarinic receptor activation is capable of suppressing information transfer in the CA3-CA1 microcircuit. Interestingly, BQCA and donepezil appear capable of also suppressing CA3 spike-CA1 field coherence. In the case of donepezil, this suppression may very well arise entirely from other actions than M_1 activation.

M₁ Activation by VU572 Renders CA3 Spikes to CA1 Less Coherent

Since spike-field coherence is a biased statistic, unbiased methods in order to quantify the effect of M₁ activation by VU572 on the organization of CA3 spikes flowing into CA1 theta field oscillations were needed. The pairwise phase consistency was developed as just such an unbiased statistic that measures whether there is a particular phase of an oscillation that spikes tend to be most consistent with, regardless of what that phase actually is. Thus, the higher the pairwise phase consistency, the more temporally ordered spikes, whereas a low pairwise phase consistency equates to a more random temporal organization of how spikes fall on a field oscillation. By computing the pairwise phase consistency for units across all 3 rats that data was recorded from, M₁ activation by VU572 at 10 mg/kg and 30 mg/kg appears to dose-dependently suppress the pairwise phase consistency of CA3 spikes relative to CA1 theta oscillations ($*p < 0.05$, $t = 2.23$, $df = 94$; $***p < 0.001$, $t = 3.90$, $df = 90$) (Figure 4.8). This suppression is consistent with the result obtained in spike-field coherence analysis and indicates that the temporal organization of CA3 spiking becomes disrupted with increasing levels of M₁ activation. In this regard, BQCA was found to very robustly depress CA3-CA1 pairwise phase-consistency, the implications of which will be discussed shortly ($***p < 0.001$, $t = 5.32$, $df = 94$) (Figure 4.8). Donepezil was found to have no significant effect on the temporal organization of CA3 spiking ($t = 1.087$, $df = 100$) (Figure 4.8).

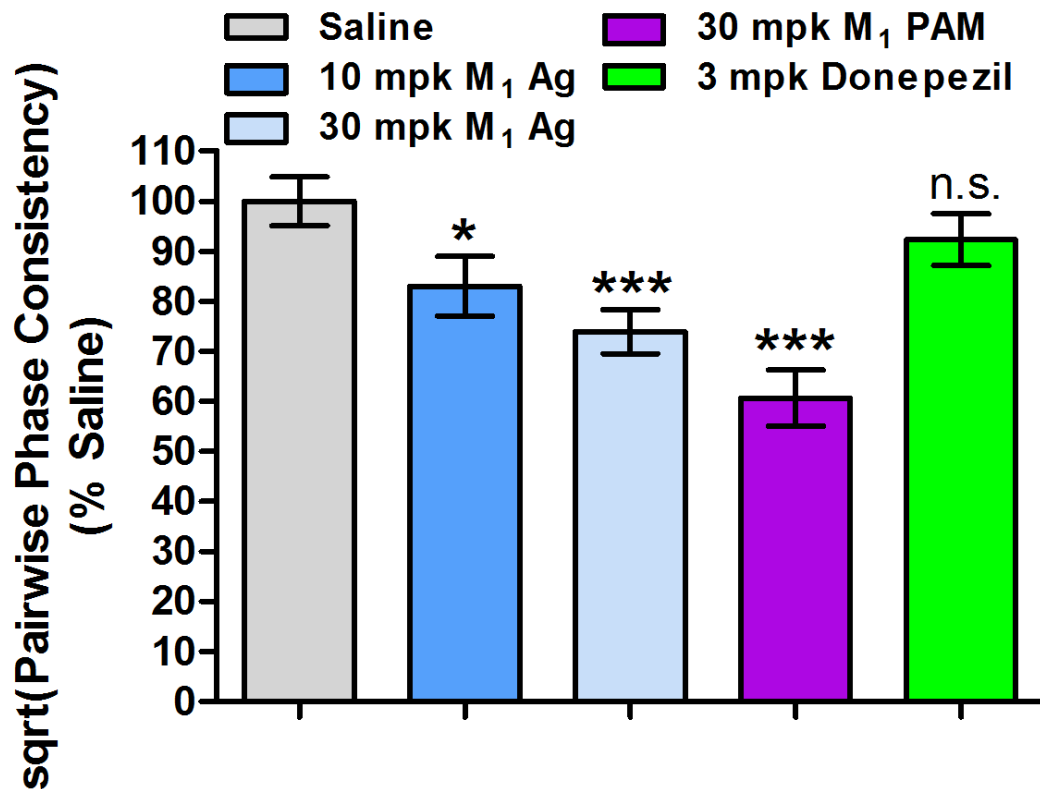


Figure 4.8. M₁ Activation by VU572 Renders CA3 Spikes to CA1 Less Coherent.

Since spike-field coherence is a biased statistic, it is hard to calculate on a unit-by-unit basis for units possessing low spike counts during a test session, which is particularly common in the CA3 subfield of interest where firing rates tend to be much lower than in CA1. In order to determine the effect of M₁ activation on the temporal organization of spiking by individual units, analysis using the unbiased statistic of pairwise phase consistency (PPC) was employed (Vinck, et al. 2010). The PPC is equal to the average dot product of the angular distance between spike pairs for a given unit. The general idea is that the higher the phase-consistency of spikes from a given neuron (that is, spikes continually fall on the same phase of oscillations over time), the smaller the angular distance between any two of those spikes. The square root of the pairwise phase

consistency is equivalent to the mean resultant length vector typically used in estimating spike-phase coherence. Thus, the higher the value of the sqrt(PPC), the more organized or coherent spikes can be said to be relative to the field oscillation of another region. Conversely, low sqrt(PPC) values indicate temporal disorganization among spikes relative to the field oscillation. Following dosing of 10 mg/kg and 30 mg/kg VU572 it appears that M₁ activation triggers a dose-dependent temporal disorganization of CA3 spikes relative to CA1 theta oscillations, as sqrt(PPC) values decrease ($*p < 0.05$, $t = 2.23$, $df = 94$; $***p < 0.001$, $t = 3.90$, $df = 90$). In a similar fashion, BQCA triggers a disorganization of CA3 spikes to an even greater degree, although such a robust suppression may not correspond to beneficial effects on spatial memory in light of the place field data discussed earlier in the manuscript ($***p < 0.001$, $t = 5.32$, $df = 94$). No significant effects on CA3 spiking organization were noted with donepezil ($t = 1.087$, $df = 100$). Error bars show \pm SEM across single units meeting firing criteria for all rats.

Discussion

In this study, the mechanisms for how M_1 mAChRs act at the level of hippocampal circuitry to mediate their therapeutic effects on memory *in vivo* begin to be uncovered for the first time. Specifically, we show a role for M_1 mAChRs in biasing how the hippocampus represents current spatial information at the level of CA3 and CA1 place cells. Additionally, a role for M_1 in suppressing CA3-CA1 connectivity is uncovered. In particular, we find that measures of CA3-CA1 field-field and spike-field coherence are reduced by increasing M_1 activation. This reduction is CA3 spike-CA1 field coherence and corresponding reduction in CA3-CA1 pairwise phase consistency indicates that increasing levels of M_1 activation serve to temporally-desynchronize CA3 spikes and compromise the information that is being conveyed to CA1. Importantly, the practical implication of this M_1 -mediated desynchronization of CA3 spiking may be illustrated by figures 4.9 and 4.10.

As previously mentioned, CA1 is known to communicate with both CA3 and EC. These channels of communication are believed to represent the convergence of previous information and current information onto CA1, respectively. Under normal baseline conditions, CA1 may be equally inclined to listen to either CA3 or EC (Figure 4.9) and this idea is consistent with the level of pattern completion and pattern separation normally observed in CA1 (Leutgeb, et al. 2005, 2007, 2008). However, in the presence of an M_1 activator that renders the information coming from CA3 less-coherent, CA3 may synchronize with CA1 less of the time. Thus, this may likely free CA1 to synchronize more with EC in the service of representing current information. It is important to note that EC and CA3 are not the only anatomically-connected regions to

CA1. Therefore, the larger implication of suppressed CA3 CA1 connectivity is that CA1 is free to synchronize with all of its anatomically-connected partners more (e.g. prefrontal cortex) in the service of representing current spatial information. Notably, the present work examines CA3 spike-CA1 theta coherence specifically. Theta was chosen as a frequency to compare CA3 spikes to, as it is by far the most prominent frequency observed during a test session in which animals are engaged free navigation. Additionally, theta serves as a global organizational framework to organize the activity of faster oscillators, so changes at the level of theta have global implications for information processing by the CA3-CA1 circuit. Future analyses will examine CA3 spike-CA1 low gamma coherence, as the low gamma frequency band should directly reflect CA3-CA1 activity.

A limitation of the current study is that we systemically deliver a drug and record brain activity at a very distant CA3-CA1 synapse. The present study was designed to most closely model the therapeutic scenario where a M_1 activator is systemically delivered and it exerts a particular effect on the brain. Our intent was to measure the resulting sum of all brain-wide M_1 activation at the level of the hippocampus. Thus, we attempt to make no claim that it is specifically CA3 M_1 receptors responsible for mediating the observed effects. Previous experimental evidence is consistent with the notion that VU572 may be exerting its actions in a manner relatively confined to hippocampal circuitry, though. Digby and colleagues examine the neuronal responsiveness to VU572 using whole cell and field recordings from three different brain regions with varying degrees of M_1 receptor reserve. Specifically, they recorded from hippocampal preparations, which are thought to have a high M_1 receptor reserve, striatal

preparations, which are thought to have a moderate M_1 receptor reserve, and mPFC preparations, which are thought to have a lower M_1 receptor reserve. What they observed was that VU572 elicited a robust increase in activity in the hippocampus, a moderate effect in the striatum, and no observable effect in mPFC. Since VU572 is a partial agonist, it makes sense that its activity tracks with the degree of receptor reserve in various brain regions. However, it also raises the provocative question of whether partial agonists for modulatory receptors particularly enriched in the hippocampus might be uniquely poised to alleviate memory disorders since such compounds can exert effects relatively confined to hippocampal circuits. Furthermore, this study raises several other provocative findings, discussed below.

First and foremost, how is BQCA degrading spatial representations if M_1 activation is supposed to be good for memory? There are several different possibilities. If this study were designed to focus on the mechanism of BQCA on hippocampal representations we would have included several different concentrations of BQCA to address this question. As it was, we only had sufficient bandwidth to include a single dose of BQCA and due to the limited literature reporting the effects of BQCA on memory tasks, our best guess came from a reversal learning study done by Nicolle and colleagues (Shirey, et al. 2009). Since reversal learning is known to be mediated via frontal circuitry more so than hippocampal circuitry it is likely that the dose of BQCA selected for the present study was very sub-optimal. Another possibility is that too much M_1 efficacy in a healthy adult brain could be a bad thing. Since healthy adult rats were utilized for the study, pushing their hippocampal circuitry to suprathreshold levels of ACh signaling may prove to be deleterious for accurately representing information. Yet

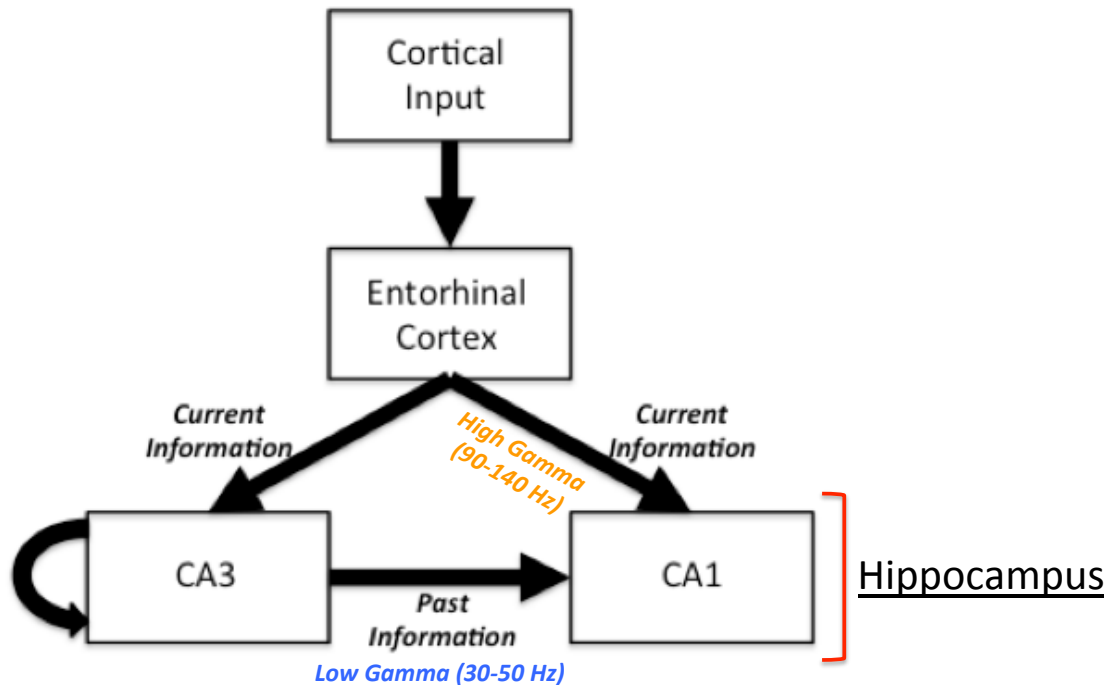


Figure 4.9. Under Normal Circumstances CA1 Listens Equally to Either CA3 or EC.

Under normal circumstances, CA1 receives its two major inputs from CA3 and entorhinal cortex (EC). Notably, these inputs can be distinctly differentiated at the spectral level as they occur in very distinct frequency bands. CA1 is known to communicate with EC at high gamma frequencies (90-140 Hz), whereas CA1 communication with CA3 takes place at low gamma frequencies (30-50 Hz). EC-CA1 activity is thought to drive coding of current, online information by the hippocampus. On the other hand, CA3-CA1 activity is thought to drive the retrieval of previously coded representations by the hippocampus. Thus, under normal conditions in a healthy hippocampus CA1 flips back and forth between EC and CA3 inputs in order to compare and contrast new incoming information with already encoded memories so that a new memory can be formed if a difference exists.

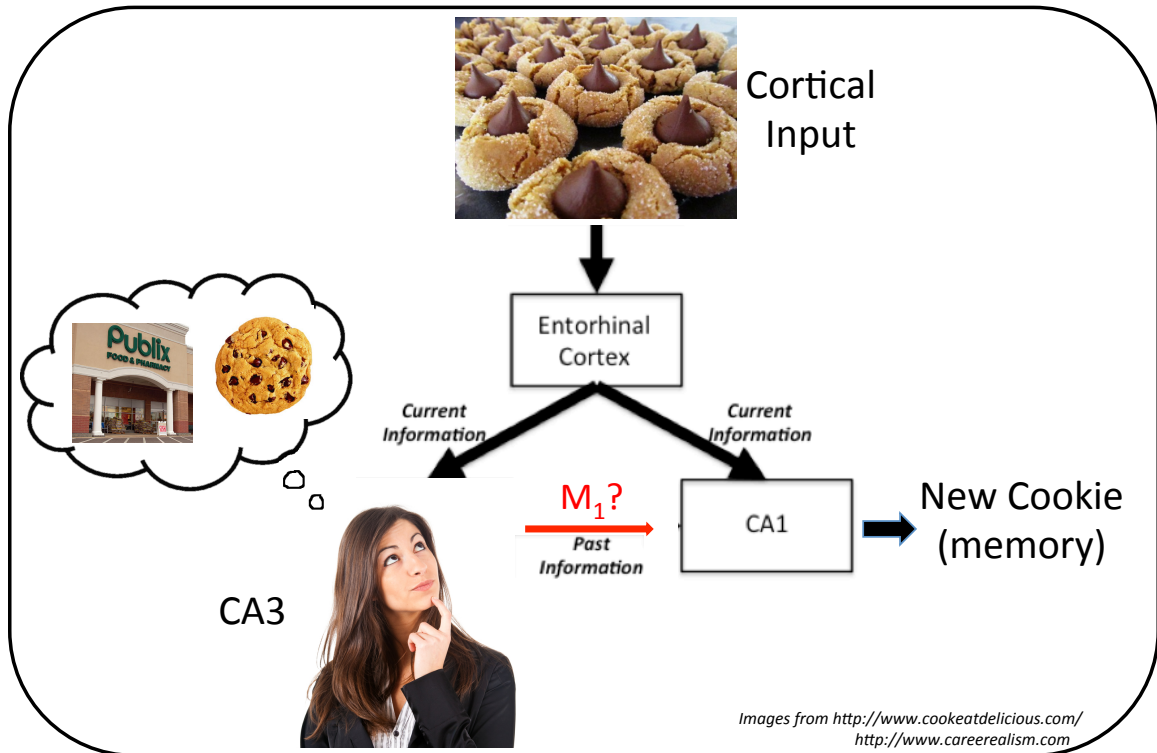


Figure 4.10. The Suppression of CA3-CA1 Circuitry by M₁ Agonists May Bias CA1 Towards Synchronizing More with Other Partners Such as EC to Drive Novel Information Encoding.

In light of the findings that M₁ activation by VU572 is capable of enhancing hippocampal place cell representation of novel spatial information while simultaneously suppressing CA3-CA1 information transfer, one plausible interpretation is given by the above figure. If cortical input is provided to the hippocampus in terms of a new cookie one encounters, one will first hold the new cookie information online (mediated by EC-CA1 activity) and compare this information to experiences with previous cookies (mediated by CA3-CA1 activity) (e.g. a chocolate chip cookie encountered during a recent visit to the grocery store) in order to determine if the present cookie is truly a new cookie or a familiar cookie. Since CA1 receives each of its prominent inputs from CA3 and entorhinal cortex (EC), M₁-mediated suppression of CA3-CA1 connections may act to increase the

availability of CA1 to synchronize more/easier with EC and increase the likelihood that the hippocampus will code the new cookie as a new memory (that is, the attention of CA1 no longer has to be divided as much between both CA3 and EC). This increase in current information encoding has important implications for states of aging and disease (e.g. schizophrenia) where the functional pathology at the level of the hippocampus is an elevation in CA3 firing rate. Additionally, this increase in availability of CA1 to synchronize more with other anatomically-connected partners following CA3-CA1 suppression may generalize to other brain areas beyond EC (e.g. prefrontal cortex).

another possibility is due to the pharmacology of BQCA itself. In the past few years it has become apparent that BQCA is not as pure of an M₁ PAM as originally thought. Namely, BQCA can most aptly be referred to as an ago-PAM because in addition to possessing activity as a potentiator it is also capable of directly activating M₁ receptors (Langmead, et al. 2012; Melancon, et al. 2012). This combination of direct activation and potentiation on top of endogenous signaling by ACh may serve to overwhelm endogenous memory circuitry. Finally, although we did not observe any dose-limiting peripheral side effects, there may very well be central off-target side effects that we could not otherwise rule out in the present study, as BQCA is a rather preliminary compound with a large degree of uncertainty regarding its ancillary pharmacology at other receptors. Future work would be needed to clarify whether the actions observed on place fields are M₁-specific or not, so M₁ PAMs as a therapeutically-relevant mechanism for improving memory should not at all be ruled out by the present work.

Apart from the actions of BQCA, a more basic, fundamental question is: how is it that M₁ receptors are acting to suppress CA3-CA1 connectivity, when one might expect *a priori* that M₁ activators would enhance CA3-CA1 connectivity since M₁ is an excitatory receptor? In addressing this question it is important to state first that we observed no changes in mean firing rates for any units recorded under the influence of VU572 compared to saline. The only changes we note in spiking apart from drug effects on place cells are a temporal desynchronization that leads to less coherent CA3 information being received by CA1. Tonegawa has actually demonstrated a functional role for M₁ receptor presynaptic inhibition in CA3 that could serve to explain why increasing concentrations of VU572 suppress activity in the CA3-CA1 microcircuit (Kremin, et al.

2006). While the M_1 receptor has been functionally implicated in this regard, it is important to point out that immunohistochemical do not detect any presynaptic levels of M_1 in the hippocampus.

A more plausible explanation for the ability of VU572 to temporally-desynchronize CA3 spikes and suppress information transfer in the CA3-CA1 circuit, may therefore derive from its pharmacology. As a direct-acting agonist, VU572 is not bound by the spatiotemporal constraints of endogenous ligand signaling. Since VU572 is an allosteric agonist and does not need ACh to activate M_1 , this compound activates M_1 both outside and inside of the temporal domain of endogenous ACh signaling. While VU572 is an agonist, the net functional effect of activating M_1 receptors at a time when they should not be active may serve to dose-dependently inject noise into neuronal circuits modulated by M_1 . Therefore, injecting noise into CA3 spike trains would render them less coherent and be expected to diminish the ability of this information to couple to CA1 cells.

Chapter V: SUMMARY AND FUTURE DIRECTIONS

In this thesis I have shown several significant findings pertaining to the role of M_1 mAChR receptors. In Aim 1 of the current thesis I focused on rigorously investigating whether or not chronic M_1 activation is a viable therapeutic mechanism to treat AD. To this end I demonstrated for the first time that chronic dosing of the first M_1 -specific agonist, VU572, is capable of preventing memory impairments and significantly curbing $A\beta_{40}$ and $A\beta_{42}$ pathology in the brains of 5X FAD mice. In particular, the action of VU572 appears to lessen $A\beta_{40}$ and $A\beta_{42}$ pathology in the hippocampus and cortex of these mice and abolishes the correlation of soluble $A\beta_{42}$ in the hippocampus with memory impairments, suggesting that VU572 also acts to decrease soluble $A\beta$ oligomers, although this remains to be determined. This finding is extremely exciting and important, as it suggests that activating M_1 during prodromal AD may work in the clinic to slow or halt the development of neuropathology and memory impairments and that therapeutically-beneficial effects can be sustained and long-lasting. Furthermore, the potential for clinical translation of this M_1 -mediated mechanism is high since the present effects were observed in the most aggressive mouse model of AD to-date. One of the most attractive aspects for clinical translation of the present work is that it demonstrates significant and sustained effects with a relatively weak M_1 activator compared with potent and robust full agonists or PAMs. Thus, the side-effect liability in the clinic is dramatically lessened by the prospect of obtaining therapeutic efficacy in prodromal AD with a much lower dose than one might otherwise give to a mid-to-late-stage AD patient.

In Aim 2 of the present thesis I examined the ability of VU572 to bias hippocampal circuitry away towards the representation of current spatial information.

Specifically, I showed that M₁ activation by VU572 can improve the ability of CA3 and CA1 hippocampal place cells to represent current spatial information. This increase in representation of current spatial information was found to be paralleled by a decrease in CA3-CA1 field-field coherence and a decrease in measures of CA3 spike-CA1 field coherence. The observed decrease in CA3 spike-CA1 field coherence was shown to be due to increasing temporal desynchronization of CA3 spike under the influence of increasing M₁ activation. This ability of M₁ to drive temporal disorganization of CA3 spiking has several important applications, discussed below.

First, aging is known to impact hippocampal circuitry in many deleterious ways (Figure 5.1) (Wilson, et al. 2006; Small, et al. 2011; Yassa, et al. 2011). The net result of the age-related loss of hippocampal circuitry modulation *in vivo* seems to be that CA3 firing rate becomes elevated. This elevation in CA3 firing rate begs the question of whether or not CA3-CA1 coherence is also pathologically high in aged and diseased animals and individual who display elevated CA3 firing. If so, this could provide a mechanism to help explain the failure of older cognitively-impaired individuals to effectively code current information.

At the level of place cells in aged rats, Wilson and colleagues have shown in several studies that CA3 place cells are able to form spatial representations in a context like a normal place cell, although if a rat is then introduced to a novel context, the original place field spatial representation remains (Figure 5.2) (Wilson, et al. 2002, 2004, 2006). In effect, the hippocampus of the animal does not recognize that the animal has changed to a new context. The failure to remap upon exposure to novel contexts for aged rats led Wilson to coin the term “rigid” when referring to the CA3 place fields of old

animals. The rigidity in CA3 place field representation and elevated CA3 firing may, therefore, reflect an overemphasis on prior information by the aged hippocampus. In light of the findings of the current thesis that M_1 activation can act to suppress CA3-CA1 connectivity, future studies are warranted that examine the potential of VU572 to reverse or help ameliorate these age-related deficits in place cell representation of spatial information.

Apart from age-related deficits how place cells represent information, place cells in Tg2576 transgenic AD mice also exhibit deficits in place cell representation of information (Figure 5.3) (Cacucci, et al. 2008). These mice are known to display larger and more disorganized CA1 place fields than their WT littermates, indicating that AD neuropathology can disrupt accurate representation of spatial information by the hippocampus. Due to the demonstrated effects in the present thesis on the ability of VU572 to guard against neuropathology and cognitive decline in a mouse model of AD, future studies are warranted to see whether or not VU572 also is able to rescue functional deficits at the circuit level in transgenic models. A major limitation of O'Keefe's work in the Tg2576 mice is that since recordings were performed in mice, only cells from CA1 were recorded. In addition to only having place cells from CA1, not many cells overall were able to be recorded since mice are so small and cannot be implanted with many tetrodes. Thus the overall yield of place cells that one can record from a mouse is very low. In terms of appreciating how disease pathology affects circuits and how drugs might influence these effects a rat model of AD would be very preferable. Fortunately, such a model was recently described by Cohen and colleagues and will prove to be a boon for the understanding of functional deficits that occur at the level of memory

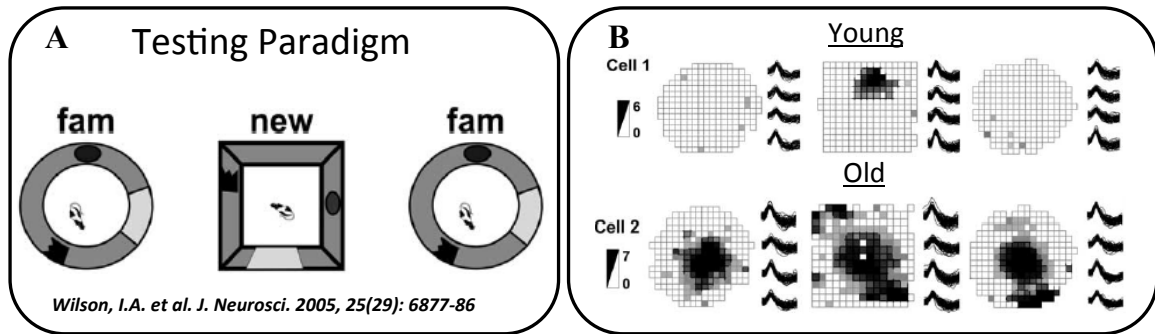


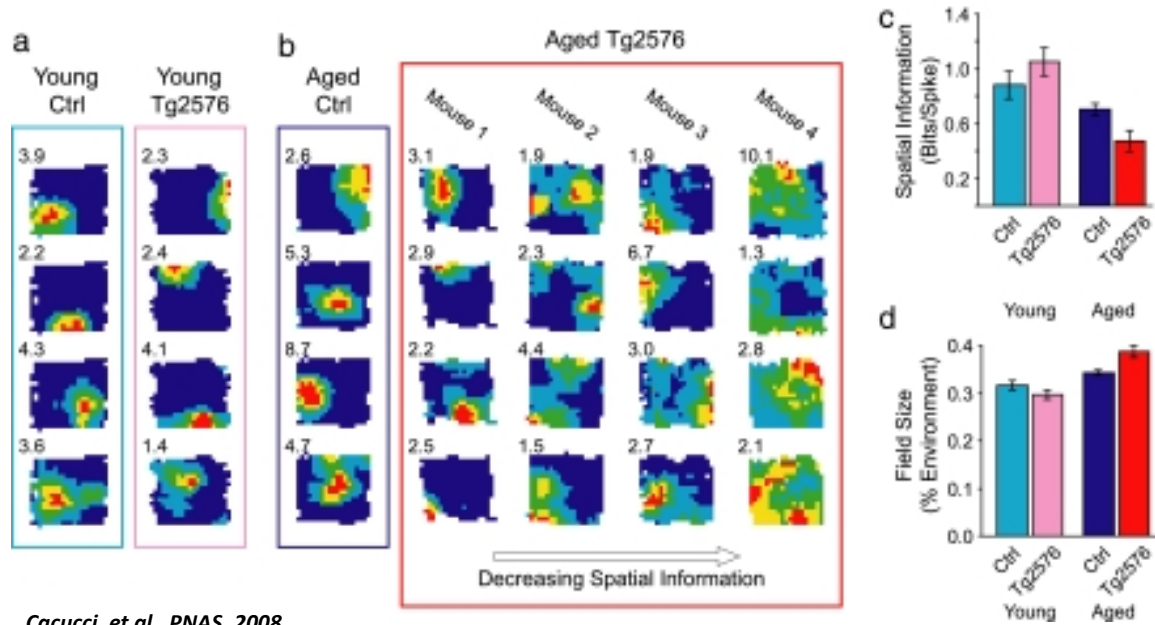
Figure 5.2. Aging Detrimentally Impacts the Ability of Place Cells to Represent Space and Biases the Hippocampus Towards Pattern Completion.

As previously mentioned, the pathological elevation in CA3 activity that accompanies aging and disease states is thought to lock hippocampal circuitry into an information retrieval state, whereby animals over-emphasize previous memories. This hypothesis bears out at the level of place cells and becomes apparent when aged rats are run through a sequence of differently shaped test enclosures (A and B), analogous to the present work (circle-square-circle test enclosures are used, above). B) Aged animals are able to form typical place fields when placed in the initial circle enclosure, however, CA3 place fields remain “rigid” and do not change when an animal encounters different context (e.g. square) that a young animal would recognize as different. In light of the present findings demonstrating that M_1 activation can both increase the ability of place cells to represent novel spatial information and suppress CA3-CA1 connectivity, future work dedicated to understanding whether M_1 activators can overcome the rigid representations formed by the aged hippocampus is crucial.

circuits in response to AD pathology (Cohen, et al. 2013). Ongoing work in the laboratory of Joseph Manns seeks to identify the earliest circuit abnormalities in these animals and whether M₁ activation with VU572 is effective in combatting these circuit deficits.

Aside from aged and AD rodent models, recent research has shown that a common tie between mild cognitive impairment (MCI), age-related cognitive decline, and schizophrenia is hippocampal CA3 overactivity (Figure 5.4). It is possible that this CA3 overactivity may lie at the heart of the memory deficits that are hallmark components of these various conditions. Thus, future work should be aimed at leveraging the present findings that M₁ activation provides a means to suppress CA3-CA1 connectivity in order to see if selective M₁ activators are efficacious in the clinic alleviating the memory impairments associated with the aforementioned conditions and whether any alleviation of memory impairments tracks with an ability of M₁ activators to suppress the ability of CA3 to communicate with CA1. Notably, Stark and Gallagher have developed pattern completion and pattern separation imaging tasks that would permit the detection of such therapeutic effects in the clinical populations of interest (Gallagher, et al. 2010; Yassa, et al. 2011a, 2011b).

Finally, the findings of present thesis with regard to the beneficial impact of chronic M₁ activation on alleviating neuropathology and preventing memory impairments in 5X FAD mice allows for the possibility of discovering new treatment avenues for AD. Namely, effects confined to A β may only represent part of the pathological and therapeutic story observed in 5X FAD mice. In this vein, future work will seek to run an unbiased proteomic screen on soluble and insoluble samples from the hippocampus and

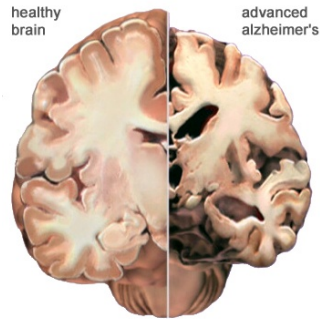


Cacucci, et al. PNAS. 2008.

Figure 5.3. Mouse Models of AD Show Disrupted Place Fields and Decreased Spatial Information Content of Place Cells.

A) Young WT control mice and Tg2576 transgenic AD mice show stereotypical place field formation with typical spatial information content (C) and place field size (D) observed. However, aged control and Tg2576 mice show overt place cell abnormalities (B-D). Aged controls show a moderate decline in spatial information relative to young mice (C) and a slight increase in place field size (D), indicating that aging may adversely impact the ability of the hippocampus to accurately represent spatial information and form episodic memories. Tg2576 mice show a marked decline in spatial information (C) and a greater increase in place field size (D) relative to young mice, indicating that the presence AD pathology may further diminish the capacity of the hippocampus to accurately represent spatial information and form episodic memories.

cortex of 5X FAD vehicle-treated mice versus mice treated with VU572. Such a screen will enable us to obtain a treatment-responsive proteome in order to more closely and globally examine if levels of particular proteins are significantly perturbed in particular tissue fractions in order to gain a better understanding of which proteins may be involved in disease pathology and which proteins may represent novel treatment targets for AD.



MCI/Alzheimer's Disease

- Early death of layer II EC glutamatergic neurons
- Hippocampal CA3 overactivity in MCI (Putcha, et al. *J. Neurosci.* 2005)



Age-Related Cognitive Decline

- Decreased cholinergic modulation of hippocampus
- Hippocampal CA3 overactivity (Bookheimer, et al. *NEJM* 2000; Wilson, et al. *J. Neurosci.* 2005)



Schizophrenia

- NMDAR hypofunction
- Hippocampal CA3 overactivity (Tamminga, et al. *Am. J. Psych.* 2010)

Can we alter hippocampal input-output dynamics to benefit states of memory impairment?

Figure 5.4. M₁ Agonists for the Treatment of Memory Dysfunction.

The findings that M₁ activation by VU572 is capable of enhancing hippocampal place cell representation of novel spatial information while simultaneously suppressing CA3-CA1 information transfer have important implications for states of aging and disease. Mild cognitive impairment (MCI), age-related cognitive decline, and schizophrenia are all conditions with memory deficits as hallmark components of the disorders. A common documented pathological tie between mild cognitive impairment (MCI), age-related cognitive decline, and schizophrenia is CA3 overactivity. Thus, in light of the present findings M₁ should be viewed as a critically relevant therapeutic mechanism for these conditions of memory impairment moving forward. The possibility of altering hippocampal input-output dynamics by M₁ activation to benefit states of memory impairments may be a realistic and valid approach to take.

DECLARATION OF CONFLICTS OF INTEREST

Evan P. Lebois holds patents surrounding the compound VU0364572, mentioned in this work, but has not received any royalties or other revenue from this intellectual property.

REFERENCES

Websites:

<http://groups.csail.mit.edu/netmit/wordpress/projects/sparse-fourier-transform/>

<http://www.alz.org>

<http://www.alzgene.org>

http://www.alz.org/alzheimers_disease_facts_figures.asp

<http://what-when-how.com/neuroscience/neurotransmitters-the-neuron-part-2/>

Primary Literature:

Abe K, Nakata A, Mizutani A, Saito H (1994) Facilitatory but nonessential role of the muscarinic cholinergic system in the generation of long-term potentiation of population spikes in the dentate gyrus in vivo. *Neuropharmacology*, 33:847-852.

Akiyama, H., Barger, S., Barnum, S., Bradt, B., Bauer, J., Cole, G. M., ... & Wyss-Coray, T. (2000). Inflammation and Alzheimer's disease. *Neurobiology of aging*, 21(3), 383-421.

Alzheimer A. Uber eine eigenartige Erkrankung der Hirnrinde. *Allg. Z. Psychiatr.* 1907; 64, 146-148.

Anagnostaras, S. G., Murphy, G. G., Hamilton, S. E., Mitchell, S. L., Rahnema, N. P., Nathanson, N. M., & Silva, A. J. (2002). Selective cognitive dysfunction in acetylcholine M1 muscarinic receptor mutant mice. *Nature neuroscience*, 6(1), 51-58.

Anagnostaras, S. G., G. G. Murphy, et al. (2003). "Selective cognitive dysfunction in acetylcholine M1 muscarinic receptor mutant mice." *Nat Neurosci* 6(1): 51-8.

- Auerbach, J. M., & Segal, M. E. N. A. H. E. M. (1994). A novel cholinergic induction of long-term potentiation in rat hippocampus. *Journal of Neurophysiology*, *72*(4), 2034-2040.
- Auerbach, J. M., & Segal, M. (1996). Muscarinic receptors mediating depression and long-term potentiation in rat hippocampus. *The Journal of Physiology*, *492*(Pt 2), 479-493.
- Avlani, V. A., Langmead, C. J., Guida, E., Wood, M. D., Tehan, B. G., Herdon, H. J., ... & Christopoulos, A. (2010). Orthosteric and allosteric modes of interaction of novel selective agonists of the M1 muscarinic acetylcholine receptor. *Molecular pharmacology*, *78*(1), 94-104.
- Bakker, A., Krauss, G. L., Albert, M. S., Speck, C. L., Jones, L. R., Stark, C. E., ... & Gallagher, M. (2012). Reduction of hippocampal hyperactivity improves cognition in amnesic mild cognitive impairment. *Neuron*, *74*(3), 467-474.
- Barker, W. W., Luis, C. A., Kashuba, A., Luis, M., Harwood, D. G., Loewenstein, D., ... & Duara, R. (2002). Relative frequencies of Alzheimer disease, Lewy body, vascular and frontotemporal dementia, and hippocampal sclerosis in the State of Florida Brain Bank. *Alzheimer Disease & Associated Disorders*, *16*(4), 203-212.
- Basile AS, Fedorova I, Zapata A, Liu X, Shippenberg T, Duttaroy A, Yamada M, Wess J (2002) Deletion of the M5 muscarinic acetylcholine receptor attenuates morphine reinforcement and withdrawal but not morphine analgesia. *Proc Natl Acad Sci USA*, *99*:11452-11457.
- Baysinger, A. N., Kent, B. A., & Brown, T. H. (2012). Muscarinic receptors in amygdala control trace fear conditioning. *PloS one*, *7*(9), e45720.

- Beattie, A., Klumpp, S., Cohen, P., & Codd, G. A. (1988). Dynamics of the Hippocampal Ensemble Code for Space. *Proc. Natl. Acad. Sci. USA*, *85*, 4991.
- Berkeley JL, Gomeza J, Wess J, Hamilton SE, Nathanson NM, Levey AI (2001) M1 muscarinic acetylcholine receptors activate extracellular signal-regulated kinase in CA1 pyramidal neurons in mouse hippocampal slices. *Mol Cell Neurosci*, *18*:512-524.
- Billings, L. M., Oddo, S., Green, K. N., McGaugh, J. L., & LaFerla, F. M. (2005). Intraneuronal A β causes the onset of early Alzheimer's disease-related cognitive deficits in transgenic mice. *Neuron*, *45*(5), 675-688.
- Bitan, G., Kirkitadze, M. D., Lomakin, A., Vollers, S. S., Benedek, G. B., & Teplow, D. B. (2003). Amyloid β -protein (A β) assembly: A β 40 and A β 42 oligomerize through distinct pathways. *Proceedings of the National Academy of Sciences*, *100*(1), 330-335.
- Bliss, T. V., & Collingridge, G. L. (1993). A synaptic model of memory: long-term potentiation in the hippocampus. *Nature*, *361*(6407), 31-39.
- Blitzer RD, Gil O, Landau EM (1990) Cholinergic stimulation enhances long-term potentiation in the CA1 region of rat hippocampus. *Neurosci Lett*, *119*:207-210.
- Bodick NC, Offen WW, Shannon HE, Satterwhite J, Lucas R, van Lier R, Paul SM (1997a) The selective muscarinic agonist xanomeline improves both the cognitive deficits and behavioral symptoms of Alzheimer disease. *Alzheimer Dis. Assoc. Disord.* *11* Suppl 4:S16-22.232.
- Bodick, N. C., Offen, W. W., Levey, A. I., Cutler, N. R., Gauthier, S. G., Satlin, A., ... & Paul, S. M. (1997b). Effects of xanomeline, a selective muscarinic receptor

- agonist, on cognitive function and behavioral symptoms in Alzheimer disease. *Archives of Neurology*, 54(4), 465-473.
- Bokil, H., Purpura, K., Schoffelen, J. M., Thomson, D., & Mitra, P. (2007). Comparing spectra and coherences for groups of unequal size. *Journal of neuroscience methods*, 159(2), 337-345.
- Bokil, H., Andrews, P., Kulkarni, J. E., Mehta, S., & Mitra, P. P. (2010). Chronux: a platform for analyzing neural signals. *Journal of neuroscience methods*, 192(1), 146-151.
- Bomben, V., Holth, J., Reed, J., Cramer, P., Landreth, G., & Noebels, J. (2014). Bexarotene reduces network excitability in models of Alzheimer's disease and epilepsy. *Neurobiology of aging*.
- Bookheimer, S. Y., Strojwas, M. H., Cohen, M. S., Saunders, A. M., Pericak-Vance, M. A., Mazziotta, J. C., & Small, G. W. (2000). Patterns of brain activation in people at risk for Alzheimer's disease. *New England journal of medicine*, 343(7), 450-456.
- Bridges, T. M., LeBois, E. P., Hopkins, C. R., Wood, M. R., Jones, C. K., Conn, P. J., & Lindsley, C. W. (2010). The antipsychotic potential of muscarinic allosteric modulation. *Drug news & perspectives*, 23(4), 229-240.
- Brown, E. N., Kass, R. E., & Mitra, P. P. (2004). Multiple neural spike train data analysis: state-of-the-art and future challenges. *Nature neuroscience*, 7(5), 456-461.

- Brun, V. H., Otnæss, M. K., Molden, S., Steffenach, H. A., Witter, M. P., Moser, M. B., & Moser, E. I. (2002). Place cells and place recognition maintained by direct entorhinal-hippocampal circuitry. *Science*, *296*(5576), 2243-2246.
- Brun, V. H., Leutgeb, S., Wu, H. Q., Schwarcz, R., Witter, M. P., Moser, E. I., & Moser, M. B. (2008). Impaired spatial representation in CA1 after lesion of direct input from entorhinal cortex. *Neuron*, *57*(2), 290-302.
- Buchhave, P., Minthon, L., Zetterberg, H., Wallin, Å. K., Blennow, K., & Hansson, O. (2012). Cerebrospinal Fluid Levels of β -Amyloid 1-42, but Not of Tau, Are Fully Changed Already 5 to 10 Years Before the Onset of Alzheimer Dementia. *Archives of general psychiatry*, *69*(1), 98-06.
- Buckner, R. L. (2004). Memory and executive function in aging and AD: multiple factors that cause decline and reserve factors that compensate. *Neuron*, *44*(1), 195-208.
- Buckner, R. L., Snyder, A. Z., Shannon, B. J., LaRossa, G., Sachs, R., Fotenos, A. F., ... & Mintun, M. A. (2005). Molecular, structural, and functional characterization of Alzheimer's disease: evidence for a relationship between default activity, amyloid, and memory. *The Journal of Neuroscience*, *25*(34), 7709-7717.
- Burgard EC, Sarvey JM (1990) Muscarinic receptor activation facilitates the induction of long-term potentiation (LTP) in the rat dentate gyrus. *Neurosci Lett*, 116:34-39.
- Burgess, N., Maguire, E. A., & O'Keefe, J. (2002). The human hippocampus and spatial and episodic memory. *Neuron*, *35*(4), 625-641.
- Buzsáki, G., & Draguhn, A. (2004). Neuronal oscillations in cortical networks. *Science*, *304*(5679), 1926-1929.

- Buzsáki, G. (2004). Large-scale recording of neuronal ensembles. *Nature neuroscience*, 7(5), 446-451.
- Buzsáki, G., & Watson, B. O. (2012). Brain rhythms and neural syntax: implications for efficient coding of cognitive content and neuropsychiatric disease. *Dialogues in clinical neuroscience*, 14(4), 345.
- Buzsáki, G., & Moser, E. I. (2013). Memory, navigation and theta rhythm in the hippocampal-entorhinal system. *Nature neuroscience*, 16(2), 130-138.
- Bymaster, F. P., Whitesitt, C. A., Shannon, H. E., DeLapp, N., Ward, J. S., Calligaro, D. O., ... & Mitch, C. H. (1997). Xanomeline: a selective muscarinic agonist for the treatment of Alzheimer's disease. *Drug development research*, 40(2), 158-170.
- Caccamo, A., Oddo, S., Billings, L. M., Green, K. N., Martinez-Coria, H., Fisher, A., & LaFerla, F. M. (2006). M1 receptors play a central role in modulating AD-like pathology in transgenic mice. *Neuron*, 49(5), 671-682.
- Cacucci, F., Yi, M., Wills, T. J., Chapman, P., & O'Keefe, J. (2008). Place cell firing correlates with memory deficits and amyloid plaque burden in Tg2576 Alzheimer mouse model. *Proceedings of the National Academy of Sciences*, 105(22), 7863-7868.
- Canals, M., Lane, J. R., Wen, A., Scammells, P. J., Sexton, P. M., & Christopoulos, A. (2012). A Monod-Wyman-Changeux mechanism can explain G protein-coupled receptor (GPCR) allosteric modulation. *Journal of Biological Chemistry*, 287(1), 650-659.
- Castello, N. A., Nguyen, M. H., Tran, J. D., Cheng, D., Green, K. N., & LaFerla, F. M. (2014). 7, 8-Dihydroxyflavone, a Small Molecule TrkB Agonist, Improves Spatial

Memory and Increases Thin Spine Density in a Mouse Model of Alzheimer Disease-Like Neuronal Loss. *PloS one*, 9(3), e91453.

- Cataldo, A. M., J. L. Barnett, et al. (1997). "Increased neuronal endocytosis and protease delivery to early endosomes in sporadic Alzheimer's disease: neuropathologic evidence for a mechanism of increased beta-amyloidogenesis." *J Neurosci*, 17(16): 6142-51.
- Cataldo, A. M., S. Petanceska, et al. (2004). "Abeta localization in abnormal endosomes: association with earliest Abeta elevations in AD and Down syndrome." *Neurobiol Aging*, 25(10): 1263-72.
- Chapman, P. F., White, G. L., Jones, M. W., Cooper-Blacketer, D., Marshall, V. J., Irizarry, M., ... & Hsiao, K. K. (1999). Impaired synaptic plasticity and learning in aged amyloid precursor protein transgenic mice. *Nature neuroscience*, 2(3), 271-276.
- Cirrito, J. R., Yamada, K. A., Finn, M. B., Sloviter, R. S., Bales, K. R., May, P. C., ... & Holtzman, D. M. (2005). Synaptic activity regulates interstitial fluid amyloid- β levels in vivo. *Neuron*, 48(6), 913-922.
- Cohen, R. M., Rezai-Zadeh, K., Weitz, T. M., Rentsendorj, A., Gate, D., Spivak, I., ... & Town, T. (2013). A transgenic Alzheimer rat with plaques, tau pathology, behavioral impairment, oligomeric $a\beta$, and frank neuronal loss. *The Journal of Neuroscience*, 33(15), 6245-6256.
- Colgin, L. L., Denninger, T., Fyhn, M., Hafting, T., Bonnevie, T., Jensen, O., ... & Moser, E. I. (2009). Frequency of gamma oscillations routes flow of information in the hippocampus. *Nature*, 462(7271), 353-357.

- Conn, P. J., Jones, C. K., & Lindsley, C. W. (2009). Subtype-selective allosteric modulators of muscarinic receptors for the treatment of CNS disorders. *Trends in pharmacological sciences*, 30(3), 148-155.
- Conn, P. J., Christopoulos, A., & Lindsley, C. W. (2009). Allosteric modulators of GPCRs: a novel approach for the treatment of CNS disorders. *Nature reviews Drug discovery*, 8(1), 41-54.
- Corder, E. H., Saunders, A. M., Strittmatter, W. J., Schmechel, D. E., Gaskell, P. C., Small, G., ... & Pericak-Vance, M. A. (1993). Gene dose of apolipoprotein E type 4 allele and the risk of Alzheimer's disease in late onset families. *Science*, 261(5123), 921-923.
- Coyle JT, Tsai G, Goff DC (2002) Ionotropic glutamate receptors as therapeutic targets in schizophrenia. *Curr Drug Target CNS Neurol Disord*, 1:183-189.
- Cramer, P. E., Cirrito, J. R., Wesson, D. W., Lee, C. D., Karlo, J. C., Zinn, A. E., ... & Landreth, G. E. (2012). ApoE-directed therapeutics rapidly clear β -amyloid and reverse deficits in AD mouse models. *Science*, 335(6075), 1503-1506.
- Dan, Y., & Poo, M. M. (2004). Spike timing-dependent plasticity of neural circuits. *Neuron*, 44(1), 23-30.
- Danysz, W., & Parsons, C. G. (2012). Alzheimer's disease, β -amyloid, glutamate, NMDA receptors and memantine—searching for the connections. *British journal of pharmacology*, 167(2), 324-352.
- Davies, P. and A. J. Maloney (1976). "Selective loss of central cholinergic neurons in Alzheimer's disease." *Lancet*, 2(8000): 1403.

- Davis, A. A., Fritz, J. J., Wess, J., Lah, J. J., & Levey, A. I. (2010a). Deletion of M1 muscarinic acetylcholine receptors increases amyloid pathology in vitro and in vivo. *The Journal of Neuroscience*, *30*(12), 4190-4196.
- Davis, A. A., Heilman, C. J., Brady, A. E., Miller, N. R., Fuerstenau-Sharp, M., Hanson, B. J., ... & Levey, A. I. (2010b). Differential effects of allosteric M1 muscarinic acetylcholine receptor agonists on receptor activation, arrestin 3 recruitment, and receptor downregulation. *ACS chemical neuroscience*, *1*(8), 542-551.
- Dawkins, E., & Small, D. H. (2014). Insights into the physiological function of the β -amyloid precursor protein: beyond Alzheimer's disease. *Journal of neurochemistry*, *129*(5), 756-769.
- deToledo-Morrell, L., Stoub, T. R., & Wang, C. (2007). Hippocampal atrophy and disconnection in incipient and mild Alzheimer's disease. *Progress in brain research*, *163*, 741-823.
- De Strooper, B., Annaert, W., Cupers, P., Saftig, P., Craessaerts, K., Mumm, J. S., ... & Kopan, R. (1999). A presenilin-1-dependent γ -secretase-like protease mediates release of Notch intracellular domain. *Nature*, *398*(6727), 518-522.
- Digby, G. J., Noetzel, M. J., Bubser, M., Utley, T. J., Walker, A. G., Byun, N. E., ... & Conn, P. J. (2012). Novel allosteric agonists of M1 muscarinic acetylcholine receptors induce brain region-specific responses that correspond with behavioral effects in animal models. *The Journal of Neuroscience*, *32*(25), 8532-8544.
- Dimitrov, M., Alattia, J. R., Lemmin, T., Lehal, R., Fligier, A., Houacine, J., ... & Fraering, P. C. (2013). Alzheimer's disease mutations in APP but not γ -secretase

modulators affect epsilon-cleavage-dependent AICD production. *Nature communications*, 4.

- Dolev, I., Fogel, H., Milshtein, H., Berdichevsky, Y., Lipstein, N., Brose, N., ... & Slutsky, I. (2013). Spike bursts increase amyloid-[beta] 40/42 ratio by inducing a presenilin-1 conformational change. *Nature neuroscience*, 16(5), 587-595.
- Doody, R. S., Dunn, J. K., Clark, C. M., Farlow, M., Foster, N. L., Liao, T., ... & Massman, P. (2001). Chronic donepezil treatment is associated with slowed cognitive decline in Alzheimer's disease. *Dementia and geriatric cognitive disorders*, 12(4), 295-300.
- Doody, R. S., Thomas, R. G., Farlow, M., Iwatsubo, T., Vellas, B., Joffe, S., ... & Mohs, R. (2014). Phase 3 trials of solanezumab for mild-to-moderate Alzheimer's disease. *New England Journal of Medicine*, 370(4), 311-321.
- Draguhn, A., Traub, R. D., Schmitz, D., & Jefferys, J. G. R. (1998). Electrical coupling underlies high-frequency oscillations in the hippocampus in vitro. *Nature*, 394(6689), 189-192.
- Duttaroy, A., C. L. Zimlik, et al. (2004). "Muscarinic stimulation of pancreatic insulin and glucagon release is abolished in m3 muscarinic acetylcholine receptor deficient mice." *Diabetes*, 53(7): 1714-20.
- Esch, F. S., P. S. Keim, et al. (1990). "Cleavage of amyloid beta peptide during constitutive processing of its precursor." *Science*, 248(4959): 1122-4.
- Fanselow, M. S., & Dong, H. W. (2010). Are the dorsal and ventral hippocampus functionally distinct structures?. *Neuron*, 65(1), 7-19.

- Farber, S. A., Nitsch, R. M., Schulz, J. G., & Wurtman, R. J. (1995). Regulated secretion of beta-amyloid precursor protein in rat brain. *The Journal of neuroscience*, *15*(11), 7442-7451.
- Fink-Jensen A, Fedorova I, Wortwein G, Woldbye DP, Rasmussen T, Thomsen M, Bolwig TG, Knitowski KM, McKinzie DL, Yamada M, Wess J, Basile A (2003) Role for M5 muscarinic acetylcholine receptors in cocaine addiction. *J Neurosci Res*, *74*:91-96.
- Fisahn, A., Yamada, M., Duttaroy, A., Gan, J. W., Deng, C. X., McBain, C. J., & Wess, J. (2002). Muscarinic induction of hippocampal gamma oscillations requires coupling of the M1 receptor to two mixed cation currents. *Neuron*, *33*(4), 615-624.
- Fisher, A., Pittel, Z., Haring, R., Bar-Ner, N., Kliger-Spatz, M., Natan, N., ... & Brandeis, R. (2003). M1 muscarinic agonists can modulate some of the hallmarks in Alzheimer's disease. *Journal of Molecular Neuroscience*, *20*(3), 349-356.
- Fitzjohn, S. M., Morton, R. A., Kuenzi, F., Rosahl, T. W., Shearman, M., Lewis, H., ... & Seabrook, G. R. (2001). Age-related impairment of synaptic transmission but normal long-term potentiation in transgenic mice that overexpress the human APP695SWE mutant form of amyloid precursor protein. *The Journal of Neuroscience*, *21*(13), 4691-4698.
- Foster, D. J., Gentry, P. R., Lizardi-Ortiz, J. E., Bridges, T. M., Wood, M. R., Niswender, C. M., ... & Conn, P. J. (2014). M5 Receptor Activation Produces Opposing Physiological Outcomes in Dopamine Neurons Depending on the Receptor's Location. *The Journal of Neuroscience*, *34*(9), 3253-3262.

- Gallagher, M., Bakker, A., Yassa, M. A., & Stark, C. E. L. (2010). Bridging neurocognitive aging and disease modification: targeting functional mechanisms of impairment. *Current Alzheimer Research*, 7(3), 197.
- Giessel, A. J., & Sabatini, B. L. (2010). M1 muscarinic receptors boost synaptic potentials and calcium influx in dendritic spines by inhibiting postsynaptic SK channels. *Neuron*, 68(5), 936-947.
- Gomez, J., H. Shannon, et al. (1999). "Pronounced pharmacologic deficits in M2 muscarinic acetylcholine receptor knockout mice." *Proc Natl Acad Sci USA* 96(4): 1692-7.
- Greicius, M. D., Srivastava, G., Reiss, A. L., & Menon, V. (2004). Default-mode network activity distinguishes Alzheimer's disease from healthy aging: evidence from functional MRI. *Proceedings of the National Academy of Sciences of the United States of America*, 101(13), 4637-4642.
- Greicius, M. D., Supekar, K., Menon, V., & Dougherty, R. F. (2009). Resting-state functional connectivity reflects structural connectivity in the default mode network. *Cerebral cortex*, 19(1), 72-78.
- Greenlee, W., Clader, J., Asberom, T., McCombie, S., Ford, J., Guzik, H., ... & Cox, K. (2001). Muscarinic agonists and antagonists in the treatment of Alzheimer's disease. *Il Farmaco*, 56(4), 247-250.
- Guzowski, J. F., Knierim, J. J., & Moser, E. I. (2004). Ensemble dynamics of hippocampal regions CA3 and CA1. *Neuron*, 44(4), 581-584.

- Haass, C., & Selkoe, D. J. (2007). Soluble protein oligomers in neurodegeneration: lessons from the Alzheimer's amyloid β -peptide. *Nature reviews Molecular cell biology*, 8(2), 101-112.
- Hamilton, S. E., Loose, M. D., Qi, M., Levey, A. I., Hille, B., McKnight, G. S., ... & Nathanson, N. M. (1997). Disruption of the m1 receptor gene ablates muscarinic receptor-dependent M current regulation and seizure activity in mice. *Proceedings of the National Academy of Sciences*, 94(24), 13311-13316.
- Hamilton SE, Nathanson NM (2001) The M1 receptor is required for muscarinic activation of mitogen-activated protein (MAP) kinase in murine cerebral cortical neurons. *J Biol Chem*, 276:15850-15853.
- Hardy, J., & Selkoe, D. J. (2002). The amyloid hypothesis of Alzheimer's disease: progress and problems on the road to therapeutics. *Science*, 297(5580), 353-356.
- Hargreaves, E. L., Rao, G., Lee, I., & Knierim, J. J. (2005). Major dissociation between medial and lateral entorhinal input to dorsal hippocampus. *Science*, 308(5729), 1792-1794.
- Hasselmo, M. E., Schnell, E., & Barkai, E. (1995). Dynamics of learning and recall at excitatory recurrent synapses and cholinergic modulation in rat hippocampal region CA3. *The Journal of neuroscience*, 15(7), 5249-5262.
- Hasselmo, M. E., & McClelland, J. L. (1999). Neural models of memory. *Current Opinion in Neurobiology*, 9(2), 184-188.
- Hasselmo, M. E. (2006). The role of acetylcholine in learning and memory. *Current opinion in neurobiology*, 16(6), 710-715.

- Haydar, S. N., & Dunlop, J. (2010). Neuronal nicotinic acetylcholine receptors-targets for the development of drugs to treat cognitive impairment associated with schizophrenia and Alzheimer's disease. *Current topics in medicinal chemistry*, 10(2), 144-152.
- Hendriks, L., C. M. van Duijn, et al. (1992). "Presenile dementia and cerebral haemorrhage linked to a mutation at codon 692 of the beta-amyloid precursor protein gene." *Nature Genetics*, 1(3): 218-21.
- Hock, C., Maddalena, A., Heuser, I., Naber, D., Oertel, W., Kammer, H., ... & Nitsch, R. M. (2000). Treatment with the Selective Muscarinic Agonist Talsaclidine Decreases Cerebrospinal Fluid Levels of Total Amyloid β -Peptide in Patients with Alzheimer's Disease. *Annals of the New York Academy of Sciences*, 920(1), 285-291.
- Holtzman, D. M., Morris, J. C., & Goate, A. M. (2011). Alzheimer's disease: the challenge of the second century. *Science translational medicine*, 3(77), 77sr1-77sr1.
- Gandy, S. E., G. L. Caporaso, et al. (1993). "Protein phosphorylation regulates relative utilization of processing pathways for Alzheimer beta/A4 amyloid precursor protein." *Ann N Y Acad Sci*, 695: 117-21.
- Giocomo, L. M., & Hasselmo, M. E. (2007). Neuromodulation by glutamate and acetylcholine can change circuit dynamics by regulating the relative influence of afferent input and excitatory feedback. *Molecular neurobiology*, 36(2), 184-200.
- Glabe, C. C. (2005). "Amyloid accumulation and pathogenesis of Alzheimer's disease: significance of monomeric, oligomeric and fibrillar A β ." *Subcell Biochem*, 38:

167-77.

- Goate, A., M. C. Chartier-Harlin, et al. (1991). "Segregation of a missense mutation in the amyloid precursor protein gene with familial Alzheimer's disease." *Nature*, 349(6311): 704-6.
- Guzowski, J. F., Knierim, J. J., & Moser, E. I. (2004). Ensemble dynamics of hippocampal regions CA3 and CA1. *Neuron*, 44(4), 581-584.
- Hill AJ, Best PJ. Effects of deafness and blindness on the spatial correlates of hippocampal unit activity in the rat. *Exp Neurol*, 1981;74(1):204-17.
- Jack Jr, C. R., Knopman, D. S., Jagust, W. J., Shaw, L. M., Aisen, P. S., Weiner, M. W., ... & Trojanowski, J. Q. (2010). Hypothetical model of dynamic biomarkers of the Alzheimer's pathological cascade. *The Lancet Neurology*, 9(1), 119-128.
- Jacobson, M. A., Kreatsoulas, C., Pascarella, D. M., O'Brien, J. A., & Sur, C. (2010). The M1 muscarinic receptor allosteric agonists AC-42 and 1-[1'-(2-methylbenzyl)-1, 4'-bipiperidin-4-yl]-1, 3-dihydro-2H-benzimidazol-2-one bind to a unique site distinct from the acetylcholine orthosteric site. *Molecular pharmacology*, 78(4), 648-657.
- Jeffery KJ, O'Keefe JM. Learned interaction of visual and idiothetic cues in the control of place field orientation. *Exp Brain Res*, 1999;127(2):151-61.
- Jin, M., Shepardson, N., Yang, T., Chen, G., Walsh, D., & Selkoe, D. J. (2011). Soluble amyloid β -protein dimers isolated from Alzheimer cortex directly induce Tau hyperphosphorylation and neuritic degeneration. *Proceedings of the National Academy of Sciences*, 108(14), 5819-5824.

- Jones, C. K., Brady, A. E., Davis, A. A., Xiang, Z., Bubser, M., Tantawy, M. N., ... & Conn, P. J. (2008). Novel selective allosteric activator of the M1 muscarinic acetylcholine receptor regulates amyloid processing and produces antipsychotic-like activity in rats. *The Journal of Neuroscience*, *28*(41), 10422-10433.
- Jones, C. K., Byun, N., & Bubser, M. (2011). Muscarinic and nicotinic acetylcholine receptor agonists and allosteric modulators for the treatment of schizophrenia. *Neuropsychopharmacology*, *37*(1), 16-42.
- Jung MW, Wiener SI, McNaughton BL. Comparison of spatial firing characteristics of units in dorsal and ventral hippocampus of the rat. *J Neurosci*, 1994;14(12):7347-56.
- Jutras, M. J., Fries, P., & Buffalo, E. A. (2009). Gamma-band synchronization in the macaque hippocampus and memory formation. *The Journal of neuroscience*, *29*(40), 12521-12531.
- Jutras, M. J., & Buffalo, E. A. (2010). Synchronous neural activity and memory formation. *Current opinion in neurobiology*, *20*(2), 150-155.
- Kajiwara, R., Wouterlood, F. G., Sah, A., Boekel, A. J., Baks-te Bulte, L. T., & Witter, M. P. (2008). Convergence of entorhinal and CA3 inputs onto pyramidal neurons and interneurons in hippocampal area CA1—an anatomical study in the rat. *Hippocampus*, *18*(3), 266-280.
- Kamenetz, F., Tomita, T., Hsieh, H., Seabrook, G., Borchelt, D., Iwatsubo, T., ... & Malinow, R. (2003). APP processing and synaptic function. *Neuron*, *37*(6), 925-937.

- Karran, E., Mercken, M., & De Strooper, B. (2011). The amyloid cascade hypothesis for Alzheimer's disease: an appraisal for the development of therapeutics. *Nature Reviews Drug Discovery*, *10*(9), 698-712.
- Kauwe, J. S., J. Wang, et al. (2008). "Novel presenilin 1 variant (P117A) causing Alzheimer's disease in the fourth decade of life." *Neurosci Lett*, *438*(2): 257-9.
- Khurana, S., I. Chacon, et al. (2004). "Vasodilatory effects of cholinergic agonists are greatly diminished in aorta from M3R^{-/-} mice." *Eur J Pharmacol*, *493*(1-3): 127-32.
- Kim, J., Basak, J. M., & Holtzman, D. M. (2009). The role of apolipoprotein E in Alzheimer's disease. *Neuron*, *63*(3), 287-303.
- Knierim, J. J., Lee, I., & Hargreaves, E. L. (2006). Hippocampal place cells: parallel input streams, subregional processing, and implications for episodic memory. *Hippocampus*, *16*(9), 755-764.
- Komorowski, R. W., Garcia, C. G., Wilson, A., Hattori, S., Howard, M. W., & Eichenbaum, H. (2013). Ventral hippocampal neurons are shaped by experience to represent behaviorally relevant contexts. *The Journal of Neuroscience*, *33*(18), 8079-8087.
- Kremin, T., Gerber, D., Giocomo, L. M., Huang, S. Y., Tonegawa, S., & Hasselmo, M. E. (2006). Muscarinic suppression in stratum radiatum of CA1 shows dependence on presynaptic M₁ receptors and is not dependent on effects at GABA_B receptors. *Neurobiology of learning and memory*, *85*(2), 153-163.

- Kuo YM, Emmerling MR, Vigo-Pelfrey C, Kasunic TC, Kirkpatrick JB, Murdoch GH, Ball MJ, Roher AE. Water-soluble Abeta (N-40, N-42) oligomers in normal and Alzheimer disease brains. *J Biol Chem*, 1996; 271(8): 4077-81.
- Lah, J. J. and A. I. Levey (2000). "Endogenous presenilin-1 targets to endocytic rather than biosynthetic compartments." *Mol Cell Neurosci*, 16(2): 111-26.
- Langmead, C. J., Austin, N. E., Branch, C. L., Brown, J. T., Buchanan, K. A., Davies, C. H., ... & Watson, J. (2008). Characterization of a CNS penetrant, selective M1 muscarinic receptor agonist, 77-LH-28-1. *British journal of pharmacology*, 154(5), 1104-1115.
- Lebois, E. P., Bridges, T. M., Lewis, L. M., Dawson, E. S., Kane, A. S., Xiang, Z., ... & Lindsley, C. W. (2009). Discovery and characterization of novel subtype-selective allosteric agonists for the investigation of M1 receptor function in the central nervous system. *ACS chemical neuroscience*, 1(2), 104-121.
- Lebois, E. P., Digby, G. J., Sheffler, D. J., Melancon, B. J., Tarr, J. C., Cho, H. P., ... & Lindsley, C. W. (2011). Development of a highly selective, orally bioavailable and CNS penetrant M₁ agonist derived from the MLPCN probe ML071. *Bioorganic & medicinal chemistry letters*, 21(21), 6451-6455.
- Leutgeb, S., Leutgeb, J. K., Treves, A., Moser, M. B., & Moser, E. I. (2004). Distinct ensemble codes in hippocampal areas CA3 and CA1. *Science*, 305(5688), 1295-1298.
- Leutgeb, S., Leutgeb, J. K., Moser, M. B., & Moser, E. I. (2005). Place cells, spatial maps and the population code for memory. *Current opinion in neurobiology*, 15(6), 738-746.

- Leutgeb, S., Leutgeb, J. K., Barnes, C. A., Moser, E. I., McNaughton, B. L., & Moser, M. B. (2005). Independent codes for spatial and episodic memory in hippocampal neuronal ensembles. *Science*, *309*(5734), 619-623.
- Leutgeb, J. K., Leutgeb, S., Treves, A., Meyer, R., Barnes, C. A., McNaughton, B. L., ... & Moser, E. I. (2005). Progressive transformation of hippocampal neuronal representations in “morphed” environments. *Neuron*, *48*(2), 345-358.
- Leutgeb, J. K., Leutgeb, S., Moser, M. B., & Moser, E. I. (2007). Pattern separation in the dentate gyrus and CA3 of the hippocampus. *science*, *315*(5814), 961-966.
- Levey AI, Kitt CA, Simonds WF, Price DL, Brann MR (1991) Identification and localization of muscarinic acetylcholine receptor proteins in brain with subtypespecific antibodies. *J Neurosci*, *11*:3218-3226.
- Levey AI, Edmunds SM, Heilman CJ, Desmond TJ, Frey KA (1994) Localization of muscarinic m3 receptor protein and M3 receptor binding in rat brain. *Neuroscience*, *63*:207-221.
- Levey AI, Edmunds SM, Koliatsos V, Wiley RG, Heilman CJ (1995) Expression of m1-m4 muscarinic acetylcholine receptor proteins in rat hippocampus and regulation by cholinergic innervation. *J Neurosci*, *15*:4077-4092.
- Levey, A. I., Edmunds, S. M., Koliatsos, V., Wiley, R. G., & Heilman, C. J. (1995). Expression of m1-m4 muscarinic acetylcholine receptor proteins in rat hippocampus and regulation by cholinergic innervation. *The Journal of neuroscience*, *15*(5), 4077-4092.
- Levy-Lahad, E., W. Wasco, et al. (1995). "Candidate gene for the chromosome 1 familial Alzheimer's disease locus." *Science* *269*(5226): 973-7.

- Levey, A. I. (1996). Muscarinic acetylcholine receptor expression in memory circuits: implications for treatment of Alzheimer disease. *Proceedings of the National Academy of Sciences*, 93(24), 13541-13546.
- Leys, C., Ley, C., Klein, O., Bernard, P., & Licata, L. (2013). Detecting outliers: Do not use standard deviation around the mean, use absolute deviation around the median. *Journal of Experimental Social Psychology*, 49(4), 764-766.
- Loewi, O. and E. Navratil (1926). "Über humorale Übertragbarkeit der Herznervenwirkung. XI. Über den Mechanismus der Vaguswirkung von Physostigmin und Ergotamin." *Pflugers Archiv für die Gesamte Physiologie Menschen und der Tiere*, 214: 689-696.
- Li, S., Hong, S., Shepardson, N. E., Walsh, D. M., Shankar, G. M., & Selkoe, D. (2009). Soluble oligomers of amyloid β protein facilitate hippocampal long-term depression by disrupting neuronal glutamate uptake. *Neuron*, 62(6), 788-801.
- Lue LF, Kuo YM, Roher AE, Brachova L, Shen Y, Sue L, Beach T, Kurth JH, Rydel RE, Rogers J. Soluble amyloid beta peptide concentration as a predictor of synaptic change in Alzheimer's disease. *Am J Pathol*, 1999; 155(3): 853-62.
- Ma, L., Seager, M. A., Wittmann, M., Jacobson, M., Bickel, D., Burno, M., ... & Ray, W. J. (2009). Selective activation of the M1 muscarinic acetylcholine receptor achieved by allosteric potentiation. *Proceedings of the National Academy of Sciences*, 106(37), 15950-15955.
- Mangialasche, F., Solomon, A., Winblad, B., Mecocci, P., & Kivipelto, M. (2010). Alzheimer's disease: clinical trials and drug development. *The Lancet Neurology*, 9(7), 702-716.

- Marino MJ, Rouse ST, Levey AI, Potter LT, Conn PJ (1998) Activation of the genetically defined m1 muscarinic receptor potentiates N-methyl-D-aspartate (NMDA) receptor currents in hippocampal pyramidal cells. *Proc Natl Acad Sci USA*, 95:11465-11470.
- Marino MJ, Conn PJ (2002) Direct and indirect modulation of the N-methyl D-aspartate receptor. *Curr Drug Targets CNS Neurol Disord*, 1:1-16.
- Markram H, Segal M (1990) Acetylcholine potentiates responses to N-methyl-Daspartate in the rat hippocampus. *Neurosci Lett*, 113:62-65.
- Matsui, M., D. Motomura, et al. (2000). "Multiple functional defects in peripheral autonomic organs in mice lacking muscarinic acetylcholine receptor gene for the M3 subtype." *Proc Natl Acad Sci USA*, 97(17): 9579-84.
- McGeer, P. L., & McGeer, E. G. (1995). The inflammatory response system of brain: implications for therapy of Alzheimer and other neurodegenerative diseases. *Brain Research Reviews*, 21(2), 195-218.
- McGeer, P. L., & McGeer, E. G. (1999). Inflammation of the brain in Alzheimer's disease: implications for therapy. *Journal of leukocyte biology*, 65(4), 409-415.
- McGeer, E. G., & McGeer, P. L. (2003). Inflammatory processes in Alzheimer's disease. *Progress in Neuro-Psychopharmacology and Biological Psychiatry*, 27(5), 741-749.
- McLean CA, Cherny RA, Fraser FW, Fuller SJ, Smith MJ, Beyreuther K, Bush AI, Masters CL. Soluble pool of Abeta amyloid as a determinant of severity of neurodegeneration in Alzheimer's disease. *Ann Neurol*, 1999; 46(6):860-6.

- McNaughton, B. L., & Barnes, C. A. (1977). Physiological identification and analysis of dentate granule cell responses to stimulation of the medial and lateral perforant pathways in the rat. *Journal of Comparative Neurology*, 175(4), 439-453.
- Melancon, B.J., Gogliotti, R.D., Tarr, J.C., Saleh, S.A., Chauder, B.A., Lebois, E.P., Cho, H.P., ... & Wood, M.R. (2012). Continued optimization of the MLPCN probe ML071 into highly potent agonists of the hM₁ muscarinic acetylcholine receptor. *Bioorganic & medicinal chemistry letters*. 22, 3467-3472.
- Melancon, B. J., Hopkins, C. R., Wood, M. R., Emmitte, K. A., Niswender, C. M., Christopoulos, A., ... & Lindsley, C. W. (2012). Allosteric modulation of seven transmembrane spanning receptors: theory, practice, and opportunities for central nervous system drug discovery. *Journal of medicinal chemistry*, 55(4), 1445-1464.
- Mitra, P. P., & Pesaran, B. (1999). Analysis of dynamic brain imaging data. *Biophysical journal*, 76(2), 691-708.
- Mizumori SJ, Perez GM, Alvarado MC, Barnes CA, McNaughton BL. Reversible inactivation of the medial septum differentially affects two forms of learning in rats. *Brain Res*, 1990; 528: 12-20.
- Mizumori, S. J. Y., Perez, G. M., Alvarado, M. C., Barnes, C. A., & McNaughton, B. L. (1990). Reversible inactivation of the medial septum differentially affects two forms of learning in rats. *Brain research*, 528(1), 12-20.
- Mizuseki, K., Sirota, A., Pastalkova, E., & Buzsáki, G. (2009). Theta oscillations provide temporal windows for local circuit computation in the entorhinal-hippocampal loop. *Neuron*, 64(2), 267-280.

- Morales, I., Guzmán-Martínez, L., Cerda-Troncoso, C., Farías, G. A., & Maccioni, R. B. (2014). Neuroinflammation in the pathogenesis of Alzheimer's disease. A rational framework for the search of novel therapeutic approaches. *Frontiers in cellular neuroscience*, 8.
- Moser, E. I., Kropff, E., & Moser, M. B. (2008). Place cells, grid cells, and the brain's spatial representation system. *Neuroscience*, 31(1), 69.
- Mossner, R., A. Schmitt, et al. (2000). "The serotonin transporter in Alzheimer's and Parkinson's disease." *J Neural Transm Suppl*, (60): 345-50.
- Mucke, L., Masliah, E., Yu, G. Q., Mallory, M., Rockenstein, E. M., Tatsuno, G., ... & McConlogue, L. (2000). High-level neuronal expression of A β 1–42 in wild-type human amyloid protein precursor transgenic mice: synaptotoxicity without plaque formation. *The Journal of neuroscience*, 20(11), 4050-4058.
- Mucke, L., E. Masliah, et al. (2000). "High-level neuronal expression of abeta 1-42 in wild-type human amyloid protein precursor transgenic mice: synaptotoxicity without plaque formation." *J Neurosci*, 20(11): 4050-8.
- Mufson, E. J., Bothwell, M., & Kordower, J. H. (1989). Loss of nerve growth factor receptor-containing neurons in Alzheimer's disease: a quantitative analysis across subregions of the basal forebrain. *Experimental neurology*, 105(3), 221-232.
- Mufson, E. J. and J. H. Kordower (2001). Cholinergic Basal Forebrain Systems in the Primate Central Nervous System: Anatomy, Connectivity, Neurochemistry, Aging, Dementia, and Experimental Therapeutics. *Functional Neurobiology of Aging*. P. R. Hof and C. V. Mobbs. San Diego, Academic Press.

- Mufson, E. J., Ma, S. Y., Dills, J., Cochran, E. J., Leurgans, S., Wu, J., ... & Kordower, J. H. (2002). Loss of basal forebrain p75^{NTR} immunoreactivity in subjects with mild cognitive impairment and Alzheimer's disease. *Journal of Comparative Neurology*, 443(2), 136-153.
- Mufson, E. J., Counts, S. E., Perez, S. E., & Ginsberg, S. D. (2008). Cholinergic system during the progression of Alzheimer's disease: therapeutic implications.
- Mullan, M., Crawford, F., et al. (1992). "A pathogenic mutation for probable Alzheimer's disease in the APP gene at the N-terminus of beta-amyloid." *Nature Genetics* 1(5): 345-7.
- Muller RU, Kubie JL. The effects of changes in the environment on the spatial firing of hippocampal complex-spike cells. *J Neurosci*, 1987 Jul;7(7):1951-68.
- Murrell, J., Farlow, M., et al. (1991). "A mutation in the amyloid precursor protein associated with hereditary Alzheimer's disease." *Science*, 254(5028): 97-9.
- Nachmansohn, D. and A. L. Machado (1943). "The formation of acetylcholine. A new enzyme choline acetylase." *J Neurophysiol*, 6: 397-403.
- Nachmansohn, D. and H. M. John (1945). "On the Formation of Acetylcholine in the Nerve Axon." *Science*, 102(2645): 250-251.
- Nafstad PH. An electron microscope study on the termination of the perforant path fibres in the hippocampus and the fascia dentata. *Z Zellforsch Mikrosk Anat*, 1967; 76: 532-542.
- Nagahara, A. H., Merrill, D. A., Coppola, G., Tsukada, S., Schroeder, B. E., Shaked, G. M., ... & Tuszynski, M. H. (2009). Neuroprotective effects of brain-derived

neurotrophic factor in rodent and primate models of Alzheimer's disease. *Nature medicine*, 15(3), 331-337.

Nagahara, A. H., Mateling, M., Kovacs, I., Wang, L., Eggert, S., Rockenstein, E., ... & Tuszynski, M. H. (2013). Early BDNF treatment ameliorates cell loss in the entorhinal cortex of APP transgenic mice. *The Journal of Neuroscience*, 33(39), 15596-15602.

Naslund J, Haroutunian V, Mohs R, Davis KL, Davies P, Greengard P, Buxbaum JD. Correlation between elevated levels of amyloid beta-peptide in the brain and cognitive decline. *JAMA*, 2000;283(12):1571-7.

Nitsch RM, Deng M, Tennis M, Schoenfeld D, Growdon JH (2000). The selective muscarinic M1 agonist AF102B decreases levels of total Abeta in cerebrospinal fluid of patients with Alzheimer's disease. *Ann Neurol*. 48(6): 913-8.

Oakley, H., Cole, S. L., Logan, S., Maus, E., Shao, P., Craft, J., ... & Vassar, R. (2006). Intraneuronal β -amyloid aggregates, neurodegeneration, and neuron loss in transgenic mice with five familial Alzheimer's disease mutations: potential factors in amyloid plaque formation. *The Journal of neuroscience*, 26(40), 10129-10140.

Oddo, S., Caccamo, A., Shepherd, J. D., Murphy, M. P., Golde, T. E., Kaye, R., ... & LaFerla, F. M. (2003a). Triple-transgenic model of Alzheimer's disease with plaques and tangles: intracellular A β and synaptic dysfunction. *Neuron*, 39(3), 409-421.

Oddo, S., Caccamo, A., Kitazawa, M., Tseng, B. P., & LaFerla, F. M. (2003b). Amyloid deposition precedes tangle formation in a triple transgenic model of Alzheimer's disease. *Neurobiology of aging*, 24(8), 1063-1070.

- Oddo, S., L. Billings, et al. (2004). "Abeta immunotherapy leads to clearance of early, but not late, hyperphosphorylated tau aggregates via the proteasome." *Neuron*, 43(3): 321-32.
- Oddo, S., A. Caccamo, et al. (2007). "Genetically augmenting tau levels does not modulate the onset or progression of Abeta pathology in transgenic mice." *J Neurochem*, 102(4): 1053-63.
- O'Keefe J, Dostrovsky J. The hippocampus as a spatial map. Preliminary evidence from unit activity in the freely-moving rat. *Brain Res*, 1971; 34(1):171-5.
- O'Keefe. Place units in the hippocampus of the freely moving rat. *Exp Neurol*, 1976; 51(1): 78-109.
- O'Keefe J, Conway DH. Hippocampal place units in the freely moving rat: why they fire where they fire. *Exp Brain Res*, 1978;31(4):573-90.
- O'Keefe J, Burgess N. Geometric determinants of the place fields of hippocampal neurons. *Nature*, 1996;381(6581):425-8.
- Palop, J. J., & Mucke, L. (2010). Amyloid-[beta]-induced neuronal dysfunction in Alzheimer's disease: from synapses toward neural networks. *Nature neuroscience*, 13(7), 812-818.
- Perry, E. K., R. H. Perry, et al. (1977). "Necropsy evidence of central cholinergic deficits in senile dementia." *Lancet*, 1(8004): 189.
- Perry, E. K., B. E. Tomlinson, et al. (1978). "Correlation of cholinergic abnormalities with senile plaques and mental test scores in senile dementia." *Br Med J*, 2(6150): 1457-9.

- Perry, E. K., Kilford, L., Lees, A. J., Burn, D. J., & Perry, R. H. (2003). Increased Alzheimer pathology in Parkinson's disease related to antimuscarinic drugs. *Annals of neurology*, *54*(2), 235-238.
- Putcha, D., Brickhouse, M., O'Keefe, K., Sullivan, C., Rentz, D., Marshall, G., ... & Sperling, R. (2011). Hippocampal hyperactivation associated with cortical thinning in Alzheimer's disease signature regions in non-demented elderly adults. *The Journal of Neuroscience*, *31*(48), 17680-17688.
- Puzzo, D., & Arancio, O. (2013). Amyloid- β Peptide: Dr. Jekyll or Mr. Hyde?. *Journal of Alzheimer's Disease*, *33*, S111-S120.
- Quinn, J. J., Loya, F., Ma, Q. D., & Fanselow, M. S. (2005). Dorsal hippocampus NMDA receptors differentially mediate trace and contextual fear conditioning. *Hippocampus*, *15*(5), 665-674.
- Quirk GJ, Muller RU, Kubie JL. The firing of hippocampal place cells in the dark depends on the rat's recent experience. *J Neurosci*, 1990; 10(6):2008-17.
- Reisberg, B., Doody, R., Stöffler, A., Schmitt, F., Ferris, S., & Möbius, H. J. (2003). Memantine in moderate-to-severe Alzheimer's disease. *New England Journal of Medicine*, *348*(14), 1333-1341.
- Rogaev, E. I., R. Sherrington, et al. (1995). "Familial Alzheimer's disease in kindreds with missense mutations in a gene on chromosome 1 related to the Alzheimer's disease type 3 gene." *Nature*, *376*(6543): 775-8.
- Rogers, J., Webster, S., Lue, L. F., Brachova, L., Harold Civin, W., Emmerling, M., ... & McGeer, P. (1996). Inflammation and Alzheimer's disease pathogenesis. *Neurobiology of aging*, *17*(5), 681-686.

- Rouse, S. T., & Levey, A. L. (1996). Expression of m1-m4 muscarinic acetylcholine receptor immunoreactivity in septohippocampal neurons and other identified hippocampal afferents. *Journal of Comparative Neurology*, 375(3), 406-416.
- Salloway, S., Sperling, R., Gilman, S., Fox, N. C., Blennow, K., Raskind, M., ... & Grundman, M. (2009). A phase 2 multiple ascending dose trial of bapineuzumab in mild to moderate Alzheimer disease. *Neurology*, 73(24), 2061-2070.
- Salloway, S., Sperling, R., Fox, N. C., Blennow, K., Klunk, W., Raskind, M., ... & Brashear, H. R. (2014). Two phase 3 trials of bapineuzumab in mild-to-moderate Alzheimer's disease. *New England Journal of Medicine*, 370(4), 322-333.
- Save E, Cressant A, Thinus-Blanc C, Poucet B. Spatial firing of hippocampal place cells in blind rats. *J Neurosci*, 1998;18(5):1818-26.
- Scheff, S. W., Price, D. A., Schmitt, F. A., & Mufson, E. J. (2006). Hippocampal synaptic loss in early Alzheimer's disease and mild cognitive impairment. *Neurobiology of aging*, 27(10), 1372-1384.
- Scheiderer CL, McCutchen E, Thacker EE, Kolasa K, Ward MK, Parsons D, Harrell LE, Dobrunz LE, McMahon LL (2006) Sympathetic sprouting drives hippocampal cholinergic reinnervation that prevents loss of a muscarinic receptor-dependent long-term depression at CA3-CA1 synapses. *J Neurosci*, 26:3745-3756.
- Scheiderer CL, Smith CC, McCutchen E, McCoy PA, Thacker EE, Kolasa K, Dobrunz LE, McMahon LL (2008) Coactivation of M(1) muscarinic and alpha1 adrenergic receptors stimulates extracellular signal-regulated protein kinase and induces long-term depression at CA3-CA1 synapses in rat hippocampus. *J Neurosci*, 28:5350-5358.

- Segal, M., & Auerbach, J. M. (1997). Muscarinic receptors involved in hippocampal plasticity. *Life sciences*, 60(13), 1085-1091.
- Selkoe, D. J. (1994). Normal and abnormal biology of the beta-amyloid precursor protein. *Annual review of neuroscience*, 17(1), 489-517.
- Selkoe, D. J., T. Yamazaki, et al. (1996). "The role of APP processing and trafficking pathways in the formation of amyloid beta-protein." *Ann N Y Acad Sci*, 777: 57-64.
- Selkoe, D. J. (2001). Alzheimer's disease: genes, proteins, and therapy. *Physiological reviews*, 81(2), 741-766.
- Sherrington, R., E. I. Rogaeve, et al. (1995). "Cloning of a gene bearing missense mutations in early-onset familial Alzheimer's disease." *Nature*, 375(6534): 754-60.
- Shinoe T, Matsui M, Taketo MM, Manabe T (2005) Modulation of synaptic plasticity by physiological activation of M1 muscarinic acetylcholine receptors in the mouse hippocampus. *J Neurosci*, 25:11194-11200.
- Shirey, J. K., Brady, A. E., Jones, P. J., Davis, A. A., Bridges, T. M., Kennedy, J. P., ... & Conn, P. J. (2009). A selective allosteric potentiator of the M1 muscarinic acetylcholine receptor increases activity of medial prefrontal cortical neurons and restores impairments in reversal learning. *The Journal of Neuroscience*, 29(45), 14271-14286.
- Sisodia, S. S., E. H. Koo, et al. (1990). "Evidence that beta-amyloid protein in Alzheimer's disease is not derived by normal processing." *Science*, 248(4954): 492-5.
- Sisodia, S. S. (1992). "Beta-amyloid precursor protein cleavage by a membrane-bound

- protease." *Proc Natl Acad Sci USA*, 89(13): 6075-9.
- Skaggs, W. E., McNaughton, B. L., Gothard, K. M., & Markus, E. J. (1993). An information-theoretic approach to deciphering the hippocampal code. In *In*.
- Skaggs, W. E., & McNaughton, B. L. (1998). Spatial firing properties of hippocampal CA1 populations in an environment containing two visually identical regions. *The Journal of neuroscience*, 18(20), 8455-8466.
- Skovronsky, D. M., D. B. Moore, et al. (2000). "Protein kinase C-dependent alphasecretase competes with beta-secretase for cleavage of amyloid-beta precursor protein in the trans-golgi network." *J Biol Chem*, 275(4): 2568-75.
- Slepian, D. (1978). Prolate spheroidal wave functions, Fourier analysis, and uncertainty—V: The discrete case. *Bell System Technical Journal*, 57(5), 1371-1430.
- Small, S. A., & Duff, K. (2008). Linking A β and tau in late-onset Alzheimer's disease: a dual pathway hypothesis. *Neuron*, 60(4), 534-542.
- Small, S. A., Schobel, S. A., Buxton, R. B., Witter, M. P., & Barnes, C. A. (2011). A pathophysiological framework of hippocampal dysfunction in ageing and disease. *Nature Reviews Neuroscience*, 12(10), 585-601.
- Spalding, T. A., Ma, J. N., Ott, T. R., Friberg, M., Bajpai, A., Bradley, S. R., ... & Burstein, E. S. (2006). Structural requirements of transmembrane domain 3 for activation by the M1 muscarinic receptor agonists AC-42, AC-260584, clozapine, and N-desmethyleclozapine: evidence for three distinct modes of receptor activation. *Molecular pharmacology*, 70(6), 1974-1983.

- Sperling, R. A., LaViolette, P. S., O'Keefe, K., O'Brien, J., Rentz, D. M., Pihlajamaki, M., ... & Johnson, K. A. (2009). Amyloid deposition is associated with impaired default network function in older persons without dementia. *Neuron*, *63*(2), 178-188.
- Sperling, R. A., Dickerson, B. C., Pihlajamaki, M., Vannini, P., LaViolette, P. S., Vitolo, O. V., ... & Johnson, K. A. (2010). Functional alterations in memory networks in early Alzheimer's disease. *Neuromolecular medicine*, *12*(1), 27-43.
- Squire LR. The hippocampus and spatial memory. *Trends Neurosci.* 1993; *16*(2): 56-7.
- Squire, L. R. (1992). Memory and the hippocampus: a synthesis from findings with rats, monkeys, and humans. *Psychological review*, *99*(2), 195.
- Steiner, H., R. Fluhrer, et al. (2008). "Intramembrane proteolysis by gamma-secretase." *J Biol Chem*, *283*(44): 29627-31.
- Steward O, Scoville SA. Cells of origin of entorhinal cortical afferents to the hippocampus and fascia dentata of the rat. *J Comp Neurol*, 1976; *169*: 347-370.
- Sullivan, D., Csicsvari, J., Mizuseki, K., Montgomery, S., Diba, K., & Buzsáki, G. (2011). Relationships between hippocampal sharp waves, ripples, and fast gamma oscillation: influence of dentate and entorhinal cortical activity. *The Journal of Neuroscience*, *31*(23), 8605-8616.
- Suzuki, T. and T. Nakaya (2008). "Regulation of amyloid beta-protein precursor by phosphorylation and protein interactions." *J Biol Chem*, *283*(44): 29633-7.
- Szekely, C. A., Thorne, J. E., Zandi, P. P., Ek, M., Messias, E., Breitner, J. C., & Goodman, S. N. (2004). Nonsteroidal anti-inflammatory drugs for the prevention of Alzheimer's disease: a systematic review. *Neuroepidemiology*, *23*(4), 159-169.

- Takahashi, R. H., C. G. Almeida, et al. (2004). "Oligomerization of Alzheimer's beta-amyloid within processes and synapses of cultured neurons and brain." *J Neurosci*, 24(14): 3592-9.
- Tamminga, C. A., Stan, A. D., & Wagner, A. D. (2010). The hippocampal formation in schizophrenia. *American Journal of Psychiatry*, 167(10), 1178-1193.
- Tamminga, C. A. (2013). Psychosis is emerging as a learning and memory disorder. *Neuropsychopharmacology*, 38(1), 247.
- Tanzi, R. E., J. F. Gusella, et al. (1987). "Amyloid beta protein gene: cDNA, mRNA distribution, and genetic linkage near the Alzheimer locus." *Science*, 235(4791): 8.
- Thinakaran, G., D. B. Teplow, et al. (1996). "Metabolism of the "Swedish" amyloid precursor protein variant in neuro2a (N2a) cells. Evidence that cleavage at the "beta-secretase" site occurs in the golgi apparatus." *J Biol Chem*, 271(16): 9390-7.
- Thinakaran, G. and E. H. Koo (2008). "Amyloid precursor protein trafficking, processing, and function." *J Biol Chem*, 283(44): 29615-9.
- Thomas, R. L., Langmead, C. J., Wood, M. D., & Challiss, R. J. (2009). Contrasting effects of allosteric and orthosteric agonists on m1 muscarinic acetylcholine receptor internalization and down-regulation. *Journal of Pharmacology and Experimental Therapeutics*, 331(3), 1086-1095.
- Thomas, S. J., & Grossberg, G. T. (2009). Memantine: a review of studies into its safety and efficacy in treating Alzheimer's disease and other dementias. *Clinical interventions in aging*, 4, 367.

- Whitehouse, P. J., D. L. Price, et al. (1981). "Alzheimer disease: evidence for selective loss of cholinergic neurons in the nucleus basalis." *Annals of Neurology*. 10(2): 122-6.
- Thompson, S., Lanctôt, K. L., & Herrmann, N. (2004). The benefits and risks associated with cholinesterase inhibitor therapy in Alzheimer's disease. *Expert opinion on drug safety*, 3(5), 425-440.
- Thomsen, M., D. P. Woldbye, et al. (2005). "Reduced cocaine self-administration in muscarinic M5 acetylcholine receptor-deficient mice." *J Neurosci* 25(36): 8141-9
- Trimper, J. B., Stefanescu, R. A., & Manns, J. R. (2014). Recognition memory and theta-gamma interactions in the hippocampus. *Hippocampus*, 24(3), 341-353.
- Tsai G, Coyle JT (2002) Glutamatergic mechanisms in schizophrenia. *Annu Rev Pharmacol Toxicol*, 42:165-179.
- Van Strien, N. M., Cappaert, N. L. M., & Witter, M. P. (2009). The anatomy of memory: an interactive overview of the parahippocampal-hippocampal network. *Nature Reviews Neuroscience*, 10(4), 272-282.
- Vinck, M., van Wingerden, M., Womelsdorf, T., Fries, P., & Pennartz, C. (2010). The pairwise phase consistency: a bias-free measure of rhythmic neuronal synchronization. *Neuroimage*, 51(1), 112-122.
- Vlassenko, A. G., Vaishnavi, S. N., Couture, L., Sacco, D., Shannon, B. J., Mach, R. H., ... & Mintun, M. A. (2010). Spatial correlation between brain aerobic glycolysis and amyloid- β (A β) deposition. *Proceedings of the National Academy of Sciences*, 107(41), 17763-17767.

- Vogt, K. E., & Regehr, W. G. (2001). Cholinergic modulation of excitatory synaptic transmission in the CA3 area of the hippocampus. *The Journal of Neuroscience*, 21(1), 75-83.
- von Koch, C. S., H. Zheng, et al. (1997). "Generation of APLP2 KO mice and early postnatal lethality in APLP2/APP double KO mice." *Neurobiol Aging*, 18(6): 661-9.
- Wainer, B. H., Levey, A. I., Rye, D. B., Mesulam, M., & Mufson, E. J. (1985). Cholinergic and non-cholinergic septohippocampal pathways. *Neuroscience letters*, 54(1), 45-52.
- Walsh, D. M., I. Klyubin, et al. (2002). "Naturally secreted oligomers of amyloid beta protein potently inhibit hippocampal long-term potentiation in vivo." *Nature*, 416(6880): 535-9.
- Walsh, D. M., I. Klyubin, et al. (2005). "The role of cell-derived oligomers of Abeta in Alzheimer's disease and avenues for therapeutic intervention." *Biochem Soc, Trans* 33(Pt 5): 1087-90.
- Walsh, D. M., M. Townsend, et al. (2005). "Certain inhibitors of synthetic amyloid betapeptide (Abeta) fibrillogenesis block oligomerization of natural Abeta and thereby rescue long-term potentiation." *J Neurosci*, 25(10): 2455-62.
- Ward, S. D., Curtis, C. A., & Hulme, E. C. (1999). Alanine-scanning mutagenesis of transmembrane domain 6 of the M1 muscarinic acetylcholine receptor suggests that Tyr381 plays key roles in receptor function. *Molecular pharmacology*, 56(5), 1031-1041.
- Weinshenker, D. (2008). "Functional consequences of locus coeruleus degeneration in

- Alzheimer's disease." *Curr Alzheimer Res*, 5(3): 342-5.
- Wess, J., Eglen, R. M., & Gautam, D. (2007). Muscarinic acetylcholine receptors: mutant mice provide new insights for drug development. *Nature Reviews Drug Discovery*, 6(9), 721-733.
- Wess, J. (1996). Molecular biology of muscarinic acetylcholine receptors. *Critical Reviews in Neurobiology*, 10(1).
- Wess, J. (2004). Muscarinic Acetylcholine Receptor Knockout Mice: Novel Phenotypes and Clinical Implications*. *Annu. Rev. Pharmacol. Toxicol.*, 44, 423-450.
- Whitehouse, P. J., Price, D. L., Struble, R. G., Clark, A. W., Coyle, J. T., & Delon, M. R. (1982). Alzheimer's disease and senile dementia: loss of neurons in the basal forebrain. *Science*, 215(4537), 1237-1239.
- Wild-Bode, C., T. Yamazaki, et al. (1997). "Intracellular generation and accumulation of amyloid beta-peptide terminating at amino acid 42." *J Biol Chem*, 272(26): 16085-8.
- Wilson, I. A., Ikonen, S., McMahan, R. W., Gallagher, M., Eichenbaum, H., & Tanila, H. (2003). Place cell rigidity correlates with impaired spatial learning in aged rats. *Neurobiology of aging*, 24(2), 297-305.
- Wilson, I. A., Ikonen, S., Gureviciene, I., McMahan, R. W., Gallagher, M., Eichenbaum, H., & Tanila, H. (2004). Cognitive aging and the hippocampus: how old rats represent new environments. *The Journal of neuroscience*, 24(15), 3870-3878.
- Wilson, I. A., Ikonen, S., Gallagher, M., Eichenbaum, H., & Tanila, H. (2005). Age-associated alterations of hippocampal place cells are subregion specific. *The Journal of neuroscience*, 25(29), 6877-6886.

- Wilson, I. A., Gallagher, M., Eichenbaum, H., & Tanila, H. (2006). Neurocognitive aging: prior memories hinder new hippocampal encoding. *Trends in neurosciences*, 29(12), 662-670.
- Wingo, T. S., Lah, J. J., Levey, A. I., & Cutler, D. J. (2012). Autosomal recessive causes likely in early-onset Alzheimer disease. *Archives of neurology*, 69(1), 59-64.
- Witter, M. P. (1993). Organization of the entorhinal—hippocampal system: A review of current anatomical data. *Hippocampus*, 3(S1), 33-44.
- Xu, H., D. Sweeney, et al. (1997). "Generation of Alzheimer beta-amyloid protein in the trans-Golgi network in the apparent absence of vesicle formation." *Proc Natl Acad Sci USA*, 94(8): 3748-52.
- Yamada, M., T. Miyakawa, et al. (2001a). "Mice lacking the M3 muscarinic acetylcholine receptor are hypophagic and lean." *Nature*, 410(6825): 207-12.
- Yamada M, Lamping KG, Duttaroy A, Zhang W, Cui Y, Bymaster FP, McKinzie DL, Felder CC, Deng CX, Faraci FM, Wess J (2001b) Cholinergic dilation of cerebral blood vessels is abolished in M(5) muscarinic acetylcholine receptor knockout mice. *Proc Natl Acad Sci USA*, 98:14096-14101.
- Yan, R., & Vassar, R. (2014). Targeting the β secretase BACE1 for Alzheimer's disease therapy. *The Lancet Neurology*, 13(3), 319-329.
- Yassa, M. A., Lacy, J. W., Stark, S. M., Albert, M. S., Gallagher, M., & Stark, C. E. (2011a). Pattern separation deficits associated with increased hippocampal CA3 and dentate gyrus activity in nondemented older adults. *Hippocampus*, 21(9), 968-979.

- Yassa, M. A., & Stark, C. E. (2011b). Pattern separation in the hippocampus. *Trends in neurosciences*, 34(10), 515-525.
- Yassa, M. A., Mattfeld, A. T., Stark, S. M., & Stark, C. E. (2011c). Age-related memory deficits linked to circuit-specific disruptions in the hippocampus. *Proceedings of the National Academy of Sciences*, 108(21), 8873-8878.
- Zeng, Y., Zhao, D., & Xie, C. W. (2010). Neurotrophins enhance CaMKII activity and rescue amyloid- β -induced deficits in hippocampal synaptic plasticity. *Journal of Alzheimer's Disease*, 21(3), 823-831.
- Zhang, W., Hao, J., Liu, R., Zhang, Z., Lei, G., Su, C., ... & Li, Z. (2011). Soluble A β levels correlate with cognitive deficits in the 12-month-old APP^{swe}/PS1^{dE9} mouse model of Alzheimer's disease. *Behavioural brain research*, 222(2), 342-350.
- Zheng, H., M. Jiang, et al. (1995). "beta-Amyloid precursor protein-deficient mice show reactive gliosis and decreased locomotor activity." *Cell*, 81(4): 525-31.
- Ziying, Z., & Creese, I. (1997). Differential regulation of expression of rat hippocampal muscarinic receptor subtypes following fimbria-fornix lesion. *Biochemical pharmacology*, 53(9), 1379-1382.